Discovery and evaluation of styrylsulfonyl-methylpyridine derivatives as anticancer agents

by

Aik Wye Goh
Master of Pharmacy (Honours)

A thesis submitted for the degree of

Doctor of Philosophy

Centre for Drug Discovery and Development
School of Pharmacy and Medical Sciences
Division of Health Sciences



University of
South Australia

January 2016

Contents

1 Introduction 1

1.1 Hallmarks of cancer 1

1.1.1 Sustaining proliferative signalling 1

1.1.2 Resisting cell death 2

1.1.3 Evading growth suppressors 4

1.1.4 Inducing angiogenesis 4

1.1.5 Enabling replicative immortality 4

1.1.6 Activating invasion and metastasis 5

1.2 Kinases 5

1.3 Kinase inhibitors 6

1.4 Types of kinase inhibitors 7

1.4.1 Type I and II inhibitors 7

1.4.2 Type III inhibitors 9

1.4.3 Type IV inhibitors 9

1.5 ON01910 10

1.5.1 Synthesis and structure activity relationship 10

1.5.2 Mechanism of action 14

1.5.2.1 Polo-like kinase 1 15

1.5.2.2 PI3K/AKT/mTOR pathway 20

1.6 Clinical efficacy 24

1.7 ADME properties 26

1.8 Research aims and design background 28

2 Discovery of (*E*)-3-((styryl-sulfonyl)methyl)pyridines as potential anti-cancer agents 31

2.1 Introduction 31

2.2 Chemistry 32

2.2.1 Synthesis of (*E*)-2-methoxy-5-(((2,4,6-trimethoxystyryl)-sulfonyl)methyl)pyridin-3-amine analogues 32

2.2.2 Synthesis of (*E*)-2-methoxy-5-(((2,4,6-trimethoxystyryl)-sulfonyl)methyl)pyridin-3-ol analogues 36

2.2.3 Modification at the R^3 position of the styryl ring 40

2.3 Evaluation of antiproliferative activity and structure-activity relationship analysis 45

2.4 Microsomal stability assay 49

2.5 Caco-2 permeability assay 51

2.6 Pharmacokinetic studies 52

2.7 Conclusion 53
3 Design, synthesis and evaluation of (*E*)-2-((styrylsulfonyl)methyl)-pyridine 55
3.1 Introduction 55
3.2 Chemistry 55
3.2.1 Synthesis of (*E*)-3-methoxy-6-(((2,4,6-trimethoxystyryl)-sulfonyl)methyl)pyridin-2-amine analogues 55
3.2.2 Modification at the R^2 position of the pyridine ring 59
3.2.3 Modification at the R^3 position of the styryl ring 62
3.2.4 Synthesis of (*E*)-2-methoxy-6-(((2,4,6-trimethoxystyryl)sulfonyl)-methyl)pyridin-3-amine 64
3.3 Structure-activity relationship analysis 66
3.4 Investigation of cellular mode of action 70
3.5 Caspase-3/7 activation 78
3.6 Cellular mechanism of action 79
3.7 Microsomal stability assay 82
3.8 Caco-2 permeability assay 84
3.9 Pharmacokinetic studies 85
3.10 *In vivo* efficacy studies 86
3.11 Conclusion 88
4 Conclusions and future work 91
4.1 Conclusions 91
4.2 Future work 93
5 Experimental 100
5.1 Chemistry 100
5.2 Antiproliferative assay 148
5.3 Cell-Cycle Analysis and Detection of Apoptosis 149
5.4 Caspase-3/7 assay 149
5.5 Western blots 150
5.6 Kinase assay 150
5.7 Microsomal stability assay 150
5.8 Pharmacokinetic determinations 151
5.9 Caco-2 permeability assay 151
5.10 *In vivo* efficacy studies 151

Declaration

This thesis presents work carried out by myself and does not incorporate without acknowledgment any material previously submitted for a degree or diploma in any university; to the best of my knowledge it does not contain any materials previously published or written by another person except where due reference is made in the text; and all substantive contributions by others to the work presented, including jointly authored publications, are clearly acknowledged.

Compounds **16**, **17**, **18a** (TL-77), **18e** and **18f** were initially synthesized by Tiangong Lu and Anran Hu at the University of Nottingham. However, the structure activity relationship of these compounds was not established. I continued the research into the medicinal chemistry of styrylsulfonyl-methylpyridine derivatives. I optimised the synthetic methodology and prepared all compounds described in this thesis.

Biological activities and *in vivo* efficacy studies were performed by Dr Julian Adams. Microsomal stability assays and pharmacokinetic studies in rodents were carried out by Mr Ben Noll, Ms Longjin Zhong and Dr Peng Li. Computational studies including binding models were performed by Dr Malika Kumarasiri.

Aik Wye Goh

Publications

Portions of this thesis have been published or prepared for publications:

Lu, T.; **Goh, A.**; Yu, M.; Adams, J.; Lam, F.; Teo, T.; Li, P.; Noll, B.; Zhong, L.; Diab, S.; Chahrour, O.; Hu, A.; Abbas, A. Y.; Liu, X.; Huang, S.; Sumby, C. J.; Milne, R.; Midgley, C.; and Wang, S. Discovery of (*E*)-3-((Styrylsulfonyl)methyl)pyridine and (*E*)-2-((Styrylsulfonyl)methyl)pyridine Derivatives as Anti-Cancer Agents: Synthesis, Structure-Activity Relationships, and Biological Activities. *J. Med. Chem.* **2014**, *57*(6), 2275-2291.

Goh, A.; Adams, J.; Yu, M.; Noll, B.; Li, P.; Lam, F.; Teo, T.; Sykes, M.; and Wang, S. Synthesis and Biological Evaluation of (*E*)-2-((Styrylsulfonyl)methyl)pyridine and (*E*)-3-((Styrylsulfonyl)methyl)pyridine Derivatives as Potent Anticancer Agents. *Eur. J. Med. Chem.* **2016**, *in preparation*.

Noll, B.; Zhong, L.; **Goh, A.**; Li, P.; Rahaman, M.; Milne, R.; and Wang, S. Metabolic Profiles and Pharmacokinetics of Novel Mitotic Kinase Inhibitors. *J. Pharm. Biomed. Anal*. **2016**, *in preparation*.

Acknowledgements

Firstly, I would like to thank my supervisor, Professor Shudong Wang, for providing this wonderful opportunity to work with her group and for her support throughout my candidature. Her passion for medicinal chemistry as well as excellent knowledge has inspired my interest in drug discovery. I would also like to thank my associate supervisor, Dr Matt Sykes, for his continuous support and encouragement throughout my candidature. His broad and excellent knowledge in drug design and metabolism has assisted me greatly during my research.

I would like to give special thanks to my colleague, Dr Mingfeng Yu for his guidance and assistance throughout my research. I will always remember his inspirational and uplifting advice which supported me during my research. I would like to thank Dr Julian Adams for his assistance throughout my candidature and for helping me understand the biological aspects of cancer. I would also like to thank Mr Ben Noll, Dr Peng Li, and Ms Longjin Zhong for assisting me with the pharmacokinetic assessment of the compounds as well as helping me understand more about the wonders of pharmacokinetics.

Many thanks to my fellow colleagues and friends in the Centre for Drug Discovery and Development: Miss Sarah Diab, Miss Theodosia Teo, Miss Sapphire Le, Mr Yi Long, and Dr Malika Kumarasiri for supporting me and cheering me up throughout my research. Their heart-warming presence in the group has made the chemistry lab a much happier place to work in, especially during late nights.

Finally and most importantly, I would like to thank my mother and sister, Florence and May Yeng, who have given me everything in life.

The pathogenesis of cancer is heavily reliant on the deregulation of kinase activity including PLK1 and PI3K. This has led to the development of kinase inhibitors for the treatment of cancer. The most common kinase inhibitors identified are ATP competitive (i.e. type I and II inhibitors). However, these inhibitors tend to have poor selectivity due to the highly conserved structural features of the ATP binding site of kinases. Promiscuous inhibitory activity against a range of kinases can cause off-target toxicity and clinically, non-ATP competitive (i.e. type III) inhibitors that target an allosteric site of the kinase are more desirable for the purpose of molecular design. An example of a type III inhibitor is ON01910 (rigosertib) which has been demonstrated to have high selectivity with a good safety profile in clinical trials.

The aim of this research was to design and synthesise a novel class of styrylsulfonyl-methylpyridine derivatives that are able to mimic the mechanism of action of ON01910. The compounds were prepared using a series of synthetic routes, with substituents introduced at key positions to study the structure activitiy relationship (SAR).

Chapter 1 summarises the biological activity and pharmacokinetic properties of ON01910, the benchmark compound. Emphasis was placed on exploring the advantages and disadvantages of this drug as a clinical candidate.

In Chapter 2, (*E*)-3-((styrylsulfonyl)methyl)pyridine derivatives were designed and synthesised. The introduction of a pyridine moiety aimed to increase the water solubility and improve biopharmaceutical properties compared to that of ON01910. The antiproliferative activities of the compounds were evaluated, with compound **17** exhibiting high potency in cancer cell lines especially in pancreatic cancer cells (GI_{50} = 0.001-0.014 μM). Compound **17** demonstrated favourable pharmacokinetic properties with an oral bioavailability of 27% in rats dosed at 40 mg/kg. Caco-2 permeability assay studies of compound **17** showed a low efflux ratio, suggesting it has low susceptibility to P-glycoprotein.

As detailed in Chapter 3, (*E*)-2-((styrylsulfonyl)methyl)pyridine derivatives were synthesised to compare the SAR with that of the (*E*)-3-((styrylsulfonyl)methyl)pyridine series. Assessment of the antiproliferative activity led to the identification of lead compound **49** (GI_{50} = 0.001-0.011 μM). Treatment of A2780 human ovarian cancer cells with **49** resulted in the accumulation of cells at the G_2/M phase of the cell cycle,

followed by caspase targeted apoptosis. Western blot studies on **49** demonstrated its ability to inhibit CDC25C, indicating cellular inhibition of PLK1. In addition to possessing good oral bioavailability (*i.e.* 44% in rats dosed at 40 mg/kg) and low efflux ratio (*i.e.* 0.79), **49** was found to be significantly less susceptible to drug clearance *in vivo* compared to **7**. *In vivo* efficacy studies conducted on A2780 tumour xenograft models demonstrated that **49** suppressed tumour growth and improved overall survival.

In summary, the identification of ON01910 mechanistic mimetics that possess superior biopharmaceutical properties to ON01910 has been achieved. Lead compounds **17** and **49** are therefore nominated as drug candidates for preclinical development.

4EBP eIF4e-binding proteins

AIBN Azobisisobutyronitrile

AKT protein kinase B

APAF1 apoptotic protease-activating factor-1

ATP adenosine triphosphate

BAD BCL-2 antagonist of cell death

Bcl-2 B-cell lymphoma 2

BH3 Bcl-2 homology 3

BID BH3 interacting-domain death agonist

BIM Bcl-2 interacting mediator of death

CDK cyclin-dependent kinase

CHK checkpoint kinase

CLL chronic lymphocytic leukaemia

CNS central nervous system

DCM dichloromethane

DISC death-inducing signalling complex

DMAP *N*,*N*-Dimethylpyridin-4-amine

DMF *N*,*N*-dimethylformamide

DMSO dimethyl sulfoxide

DNA deoxyribonucleic acid

eIF4E eukaryotic initiation factor 4E

eIF4G eukaryotic initiation factor 4G

ERK extracellular signal regulated kinases

Flt1 vascular endothelial growth factor receptor 1

FOXO foxhead box proteins

GSK3 glycogen synthase kinase 3

HRMS high resolution mass spectroscopy

IP intraparenteral

IR insulin receptors

IRS-1 insulin receptor substrate 1

IV intravenous

LC/MS/MS liquid chromatography with tandem mass spectrometry

MAPK mitogen-activated protein kinases

MCL mantle cell lymphoma

mdm2 mouse double minute-2 homolog

MNK mitogen activated protein kinase-activated protein kinase

mTOR mammalian target of rapamycin

MTT 3-(4,5-dimethylthiazol-2-yl)-2,5 diphenyl tetrazolium bromide

NBS *N*-bromosuccinimide

NF-κB nuclear factor kappa-light-chain-enhancer of activated B cells

NLP Ninein-like protein

NMP *N*-methyl-2-pyrrolidone

NMR nuclear magnetic resonance

PAMPA parallel artificial membrane permeability assay

PARP poly(ADP-ribose) polymerase

PBD polo-box domain

PDGFR platelet-derived Growth Factor receptor

PDK1 phosphoinositide-dependant kinase-1

PI3K phosphoinositide 3-kinase

PIP_2 phosphatidylinositol 4,5-bisphosphate

PIP_3 phosphatidylinositol (3,4,5)-triphosphate

PLK1 Polo like kinase 1

p-AKT phosphorylated AKT

P-gp p-glycoprotein

p-mTOR phosphorylated mTOR

po oral gavage

PTEN phosphatidylinositol-3,4,5-trisphosphate 3-phosphatase

RAL RAS-like

RAS rat sarcoma

RBD RAS-binding domain

ROS reactive oxygen species

RTKs receptor tyrosine kinases

S6K ribosomal protein S6K

SUMO*RanGAP1 SUMO-conjugated RanGAP1

TBS *t*-butyldimethylsilyl

THF tetrahydrofuran

TLC thin layer chromatography

Topors topoisomerase I-binding proteins

Figure 1.1: The six distinct capabilities of cancer cells in enabling uncontrolled cell growth and metastasis.

Figure 1.2: The extrinsic (death receptor mediated) and intrinsic (mitochondrial mediated) apoptotic pathways.

Figure 1.3: The general structure of the catalytic domain of kinases.

Figure 1.4: Chemical structures of type I inhibitor gefitinib and type II inhibitor imatinib.

Figure 1.5: Chemical structure of ON01910 (rigosertib).

Figure 1.6: Chemical structure of ON01500, ON01910, ON013100, and ON013105.

Figure 1.7: Model representation and crystal structure of PLK1.

Figure 1.8: The two models for PBD-mediated substrate targeting as proposed by Lowery *et al*.

Figure 1.9: Regulation of the CDK1-cyclinB1 complex and CDC25C activities.

Figure 1.10: Chemical structures of BI 6727, GSK461364, and HMN-214.

Figure 1.11: The PI3K/AKT/mTOR pathway.

Figure 1.12: Chemical structures of NVP-BEZ235, BGT226, and GSK2126458.

Figure 1.13: General chemical structure of designed and synthesised styrylsulfonyl-methylpyridine derivatives.

Figure 2.1: General chemical structure of (*E*)-2-methoxy-5-(((2,4,6-trimethoxy-styryl)sulfonyl)methyl)pyridine derivatives.

Figure 2.2: Proposed mechanism of the Verley-Doebner modification of Knoevenagel condensation using benzylamine as the catalyst.

Figure 2.3: Proposed decarboxylation mechanism of **14**.

Figure 2.4: Mechanism of formation of the diazonium salt from aniline using sodium nitrite.

Figure 2.5: Proposed mechanism of Wohl-Ziegler bromination of benzylic CH_3.

Figure 2.6: Chemical structures depicting the keto-enol tautomerism of 4-hydroxy-2,6-dimethoxybenzaldehyde **31**.

Figure 2.7: Mechanism of O-demethylation.

Figure 2.8: Proposed major metabolite of **17**.

Figure 3.1: Stabilization of the anion of 2-aminopyridine *via* resonance.

Figure 3.2: Proposed decarboxylation mechanism of **47**.

Figure 3.3: Cell cycle effects of **49** and **50a** on A2780 cells.

Figure 3.4: Cell cycle effects of **59a**, **63b** and ON01910 on A2780 cells.

Figure 3.5: Cell cycle effects of **49**, **50a** and ON01910 on WI-38 cells.

Figure 3.6: Annexin V/PI binding assay on A2780 cells treated with **49**, **50a**, and ON01910.

Figure 3.7: Annexin V/PI binding assay on A2780 cells treated with **59a**, **63b**, and ON01910.

Figure 3.8: Annexin V/PI binding assay on HCT-116 cells treated with **63b** and ON01910.

Figure 3.9: Annexin V/PI binding assay on WI-38 cells treated with **49**, **50a**, and ON01910.

Figure 3.10: Caspase-3/7 activity in A2780 or WI-38 cells after treatment with **49**, **50a**, ON01910 for 24 h.

Figure 3.11: Western blot analysis of A2780 cells treated with **49**, **50a** or ON01910 for 24 h at the concentrations shown.

Figure 3.12: Screening of **49** against a panel of 57 kinases.

Figure 3.13: Proposed major metabolite of **49**.

Figure 3.14: *In vivo* antitumour activity of **49** in an A2780 ovarian cancer xenograft model.

Figure 3.15: Kaplan−Meier analysis of animal survival in an A2780 ovarian cancer xenograft model treated with compound **49**.

Figure 4.1: General structure of synthesised analogues.

Figure 4.2: Binding model of **49** on the PBD of PLK1.

Figure 4.3: (A) The lowest energy structure of the RBD of B-RAF with ON01910 in complex I and II. (B) Interactions of ON01910 with the amino acid residues of the RBD in complex I and II.

Figure 4.4: Preliminary binding model of **49** and ON01910 on the RBD of B-RAF.

Figure 4.5: Crosstalk between the PI3K/AKT/mTOR and RAF/MEK/ERK signalling pathways.

Tables

Table 1.1: Summary of clinical trials of ON01910. 25

Table 2.1: Structure and biological activity of (*E*)-3-((styrylsulfonyl)methyl)-pyridines..... 47

Table 2.2: Biological activity of **17**, **18a** and ON01910 against a panel of human cell lines 49

Table 2.3: Metabolic stability of compounds in rat liver microsomes 50

Table 2.4: Caco-2 permeability of **17** and **18a** 52

Table 2.5: Rat pharmacokinetic comparison of IV and orally administered **17** 53

Table 3.1: Summary of structure and biological activity 68

Table 3.2: Antiproliferative activity of **49**, **50a** and ON01910 against a panel of human cell lines 69

Table 3.3: Metabolic stability of compounds in rat liver microsomes 83

Table 3.4: Caco-2 permeability of **49** and **50a** 85

Table 3.5: Rat pharmacokinetic comparison of IV and orally administered **49**, **50a**, and **63b** .. 86

1 Introduction

1.1 Hallmarks of cancer

Cancer is a disease in which cell cycle misregulation leads to uncontrolled cell growth and proliferation. The transformation of normal cells to malignant cancer cells is a multistep process that involves somatic mutations to genes that regulate cell proliferation and development. According to Hanahan and Weinberg in their landmark review titled “The Hallmarks of Cancer”, cancer cells have six important capabilities that enable uncontrolled cell growth and metastatis (**Figure 1.1**).[1-2]

1.1.1 Sustaining proliferative signalling

In normal tissues, cell growth is regulated by the controlled release of mitogenic growth signals. In contrast, cancer cells possess a sustained proliferative signaling due to their ability to (a) produce growth factors by themselves; (b) stimulate neighbouring normal cells to exogenously release growth factors; (c) elevate the levels of receptor proteins on the surface of cancer cells, causing them to be hypersensitive exogenous growth factors.

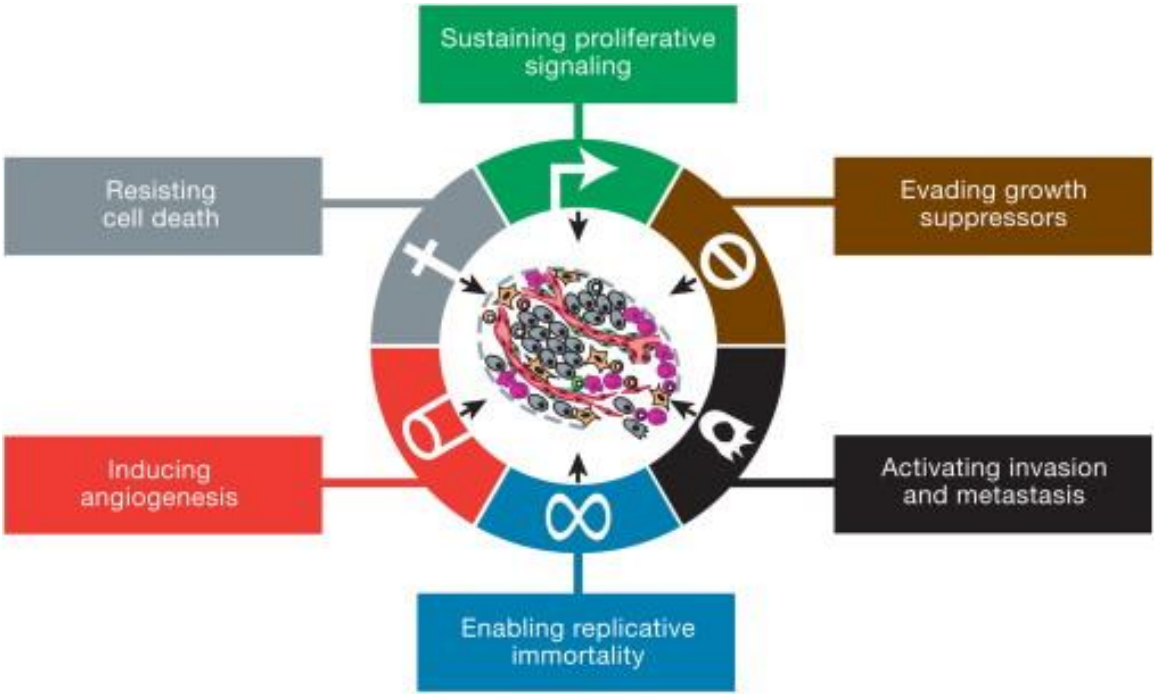


Figure 1.1: The six distinct capabilities of cancer cells in enabling uncontrolled cell growth and metastasis. (Reprinted with permission from Cell, March 2011, Vol. 144, Pages 646-674.[1] Copyright (2011) Elsevier Inc.)

1.1.2 **Resisting cell death**

Apoptosis, the process of controlled cell death, is an important barrier to the development of cancer. The signal transduction of the apoptotic process occurs by two distinct pathways which are the extrinsic pathway (death receptor mediated pathway) and intrinsic pathway (mitochondrial pathway) (**Figure 1.2**). The extrinsic pathway involves the activation of cell surface death receptors, which leads to the recruitment of TNFR-associated death domain protein (TRADD) and FAS-associated death domain protein (FADD).[3-4] These proteins lead to the activation of caspase-8, which in turn activates the effector caspases-3 and -7. Meanwhile, the intrinsic pathway involves the release of cytochrome c from the mitochondria. Activation of BH3-only proteins by several apoptotic signals (including DNA damage, oncogenesis, and hypoxia) activates Bcl-2 associated X protein (BAX).[5] The binding of activated BAX on the outer membrane of the mitrochondria then triggers the release of cytochrome c. The latter can also be trigerred by Bcl‑2 antagonist/killer (BAK), which is activated by truncated BH3 interacting-domain death agonist (tBID).[6] Cytochrome c subsequently complexes with

apoptotic protease-activating factor-1 (APAF1), forming the apoptosome which activates caspase 9.[7] Similar to caspase-8, caspase-9 activates the effector caspases-3 and -7 which subsequently leads to the induction of apoptosis.

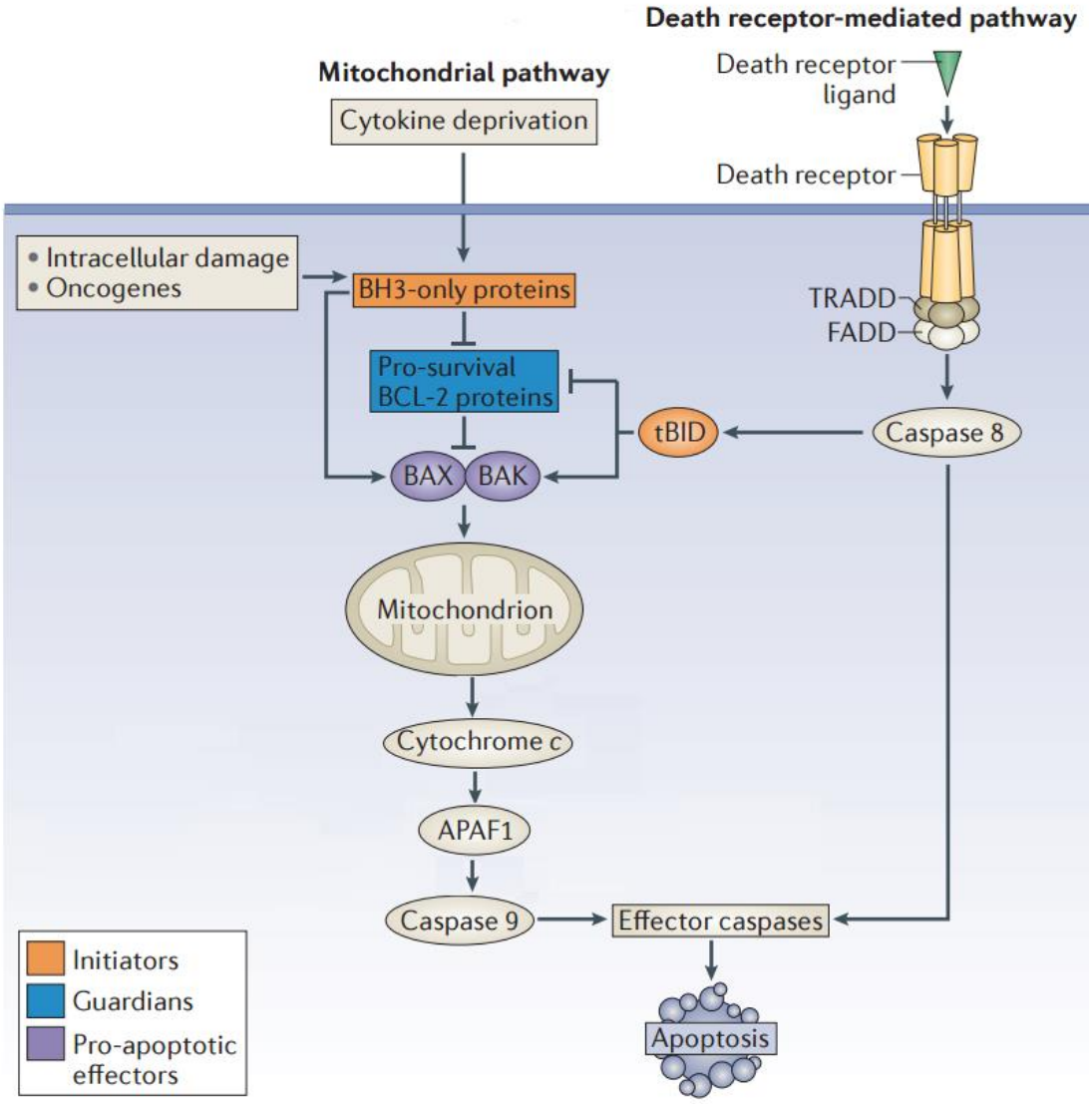


Figure 1.2: The extrinsic (death receptor mediated) and intrinsic (mitochondrial mediated) apoptotic pathways. The extrinsic pathway is initiated by the activation of transmembrane death receptors while the intrinsic pathway involves the release of cytochrome c by the mitochondria *via* the activation of BAX/BAK. (Reprinted with permission from Nature Reviews Molecular Cell Biology, December 2013, Vol. 15, Pages 49-63.[4] Copyright (2014) Nature Publishing Group.)

However, cancer cells have several strategies that allow them to disrupt the apoptotic machinery. These include the upregulation of antiapoptotic proteins (Bcl-2, Bcl-x_1,

survivin) [8-10] or of survival signals (IGF1/2),[11] and the downregulation of pro-apoptotic regulators (BAX, BAK).[12-13]

1.1.3 Evading growth suppressors

Tumour suppressors, including the two central supressors retinoblastoma protein (RB) and p53, are involved in the regulation of the cell cycle, induction of apoptosis, and maintenance of genome stability.[14] Despite that, these suppressors are usually inhibited in cancer cells, either due to overexpression of oncogenic proteins or to the presence of genetic mutations.[15-17] Loss of function of suppressor proteins due to gene mutations has also been implicated in the formation of cancers.[18-22]

1.1.4 Inducing angiogenesis

The growth and metastatis of cancer cells are highly dependent on the ability of cancer cells to promote angiogenesis. In normal tissues, angiogenesis is only activated during processes, including wound healing and the female menstrual cycle. However, in cancer cells, upregulation of angiogenesis growth factors such as vascular endothelial growth factor (VEGF) and fibroblast growth factors, results in constant activation of angiogenesis, thereby allowing growth sustenance.[23-24]

1.1.5 Enabling replicative immortality

Unlike normal cells which can only undergo cell division for a limited number of times, cancer cells, which are virtually immortalized, are able to replicate without limit. In normal cells, telomeres, which are caps at the end of DNA strands and consist of TTAGGG repeats, shorten progressively with each cycle of cell division. As telomeres protect the ends of chromosomes and prevent them from fusing, the gradual shortening of telomeres eventually causes them to lose their protective function.[25] This subsequently leads to a loss of cell viability. In contrast, cancer cells are able to reverse telomere shortening by enhancing the activity of telomerases, a ribonucleoprotein that synthesises telomeric DNA.[26]

1.1.6 Activating invasion and metastasis

During the progression of cancer, cancer cells, especially transformed epithelial cells, acquire the ability to invade and colonize new sites in the body. The downregulation of E-cadherin, an antagonist of invasion and metastasis, is commonly observed in aggressive carcinomas.[21, 27] Additionally, adhesion proteins, including CD44 and N-cadherin which promote cell migration, are commonly upregulated in invasive cancers.[28-29]

1.2 Kinases

Kinases are phosphotransferases that catalyze the transfer of a phosphoryl group from ATP to the hydroxyl group of a serine, threonine, or tyrosine residue on the protein substrate. Thus, kinases are categorized based on the amino acid residue that they phosphorylate. Phosphorylation of target proteins plays a key role in cellular signaling by modifying their activity or function, which in turn affects downstream responses.

The general structure of kinases consists of a catalytic domain (250-300 amino acid residues),[30] with the N-terminal lobe composed primarily of β-sheets and a single α-helix, and is linked to the C-terminal lobe (**Figure 1.3**). The hinge region that connects the N- and C- terminal lobes serves as the ATP binding site as its residues form hydrogen bonds with the adenine group of ATP.[31] Within the ATP binding site, the conserved DFG motif in the activation loop is important for the catalytic activity of the kinase. In the active confirmation of the kinase, the 'in conformation' of the DFG motif allows its Asp residue to chelate Mg^{2+} and orientate ATP.[32] In the inactive state, the Phe residue of the motif is directed towards the ATP binding site, thereby preventing access of ATP to its site.[33] The first residue of the hinge region is called the gatekeeper as it plays an important role in restricting access to a hydrophobic pocket adjacent to the ATP binding site.

The importance of kinases has been observed in a variety of biological processes including cellular proliferation, central nervous system (CNS) processes, cardiovascular system and cellular metabolism. Likewise, the dysregulation of kinases in these systems have been implicated in a variety of diseases including rheumatoid arthritis,[34] Parkinson's disease,[35] cardiovascular diseases,[36] and type 2 diabetes.[37] However, the

vast majority of studies are concentrated on the role of aberrantly activated kinases in the development of cancers.

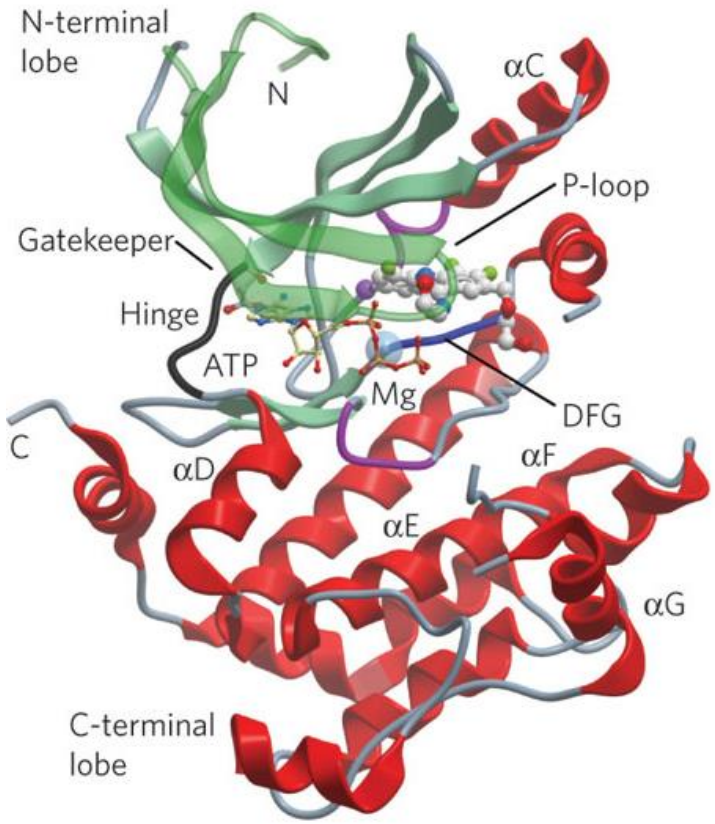


Figure 1.3: The general structure of the catalytic domain of kinases. (Reprinted with permission from Nature Chemical Biology, March 2010, Vol. 6, Pages 166–169.[38] Copyright (2010) Nature Publishing Group.)

1.3 **Kinase inhibitors**

According to Zhang *et al*, kinase targets are classed into three different types in regards to inhibitor design. The first type of targets are kinases that become resistant to regulatory mechanisms following genetic mutations that either activate or amplify their oncogenic activity.[39] Enhanced activities of these kinases are often essential for the growth and survival of the cancer cells. Therefore, the development of kinase inhibitors has drawn great attention as an effective anti-cancer therapeutic strategy. Imatinib (Gleevec) was the first kinase inhibitor developed, and is a BCR-ABL inhibitor used as a first line therapy for the treatment of chronic myelogenous leukemia (CML). CML is

characterized by an overexpression of the BCR-ABL protein due to the Philadelphia chromosome, which allows the maintenance and progression of this disease.[40-41]

The second type of kinase targets consists of kinases that have a synthetic lethal interaction with a mutated cancer gene. Two genes are said to have a synthetic lethal interaction when mutations occurring on both genes lead to cell death, while mutation on either gene alone maintains cell viability.[42] Therefore, inhibition of kinases that are encoded by genes that have a synthetic lethal interaction with cancer relevant mutations will selectively kill cancer cells.[43] Although these kinases are not oncogenic and are rarely mutated in cancer cells, these kinases are often necessary for the growth/survival of cancer cells and may be part of a key signaling pathway involved in the development of cancer. Example of kinases that have synthetic lethal interactions includes mammalian target of rapamycin (mTOR),[44] cyclin dependent kinases (CDKs),[45] and polo-like kinase 1 (PLK1).[46]

The third type of kinases involves those that are expressed in tumours or neighbouring tissues and regulate processes including cell survival, metastasis and angiogenesis. Examples of these kinases include vascular endothelial growth factor receptor (VEGFR) and FGFR which are important for angiogenesis,[47-48] tropomyosin receptor kinase B (TrkB) which promotes cancer cell invasion and metastasis, and the M2 isoform of pyruvate kinase which promotes aerobic glycolysis and tumour growth.[49]

The main advantage of kinase inhibitors compared to conventional chemotherapeutic agents is the ability of normal cells to tolerate the effect of kinase inhibition as certain kinases are not essential for the survival of normal cells. Targeting these kinases is often less damaging and more tolerable compared to other inhibition targets.

1.4 Types of kinase inhibitors

Kinase inhibitors can be categorized into four different types of inhibitors depending on their mode of binding.

1.4.1 Type I and II inhibitors

Type I kinase inhibitors are ATP competitive inhibitors that bind to the catalytically active conformation of the kinase at the ATP binding site, and are by far the most

common type of kinase inhibitors. Examples of type I inhibitors include SB203580,[50] PD166326,[51] gefitinib (**Figure 1.4**), and erlotinib.[52] Type I inhibitors typically contain a heteroaryl moiety which allows them to mimic the hydrogen bonds between the adenosine group of ATP and the amino acid residues of the ATP binding site.[31]

Unlike type I inhibitors which bind to the active conformation of the kinase, type II inhibitors, including imatinib (**Figure 1.4**), sorafenib,[53] and nilotinib,[54] bind to the inactive conformation where the rearrangement of the DFG motif to the DFG-out conformation exposes an additional hydrophobic pocket. Type II inhibitors possess a hydrophobic moiety that is able to form van der Waals interactions with residues in this pocket. Due to the lower affinity of this conformation for ATP, type II inhibitors tend to have higher cellular potency than type I inhibitors due to their low competition with ATP.[55] Furthermore, high kinase selectivity can also be achieved with type II inhibitors as the amino acid residues of the hydrophobic pocket exposed in the DFG-out conformation are less conserved compared to the residues of the ATP binding site.[56]

One of the limitations of targeting the ATP binding site of kinases is the risk of resistance due to mutations. Mutations to the gatekeeper residue of the ATP binding site are common problems observed with a wide variety of kinase inhibitors including imatinib, gefitinib and erlotinib.[57-58] As the gatekeeper residue determines the entry and binding of the inhibitor to the ATP binding site, mutation of the gatekeeper residue to a residue with a large side chain can significantly decrease the affinity of the ATP binding site to the kinase inhibitor. Furthermore, mutation to the gatekeeper residue has minimal effect on the binding of ATP, thus maintaining the activity of the kinase. Mutation at the ATP binding site has also been linked to the enhancement of ATP affinity, thereby reducing binding and potency of the inhibitor.[58]

Another limitation of ATP competitive inhibitors is the lack of selectivity across kinases due to the highly conserved nature of the ATP binding site, which may lead to toxicity problems and the inhibition of apoptosis promoting kinases including PLK 2 and p38.[59-61] Due to the hydrophobic moiety of type II inhibitors, these inhibitors also tend to have poor water solubility which may limit their *in vivo* activity as well as their bioavailability.[62]

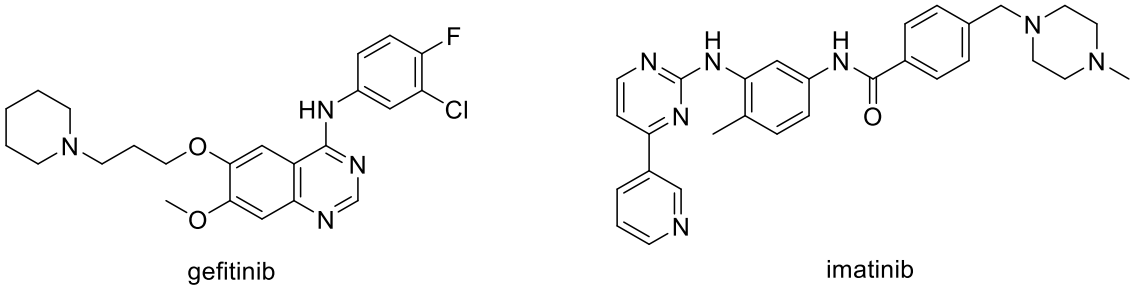


Figure 1.4: Chemical structures of type I inhibitor gefitinib and type II inhibitor imatinib.

1.4.2 Type III inhibitors

The high sequence similarity in the ATP binding site among members of the kinase families often results in low selectivity of ATP competitive inhibitors. In contrast, by targeting the less conserved allosteric site of kinases, type III inhibitors can acheive high specificity, thereby achieving a safer therapeutic profile.[63-65] Targeting the allosteric site can either modulate the enzymatic activity of the kinase or inhibit the activation of the kinase.[66] The most well characterized type III inhibitors are the MEK 1/2 allosteric inhibitors including CI-1040 and PD0325901 that bind to an allosteric site adjacent to the ATP binding site.[62] Other examples of a type III inhibitor are the BCR-ABL inhibitors GNF-2 and GNF-5 which were designed to circumvent resistance linked with imatinib administration.[67-69]

Due to the poorly conserved nature of the allosteric binding site, the identification and development of type III inhibitors are more difficult compared to the ATP competitive inhibitors. Allosteric inhibitors that inhibit kinase activation or signal transduction are also not identified by functional assays commonly used for the identification of ATP competitive kinase inhibitors if they do not inhibit the enzymatic activity of the kinase.[70]

1.4.3 Type IV inhibitors

Type IV inhibitors bind to the protein covalently, resulting in irreversible inhibition. A cysteine residue is commonly targeted for covalent binding due to its susceptibility to electrophilic attack.[71] This type of inhibitor can be used to target kinases that have

mutations to the ATP binding site which confers resistance to type I and type II inhibitors. The irreversible action of type IV inhibitors negates the need for high affinity compared to type I and type II inhibitors that require high affinities to compete with ATP.[72] Another significant advantage of type IV inhibitors is their sustained duration of action due to their irreversible covalent binding, allowing the design of effective treatments and avoiding the rise of resistance.[71]

1.5 ON01910

ON01910 (Rigosertib, Estybon, **Figure 1.5**) is a type III mitotic inhibitor that was developed by Onconova Therapeutics. ON01910 is currently in multiple clinical trials as a single agent for the treatment of conditions including solid tumours (Phase I), squamous cell carcinoma (Phase II),[73] higher risk myelodysplastic syndrome (MDS) in patients unresponsive to azacitidine or decitabine (Phase III),[74] and lower risk MDS *via* oral dosing (Phase II). A combination of ON01910 with azacitidine is also being evaluated in phase I/II clinical trials for the treatment of MDS,[75] acute myeloid leukemia (AML) and chronic myelomonocytic leukemia (CMML).[76]

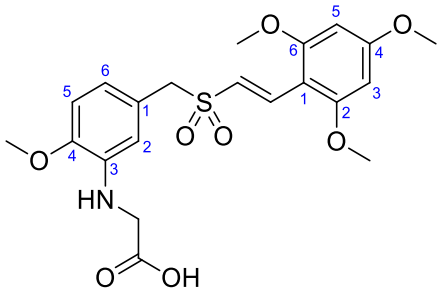


Figure 1.5: Chemical structure of ON01910 (rigosertib).

1.5.1 Synthesis and structure activity relationships

Several studies have reported the anticancer ability of certain styryl sulfones and their related biological activities.[77-79] Substituents on the styryl ring have an important effect on the anticancer activity of styryl sulfones, with electron donating substituents favoured for potent anticancer activity. The relative configuration of the alkene is also important, thus the *E* configuration of the styryl group ON01910 has been shown to be more potent compared to the respective *Z*-isomer. Interestingly, certain (*Z*)-styryl-2-

acetoxyphenyl sulfides and sulfones have exhibited inhibitory activity against cyclooxygenase-2, an enzyme involved in pain and inflammation signaling pathways.[80]

An important breakthrough in the development of styryl sulfones as anticancer agents came with the discovery of (*E*)-styrylbenzylsulfones including ON01500, ON01910, ON013100 and ON013105 (**Figure 1.6**).[81-82] The syntheses of these compounds were conducted by Onconova and are highlighted in **Scheme 1.1**. Both syntheses of ON01910 and ON13100 follow a common synthetic pathway involving the reaction of the corresponding benzyl halides **1a** and **1b** with thioglycolic acid to give carboxylic acids **2a** and **2b**. Deprotection of **2b** using TBAF in THF gave **2c**, and oxidation of **2a** and **2c** resulted in **3a** and **3c**, respectively. The Knoevenagel condensation reaction of the latter compounds with 2,4,6-trimethoxybenzaldehyde gave **4a** and **4c** (ON01500). Reduction of **4a** gave **5a**, which was treated with methyl bromoacetate followed by hydrolysis to give **5e** (ON01910).

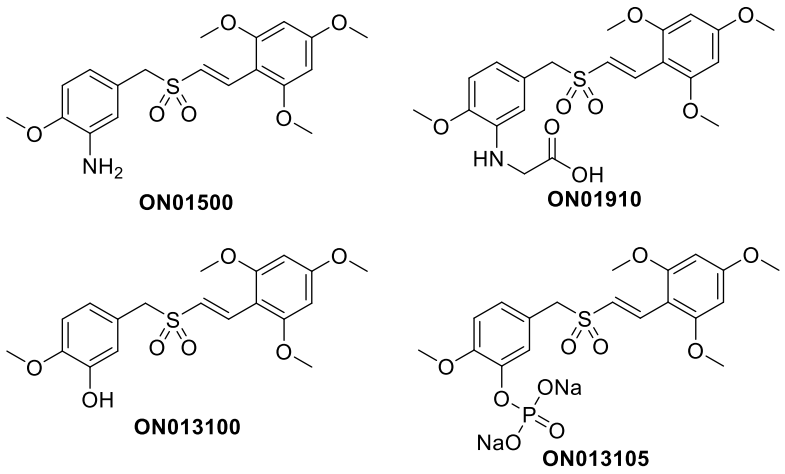
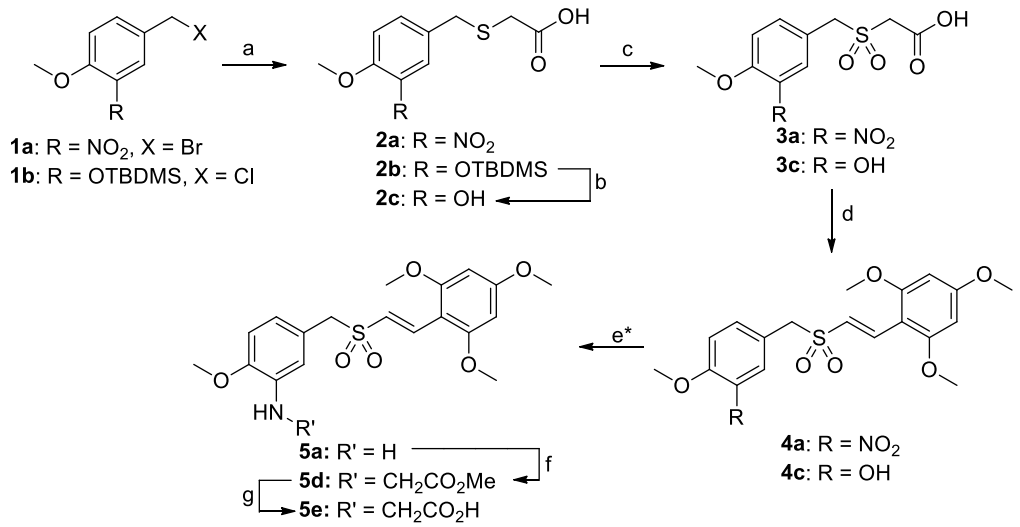


Figure 1.6: Chemical structure of ON01500, ON01910, ON013100, and ON013105.

An alternative synthetic route for **4a** is shown in **Scheme 1.2**. Treatment of 2,4,6-trimethoxybenzaldehyde with bromomethyltriphenylphosphonium bromide in the presence of potassium *t*-butoxide gave **7**. Dehydrobromination of **7** using potassium *t*-butoxide in THF afforded **8**.

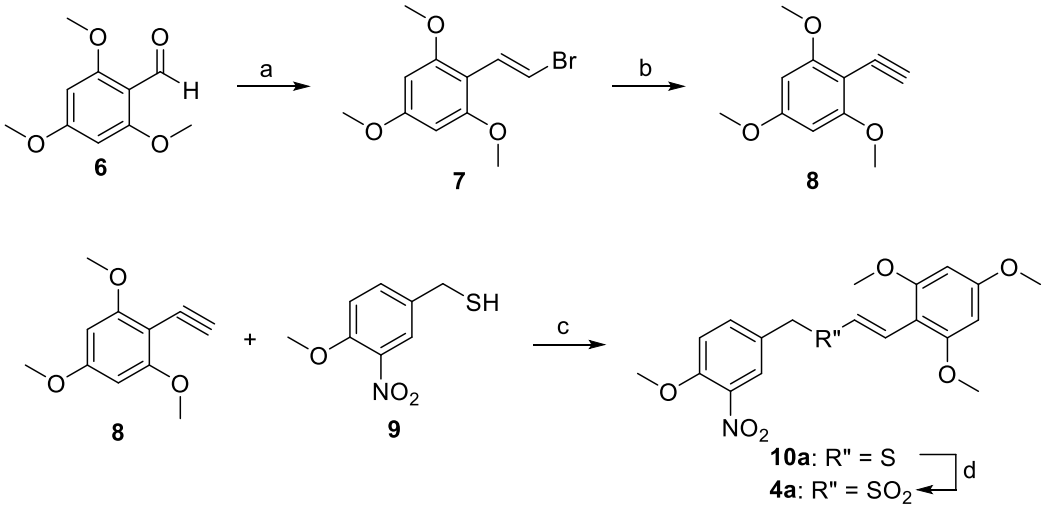
The formation of *E*- and *Z*-isomers in the free radical reaction between **8** and **9** was highly dependent on the solvent used. While reactions in non-polar solvents including benzene and toluene gave high proportions of the Z-isomer, the addition of methanol

completely shifted the stereoselectivity to the *E*-isomer **10a** with higher yields obtained. The subsequent oxidation of **10a** using 30% hydrogen peroxide gave **4a**.



Scheme 1.1: Reagents and conditions: (a) thioglycolic acid, MeOH, NaOH, rt, 3-5 h, 93-96%; (b) TBAF, THF, rt, 2 h, 50%; (c) 30% H_2O_2, CH_3CO_2H, 18-24 h, rt, 50-51%; (d) **4a**: 2,4,6-trimethoxybenzaldehyde, benzylamine, CH_3CO_2H, reflux, 2-8 h, 56%; **4c**: 2,4,6-trimethoxybenzaldehyde,piperidine, benzoic acid, toluene, 120 °C, 2-4 h, 63%; (e) *only for reduction of **4a**, acetone/H_2O (2:1), sodium hydrosulfite, 50 °C, 30 min, 48%; (f) methyl bromoacetate, sodium acetate, MeOH, reflux, 70%; (g) NaOH, H_2O, EtOH/CH_2Cl_2 (1:5), 20 °C, 3-4 h, 80%.

The cytotoxicity of the (*E*)-styrylbenzylsulfones was analysed by Onconova using a trypan blue exclusion assay conducted on human cancer cells including DU145 (prostate), K562 (leukemia), BT20 (breast), H157 (lung), and DLD1 (colorectal) cell lines.[81-82] Structure activity relationship (SAR) analysis suggested that while a hydrogen at the 3-position of the benzyl ring gave good activity (IC_{50} = 0.020-0.030 μM), the introduction of an amino (ON01500), hydroxyl (ON013100) or disodium phosphate (ON013105) group at this position increased the activity (IC_{50} = 0.003-0.010 μM). The modification of the amino group of ON01500 with glycine and glycine ester residues were generally tolerated. Of the amino acid derivatives, introduction of a glycine (*i.e.* ON01910, IC_{50} = 0.015-0.100 μM), aniline (IC_{50} = 0.015-0.025 μM), 2-amino-3,3,3-trifluoropropanoic acid (IC_{50} = 0.020-0.075 μM), and 2-amino-2-phenylacetic acid (IC_{50} = 0.015-0.020 μM) groups at the 3-position gave the best activities.



Scheme 1.2: Reagents and conditions: (a) bromomethyltriphenylphosphonium bromide, *t*-BuOK, THF, rt, 8 h, 68%; (b) *t*-BuOK, THF, reflux, 2 h, 65%; (c) Et_3B in hexane, MeOH (4 eq), toluene or benzene, 0 or 25 °C, 2 h, 92-95%; (d) 30% H_2O_2, CH_3CO_2H, 60 °C, 6 h, 80%.

On the 4-position of the benzyl ring, the methoxy group was found to be important as replacement of this methoxy in ON01500 and ON013100 with fluoride, bromide, nitro, cyanide, carboxyl, or hydroxyl groups decreased anticancer activity. Furthermore, changing the position of the methoxy from the 4-position to the 6-position of the benzyl ring resulted in a significant drop in activity (IC_{50} = 7.5 μM).

The 2,4,6-tri-substituted methoxy group of the styryl ring was found to be important for maximum anticancer activity (IC_{50} = 0.003-0.004 μM). Thus, the 2,6-dimethoxy analogue (*i.e.* (*E*)-5-(((2,6-dimethoxystyryl)sulfonyl)methyl)-2-methoxyaniline) was 10-fold less active (IC_{50} = 0.050 μM) compared to ON01500. Replacement of the 4-methoxy of the styryl ring of ON01500 with a hydroxyl or a butyric acid group also reduced the activity (IC_{50} = 0.200-25.00 μM). The 2,4,5- or 3,4,5-trimethoxy styryl analogues also exhibited significantly lower activity (IC_{50} = 0.250 -20.00 μM) compared to their 2,4,6-trimethoxystyryl counterparts.

The oxidative state of the sulfur was also found to have an impact on the biological activity of the compound. The thio and sulfinyl analogues of ON01500 gave lower cellular potencies (IC_{50} = 0.020-0.050 μM) when compared to ON01500.

1.5.2 Mechanism of action

ON01910 has been found to be active against a wide range of cancer cell lines *in vitro*, with IC_{50} values ranging from 10 nM to 170 nM.[82] ON01910 was found to be active against multi drug resistant tumour cell lines that are resistant to various drugs including doxorubicin and paclitaxel.[82] Attempts to develop resistant cell lines by prolonged exposure to ON01910 have failed.[83] The lack of resistance to ON01910 may be due to its simultaneous activity on several key pathways necessary for cancer cell survival. It has been proposed by Gumireddy *et al*. that its activity on the allosteric site instead of the ATP binding site limits the chance of resistance. Additionally, the same study proposed that while mutations to the ATP binding site have a limited effect on the binding of ATP, mutations in the allosteric sites have a detrimental effect on substrate binding which decreases kinase activity.[84] However, this proposal may be inaccurate as studies have demonstrated the ability of allosteric site mutations in conferring resistance to type III inhibitors without any detrimental effect on kinase activity.[85-86]

The anticancer activity of ON01910 originates from its ability to disrupt the cell cycle of cancer cells by arresting the cells at the G_2/M phase, which leads to the eventual induction of apoptosis.[84] Studies have previously linked this effect to its ability to inhibit PLK1, a kinase which is important in the promotion of cancer growth.[84] PLK1 promotes G_2/M transition through several roles including activation of the cyclin B/CDK1 complex, coordination of the centrosomes, and regulation of spindle assembly.[87] ON01910-treated HeLa cells were found to accumulate in the G2/M phase of the cell cycle.[84] G_2/M arrest eventually leads to the apoptosis of the cells as the cells cannot remain arrested in the G_2/M phase for extended periods of time. A recent study has also linked the G_2/M phase arrest of ON01910 to its ability to induce the hyperphosphorylation of SUMO-conjugated RanGAP1 (SUMO*RanGAP1), a complex that is involved in the regulation of mitosis.[88-89] However, it is currently unknown whether the hyperphosphorylation of this complex plays a role in the induction of apoptosis.

Subsequent studies have discovered the ability of ON01910 to induce apoptosis by the activation of the mitochondrial apoptosis pathway *via* the release of cytochrome c from the mitochondria.[90] Studies conducted on ON01910-treated mantle cell lymphoma cells have shown an increased release of cytochrome c from the mitochondria.[90] ON01910-

treated HeLa cells have been found to enhance caspase-3 activity while ON01910-treated mantle cell lymphoma (MCL) cell lines activated caspase-3, caspase-7, and caspase-9 activity.[84, 90] In ON01910-treated mantle cell lymphoma cells, the release of cytochrome c from the mitochondria is most likely promoted by truncated BH3 interacting-domain death agonist (tBID) which is the active cleaved form of BID.[7, 90] Increased expression of cleaved PARP was also found in ON01910 treated mantle cell lymphoma cells and HeLa cells, which further indicates the involvement of cytochrome c, caspase-3 and caspase-7 in the induction of apoptosis by ON01910.[84, 90]

The ability of ON01910 to induce apoptosis in cancer cells has been linked to the induction of reactive oxygen species (ROS). Treatment of chronic lymphocytic leukaemia (CLL) cells with ON01910 resulted in an increased level of ROS and pre-treatment of these cells with the antioxidant N-acetylcysteine decreased the apoptotic effect of ON01910.[91] The induction of ROS in cancer cells is a novel strategy for targeted cancer cell death. As cancer cells are under higher oxidative stress compared to normal cells, the induction of further reactive oxygen species may result in cellular damage which can eventually lead to cell death.[92] The induction of ROS in cancer cells is also able to trigger the release of cytochrome c from the mitochondria, possibly due to ROS damaging the mitochondria or the activation of Bcl-2 interacting mediator of death (BIM).[92] The induction of ROS by ON01910 has been linked to the activation of the JNK/AP-1 pathway which leads to the increased expression of ATF3, a pro-apoptotic protein.[91, 93-94] The induction of ROS in ON01910-treated CLL cells also increased the expression of the pro-apoptotic protein NOXA. Down-regulation of NOXA in Jeko-1 cell lines significantly decreased the apoptotic effect of ON01910.[91] CLL is an incurable disease that is frequently linked with resistance to anticancer agents including cytotoxic and DNA alkylating agents, which is mainly due to the loss of p53 function.[95] Increasing the expression of NOXA *via* ROS induction in CLL cells was discovered to be one of the methods able to induce apoptosis in these cells independent of the levels of p53.[95] Thus, the effect on the increase of NOXA suggests the therapeutic potential of ON01910 in the treatment of CLL.

1.5.2.1 **Polo-like kinase 1**

The inhibition of PLK1 by ON01910 has been well studied throughout the years, with several studies either demonstrating or refuting its PLK1 inhibition activity. PLKs are

serine/threonine kinases and five isoforms *i.e.* PLKs 1, 2, 3, 4, and 5 have been discovered to date. In addition to the usual structural features of kinases, PLKs have unique polo-boxes (PB) in their C-terminal lobe (**Figure 1.7**). The kinase domains of PLKs are linked to the polo-box domain (PBD) *via* an interdomain linker (IDL). The PBD is essential for the activity and localization of PLK1 as inhibition of the PBD results in the inhibition of PLK1 activity as well as an increase in mitotic arrest and apoptosis.[96-98] It has been proposed by Lowery *et al* that the PBD functions using two distinct models which are (i) the distributive phosphorylation model in which the PBD binds to a protein (neighbouring the substrate targeted by the PLK) for localization of the kinase, and (ii) the processive phosphorylation model whereby the binding of the PBD to a protein positions the protein for phosphorylation by PLK (**Figure 1.8**).[99]

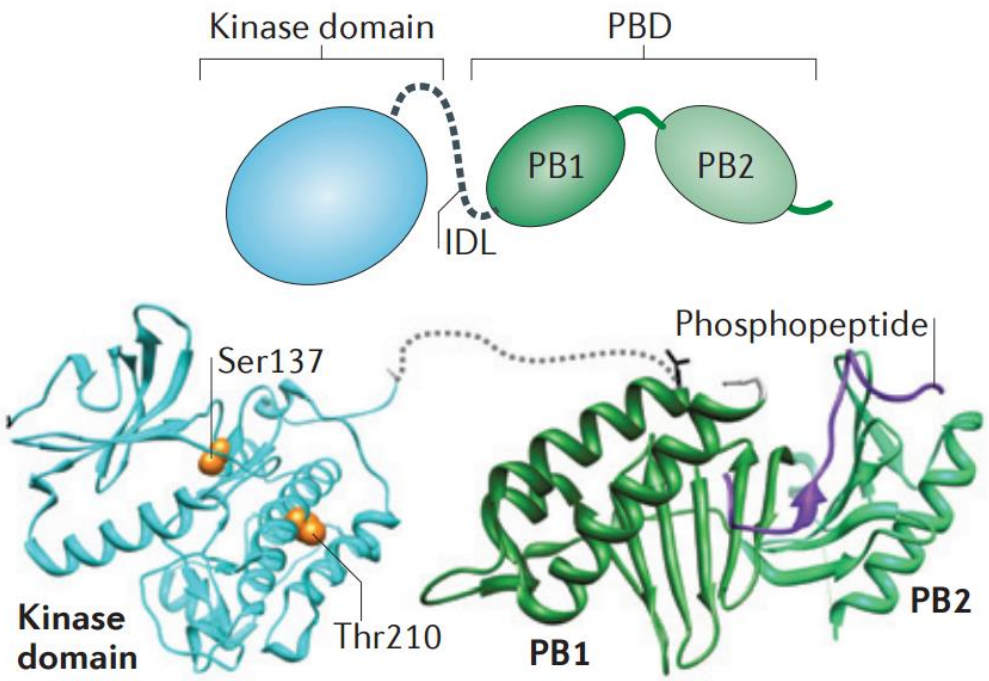


Figure 1.7: Model representation and crystal structure of PLK1. (Reprinted with permission from Nature Reviews Molecular Cell Biology, June 2014, Vol. 15, Pages 433-452.[100] Copyright (2014) Nature Publishing Group.)

PLK1 has been found to be involved in several processes during mitosis which includes the formation of bipolar spindles, centrosome maturation, kinetochore attachment, and in cytokinesis.[101-102] The importance of PLK1 in mitosis has been demonstrated in

several studies. In one study, it was found that a PLK1 knockout was embryonically lethal as it was observed that embryos lacking PLK1 expression died during the early stages of development.[103]

PLK1 promotes the transition from the G_2 phase to the M phase of the cell cycle by regulating the activities of the CDK1-cyclin B1 complex and CDC25C (**Figure 1.9**). In the interphase, the CDK1-cyclin B1 complex is kept inactive by the phosphorylation of Thr^{14} and Tyr^{15} by WEE1 and MYT1 while CDC25C is localized in the cytoplasm due to its binding with 14-3-3 proteins.[104-105] At the G_2/M transition, CDK activating kinase (CAK) phosphorylates Thr^{161} of CDK1, which opens its catalytic site.[106] PLK1 subsequently promotes the nuclear translocation of the CDK1-cyclin B1 complex by phosphorylating Ser^{147} on cyclin B1.[107] Meanwhile, PLK1 phosphorylates Ser^{198} on CDC25C which promotes its dissociation from 14-3-3 proteins.[108] This phosphorylation also promotes the nuclear translocation of CDC25C. Additionally, PLK1 inhibits checkpoint kinase 2 (CHK2) and p53, and downregulates CDC25C.[109-111] In the nucleus, CDC25C dephosphorylates Thr^{14} and Tyr^{15} on CDK1 which activates the CDK1-cyclin B1 complex to initiate mitosis.[112]

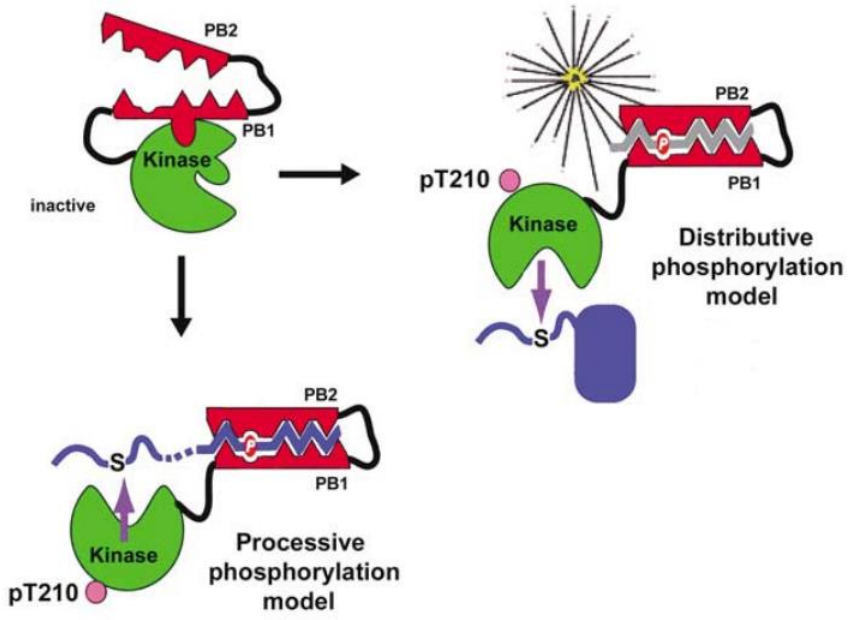


Figure 1.8: The two models for PBD-mediated substrate targeting as proposed by Lowery *et al.*[99] In the distributive phosphorylation model, PBD binds to a protein (neighbouring the substrate targeted by the PLK) for localization of the kinase. In the processive phosphorylation model, binding of the PBD to a protein positions it for

phosphorylation by the PLK. (Reprinted with permission from Oncogene, January 2005, Vol. 24, Pages 248-259.[99] Copyright (2005) Nature Publishing Group.)

During the cell division, PLK1 is important for centrosome maturation, a crucial process for the formation of bipolar spindles. The exact mechanism by which PLK1 facilitates centrosome maturation is currently unknown, though it is believed that PLK1 exerts its effect by phosphorylating the centrosomal ninein-like protein (Nlp).[113-114] The importance of PLK1 in mitosis has been demonstrated by several studies conducted on PLK1 inhibitors. Inhibition of PLK1 results in the disruption of centrosomal function and spindle abnormalities, thus inducing cell death.[84, 114-116]

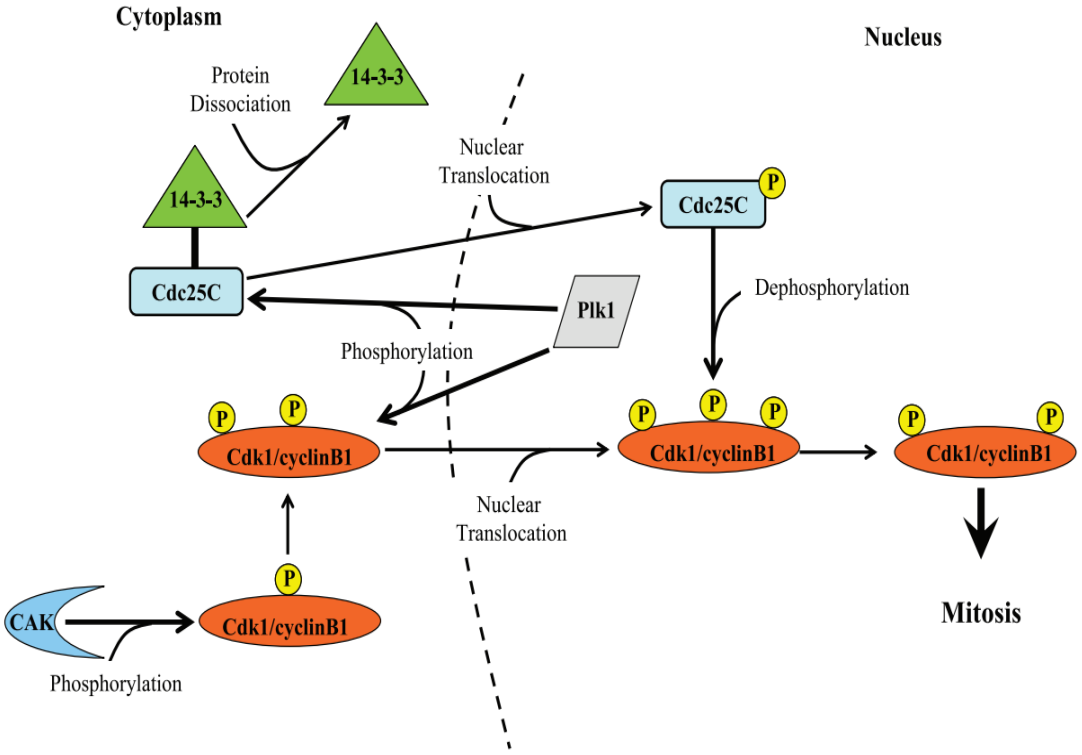


Figure 1.9: Regulation of the CDK1-cyclinB1 complex and CDC25C activities. PLK1 promotes the nuclear translocation of the complex and CDC25C *via* phosphorylation. In the nucleus, CDC25C dephosphorylates CDK1 which activates the complex and allows it to initiate mitosis. (Reprinted with permission from Molecular Cancer Therapeutics, July 2007, Vol. 6, Pages 1920-1931.[106] Copyright (2007) American Association for Cancer Research.)

PLK1 has been found to be overexpressed in cancer cells including cancers of breast, prostate, lung, skin, oesophagus, and liver.[117-122] PLK1 was found to inhibit the tumour suppressor p53 in cancer cells. In cells with normal p53 function, the activation of p53

leads to the transactivation of genes that are involved in several functions including DNA repair, cell cycle arrest and the induction of apoptosis.[101, 123] PLK1 was found to bind to the DNA binding region of p53, which thus inhibits the transactivation of genes encoding proteins including Bax,[124] phorbol-12-myristate-13-acetate-induced protein 1 (NOXA),[125] and p53 upregulated modulator of apoptosis (PUMA).[126-127] The effect of PLK1 on p53 can also be seen from the phosphorylation of topoisomerase I-binding proteins (topors) at its Ser^{718}.[128] Topors has both ubiquitin and SUMO-1 E3 ligase activity, and has several target proteins including p53. The phosphorylation of topors by PLK1 increased ubiquitination leading to the degradation of p53. PLK 1 also decreased the sumoylation activity of p53.[128]

The involvement of PLK1 in tumourigenesis and development has led to the development of several PLK1 inhibitors, including BI 6727, HMN-214, and GSK461364 (**Figure 1.10**), which have been evaluated in clinical studies. BI 6727, an ATP competitive inhibitor developed by Boehringer Ingelheim, was found to be a highly potent PLK inhibitor with an IC_{50} of 0.83, 5, and 56 nM against PLK1, PLK2 and PLK3 respectively.[129] GSK461364 is another ATP competitive inhibitor that is currently in phase I clinical trials. GSK461364 has higher selectivity for PLK1 compared to PLK2 and PLK3.[130] GSK461364 has been found to have a similar adverse effect profile to BI 6727, however reports have indicated the increased incidence of venous thrombosis compared to patients undergoing BI2536 or ON01910 therapies.[130-131] This indicates that GSK461364 may affect other undiscovered targets, which may limit its therapeutic use in patients.

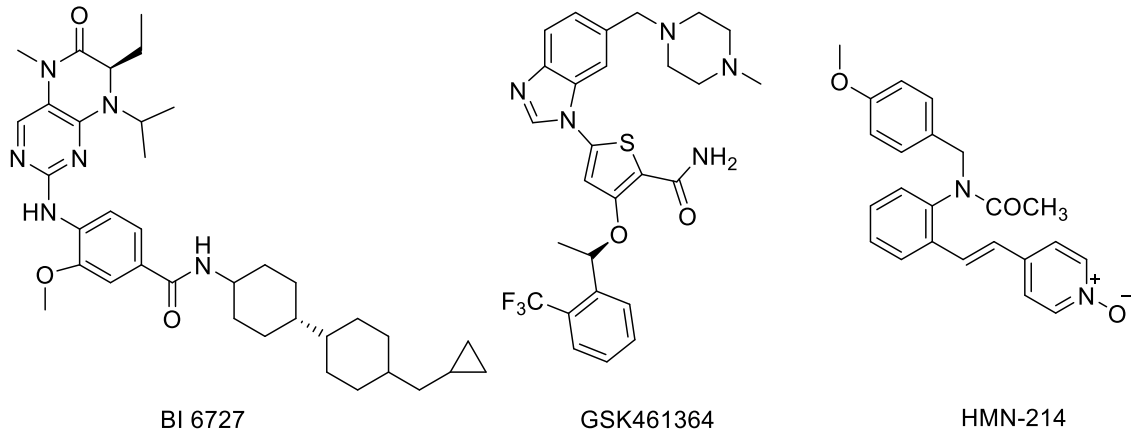


Figure 1.10: Chemical structures of BI 6727, GSK461364, and HMN-214.

The activity of ON01910 on PLK1 has been demonstrated by a series of studies conducted by Gumireddy *et al*.[84] In the study, ON01910 was shown to inhibit PLK1 *via* targeting its substrate CDC25C in a dose-dependent manner. The inhibition of ON01910 seemed ATP non-competitive. ON01910 was shown to inhibit PLK1 with an IC_{50} of 9 nM in both biochemical and cell based assays.[84] Studies on pancreatic cancer cell lines have also demonstrated the ability of ON01910 to inhibit the phosphorylation of CDC25C hence providing a link to its PLK1 inhibition.[132]

However, *in vitro* kinase assays have shown that ON01910 only inhibits PLK1 above 30 μM.[133-134] More studies will be needed to determine the binding modes of ON01910.

1.5.2.2 **PI3K/AKT/mTOR pathway**

The involvement of the PI3K/AKT/mTOR pathway (**Figure 1.11**) in cancer pathogenesis is of interest, as several studies have indicated the involvement of the components of the pathway in cancer development.[135-138] Though this pathway is also involved in normal cell cycle progression, increased and unregulated signalling in this pathway often leads to an increase in the translation of tumour promoters and anti-apoptotic proteins, which promotes carcinogenesis.

Phosphoinositide 3-kinase (PI3K) phosphorylates phosphatidylinositol 4,5-bisphosphate (PIP_2) which then generates phosphatidylinositol (3,4,5)-triphosphate (PIP_3). The active PIP_3 then proceeds by activating phosphoinositide-dependant kinase-1 (PDK-1) *via* phosphorylation which in turn activates protein kinase B (PKB), also known as AKT. The latter phosphorylates mammalian target of rapamycin complex 1 (mTORC1) *via* the phosphorylation and inactivation of tuberous sclerosis 1/2 (TSC1/2) which normally inhibits the activity of Rheb. TSC1/2 act as GTPase activating proteins of Rheb, which leads to the accumulation of the inactive GDP bound form of Rheb.[139] Inactivation of TSC1/2 leads to the accumulation of the active GTP bound Rheb, which activates mTORC1.[139] The activated mTORC1 then promotes the translation of proteins required for cell growth. Besides promoting cellular growth, the PI3K/AKT/mTOR pathway is involved in other processes including cell migration/invasion and glucose metabolism.[140-141]

The activity of this pathway is negatively regulated by the tumour suppressor, phosphatase and tensin homolog (PTEN). PTEN suppresses this pathway by

dephosphorylating PIP_3, thereby inhibiting the activity of PI3K. In addition, PTEN is involved in several PI3K-independent functions including the maintenance of DNA stability, DNA repair,[142] and cellular senescence.[143] The importance of PTEN as a barrier to cancer has been well demonstrated, with studies linking the loss of PTEN function with cancer development.[144-145] In cancer cells with impaired PTEN function, elevated levels of PIP_3 and phosphorylated AKT are commonly detected.[146-147] Loss of PTEN function can occur through somatic mutations, transcriptional silencing or protein instability.[148] Somatic mutations to PTEN have been observed in a wide variety of cancers, especially in endometrium, skin, and central nervous system cancers.[144, 149-150]

While dysregulation of the PI3K/AKT/mTOR pathway is mainly linked to loss of PTEN function, mutations to the subunits of the PI3K structure has often resulted in enchanced PI3K activity.[151] Of the three classes of PI3Ks, the class 1A PI3Ks were found to be highly involved in cancer development. Mutations to the PI3KCA gene that encodes p110α, the catalytic subunit of the class 1A PI3Ks, have been found to increase the enzymatic activity and oncogenicity of the kinase.[152] PI3KCA mutations are frequently observed in prostate, breast, and endometrium cancers.[153]

AKT is also involved in several other pathways in oncogenesis. It activates nuclear factor kappa-light-chain-enhancer of activated B cells (NF-κB), a protein that promotes cancer cell survival.[154-155] AKT has also been implicated in the activation of murine double minute-2 gene product (MDM2), a protein that inhibits the activity of p53.[154, 156] Moreover, AKT inhibits the activity of pro-apoptotic BCL-2 antagonist of cell death (BAD) and BCL-2 interacting mediator of cell death (BIM).[157-158] AKT is also involved in the deactivation of glycogen synthase kinase 3 (GSK3), a protein that increases the degradation of cyclin D1.[158]

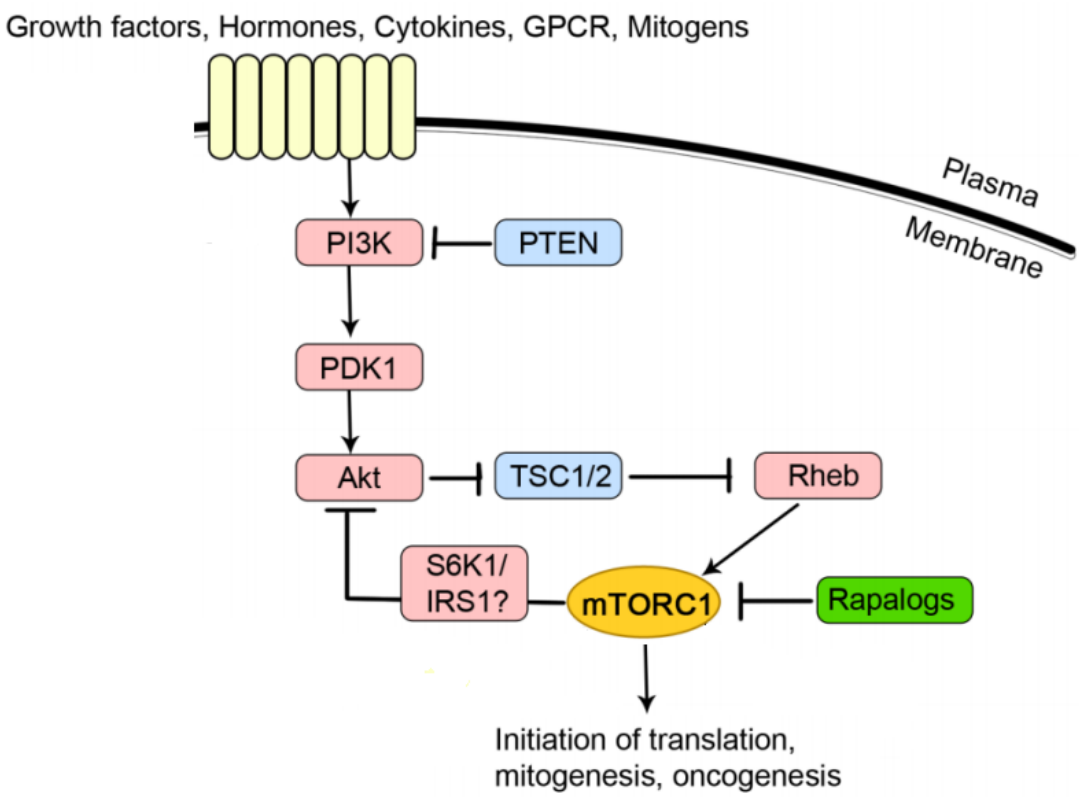


Figure 1.11: The PI3K/AKT/mTOR pathway. Activation of PI3K leads to a cascade of events including the activation of AKT and mTORC1. mTORC1 subsequently initiates the translation of proteins required for cell growth and oncogenesis.[159]

The involvement of the PI3K/AKT/mTOR pathway in oncogenesis indicates the therapeutic potential of targeting this pathway for cancer treatment. Several inhibitors which target the components of this pathway have been studied, including rapalogs and allosteric inhibitors of mTORC1. However, these inhibitors only displayed modest efficacy against specific cancers including renal cancers,[160] neuroendocrine cancers,[161-162] and lymphomas.[163-164], due to the activation of compensatory negative feedback mechanisms.[165] It was found that the inhibition of mTORC1 by rapalogs increases the activity of insulin receptor substrate 1 (IRS-1), a protein which activates PI3K *via* binding to insulin receptors (IR).[166] In normal cells, the activation of mTORC1 leads to the activation of p70 S6K1, which leads to the phosphorylation and degradation of IRS-1.[167] In rapalog-treated cells, the inhibition of mTORC1 also leads to the inhibition of S6K1 activity, which eventually leads to the accumulation of IRS-1.[166-167]

The structural similarities of the active sites of mTOR and the p110 subunit of PI3K have led to the development of dual PI3K/mTOR inhibitors including NVP-BEZ235, BGT226, and GSK2126458 (**Figure 1.12**) to circumvent this feedback mechanism.[168-171] These inhibitors have displayed encouraging results, for example NVP-BEZ235 has been found to be more effective than the rapamycin analogue everolimus.[172] However, NVP-BEZ235 induces cytostatic effects, not apoptosis, and should be used in combination with a cytotoxic agent.[168]

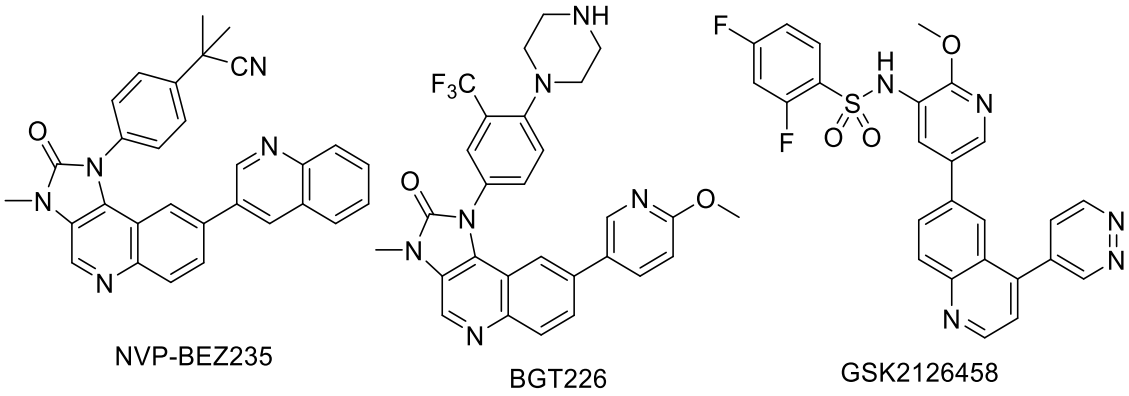


Figure 1.12: Chemical structures of NVP-BEZ235, BGT226, and GSK2126458.

The targeting of the PI3K/AKT/mTOR pathway by ON01910 has been studied using mantle cell lymphoma (MCL) cell lines and several leukemia cell lines.[90-91, 173] MCL exhibits enhanced expression of cyclin D1, an oncogenic protein that is modulated by the AKT/GSK-mediated pathway. Enhanced activation of the PI3K/AKT/mTOR pathway is often associated with an increase in cyclin D1 expression in cancer.[174-175] ON01910 down-regulates cyclin D1 expression *via* inhibition of the PI3K/AKT/mTOR pathway.[90] Furthermore, ON01910 did not affect the Ras/Raf/MEK1/2/ERK pathways, suggesting it is an AKT-mediated mechanism.[90] Decreased levels of phosphorylated mTOR (p-mTOR), phosphorylated eIF4e-binding proteins (4EBP), and phosphorylated AKT (p-AKT) were found in MCL and MLL lines treated with ON01910, which indicates ON01910 inhibitory activity associated with this pathway.[90, 173] Furthermore, chronic lymphocytic leukemia (CLL) cells treated with ON01910 were found to exhibit significantly decreased levels of p-AKT, thereby indicating that ON01910 exerts its inhibitory effect upstream of AKT.[91] In enzyme linked immunosorbent assay studies conducted using MCL cell lines, immunoprecipitated PI3K acquired from cells treated with ON01910 also exhibited significantly decreased activity compared to the immunoprecipitated PI3K acquired from the control cells.[90] The efficacy of ON01910 in

inhibiting this pathway was further demonstrated in phase I/II clinical studies whereby the administration of ON01910 in patients unresponsive to hypomethylating agents resulted in the inhibition of AKT phosphorylation in CD34+ cells.[176]

The main advantage of ON01910 compared to other known inhibitors targeting the PI3K/AKT/mTOR pathway is its additional ability to induce apoptosis by its activity on the mitotic machinery. Inhibition of the PI3K pathway has been linked to the activation of compensatory signaling pathways including extracellular signal-regulated kinase (ERK),[177] human epidermal growth factor receptor (HER) 2 and 3,[178] and v-myc avian myelocytomatosis viral oncogene homolog (MYC) pathways.[179] Unlike most known pan-PI3K inhibitors (as well as mTOR inhibitors) which are predominantly cytostatic, ON01910 has the advantage of inducing apoptosis which is possibly *via* its targeting of the mitochondrial apoptotic pathway [91, 168, 180-181] making it an highly attractive therapeutic agent.

1.6 Clinical efficacy

The clinical trials conducted on ON01910 are summarized in **Table 1.1**. Phase I trials were conducted against solid tumours and haematological cancers while most of the ongoing phase II or III trials are concentrated on the treatment of MDS and leukaemias.[182-184]

The potential of ON01910 for the treatment of MDS is based on the involvement of the PI3K pathway in the development of this disease. MDS is a haematological disorder which often precedes the development of AML and is characterized by impaired haematopoiesis.[185] Dysregulation of the PI3K pathway is a common hallmark in the development of MDS, with studies demonstrating elevated levels of phosphorylated AKT and cyclin D1 in patient cells.[186-187] In phase I studies, 12 patients with MDS were given ON01910 at 800-1000 mg/m^2, 72-120 hours continuous IV infusion every 2 weeks, which resulted in improved blood counts in six (50%) patients.[74] Administration of ON01910 in these patients also decreased the expression of cyclin D1 in their CD34+ peripheral blood cells. In a separate phase I/II study conducted on 13 MDS patients unresponsive to hypomethylating agents, seven (53%) patients demonstrated a high degree of disease stabilization following treatment (800-1800 mg/m^2, 72 hours continuous IV infusion, every 2 weeks) with ON01910.[176] Furthermore, phosphorylated

AKT levels in patient CD34+ peripheral blood cells were found be decreased after ON01910 treatment. While phase I studies have demonstrated the potential of ON01910 for the treatment of MDS, randomized phase III studies are required to demonstrate its efficacy in improving the survival of patients as well as its ability in delaying the progression of MDS to AML. The potential of ON01910 for the treatment of haematological cancers has also been demonstrated by a phase I study conducted on 14 patients with B-cell malignancies including CLL and MCL patients.[188] In this study, seven (50%) patients exhibited disease stabilization following treatment (1500-1800 mg/m^2, 48-72 hours continuous IV infusion, every 2 weeks).

Table 1.1: Summary of clinical trials of ON01910.

Conditions	Phase	Route	Ref
Solid cancers	I	2 hr IV infusion every 3 days for 28 days	189
Advanced cancers that are metastatic or unresectable	I	72 hr continuous IV infusion every 2 weeks	190
Advanced solid cancers	I	Oral in fasting state, twice daily for 21 days	73
Relapsed B-cell malignancies	I	72 hr continuous IV infusion every 2 weeks	188
Higher risk MDS	I	72-120 hr continuous IV infusion every 2 weeks	74
Higher risk MDS unresponsive to hypomethylating agents	I/II	72-120 hr continuous IV infusion every 2 weeks	191
Lower risk MDS	II	Oral in fasting state, twice daily for 14 days	192

In addition, the anticancer activity of ON01910 has been demonstrated in patients with solid cancers. In a phase I study conducted on 46 patients with advanced solid cancers, two (4%) patients exhibited tumour regression while disease stabilization was observed in eight (17%) other patients following ON01910 administration (oral, 70 mg twice daily).[73] In a separate phase I study on 20 patients with solid tumours, one patient (5%) who exhibited a partial response remained progression free for a period of 24 months following treatment of ON01910 (4370 mg, 2 hours IV infusion, every 4 days for four cycles).[189]

It is noticeable in clinical studies that the efficacy of ON01910 is highly dependent on its route of administration. Clinical studies with 72 hour continuous IV infusion had a significantly higher percentage of patients with stable disease compared to studies using other methods of administration including 2 hour IV infusion and oral dosing. The difference may be due to the pharmacokinetic profile of ON01910, and a 72 hour continuous IV infusion was required to maintain therapeutically viable levels in the plasma. Indeed, Roschewski *et al* reported that the treatment of MDS is more effective with a 72 hour infusion compared to a 48 hour infusion.[188]

Treatment with ON01910 is generally well tolerated by patients, with fatigue and gastrointestinal disturbances being the most common side effects reported in phase I studies. ON01910 has shown a low degree of haematological side effects such as thrombocytopenia and neutropenia in the clinic when compared to PLK1 ATP competitive inhibitors *i.e.* BI 2536 and GSK461364.[130, 193-195] Interestingly, dose dependent urinary side effects including dysuria, haematuria, and cystitis are highly prevalent in patients on oral ON01910, compared to patients on IV dosing which exhibited a low incidence of these side effects.[73, 176, 189, 196] In phase I studies in patients with advanced solid cancers, 36% (14/47) of patients exhibited grade 2 urinary side effects, with most of these side effects occurring at higher doses. It has been proposed by Bowles *et al* that the acidification of the compound and first pass metabolism may be responsible for the urinary effects.[73]

1.7 ADME properties

The absorption, distribution, metabolism, and excretion (ADME) properties of ON01910 have been extensively studied during preclinical development and phase I clinical trials. ON01910 is not orally bioavailable.[197-199] The low oral bioavailability of ON01910 may be due to it being a substrate of P-glycoprotein (P-gp), which can increase the efflux of the drug molecules from the epithelial cells into the intestinal lumen.[198] As a major membrane transporter protein, P-gp is present in a variety of cells including intestinal epithelial cells, liver hepatocytes, epithelial cells of the proximal renal tubule, brain endothelial cells, trophoblasts of the placenta, and the sertoli cells in the blood-testis barrier.[200-201] The expression of P-gp in certain cancers is also implicated with the development of anticancer drug resistance as P-gp promotes the

efflux of anticancer agents, reducing the therapeutic effect of the drug.[202] The expression of P-gp in the intestinal epithelia is important in limiting the absorption of xenobiotics into the systemic circulation. Additionally, expression of P-gp on hepatocytes in a healthy liver is too low to promote biliary excretion of drug molecules, though studies have demonstrated a significant increase in P-gp expression in diseased liver cells.[203] While P-gp has a vast range of substrates and is not selective for any particular chemical moiety, P-gp substrates are generally amphipathic with spatially separated hydrophobic and hydrophilic moieties.[204]

To determine whether a drug molecule is a substrate of P-gp, a cell based permeability assay using cell lines expressing P-gp can be employed.[205] Caco-2 permeability studies on ON01910 have demonstrated a high efflux ratio of the compound, which indicates that ON01910 is susceptible to the effects of P-gp.[198] Furthermore, the addition of the P-gp inhibitor cyclosporine during the assay resulted in a significant decrease in the efflux ratio, confirming that ON01910 is a substrate of P-gp.[198] Certain cancers which exhibit high expression of P-gp may also be resistant to ON01910 as P-gp may limit the intracellular concentration and potency of ON01910. While *in vitro* cytoxicity assays on multidrug resistant cell lines using ON01910 demonstrated high potency, these assays do not take the plasma protein binding and drug clearance which occur *in vivo* into consideration.[82, 206] The combination of these factors *in vivo* may limit the exposure of cancer cells to ON01910 which can impair its effectiveness towards cancers which express P-gp.

Animal studies conducted on mouse, rats, and dogs showed a high plasma protein binding (98%) of ON01910, and this was shown to increase with decreasing concentrations of ON01910.[207] While plasma protein binding is conversely related with drug metabolism,[206] drug molecules with high plasma protein binding may be problematic for intracellular targets especially in the presence of efflux proteins.[208-210] Furthermore, studies conducted on DU145 prostate carcinoma cell lines found that the presence of fetal bovine serum or albumin in the cell culture medium resulted in a significant drop in anticancer activity of ON01910, which indicates that the high plasma protein binding of ON01910 has a negative effect on the activity of the drug.[207]

In pharmacokinetic studies conducted, the elimination of the drug from plasma followed a 2 phase elimination profile which consisted of a rapid decrease of plasma

concentration after bolus intravenous (IV) injection for a few hours followed by a slow decrease of plasma concentration.[207] The initial phase in which the drug is rapidly eliminated from the plasma may limit the exposure of the cancer cells to the drug as the concentration of the drug during the second elimination phase is too low to have any effect on the cancer cells. The rapid elimination during the initial phase may indicate the high rate of metabolism and poor metabolic stability of ON01910, which is supported by the fact that the drug accumulates primarily in the liver in mice studies.[207] During phase I trials, the plasma concentration profile of the drug followed an initial rapid decrease in plasma concentration after 2 hours IV infusion followed by a steady and slow decrease in plasma concentration similar to that seen in animal studies.[189, 207] Whether the initial rapid decrease in plasma concentration is due to the distribution of the drug to the tumour sites or whether the drug is rapidly eliminated is currently unknown.

The expression of P-gp in the epithelial cells of the proximal renal tubule may contribute to the renal clearance ON01910. Several studies have implicated the role of P-gp in the renal excretion of drug molecules into the urine.[211-214] Studies on rats administered with ON01910 by IV reported high renal excretion at the dose of 300 mg/kg, indicating that renal excretion is a primary route of clearance.[207] Phase 1 clinical trials of IV ON01910 on patients with advanced cancer reported rapid renal clearance following IV administration.[190] While the high plasma protein binding of ON01910 limits the overall renal clearance of the drug, the excessive renal excretion decreases the therapeutic effect of ON01910. Moreover, clinical trials involving oral administration of ON01910 reported a high prevalence of urinary side effects including dysuria, haematuria and cystitis. It is currently unknown whether these effects are attributable to the excretion of ON01910 from the kidney or to the direct effect of ON01910 on the urinary system; more studies will need to be conducted to determine this.

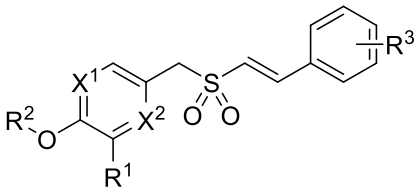
1.8 Research aims and design background

Although ON01910 is highly active against a wide variety of cancer cell lines including multidrug resistant cell lines *in vitro*, the combination of high plasma protein binding and P-gp susceptibility, poor oral bioavailability, and a mediocre pharmacokinetic profile *in vivo* may limit the exposure of the cancer cells to the drug *in vivo*. This in turn

limits its efficacy and necessitates a long and continuous IV infusion administration regime.

Therefore, novel compounds which are able to mimic the mechanism of action of ON01910 are desirable. Ideally, design of a new chemical class should aim to yield compounds which have potent anticancer activity, selectivity towards cancer cells, and improved pharmacokinetic profile. The main aim of this research project is therefore to design and synthesise a novel class of anticancer agents with superior anticancer activity, bioavailability, and pharmacokinetic properties.

In this study, a novel series of styrylsulfonyl-methylpyridine derivatives were designed and synthesised to mimic the mechanism of action of ON01910. The introduction of a pyridine ring has been strategically employed by medicinal chemists in the mitigation of metabolism and in the improvement of water solubility.[215] The introduction of N to the aromatic ring decreases the electron density of the ring and increases the polarity of the molecule, thereby reducing the metabolism of the compound by CYP450s which have high selectivity for hydrophobic molecules.[216-217] A selection of substituents was introduced at the R^1, R^2, and R^3 positions to study the structure activity relationship (SAR) of substituents at these positions (**Figure 1.13**). Further biological and pharmacological evaluations were conducted subsequently on compounds which exhibit potent antiproliferative activity to understand their mechanism of action and drug like properties.



X^1 = C, X^2 = N
or
X^1 = N, X^2 = C

Figure 1.13: General chemical structure of designed and synthesised styrylsulfonyl-methylpyridine derivatives.

2 Discovery of (*E*)-3-((styryl-sulfonyl)methyl)pyridines as potential anti-cancer agents

2.1 Introduction

This chapter encompasses the design, synthesis, and biological evaluation of (*E*)-3-((styrylsulfonyl)methyl)pyridines to evaluate the effect of replacing the benzene moiety of ON01910 with a pyridine ring on the pharmaceutical properties of the compounds. To determine the key molecular features required for optimum activity, a variety of substituents were introduced progressively at the R^1 and R^3 positions (**Figure 2.1**).

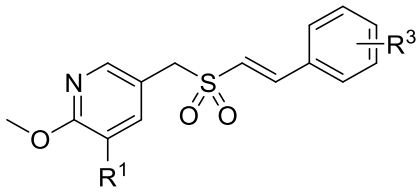


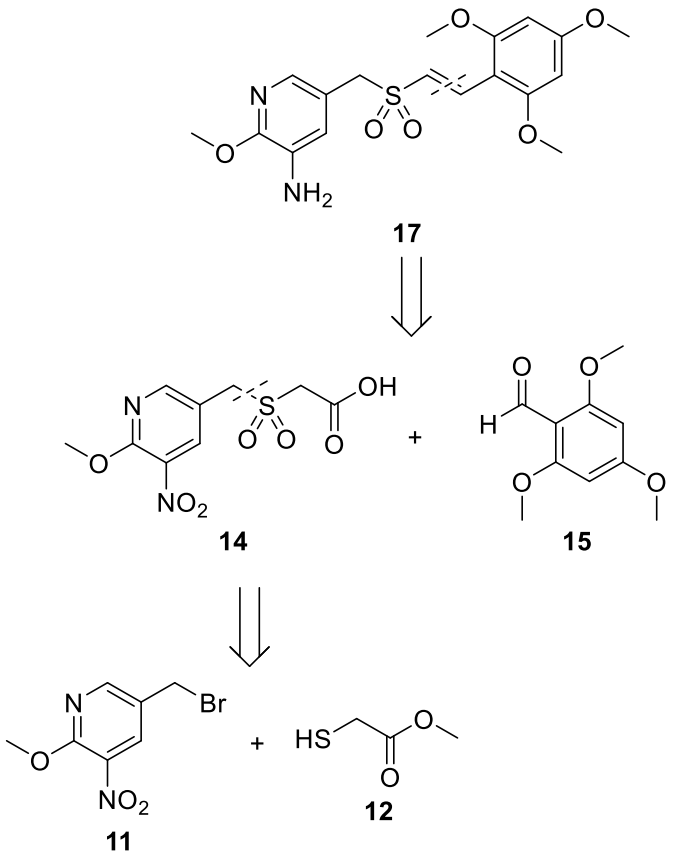
Figure 2.1: General chemical structure of (*E*)-2-methoxy-5-(((2,4,6-trimethoxy-styryl)sulfonyl)methyl)pyridine derivatives.

2.2 Chemistry

2.2.1 Synthesis of (*E*)-2-methoxy-5-(((2,4,6-trimethoxystyryl)-sulfonyl)methyl)pyridin-3-amine analogues

The retrosynthetic analysis of (*E*)-2-methoxy-5-(((2,4,6-trimethoxystyryl)sulfonyl)-methyl)pyridin-3-amine **17** is outlined in **Scheme 2.1**. Construction of **17** can be performed with the coupling of 2-(((6-methoxy-5-nitropyridin-3-yl)methyl)-sulfonyl)acetic acid **14** and the commercially available 2,4,6-trimethoxybenzaldehyde 1**5**, followed by reduction of the nitro group. Compound 1**4** can be synthesised from the nucleophilic substitution of 5-(bromomethyl)-2-methoxy-3-nitropyridine **11** with methyl 2-mercaptoacetate **12**, followed by oxidation of the thioether and then hydrolysis. While thioglycolic acid could be used instead of **12** in the coupling with **11** as adopted in the synthesis of ON01910 (*vide supra*, **Scheme 1.1**) it was envisioned that the coupling with **11** allows the formation of an ester, which is easier for purification compared to a carboxylic acid. Although **17** can also be synthesized *via* the formation of **8** as highlighted in **Scheme 1.2**, this scheme was not employed due to the impracticality of using the highly pyrophosphoric triethylborane, especially in larger scale reactions.

Compound **17** was synthesised using the process outlined in **Scheme 2.2**. The commercially available **11** was reacted with methyl 2-mercaptoacetate in the presence of potassium carbonate, with the residue subsequently oxidised with 30% hydrogen peroxide in glacial acetic acid to give methyl 2-(((6-methoxy-5-nitropyridin-3-yl)methyl)sulfonyl)acetate **13** in 79% yield. Saponification of **13** with potassium carbonate in a mixture of methanol and water afforded the carboxylic acid **14** in near quantitative yield.



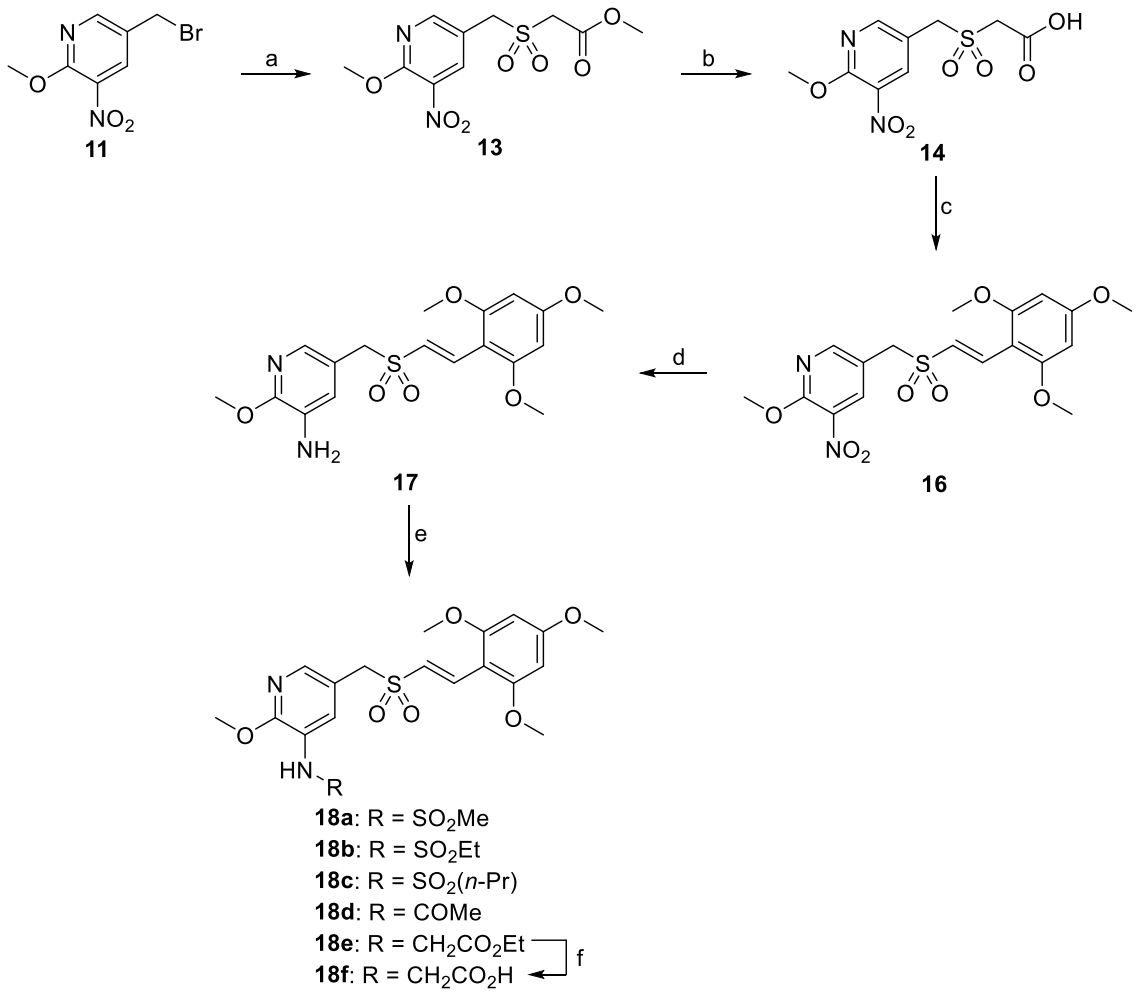
Scheme 2.1: Retrosynthetic analysis of **17**.

Synthesis of the key intermediate (*E*)-2-methoxy-3-nitro-5-(((2,4,6-trimethoxystyryl)-sulfonyl)methyl)pyridine **16** was attempted *via* Verley-Doebner modification of the Knoevenagel condensation of **14** and 2,4,6-trimethoxybenzaldehyde **15** was attempted using several different methods. The first method reported in the manufacture of ON01910, [218] used acetic acid as the coupling reagent, with toluene as the solvent. However the reaction failed to produce the target compound. A second method was attempted by employing benzylamine as the catalyst and glacial acetic acid as the solvent. [82] The reaction was successful, giving **16** in 14% yield. The reaction mechanism is proposed in **Figure 2.2**. In this reaction, benzylamine catalyzes the formation of the enolate anion which reacts with the aldehyde.[219-220] Subsequent decarboxylation and elimination of water results in the formation of the desired α,β-unsaturated compound. However, the acidic conditions of the reaction promoted decarboxylation of **14** (**Figure 2.3**), resulting in the formation of 2-methoxy-5-((methylsulfonyl)methyl)-3-nitropyridine **19** in 56% yield. Furthermore, the presence of **19** in the reaction mixture also complicates the purification process due to a similar R_f to

16 in a wide range of thin layer chromatography (TLC) mobile phases. The third method utilised a mixture of benzoic acid and piperidine in toluene.[81] The synthesis of **16** was successfully achieved using this method, obtaining a yield of 41%. The purification of the compound was also simpler as washing with methanol was sufficient to yield the pure compound.

^{1}H nuclear magnetic resonance (^{1}H-NMR) and mass spectrometry methods were employed to characterize the structure of all compounds prepared and were in agreement with the expected structures (*vide infra*, Chapter 5). In the ^{1}H NMR spectrum of **16**, coupling constants of the doublets at 7.09 and 7.46 ppm (J = 15.5 Hz) indicated that the double bond of the styryl group was present in the *E*-configuration. In contrast, the alkenyl hydrogen of a *Z*-isomer would have exhibited a coupling constant of 6-12 Hz. No *Z*-isomer was isolated from the reaction mixture during the synthesis of **16**. The coupling constant of the doublets at 8.44 and 8.45 ppm (J = 2 Hz) demonstrated the meta coupling of the pyridine protons, confirming the (*E*)-3-((styrylsulfonyl)methyl)-pyridine structure of the compound. A singlet at 6.29 ppm (2H) corresponds to the protons on the 3- and 5-positions of the styryl ring while a singlet at 4.63 ppm (2H) corresponds to the methylene linking the pyridine ring with the sulfonyl. Singlets at 3.85 (6H), 3.86 (3H) and 4.03 ppm (3H) correspond to methoxy protons. Meanwhile in the ^{13}C NMR spectrum, the number of signals in the spectrum tallies with the total number of carbons in the molecule. High resolution mass spectrometry (HRMS) analysis of **16** also confirmed the molecular mass of the compound (*m/z* 425.0991 $[M+H]^{+}$). Compound **16** was subsequently reduced with iron in a mixture of glacial acetic acid and methanol, [221-222] giving the amine **17** in 68% yield.

A selection of substituents was introduced to the amino group to further develop the structure activity relationship at that position. Reaction of **17** with alkylsulfonyl chlorides, acetyl chloride or ethyl bromoacetate in the presence of pyridine or potassium carbonate afforded the corresponding sulfonamides **18a** (R = $NHSO_2Me$), **18b** (R = $NHSO_2Et$), **18c** (R = $NHSO_2$(*n*-Pr)); acetamide **18d** (R = NHCOMe); and ethyl acetate **18e** (R = $NHCH_2CO_2Et$) (**Scheme 2.2**). Hydrolysis of **18e** was conducted using sodium hydroxide in a mixture of water and methanol, affording the carboxylic acid **18f** in 60% yield.



Scheme 2.2: Reagents and conditions: (a) (i) methyl thioglycolate, K_2CO_3, MeOH, rt, 2 h; (ii) 30% H_2O_2, CH_3CO_2H, 50 °C, 12 h, 79%; (b) K_2CO_3, MeOH/H_2O (1:1), rt, 12 h, 98%; (c) 2,4,6-trimethoxybenzaldehyde **15**, benzoic acid, piperidine, toluene, reflux, 3 h, 41%; (d) Fe, MeOH/CH_3CO_2H (3:4), 50 °C, 3 h, 68%; (e) **18a**: methanesulfonyl chloride, pyridine, 0 °C to rt, 13 h, 76%; **18b**: ethanesulfonyl chloride, pyridine, 0 °C to rt, 12 h, 84%; **18c**: propane-1-sulfonyl chloride, pyridine, 0 °C to rt, 12 h, 71%; **18d**: acetyl chloride, pyridine, rt, 2 h, 86%; **18e**: ethyl bromoacetate, K_2CO_3, DMF, 60 °C, 16 h, 51%; (f) NaOH, MeOH/H_2O (1:2), rt, 12 h, 60%.

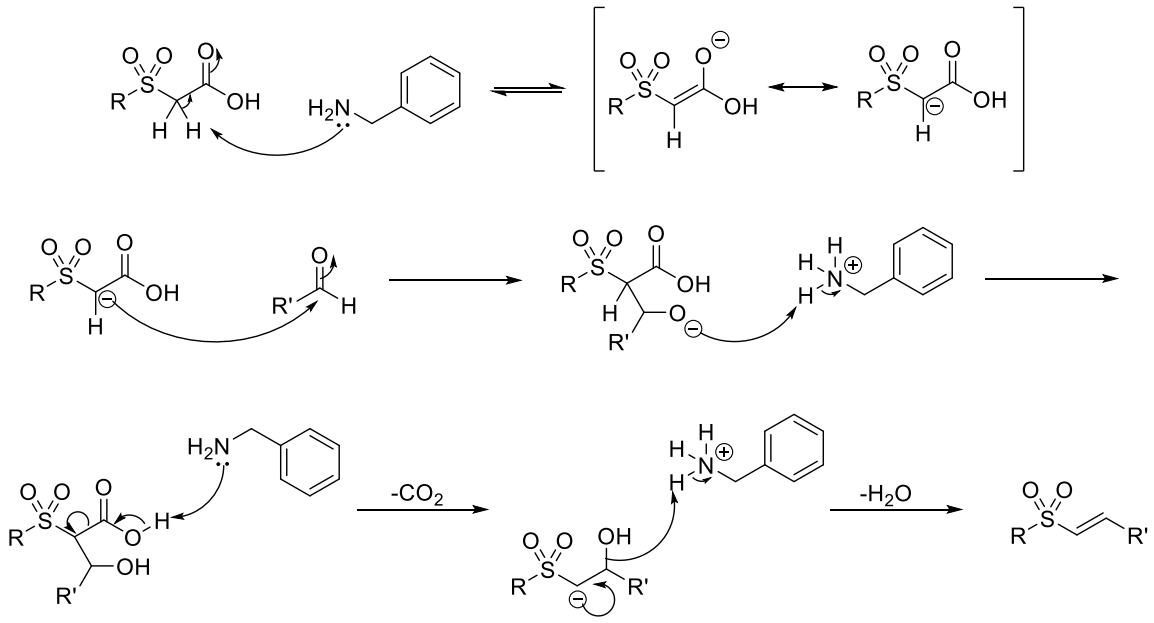


Figure 2.2: Proposed mechanism of the Verley-Doebner modification of Knoevenagel condensation using benzylamine as the catalyst.

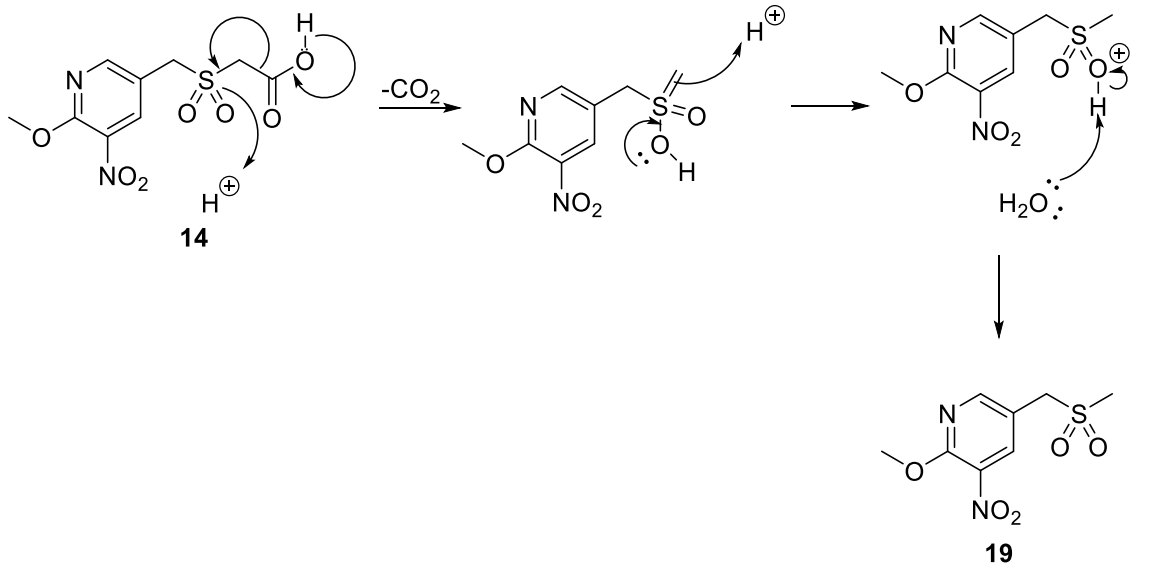


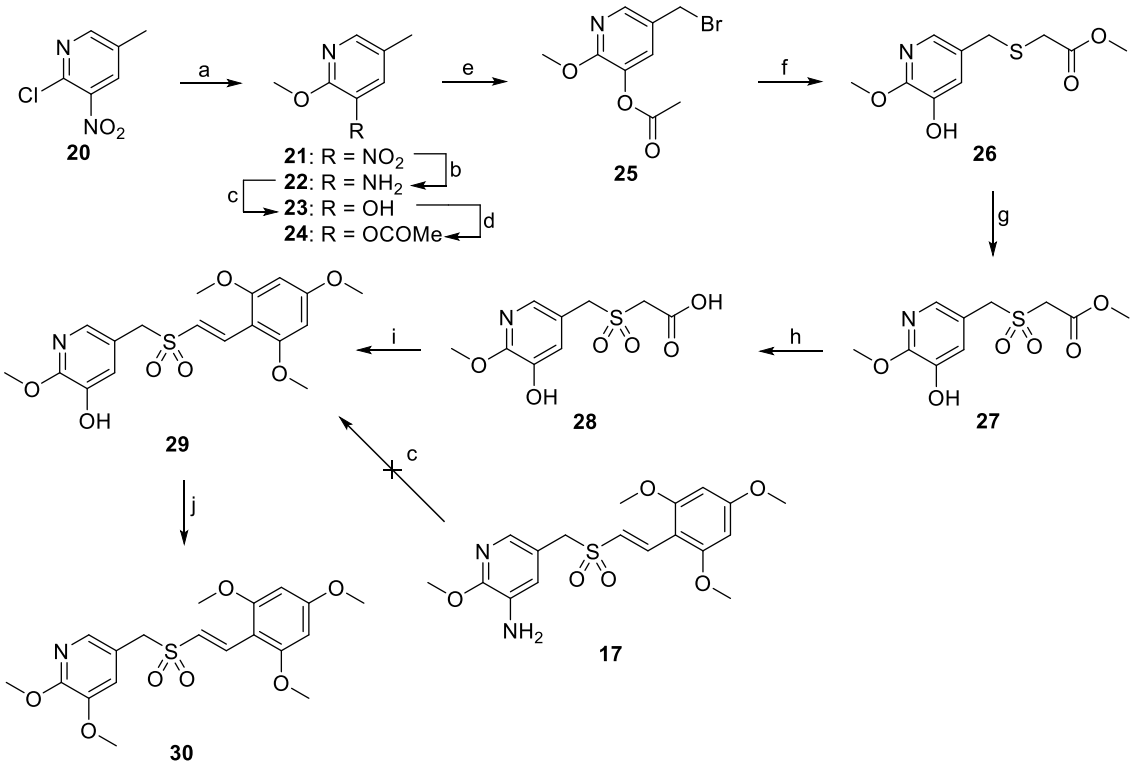
Figure 2.3: Proposed decarboxylation mechanism of **14**.

2.2.2 Synthesis of (*E*)-2-methoxy-5-(((2,4,6-trimethoxystyryl)-sulfonyl)methyl)pyridin-3-ol analogues

The next part of the study involved the replacement of the amino group of **17** with a hydroxyl group. Both groups have the ability to form hydrogen bonds with a biological

target. Pharmaceutically, while primary amines may be susceptible to CYP450 catalysed oxidation *in vivo*, hydroxyl groups are significantly less susceptible to phase I metabolism. [223]

The synthesis of (*E*)-2-methoxy-5-(((2,4,6-trimethoxystyryl)sulfonyl)methyl)pyridin-3-ol **29** from **17** was initially attempted *via* the formation of a diazonium salt (**Figure 2.4**) using sodium nitrite in cold aqueous sulfuric acid (**Scheme 2.3**).[224] The addition of sodium nitrite results in the formation of the nitrosonium ion which reacts with the nucleophilic aromatic primary amine to form the diazonium salt. Substitution of the diazonium with a hydroxyl group can be conducted by simply heating the reaction mixture, giving the phenol. However, the reaction failed. Consequently, compound **29** was synthesised using the procedure outlined in **Scheme 2.3**. Commercially available 2-chloro-5-methyl-3-nitropyridine **20** was reacted with sodium methoxide in methanol, affording 2-methoxy-5-methyl-3-nitropyridine **21** in 96% yield. Reduction of the nitro group of **21** using hydrogen gas in the presence of 10% palladium on carbon gave 2-methoxy-5-methylpyridin-3-amine **22** in 94% yield. Conversion of **22** to a diazonium salt using sodium nitrite in 10% sulfuric acid solution,[224] followed by hydrolysis gave 2-methoxy-5-methylpyridin-3-ol **23** in 81% yield. Protection of the hydroxyl group was warranted to prevent it from reacting with NBS during the Wohl-Ziegler bromination in the next step as well as the formed bromomethyl compound. The hydroxyl group of **23** was therefore protected using acetyl anhydride in the presence of pyridine,[225] giving 2-methoxy-5-methylpyridin-3-yl acetate **24** in quantitative yield.



Scheme 2.3: Reagents and conditions: (a) NaOMe, MeOH, reflux, 2 h, 96%; (b) H_2, 10% Pd/C, MeOH, rt, 4 h, 94%; (c) $NaNO_2$, H_2SO_4, H_2O, 0 °C for 30 min, 70 °C for 1 h, 81%; (d) Ac_2O, C_5H_5N, rt, 5 h, 100%; (e) NBS, AIBN, CH_2Cl_2, reflux, 42 h, 47%; (f) methyl thioglycolate, Na_2CO_3, MeOH, rt, 2 h, 84%; (g) 30% H_2O_2, CH_3CO_2H, 50 °C, 4 h, 83%; (h) Na_2CO_3, H_2O, MeOH, rt, 18 h, 94%; (i) 2,4,6-trimethoxybenzaldehyde **15**, benzoic acid, piperidine, toluene, reflux, 2 h, 41%; (j) MeI, K_2CO_3, DMF, rt, 12 h, 65%.

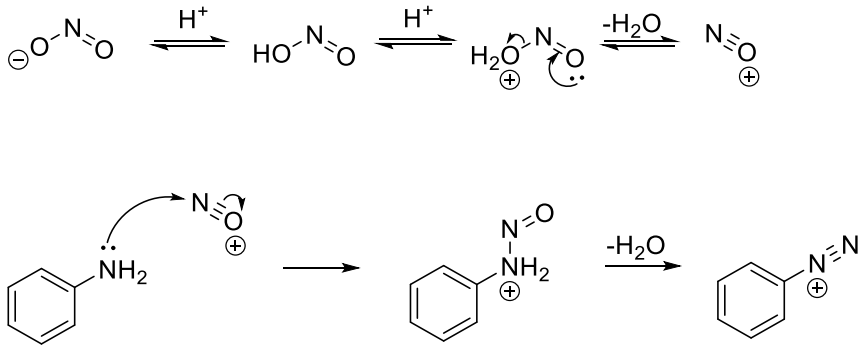


Figure 2.4: Mechanism of formation of the diazonium salt from aniline using sodium nitrite.

The Wohl-Ziegler bromination reaction in carbon tetrachloride follows a free radical mechanism (**Figure 2.5**). Due to its non-polar nature and the low solubility of NBS in carbon tetrachloride, the reaction maintains a low concentration of bromine which

facilitates mono-bromination of a benzylic methyl group.[226] Succinimide, a by-product of this reaction that is insoluble in carbon tetracholoride, precipitates out which thus prevents it from further participating in the reaction. However due to the unavailability of carbon tetrachloride in Australia, a different solvent had to be selected. The Wohl-Ziegler bromination of **24** with NBS in the presence of 2,2′-azobis(2-methylpropionitrile (AIBN) was conducted, affording 5-(bromomethyl)-2-methoxypyridin-3-yl acetate **25** in 47% yield. As the isotopic abundance of ^{79}Br and ^{81}Br are known to be similar, two peaks with similar heights at 259.9817 and 261.9795 *m/z* were present in the mass spectrum of **25**, which confirms the presence of a bromine in the molecule. ^{1}H NMR analysis of **25** further confirmed the mono-bromination of the methyl group of the pyridine ring with the singlet at 4.45 ppm (2H) corresponding to the two protons of the brominated methyl while singlets at 2.33 (3H) and 3.97 ppm (3H) correspond to the protons of the acetate and methoxy groups, respectively. The coupling constant of the doublets at 7.40 and 8.03 ppm (J = 2.0 & 2.5 Hz) confirmed the meta coupling of the pyridine protons.

Nucleophilic substitution of **25** with methyl 2-mercaptoacetate and concurrent deprotection in the presence of potassium carbonate afforded methyl 2-(((5-hydroxy-6-methoxypyridin-3-yl)methyl)thio)acetate **26** in 84% yield. Oxidation of **26** using 30% hydrogen peroxide in glacial acetic acid gave methyl 2-(((5-hydroxy-6-methoxypyridin-3-yl)methyl)sulfonyl)acetate **27** in 83% yield. Compound **27** was hydrolysed using sodium carbonate in a mixture of methanol and water, giving 2-(((5-hydroxy-6-methoxypyridin-3-yl)methyl)sulfonyl)acetic acid **28** in 94% yield. Coupling of **28** with 2,4,6-trimethoxybenzaldehyde **15** *via* Verley-Doebner modification of the Knoevenagel condensation using a mixture of benzoic acid and piperidine in toluene afforded (*E*)-2-methoxy-5-(((2,4,6-trimethoxystyryl)sulfonyl)methyl)pyridin-3-ol **29** in 41% yield. To determine the importance of the hydrogen bond donating effect of the hydroxyl group, compound **29** was alkylated with methyl iodide to afford (*E*)-2,3-dimethoxy-5-(((2,4,6-trimethoxystyryl)sulfonyl)methyl)pyridine **30** in 65% yield.

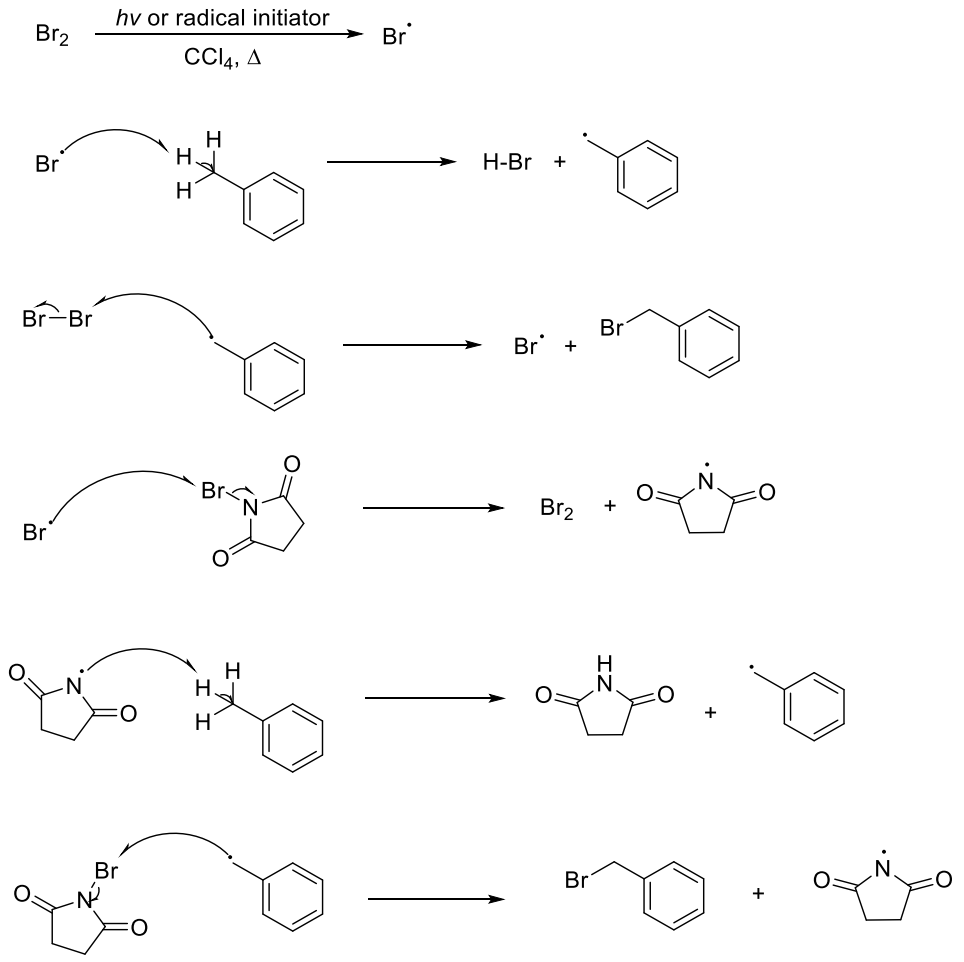


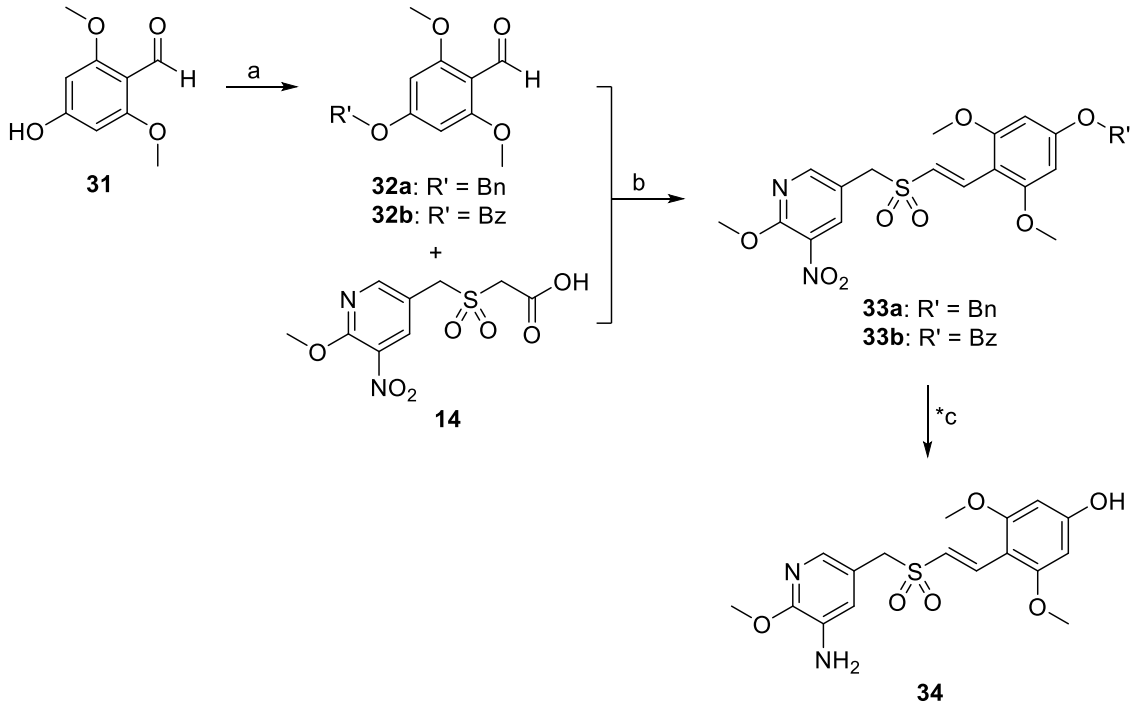
Figure 2.5: Proposed mechanism of Wohl-Ziegler bromination of benzylic CH_3.

2.2.3 **Modification at the R^3 position of the styryl ring**

While the 2,4,6-trimethoxy substitution of the styryl ring in **17** gives potent anticancer activity, it was unknown whether replacement of the methoxy groups at these positions would be tolerated. It was envisioned that replacement of the methoxy groups at these positions with phenolic hydroxy groups may reduce metabolism and increase polarity. As the primary amine at the R^1 position is necessary for optimum antiproliferative activity, this group was maintained at this position for the investigation of the R^3 position.

Replacement of the methoxy group at the 4-position with a hydroxyl group, compound **34**, was conducted as described in **Scheme 2.4**. Direct Verley-Doebner modification of the Knoevenagel condensation of **14** with 4-hydroxy-2,6-dimethoxybenzaldehyde **31**

was initially attempted, however the reaction failed to progress. This might be attributed to the formation of keto-enol tautomers (**Figure 2.6**), decreasing the reactivity of the carboxylic acid with the aldehyde. Thus, the use of a protecting group on the phenol was warranted to prevent it from forming keto-enol tautomers. The protection of **31** was initially attempted using a *t*-butyldimethylsilyl (TBS), a group that is commonly used for the protection of alcohols and phenols; however, the reaction failed to form the desired product due to its poor stability under silica purification.

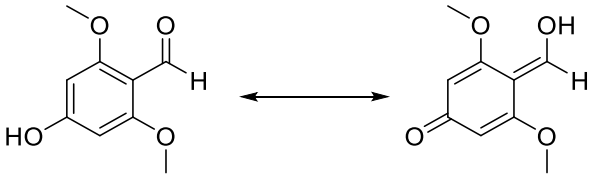


Scheme 2.4: Reagents and conditions: (a) **32a**: Benzyl bromide, K_2CO_3, DMF, rt, 3 h, 82%; **32b**: Benzoyl chloride, Et_3N, EtOAc, rt, 12 h, 39%; (b) benzoic acid, piperidine, toluene, reflux, 2 h, 49-58%; (c) *only for reduction of **33b**, Fe, MeOH/CH_3CO_2H (1:1), 50 °C, 2 h, 20%.

The second protecting group employed was the benzyl protecting group that is stable in basic conditions and mild acidic conditions.[225] The benzyl protecting group was attached to **31** using benzyl bromide and potassium carbonate in DMF to form 4-(benzyloxy)-2,6-dimethoxybenzaldehyde **32a** in 82 % yield. The benzyl protected **32a** was then reacted with **14** *via* Knoevenagel condensation to form (*E*)-5-(((4-(benzyloxy)-2,6-dimethoxystyryl)sulfonyl)methyl)-2-methoxy-3-nitropyridine **33a** in 49% yield. The nitro reduction of **33a** was then attempted using glacial acetic acid in methanol in the

presence of iron as a catalyst, though the use of acetic acid in the reaction was insufficient to remove the benzyl protecting group. While deprotection of this group conventionally involves the use of Pd/C in the presence of hydrogen, this condition was not employed for the deprotection of **33a** due to concerns of its effects on the double bond of the styryl group.

The third protecting group employed was the benzoate group, which is very stable in acidic conditions.[225] The benzoate protection group was attached to **31** using benzoyl chloride with triethylamine in ethyl acetate, giving 4-formyl-3,5-dimethoxyphenyl benzoate **32b** in 39% yield. Verley-Doebner modification of the Knoevenagel condensation of **32b** with **14** in the presence of benzoic acid and piperidine was conducted, yielding (*E*)-3,5-dimethoxy-4-(2-(((6-methoxy-5-nitropyridin-3-yl)methyl)sulfonyl)-vinyl)phenyl benzoate **33b** in 58% yield. Nitro reduction of **33b** using iron in a mixture of methanol and glacial acetic acid, followed by subsequent deprotection *via* saponification gave **34** in 20% yield. Isolation of **34** proved to be a challenging task due to its high polarity and pronounced streaking during flash column chromatography. Various solvent systems including ethyl acetate/dichloromethane (50% ethyl acetate in DCM) and acetone/dichloromethane (50% acetone in DCM) were trialled on TLC, but no appropriate R_f value (aiming for 0.2 - 0.3 R_f range) was achievable. Eventually, flash column chromatography of the reaction mixture using a mixture of 10% MeOH in DCM resulted in **34** in high purity (> 97%, Chapter 5).



31

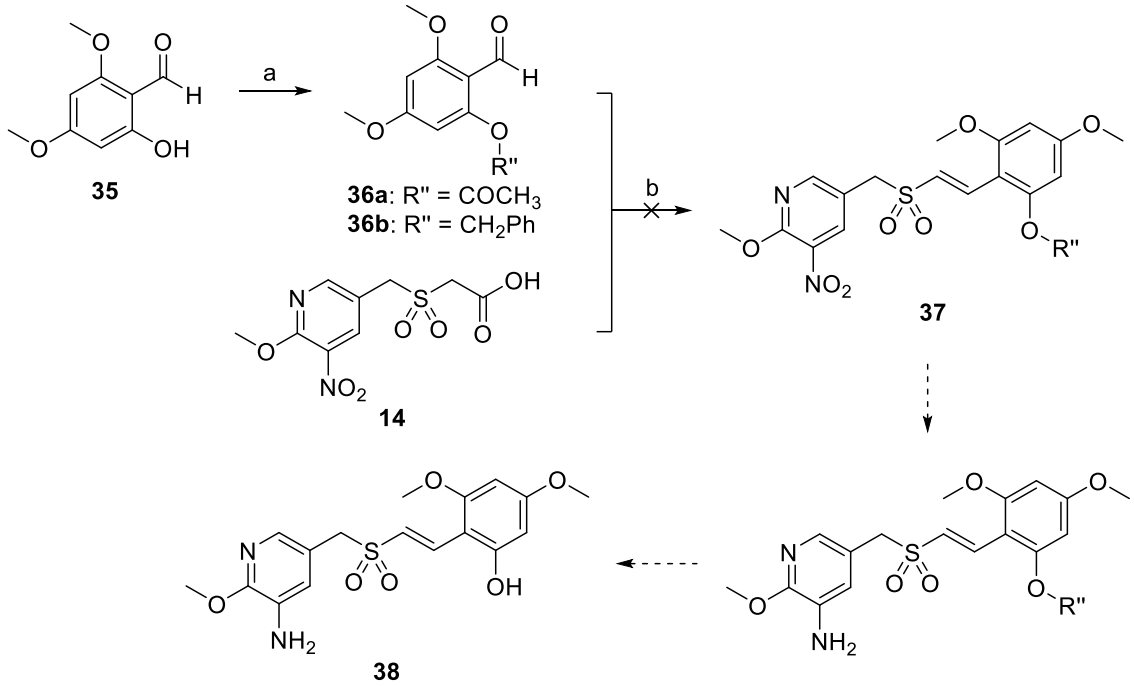
Figure 2.6: Chemical structures depicting the keto-enol tautomerism of 4-hydroxy-2,6-dimethoxybenzaldehyde **31**.

Subsequently, the synthesis of (*E*)-2-(2-(((5-amino-6-methoxypyridin-3-yl)methyl)sulfonyl)vinyl)-3,5-dimethoxyphenol **38** was attempted using the route outlined in **Scheme 2.5** to determine the effect of replacing the methoxy group at the 2-position of the styryl ring with a hydroxy group. Similar to the synthesis of **34**, the application of a protecting group was warranted as the condensation of **14** and 2-

hydroxy-4,6-dimethoxybenzaldehyde **35** was unsuccessful. The acetate protecting group was introduced by reacting **35** with acetyl chloride in the presence of triethylamine, giving 2-formyl-3,5-dimethoxyphenyl acetate **36a** in 70% yield. However, the condensation of **36a** with **14** in the presence of benzoic acid and piperidine failed to give the product due to the lability of the acetate group.

The next protecting group used was the benzyl protecting group which was introduced to **35** by reacting it with benzyl bromide in the presence of potassium carbonate and DMF, affording 2-(benzyloxy)-4,6-dimethoxybenzaldehyde **36b** in 82% yield. Despite the enhanced stability of the benzyl protecting group, the condensation of **36b** with **14** failed to generate the desired product, which might be attributed to the bulkiness of the benzyl group, conferring steric effects which prevent the formyl group from reacting with **14**. Therefore, a less bulky protecting group was needed to reduce the steric bulk conferred. While the methoxymethyl (MOM) protecting group would be an ideal protecting group due to its relatively small size, the protection of **35** with this group was not attempted due to the carcinogenicity of chloromethyl methyl ether which is used to introduce this group. The protection of **35** was therefore not pursued further.

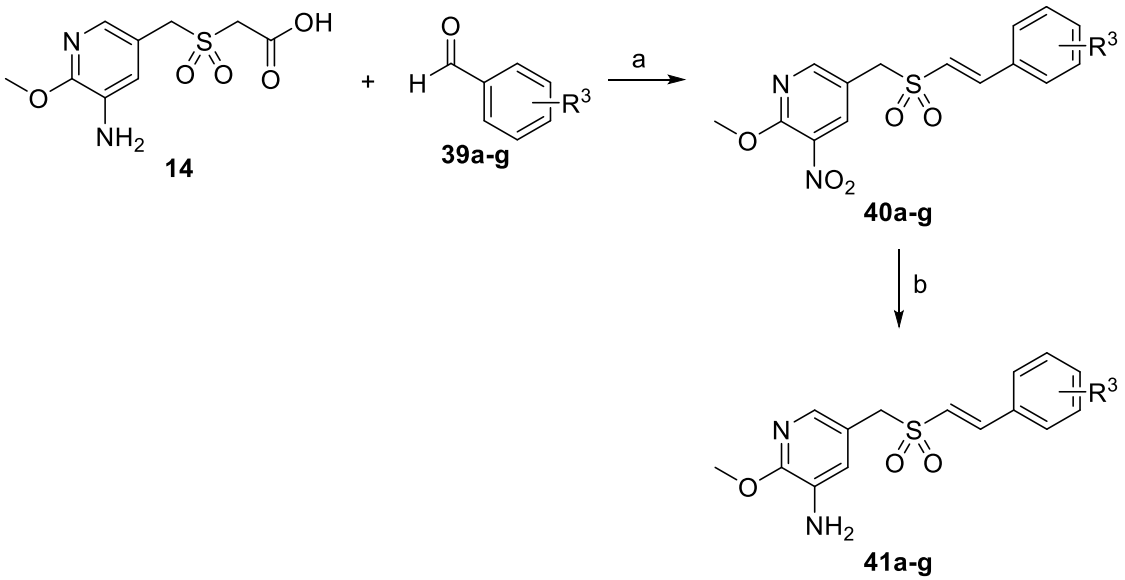
To further study the SAR of the phenyl moiety, a series of compounds with different substituents on the R^3 position were synthesised to determine the effects of these substituents on the activity and metabolic stability of the compounds. These analogues were synthesised as outlined in **Scheme 2.6**.



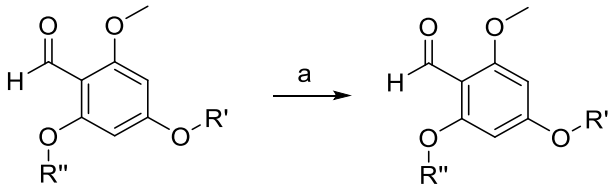
Scheme 2.5: Reagents and conditions: (a) **36a**: acetyl chloride, Et_3N, CH_2Cl_2, rt, 2 h, 70%; **36b**: benzyl bromide, K_2CO_3, DMF, rt, 3 h, 82% (b) benzoic acid, piperidine, toluene, reflux, 2 h.

The susceptibility of ether groups to O-dealkylation are highly dependent on the chain length of the alkyl group attached to oxygen, with longer chain lengths having less susceptibility compared to O-methyl groups which are highly susceptible.[227-229] Therefore, replacement of the methoxy group either at the 2 or 4-positions with an ethoxy group was conducted to determine its effects on the metabolic stability of the compounds. Compounds 4-ethoxy-2,6-dimethoxy-benzaldehyde **39a** and 2-ethoxy-4,6-dimethoxybenzaldehyde **39b** were synthesised as outlined in **Scheme 2.7**. Alkylation of **31** and **35** with ethyl iodide in the presence of potassium carbonate and DMF at room temperature yielded compounds **39a** (87% yield) and **39b** (89% yield) respectively. Coupling of **4** with **39a-g** *via* Knoevenagel condensation in the presence of benzoic acid and piperidine afforded **40a-g** (35-76% yield), which were subsequently reduced using iron in a mixture of acetic acid and methanol to give **41a-g** (21-87% yield). The poor yield obtained for **41g** (21% yield) is attributed to difficulties in purifying the extracted residue. During the flash column chromatography of **41g**, pronounced streaking developed when the solvent polarity was ramped, leading to poor isolation of the

compound. Further purification of the isolates *via* recrystallization was necessary to acquire the pure product.



Scheme 2.6: Reagents and conditions: (a) benzoic acid, piperidine, toluene, reflux, 2 h, 35-76%; (b) Fe, MeOH/CH_3CO_2H (2:1), 50 °C, 2 h, 21-87%.



Scheme 2.7: Reagents and conditions: (a) EtI, K_2CO_3, DMF, rt, 12-15 h, 87-89%.

2.3 Evaluation of antiproliferative activity and structure-activity relationship analysis

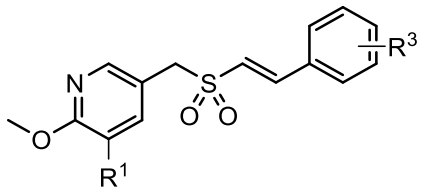
Antiproliferative activity of the synthesised compounds was determined using the 3-(4,5-dimethyl-2-thiazolyl)-2,5-diphenyl-2H-tetrazolium bromide (MTT) assay. MTT is metabolized *via* reduction in the cells to form formazan, which is a purple and insoluble compound. As the amount of MTT converted to formazan is dependent on the number of viable cells, this assay can be used to determine the cytotoxic potency of anticancer agents. The MTT assay can also be used to determine toxic effects of the drug on normal cell lines.

The anti-proliferative activity of compounds was examined in colorectal carcinoma (HCT-116), breast carcinoma (MCF-7), and ovarian carcinoma (A2780) cell lines, with ON01910 being used as a positive control. The MTT assay results are summarized in **Table 2.1**. In the (*E*)-2-methoxy-5-(((2,4,6-trimethoxystyryl)sulfonyl)methyl)pyridine series of compounds (R^3 = 2,4,6-OMe), the antiproliferative activity of a particular compound is highly dependent on the substituent at the 3-position (R^1) of the pyridine ring. While **16** (R^1 = NO_2, R^3 = 2,4,6-OMe) was found to have mediocre antiproliferative activity (GI_{50} = 5.22-7.43 μM), reduction of the nitro group to form **17** (R^1 = NH_2, R^3 = 2,4,6-OMe) resulted in significantly enhanced activity with GI_{50} = 5-6 nM against all three cell lines. The high potency of **17** was in line with the potency of the (*E*)-styrylbenzylsulfone derivative ON01500 (*vide supra*, section 1.5.1).

Replacement of the amino group with a methylsulfonamide as in **18a** (R^1 = $NHSO_2Me$, R^3 = 2,4,6-OMe) resulted in modest antiproliferative activity (GI_{50} = 0.317-0.780 μM), though a bulkier alkyl group attached to the sulfonamide as in **18b** (R^1 = $NHSO_2Et$, R^3 = 2,4,6-OMe) and **18c** (R^1 = $NHSO_2$*n*-Pr, R^3 = 2,4,6-OMe) abolished antiproliferative activity. Substitution of the amino group with an acetamide as in **18d** (R^1 = NHCOMe, R^3 = 2,4,6-OMe) resulted in a significant reduction in antiproliferative activity (GI_{50} = 7.095-8.219 μM). Both the ethyl glycinate **18e** and glycine **18f** derivatives displayed modest antiproliferative activity (GI_{50} = 0.376-0.940 μM). Compound **18f** was found to be less active than its analogue ON01910 (GI_{50} = 0.050-0.070 μM), which may be potentially due to an intramolecular interaction of the glycine group with the N of the pyridine ring, potentially reducing its binding to the receptor and consequently reducing its activity.

The importance of the primary amine at the 3-position of the pyridine ring in providing optimum activity was demonstrated with **17,** but a hydroxyl group at the position as in **29** (R^1 = OH, R^3 = 2,4,6-OMe) decreased the activity (GI_{50} = 0.048-0.051 μM). In contrast, their (*E*)-styrylbenzylsulfone counterparts ON01500 and ON13100 (*vide supra*, section 1.5.1) have similar potencies. Additionally, replacement of the hydroxyl group with a methoxy group as in **30** (R^1 = OMe, R^3 = 2,4,6-OMe) significantly decreased the antiproliferative acitivity of the compound, reinforcing that the hydrogen bond donating ability of the hydroxyl and amino groups are necessary for activity.

Table 2.1: Structure and biological activity of (*E*)-3-((styrylsulfonyl)methyl)-pyridines[a]



Code	Structure		Antiproliferative activity, GI_{50} (μmol/L) ± sd		
	R^1	R^3	A2780	MCF-7	HCT-116
16	NO_2	2,4,6-OMe	7.210 ± 0.950	5.220 ± 0.160	7.430 ± 0.280
17	NH_2	2,4,6-OMe	0.005 ± 0.001	0.006 ± 0.001	0.005 ± 0.001
18a	$NHSO_2Me$	2,4,6-OMe	0.317 ± 0.179	0.780 ± 0.041	0.570 ± 0.023
18b	$NHSO_2Et$	2,4,6-OMe	>10	>10	>10
18c	$NHSO_2$(*n*-Pr)	2,4,6-OMe	>10	>10	>10
18d	NHCOMe	2,4,6-OMe	7.095 ± 0.962	7.500 ± 1.060	8.219 ± 0.473
18e	$NHCH_2CO_2Et$	2,4,6-OMe	0.409 ± 0.133	0.940 ± 0.010	0.517 ± 0.078
18f	$NHCH_2CO_2H$	2,4,6-OMe	0.376 ± 0.093	-	0.410 ± 0.099
29	OH	2,4,6-OMe	0.051 ± 0.013	-	0.048 ± 0.006
30	OMe	2,4,6-OMe	0.926 ± 0.113	-	2.814 ± 0.295
34	NH_2	2,6-OMe, 4-OH	0.424 ± 0.101	-	0.668 ± 0.027
41a	NH_2	2,6-OMe, 4-OEt	0.052 ± 0.009	-	0.083 ± 0.003
41b	NH_2	2-OEt, 4,6-OMe	0.035 ± 0.006	-	0.039 ± 0.014
41c	NH_2	2,6-OMe	0.440 ± 0.018	-	0.662 ± 0.065
41d	NH_2	3,5-OMe	> 10	-	> 10
41e	NH_2	4-OMe	> 10	-	> 10
41f	NH_2	2,4-OMe	0.572 ± 0.128	-	3.974 ± 0.276
41g	NH_2	2,4,6-F	> 10	-	> 10
ON01910	-	-	0.062 ± 0.004	0.050 ± 0.010	0.070 ± 0.003

[a] Performed by Julian Adams

The methoxy group at the 4-position of the styryl ring of **17** seemed essential for optimum activity as its replacement with a hydroxyl (**34**)(GI_{50} = 0.424-0.668 μM) or ethoxy (**41a**)(GI_{50} = 0.052-0.083 μM) resulted in a decrease in antiproliferative activity. Furthermore, while replacement of the 2,4,6-trimethoxy in ON01500 with a 2,6-dimethoxy moiety was tolerated (*vide supra*, section 1.5.1), the same replacement

conducted on **17** was poorly tolerated as the activity significantly decreased (GI_{50} = 0.440-0.662 μM).

In the study of the 2-position of the styryl ring, the replacement of the methoxy group with an ethoxy group as in **41b** ($R^1 = NH_2$, R^3 = 2-OEt, 4,6-OMe) was found to yield compounds with potent antiproliferative activity (GI_{50} = 0.035-0.039 μM). However, substitution of the methoxy at this position with a hydrogen as in **41f** ($R^1 = NH_2$, R^3 = 2,4-OMe) resulted in a significant decrease in activity (GI_{50} = 0.572-3.974 μM). This indicates that the presence of the electron donating methoxy or ethoxy groups at this position is required for potent antiproliferative activity.

It was therefore envisioned that removal of the methoxy group(s) on the styryl ring could be used to circumvent demethylation and therefore increase metabolic stability. However, replacement of the methoxy groups at the 2-, 4-, or 6-position with hydrogen resulted in a significant decrease in activity. Substitution of the methoxy groups at the 2- and 6-positions of the styryl ring as in compound **41e** ($R^1 = NH_2$, R^3 = 4-OMe) resulted in complete abolishment of the antiproliferative activity. The 3,5-dimethoxy analogue **41d** ($R^1 = NH_2$, R^3 = 3,5-OMe) was also found to be inactive, indicating that the 2,4,6-trimethoxystyryl moiety is required for optimum activity.

To further study the SAR of the compounds, **41g** ($R^1 = NH_2$, R^3 = 2,4,6-F) was synthesised to study the effect of replacing the electron donating methoxy group with the electron withdrawing fluoride group. The fluoride group has been tactically employed in the design of various drug molecules to mitigate metabolism.[215] However, substitution of the methoxy groups with fluoride as in **41g** resulted in complete abolishment of antiproliferative activity, indicating that the electron donating methoxy at the 2-, 4-and 6-positions of the styryl ring is required for activity.

Compounds **17** and **18a** were further tested against a panel of 15 human cancer cell lines including brain, breast, cervical, colon, ovarian, pancreatic, and prostate cancer cell lines. The results are summarized in **Table 2.2**. Compound **17** was found to be highly cytotoxic with GI_{50} = 0.001-0.014 μM, approximately 10-fold more potent than ON01910. Compound **18a** showed good activity with GI_{50} in a range of 0.317-0.875 μM, being ~100-fold less potent compared to **17**. Interestingly, **17** was found to be more potent against the PANC-1 pancreatic cancer cell line which is known to exhibit high

levels of PLK1.[230-231] Whether this is solely due to activity against PLK1 is currently unknown and further studies will need to be conducted to determine the targets affected by this compound. The compounds were further tested against the untransformed human lung fibroblast cell line WI-38. Despite their potent antiproliferative activities in cancer cell lines, these compounds exhibited low toxicity (GI_{50} >10 μM) against WI-38. This indicates that the compounds are highly selective for cancer cells compared to normal cells.

Table 2.2: Biological activity of 17, 18a and ON01910 against a panel of human cell lines[a]

Human cell lines		**Antiproliferative activity,[a] GI_{50} (μmol/L) ± sd**		
Origin	**Designation**	**17**	**18a**	**ON01910**
Brain	DAOY	0.004 ± 0.001	-	0.047 ± 0.004
	D283	0.005 ± 0.002	-	0.035 ± 0.011
	D458	0.003 ± 0.001	-	0.007 ± 0.001
Breast	MCF-7	0.006 ± 0.001	0.780 ± 0.041	0.050 ± 0.010
	MDA-MB231	0.006 ± 0.001	0.671 ± 0.056	0.057 ± 0.001
Cervical	Hela	0.004 ± 0.001	0.682 ± 0.112	0.012 ± 0.001
Colon	HCT-116	0.005 ± 0.001	0.570 ± 0.023	0.070 ± 0.003
	Colo205	0.004 ± 0.001	-	0.050 ± 0.004
	HT-29	0.014 ± 0.010	-	0.075 ± 0.019
	KM12	0.007 ± 0.001	-	0.058 ± 0.004
Ovarian	A2780	0.005 ± 0.004	0.317 ± 0.179	0.062 ± 0.004
Pancreatic	PANC-1	< 0.001	0.875 ± 0.274	0.039 ± 0.006
Prostate	LNCaP	0.003 ± 0.006	-	0.025 ± 0.003
	DU-145	0.005 ± 0.008	-	0.075 ± 0.006
	PC-3	0.008 ± 0.001	-	0.647 ± 0.011
Untransformed	WI-38	> 10	> 10	> 10

[a] Performed by Julian Adams

2.4 Microsomal stability assay

Prior to conducting pharmacokinetic studies, the metabolic stability of the compounds was assessed using rat liver microsomes. The method is detailed in section 5.7. Briefly, compounds were incubated with rat liver microsomes, and samples were collected at 15

minute intervals for 120 minutes. The concentration of compound remaining in these samples was quantified using liquid chromatography with tandem mass spectroscopy (LC/MS/MS) and the half-life was calculated.

Microsomal stability assays using rat liver microsomes were conducted on a selection of compounds exhibiting good antiproliferative activity, with the results summarized in **Table 2.3**.

Table 2.3: Metabolic stability of compounds in rat liver microsomes[a]

Compound code	Half-life, $t_{½}$ (min)[b]
17	20
18a	70
29	21
34	17
41a	10
41b	3
ON01910	>120

[a] Performed by Ben Noll
[b] Values are means of at least two replicates

Compound **17** exhibited mediocre metabolic stability with a half life of 20 minutes. The mediocre metabolic stability may be attributed to the presence of the methoxy groups which are prone to O-demethylation (**Figure 2.7**).[232] Recent studies conducted by Noll *et al*. in our laboratory (unpublished result) identified that demethylation of the methoxy group on the pyridine ring was identified as the major site of metabolism for **17**, with (*E*)-3-amino-5-(((2,4,6-trimethoxystyryl)sulfonyl)methyl)pyridin-2(1*H*)-one being proposed as the major metabolite formed (**Figure 2.8**).

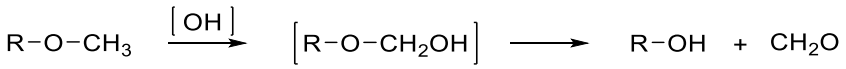


Figure 2.7: Mechanism of O-demethylation.[232]

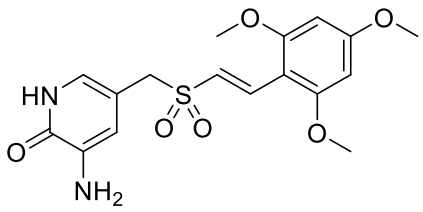


Figure 2.8: Proposed major metabolite of **17**.

In contrast, ON01910 was found to be highly stable in rat liver microsomes which may be due to the presence of the acetic acid solubilizing chain.[233] Metabolism by CYP450 is highly dependent on the polarity of the drug due to its hydrophobic substrate binding site that has a high affinity for lipophilic drug molecules.[234] One of the strategies that can be utilised to improve metabolic stability is by reducing the lipophilicity of the drug molecule, which can be conducted by introduction of solubilizing chains or replacement of hydrophobic moieties.[215, 235] The introduction of the methyl sulfonamide side group as in **18a** resulted in a significant increase in metabolic stability. This indicates that the introduction of polar side groups at the amino group on the pyridine ring is a viable strategy in improving the metabolic stability of the compound. However, the introduction of side groups on the amino also results in a significant decrease in anti-proliferative activity of the compound. Therefore, a suitable balance between activity and metabolic stability should be pursued.

Though it was initially envisioned that substitution of the methoxy group of the styryl ring with a hydroxyl group as in **34** would improve the metabolic stability of the compounds by increasing the polarity of the compound, the metabolic stability did not improve with this substitution ($t_{½}$ = 17 min). The presence of an ethoxy group in the structures of **41a** and **41b** also decreased the metabolic stability ($t_{½}$ = 3-10 min) of the compounds.

2.5 Caco-2 permeability assay

The Caco-2 monolayer permeability assay was conducted on the compounds to predict their permeability across the intestinal epithelium. The Caco-2 cell monolayer, which mimics the epithelial cells in the small intestines, allows the determination of the movement of drug molecules from the apical (A) to the basolateral (B) side and vice

versa. The apparent permeability coefficients (P_{app}) of the movement from A-B (P_{app}A-B) and B-A (P_{app}B-A) can then be used to obtain the efflux ratio.[236] The efflux ratio obtained can also illustrate the susceptibility of the compounds to P-gp due to the high expression of P-gp in the cell membrane of the Caco-2 cell line.[237]

The Caco-2 permeability assay results of **17** and **18a** are summarized in **Table 2.4**. Compound **17** was found to be highly permeable across the cell membrane, with a P_{app}A-B of 42.3 × 10^{-6} cm/s. The efflux ratio of the compound was also less than 1, indicating that the compounds have minimal susceptibility to active transport. In contrast, the methyl sulfonamide analogue **18a** was found to have a relatively high efflux ratio, with a value of 5.29 obtained.

Table 2.4: Caco-2 permeability of 17 and 18a[a]

Compound	17	18a
P_{app} A-B (10^{-6} cm/s)	42.3	8.9
P_{app} B-A (10^{-6} cm/s)	21.5	47.1
Efflux ratio	0.51	5.29

[a] Performed by Cyprotex (Macclesfield, UK)

Contrary to the impressive Caco-2 permeability of **17**, ON01910 was reported to have very poor Caco-2 permeability (efflux ratio ≥ 70),[198] explaining the poor bioavailability reported in clinical trials. Furthermore, concomitant administration of ON01910 with cyclosporine, a P-gp inhibitor, during the Caco-2 permeability assay resulted in a significant reduction in the efflux ratio (efflux ratio = 4.3). This indicates that ON01910 is highly susceptible to the effects of P-gp, limiting the potential of ON01910 as an oral drug and against multidrug resistant cancers expressing P-gp.

2.6 **Pharmacokinetic studies**

Pharmacokinetic properties of **17** were obtained in rats following an intravenous (IV) dose of 10 mg/kg or an oral dose of 40 mg/kg. The plasma concentrations were measured using LC/MS and the results were used to calculate the pharmacokinetic parameters listed in **Table 2.5**.

Following IV administration, the elimination half-life was found to be significantly longer ($t_{½}$ = 2.3 hours) than that of ON01910 ($t_{½}$ = 24-28 min).[207] Compound **17** also

exhibited superior pharmacokinetic properties with high oral bioavailability ($F_{0\text{-}t}$ = 27%) to ON01910 ($F_{0\text{-}t}$ = 10-14%).[198]

Although the $AUC_{0\text{-}t}$ of both oral and IV doses were found to be similar, the half-life of **17** was found to be significantly longer than its IV profile. As the oral dose is higher (40 mg/kg) than the IV dose (10 mg/kg), the slow absorption of the compound counteracts the elimination of the drug which results in a slow decrease in plasma concentration.[238]

Table 2.5: Rat pharmacokinetic comparison of IV and orally administered 17[a]

Dose	Cmax (μM)	$AUC_{0\text{-}t}$ (μM·h)	Half-life $t_{½}$ (h)	Bioavailability $F_{0\text{-}t}$ (%)
IV 10 mg/kg	26.4	24.6	2.3	N/A
Oral 40 mg/kg	3.0	26.1	61.8	26.5

[a] Performed by Peng Li and Longjin Zhong

2.7 Conclusion

A series of (*E*)-2-((styrylsulfonyl)methyl)pyridine derivatives were synthesised. A selection of substituents were incorporated at the R^1 and R^3 positions to assess the effect on their anti-cancer activity. SAR analysis of the compounds indicates that a primary amino group and 2,4,6-trimethoxy moiety at the R^1 and R^3 positions respectively are necessary for optimum antiproliferative activity.

Thus, **17** exhibited the highest potency with broad-spectrum activity against a panel of human cancer cell lines. Compound **17** was found to possess good microsomal stability and Caco-2 permeability. The pharmacokinetic studies on rats confirmed its superior drug properties compared to ON01910.

3 Design, synthesis and evaluation of (*E*)-2-((styrylsulfonyl)methyl)-pyridine

3.1 Introduction

The attention of this research subsequently shifted to the development of (*E*)-2-((styrylsulfonyl)methyl)pyridine analogues. Changing the nitrogen position of the pyridine ring from the X^1 to the X^2 position was conducted to compare the SAR and pharmaceutical property differences between the (*E*)-2-((styrylsulfonyl)methyl)-pyridine and (*E*)-3-((styrylsulfonyl)methyl)pyridine series. In addition to investigating the R^1 and R^3 positions as highlighted in chapter 2, the SAR of the R^2 position was also studied in this series of analogues.

3.2 Chemistry

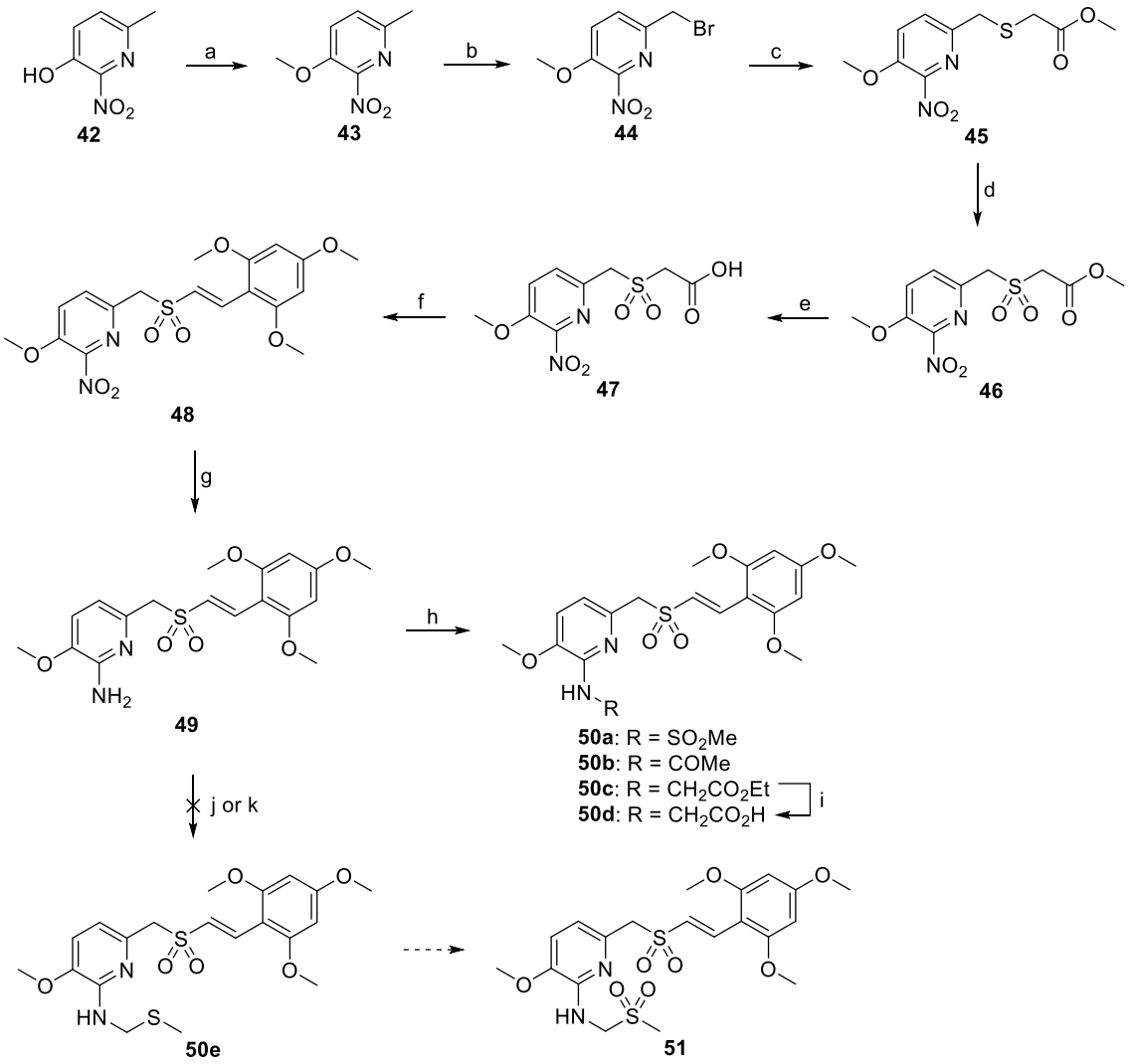
3.2.1 Synthesis of (*E*)-3-methoxy-6-(((2,4,6-trimethoxystyryl)-sulfonyl)methyl)pyridin-2-amine analogues

The synthesis of (*E*)-3-methoxy-6-(((2,4,6-trimethoxystyryl)sulfonyl)methyl)pyridin-2-amine **49** is outlined in **Scheme 3.1**. 6-Methyl-2-nitropyridin-3-ol **42** was reacted with iodomethane in the presence of potassium carbonate to give 3-methoxy-6-methyl-2-nitropyridine **43** in 96% yield.

The bromination of **43** was attempted using dichloromethane or chloroform as the solvent. [239-242] However, the reaction failed to progress. The position of the N of the pyridine ring which is *ortho* to the methyl may reduce the electron density at the methyl *via* inductive effects, decreasing the reactivity of the methyl group towards free radicals. Several studies have reported the use of microwave irradiation in Wohl-Ziegler bromination, with the attainment of significantly improved reaction times.[243-244] Therefore, a mixture of **43,** NBS and benzoyl peroxide in acetonitrile was heated at 120 °C under microwave irradiation for 45 minutes, affording 6-(bromomethyl)-3-methoxy-2-nitropyridine **44** in 42% yield.

Nucleophilic substitution of **44** with methyl thioglycolate in the presence of potassium carbonate gave methyl 2-(((5-methoxy-6-nitropyridin-2-yl)methyl)thio)acetate **45** in 91% yield. Oxidation of the thioether in the presence of 30% hydrogen peroxide in glacial acetic acid afforded methyl 2-(((5-methoxy-6-nitropyridin-2-yl)methyl)sulfonyl)acetate **46** in 98% yield. Saponification of **46** using potassium carbonate in a mixture of water and methanol yielded its carboxylic acid 2-(((5-methoxy-6-nitropyridin-2-yl)methyl)sulfonyl)acetic acid **47** in quantitative yield. Compound **47** was reacted with 2,4,6-trimethoxybenzaldehyde *via* Verley-Doebner modification of Knoevenagel condensation in the presence of benzoic acid and piperidine in toluene, giving (*E*)-3-methoxy-2-nitro-6-(((2,4,6-trimethoxystyryl)-sulfonyl)methyl)pyridine **48** in 31% yield. In the ^{1}H NMR spectrum of **48,** the coupling constants of doublets at 7.14 and 7.55 ppm (J = 15.5 & 16.0 Hz) correspond to the *E*-configuration of the double bond. Ortho coupling of the pyridine proton is also demonstrated by the coupling constants of the doublets at 7.82 and 8.02 ppm (J = 8.5 & 9.0 Hz). Singlets at 4.66 (2H) and 6.30 ppm (2H) correspond to the methylene and styryl ring protons respectively. Meanwhile, singlets at 3.85 (9H) and 3.98 ppm (3H) correspond to the methoxy groups. In the ^{13}C NMR analysis of **48**, the number of signals in the spectrum tallies with the total number of carbons in the molecule. High resolution mass spectrometry (HRMS) analysis of **48** confirmed the molecular mass of the compound (*m/z* 425.1013 $[M+H]^{+}$).

Reduction of **48** was conducted using iron powder in a mixture of glacial acetic acid and methanol, affording (*E*)-3-methoxy-6-(((2,4,6-trimethoxystyryl)sulfonyl)methyl)-pyridin-2-amine **49** in 94% yield.



Scheme 3.1*:* Reagents and conditions: (a) MeI, K_2CO_3, acetone/H_2O (5:2), reflux, 24 h, 96%; (b) NBS, benzoyl peroxide, MeCN, microwave, 120 °C, 45 min, 42%; (c) methyl thioglycolate, K_2CO_3, MeOH, 0 °C to rt, 12 h, 91%; (d) 30% H_2O_2, CH_3CO_2H, 50 °C, 12 h, 98%; (e) K_2CO_3, MeOH/H_2O (3:2), rt, 12 h, 100%; (f) 2,4,6-trimethoxybenzaldehyde **15**, benzoic acid, piperidine, toluene, reflux, 4 h, 31%; (g) Fe, MeOH/CH_3CO_2H (2:1), 50 °C, 2 h, 94%; (h) **50a**: methanesulfonyl chloride, pyridine, 0 °C to rt, 14 h, 50%; **50b**: acetyl chloride, pyridine, rt, 2 h, 42%; **50c**: ethyl bromoacetate, NaH, DMF, 50 °C, 48 h, 25%; (i) NaOH, MeOH/H_2O (1:2), rt, 18 h, 74%; (j) chloromethyl methyl sulfide, NaH, DMF, 0 °C to rt, 1 h; (k) chloromethyl methyl sulfide, *n*-Butyllithium, DMF, 0 °C to rt, 1 h.

To further study the SAR at this position, several substituents were selected and introduced to the amino group. Sulfonation of **49** with methanesulfonyl chloride was

effective using pyridine as both base and solvent, yielding (*E*)-*N*-(3-methoxy-6-(((2,4,6-trimethoxystyryl)sulfonyl)methyl)pyridin-2-yl)methanesulfonamide **50a** in 50% yield. Acylation of **49** with acetyl chloride in pyridine afforded **50b** (*E*)-*N*-(3-methoxy-6-(((2,4,6-trimethoxystyryl)sulfonyl)methyl)pyridin-2-yl)acetamide in 42% yield.

Alkylation of **49** with ethyl bromoacetate in DMF with different bases including potassium carbonate, caesium carbonate and sodium hydroxide failed to generate ethyl (*E*)-(3-methoxy-6-(((2,4,6-trimethoxystyryl)sulfonyl)methyl)pyridin-2-yl)glycinate **50c**. The reaction was subsequently performed in the presence of sodium hydride, with the reaction mixture stirred at 50 °C for 48 h affording **50c** in 25% yield. Hydrolysis of **50c** in the presence of sodium hydroxide in a mixture of methanol/water gave (*E*)-(3-methoxy-6-(((2,4,6-trimethoxystyryl)sulfonyl)methyl)pyridin-2-yl)glycine **50d** in 74% yield.

To determine the effect of adding a methylene bridge between the amine and the methane sulfonyl group in **50a**, the synthesis of (*E*)-3-methoxy-*N*-((methylthio)methyl)-6-(((2,4,6-trimethoxystyryl)sulfonyl)methyl)pyridin-2-amine **50e** and (*E*)-3-methoxy-*N*-((methylsulfonyl)methyl)-6-(((2,4,6-trimethoxystyryl)sulfonyl)methyl)pyridin-2-amine **51** was attempted. Treatment of **49** with chloromethyl methyl sulfide in the presence of sodium hydride in DMF was conducted. However, the reaction failed to produce the desired product. The reaction was subsequently repeated using a stronger base *n*-butyllithium, although the reaction still failed to generate the desired product.

The poor reactivity of the amino group of **49** is due to its low nucleophilicity. In 2- and 4-aminopyridines, the electron density of the amino group is reduced due to delocalization of the electron pair *via* resonance.[245] Meanwhile, the nucleophilicity of C4 and C6, and heteroatom N of the pyridine ring is increased. Furthermore, studies on 2-aminopyridines have demonstrated the acidity of the amino group, as the formed anions are stabilized by resonance (**Figure 3.1**).[246-248] In contrast, the amino of 3-aminopyridines resemble the amino of aniline as the presence of the heteroatom N of the pyridine ring has minimal effect on the electron density of the meta amino group. This explains the higher reactivity of the amino group in **17** compared to that of **49**.

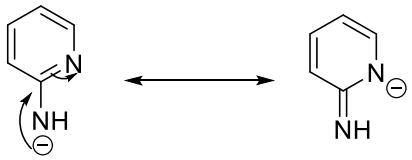


Figure 3.1: Stabilization of the anion of 2-aminopyridine *via* resonance.

3.2.2 Modification at the R^2 position of the pyridine ring

Whilst the methoxy group at the R^2 position gives potent antiproliferative activity, it was unknown whether replacement of the methoxy group with other side groups could be tolerated. Therefore, a variety of substituents were introduced at this position to study its SAR and to determine whether improvements to the metabolic stability could be obtained.

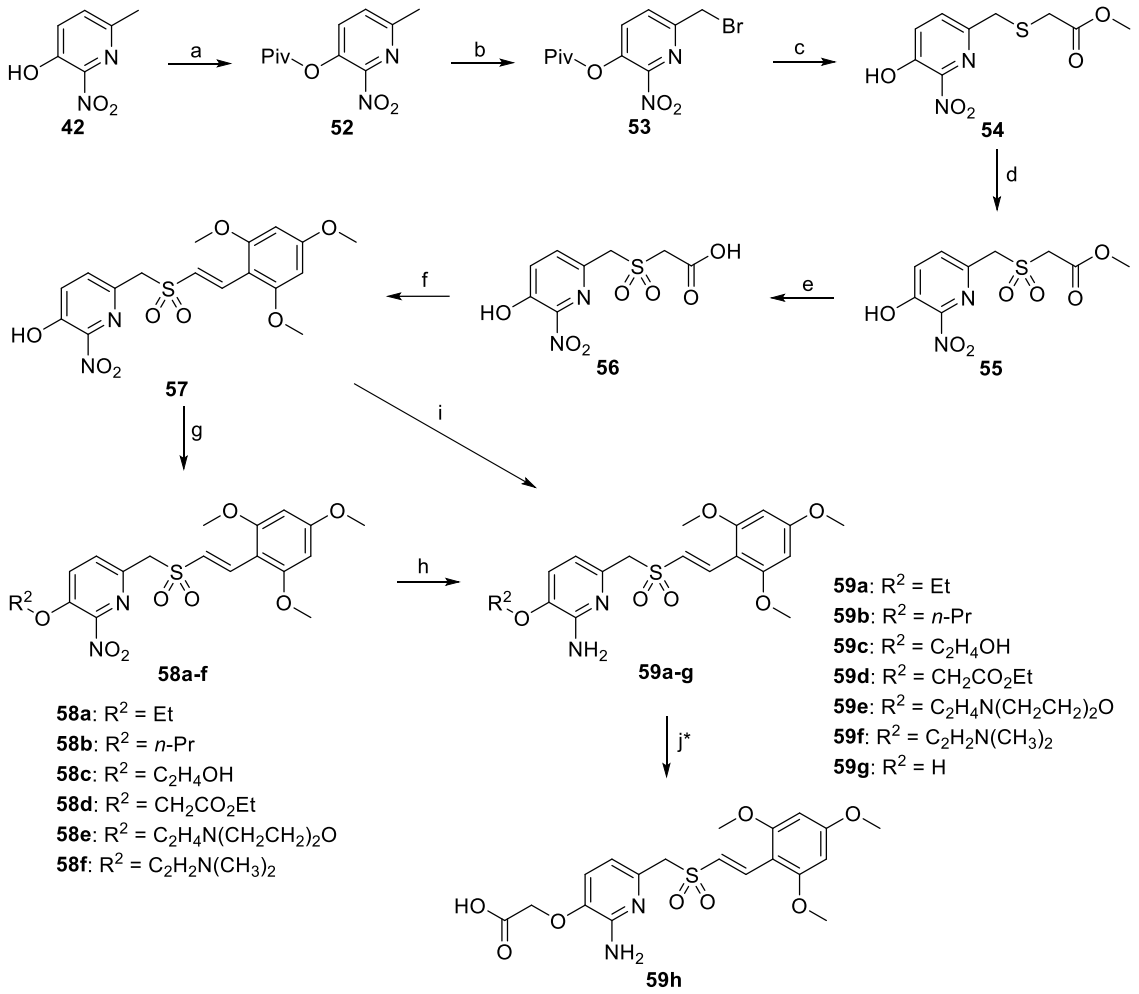
Synthesis of the analogues of **49**, i.e. **59a-h** is outlined in **Scheme 3.2**. As the bromination of the methyl group was necessary for the subsequent attachment of the methyl thioglycolate chain, the hydroxyl group of **52** was protected to prevent it from reacting with the following bromo compound. The first protecting group used was the trityl protecting group which was attached using trityl chloride. However, the protecting group was cleaved off during purification with silica flash column chromatography. The next protecting group that was employed was the benzoyl protecting group. The benzoyl protecting group was attached using benzoyl chloride, using triethylamine and DMAP as the base and catalyst respectively. The formed benzoate was then reacted with NBS in the presence of AIBN in acetonitrile. However, the reaction failed to produce the desired compound which may be due to the electron withdrawing effect of the benzoate group. The electron withdrawing effect of the benzoate decreases the electron density of the methyl side group, thus decreasing its reactivity with the electrophilic bromine free radical.

The pivalate group was subsequently selected due to the presence of the electron donating isobutane moiety. The pivalate group was attached to the hydroxyl using pivaloyl chloride in dichloromethane, with triethylamine as the base, affording 6-methyl-2-nitropyridin-3-yl pivalate **52** in quantitative yield. Unlike the bromination of **53** which was conducted under microwave irradiation, the bromination of **52** was conducted under reflux in acetonitrile to prevent side reactions occurring on the

protecting group. Wohl-Ziegler bromination of **52** with NBS in the presence of AIBN gave **53**, which was subsequently reacted with methyl thioglycolate in the presence of potassium carbonate to afford the thioether methyl 2-(((5-hydroxy-6-nitropyridin-2-yl)methyl)thio)acetate **54** in 69% yield. Oxidation of **54** with 30% hydrogen peroxide in glacial acetic acid afforded methyl 2-(((5-hydroxy-6-nitropyridin-2-yl)methyl)-sulfonyl)acetate **55** in 88% yield, which was subsequently hydrolysed using sodium carbonate in a mixture of water and methanol to give the carboxylic acid 2-(((5-hydroxy-6-nitropyridin-2-yl)methyl)sulfonyl)acetic acid **56** in 93% yield. Knoevenagel condensation of **56** with 2,4,6-trimethoxybenzaldehyde **15** in the presence of benzoic acid and piperidine gave (*E*)-2-nitro-6-(((2,4,6-trimethoxystyryl)sulfonyl)methyl)-pyridin-3-ol **57** in 43%.

The successful synthesis of **57** allowed the attachment of a variety of side groups, enabling the further study of the effects of attaching different side groups to the R^2 position.

Alkylation of **57** with ethyl iodide, *n*-propyl iodide, 2-bromoethanol, ethyl bromoacetate, 4-(2-chloroethyl)morpholine hydrochloride, and 2-chloro-*N*,*N*-dimethylethylamine hydrochloride in the presence of potassium carbonate yielded **58a** (R^2 = Et), **58b** (R^2 = *n*-Pr), **58c** (R^2 = C_2H_4OH), **58d** (R^2 = CH_2CO_2Et), **58e** (R^2 = $C_2H_4N(CH_2CH_2)_2O$), and **58f** (R^2 = $C_2H_4N(CH_3)_2$), which were subsequently reduced using iron in a mixture of acetic acid and methanol to give the amines **59a-f**. However, the reduction of **58d** using these conditions resulted in a mixture of **59d** (R^2 = CH_2CO_2Et) and the carboxylic acid **59h** (R^2 = CH_2CO_2H), indicating the instability of the acetate group under these conditions. Attempts to purify this mixture *via* flash column chromatography failed due to the similarity of the R_f values of **59d** and **59h** in a variety of solvent systems. Therefore, the mixture was subsequently stirred with sodium hydroxide in a mixture of water and methanol, affording (*E*)-2-((2-amino-6-(((2,4,6-trimethoxystyryl)sulfonyl)methyl)-pyridin-3-yl)oxy)acetic acid **59h** solely in 48% yield.



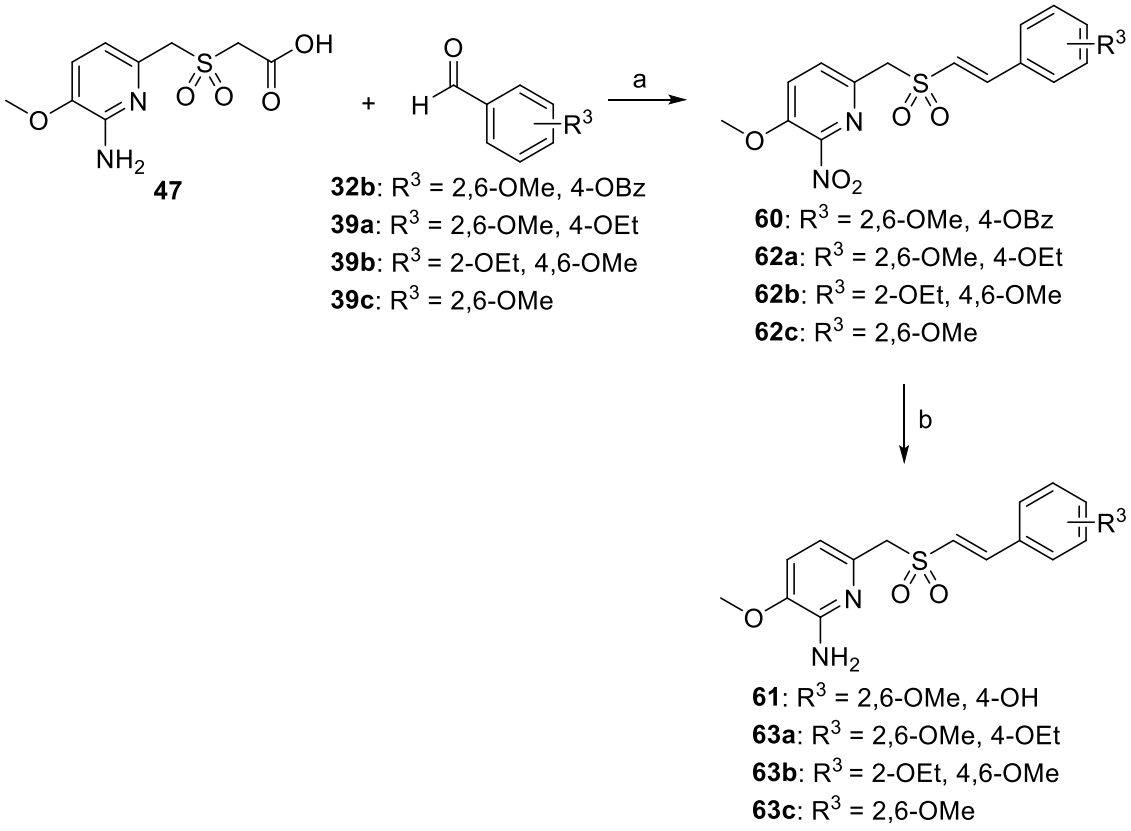
Scheme 3.2: Reagents and conditions: (a) pivaloyl chloride, Et_3N, CH_2Cl_2, rt, 2 h, 100%; (b) NBS, AIBN, MeCN, reflux, 12 h; (c) methyl thioglycolate, Na_2CO_3, MeOH, rt, 2 h, 69%; (d) 30% H_2O_2, CH_3CO_2H, 50 °C, 12 h, 88%; (e) Na_2CO_3, H_2O, MeOH, rt, 18 h, 93%; (f) 2,4,6-trimethoxybenzaldehyde **15**, benzoic acid, piperidine, toluene, reflux, 2 h, 43%; (g) **58a**: EtI, K_2CO_3, DMF, rt, 14 h, 62%; **58b**: 1-iodopropane, K_2CO_3, DMF, rt, 48 h, 78%; **58c**: 2-bromoethanol, K_2CO_3, DMF, rt to 50 °C, 24 h, 76%; **58d**: ethyl bromoacetate, K_2CO_3, DMF, rt, 12 h, 83%; **58e**: 4-(2-chloroethyl)morpholine hydrochloride, K_2CO_3, DMF, 50 °C, 48 h, 98%; **58f**: 2-chloro-*N*,*N*-dimethylethylamine hydrochloride, K_2CO_3, DMF, 50 °C, 48 h, 55%; (h) Fe, MeOH/CH_3CO_2H (1:1), 50 °C, 2 h, 37-75%; (i) H_2, 10% Pd/C, MeOH, rt, 6 h, 53%; (j) *only for hydrolysis of **59d**, NaOH, H_2O/MeOH, rt to 80 °C, 14 h, 48%.

To determine the effect of replacing the methoxy group of **49** with a phenolic hydroxyl, the synthesis of (*E*)-2-amino-6-(((2,4,6-trimethoxystyryl)sulfonyl)methyl)pyridin-3-ol **59g** was attempted *via* direct nitro reduction of **57** which was initially attempted using iron in a mixture of acetic acid and methanol. However this method failed to produce the desired product due to the complexation of the phenolic hydroxyl with the formed Fe^{3+}. Therefore, an alternative reducing agent was required for the reduction of **57**. Unlike iron which acts as an electron donor, the use of palladium in this reaction does not lead to the formation of palladium by-products as palladium acts as a surface catalyst. Consequently, palladium on carbon was selected as the reducing agent. As palladium is able to catalyse the reduction of carbon-carbon double bonds with long reaction times and mild heating,[249] the reduction of **57** with palladium on carbon in methanol was conducted under hydrogen gas at room temperature and hourly monitoring. Compound **59g** was successfully synthesised using these conditions, obtaining a yield of 53%.

3.2.3 **Modification at the R^3 position of the styryl ring**

To study the SAR of substituents at the R^3 position, a series of compounds were synthesised as outlined in **Scheme 3.3**. In view of the potent antiproliferative activity of **41a** (R^3 = 2,6-OMe, 4-OEt), **41b** (R^3 = 2-OEt, 4,6-OMe), and **41c** (R^3 = 2,6-OMe) (*vide supra*, section 2.3), substitution of the styryl moiety in these compounds was adopted for the design of **63a-c**. Knoevenagel condensation of **47** with **32b** in the presence of benzoic acid and piperidine in toluene yielded (*E*)-3,5-dimethoxy-4-(2-(((5-methoxy-6-nitropyridin-2-yl)methyl)sulfonyl)vinyl)phenyl benzoate **60** in 29% yield. Compound **60** was reduced using iron powder in a mixture of glacial acetic acid and methanol, followed by subsequent deprotection *via* saponification to give (*E*)-4-(2-(((6-amino-5-methoxy-pyridin-2-yl)methyl)sulfonyl)vinyl)-3,5-dimethoxyphenol **61** in 38% yield. Similarly, Knoevenagel condensation of **47** with **39a-c** in the presence of benzoic acid and piperidine yielded **62a-c** (37-43% yield), which were subsequently reduced to give **63a-c** (42-72% yield). It was noticed that the Knoevenagel condensation of **47** with benzaldehydes **15**, **32b**, and **39a-c** produced **48**, **60** and **62a-c** at lower yields (29-43%) compared to the yields exhibited in the synthesis of **16**, **33b**, and **41a-c** (41-76%) (*vide supra*, section 2.2.1 and 2.2.3). Compound **47** was found to be highly susceptible to

decarboxylation, resulting in 3-methoxy-6-((methylsulfonyl)methyl)-2-nitropyridine **64** (**Figure 3.2**), which was isolated from reaction mixtures in yields of 23-35%. ^{1}H NMR spectroscopic analysis confirmed the structure of **64** in which singlets at 3.99 (3H) and 4.69 ppm (2H) were assigned to methoxy and methylene protons respectively, alongside the appearance of SCH_3 as a singlet at 3.03 ppm (3H). The HRMS spectrum revealed a peak at 247.0396 *m/z* ($[M+H]^+$) in the molecular ion region, confirming the molecular mass of **64**.



Scheme 3.3: Reagents and conditions: (a) benzoic acid, piperidine, toluene, reflux, 2 h, 29-43%; (b) Fe, MeOH/CH_3CO_2H (2:1), 50 °C, 2 h, 38-72%.

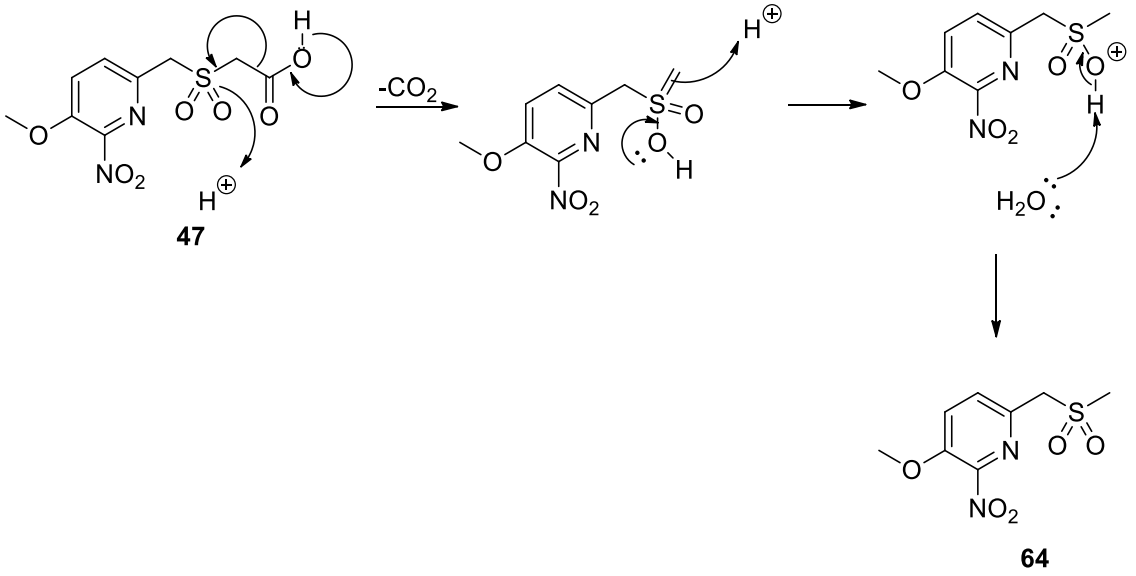
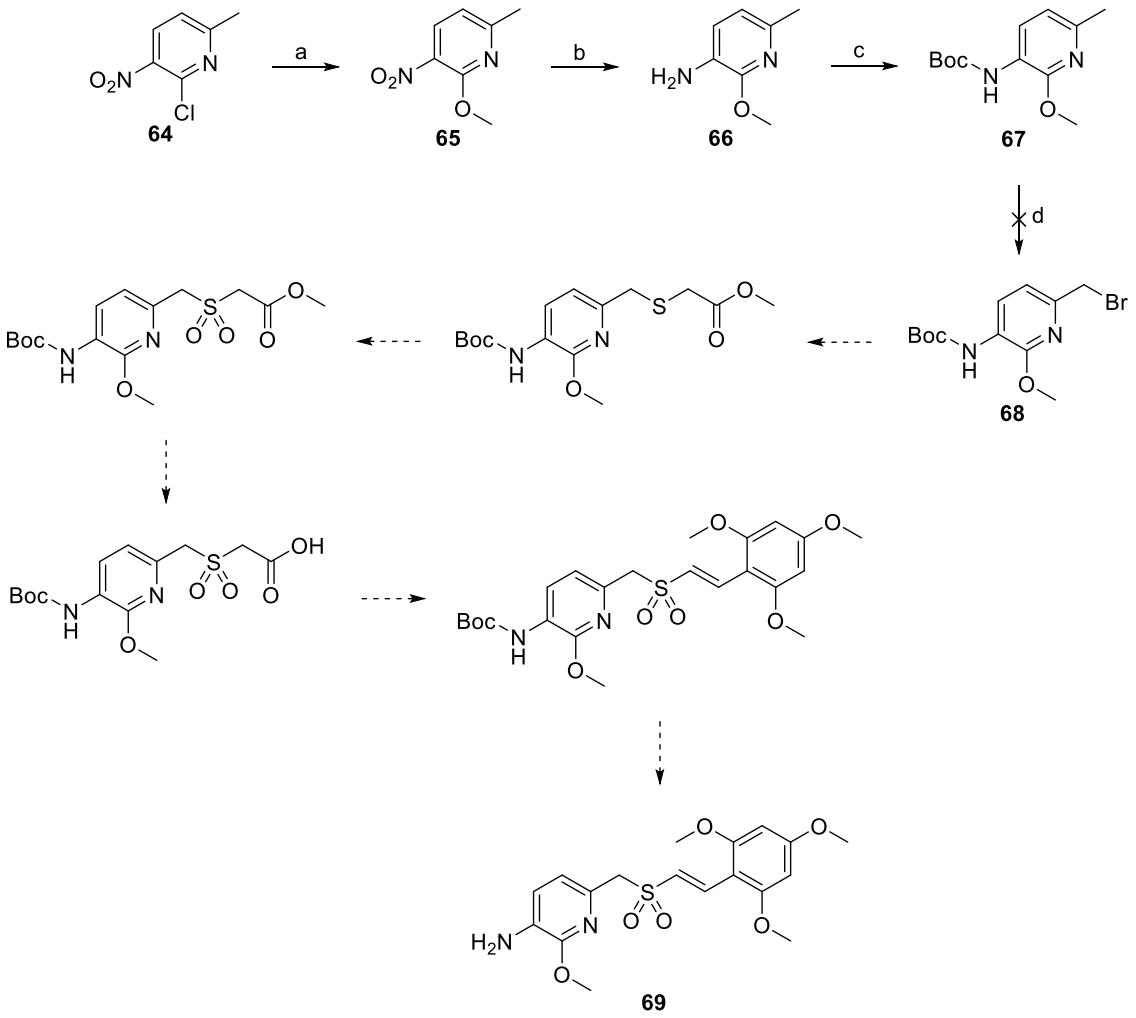


Figure 3.2: Proposed decarboxylation mechanism of **47**.

3.2.4 Synthesis of (*E*)-2-methoxy-6-(((2,4,6-trimethoxystyryl)sulfonyl)-methyl)pyridin-3-amine

The synthesis of (*E*)-2-methoxy-6-(((2,4,6-trimethoxystyryl)sulfonyl)methyl)pyridin-3-amine **69** was attempted using the route outlined in **Scheme 3.4** to determine the effect of switching the position of the methoxy and amino groups attached to the pyridine ring. Compound 2-chloro-6-methyl-3-nitropyridine **64** was reacted with sodium methoxide in methanol to give 2-methoxy-6-methyl-3-nitropyridine **65** in 90% yield. Wohl-Ziegler bromination of **65** with NBS and AIBN was initially attempted, however the reaction failed to generate the desired product. This may be due to the position of the nitro group on the pyridine ring which is *para* to the methyl group, reducing the electron density on the methyl group *via* resonance. To introduce functionality to the methyl group, the oxidation of **65** using selenium dioxide in 1,4-dioxane was attempted. However, the reaction failed to generate the desired product. These failures necessitated the replacement of the nitro group to allow Wohl-Ziegler bromination to occur. Compound **65** was subsequently reduced using 10% palladium on carbon in the presence of hydrogen gas, affording 2-methoxy-6-methylpyridin-3-amine **66** in 87% yield. The amino group of **66** was protected with a Boc group using Boc anhydride in t-

butanol, giving tert-butyl(2-methoxy-6-methyl-pyridin-3-yl)carbamate **67** in quantitative yield.



Scheme 3.4: Reagents and conditions: (a) NaOMe, MeOH, reflux, 2 h, 90%; (b) H_2, 10% Pd/C, MeOH, rt, 5 h, 87%; (c) Boc anhydride, *t*-butanol, 40 °C, 36 h, 100%, (d) NBS, AIBN, CH_3CN, reflux, 22 h.

Bromination of **67** using NBS and AIBN in acetonitrile was subsequently attempted. However, the reaction failed to produce the desired product *tert*-butyl(6-(bromomethyl)-2-methoxypyridin-3-yl)carbamate **68** as bromination occurred on the pyridine ring instead of the methyl group. Bromination of the pyridine ring was further confirmed using ^{1}H nuclear magnetic resonance (NMR) and high resolution mass spectrometry (HRMS) as one of the hydrogens of the pyridine ring was found to be substituted by bromine while the methyl group was retained. This may be due to the stabilization conferred by the amino group *via* resonance to the pyridine carbon ortho to the amino

group, therefore allowing the attached hydrogen to be replaced by bromine. Attempts to react the formed compound with methyl thioglycolate in the presence of sodium carbonate also failed, further confirming that bromination did not occur on the methyl group. Due to the failure to brominate the methyl group, the synthesis of **69** was not pursued further.

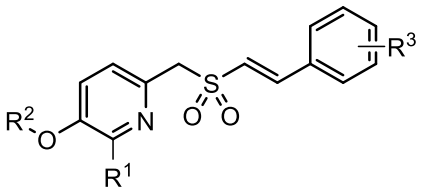
3.3 **Structure-activity relationship analysis**

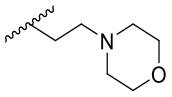
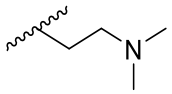
To determine the antiproliferative activity of the compounds, 72 h MTT assays were conducted on A2780 and HCT-116 cell lines. The results are summarized in **Table 3.1**. In evaluation of the R^1 position, the antiproliferative activity of the (*E*)-2-(((2,4,6-trimethoxystyryl)sulfonyl)methyl)pyridine series was found to be similar to the activity profile of the (*E*)-3-(((2,4,6-trimethoxystyryl)sulfonyl)methyl)pyridine series. Compound **48** (R^1 = NO_2, R^2 = Me, R^3 = 2,4,6-OMe) was inactive (GI_{50} >10 μM) whilst its amino derivative **49** (R^1 = NH_2, R^2 = Me, R^3 = 2,4,6-OMe) was found to be highly active (GI_{50} = 7-8 nM), with similar activity to **7**. However, the attachment of substituents on the amino group decreased the antiproliferative activity, which indicates that the primary amine group may be necessary for optimum activity. Replacement of the amino group with a methylsulfonamide as in **50a** (R^1 = $NHSO_2Me$, R^2 = Me, R^3 = 2,4,6-OMe) gave modest antiproliferative activity (GI_{50} = 0.320-0.610 μM) similar to its (*E*)-3-((styrylsulfonyl)methyl)pyridine counterpart **18a**. Interestingly, the introduction of an acetamide group as in **50b** (R^1 = NHCOMe, R^2 = Me, R^3 = 2,4,6-OMe) resulted in enhanced antiproliferative activity with GI_{50} = 0.320-0.610 μM compared to its analogue **18d** (GI_{50} = 7.095-8.219 μM). Conversely, the activity of **50c** (R^1 = $NHCH_2CO_2Et$, R^2 = Me, R^3 = 2,4,6-OMe) (GI_{50} = 5.450-6.906 μM) was found to be significantly lower than its counterpart **18e** (GI_{50} = 0.409-0.940 μM). Hydrolysis of **50c** resulted in **50d** (R^1 = $NHCH_2CO_2H$, R^2 = Me, R^3 = 2,4,6-OMe) which exhibited a significant increase in antiproliferative activity (GI_{50} = 0.253-0.329 μM), but remained more than 36-fold less potent than **49**. Similar to **18f**, **50d** was found to be significantly less active than its analog ON01910 (GI_{50} = 0.050-0.070 μM). The primary amine was subsequently retained at the R^1 position and modifications were then conducted on the R^2 position.

At the R^2 position, introduction of an ethoxy as in **59a** (R^1 = NH_2, R^2 = Et, R^3 = 2,4,6-OMe) gave potent antiproliferative activity (GI_{50} = 0.012-0.033 μM). However, substitution with an *n*-propyl group as in **59b** was not tolerated, resulting in a significant loss in activity (GI_{50} = 0.455-0.498 μM). As observed from the MTT assay results, increasing the length of the alkyl chain at this position results in a reduction in activity. While it was envisioned that the introduction of polar side groups at the R^2 position may improve the metabolic stability of the compound series, this resulted in a significant drop in antiproliferative activity. Substitution with an ethyl hydroxyl group as in **59c** (R^1 = NH_2, R^2 = C_2H_4OH, R^3 = 2,4,6-OMe) gave modest antiproliferative activity (GI_{50} = 0.494-0.506 μM). However, replacement of the methoxy group with solubilizing side groups as in **59e** (R^1 = NH_2, R^2 = $C_2H_4N(CH_2CH_2)_2O$, R^3 = 2,4,6-OMe), **59f** (R^1 = NH_2, R^2 = $C_2H_2N(CH_3)_2$, R^3 = 2,4,6-OMe) and **59h** (R^1 = NH_2, R^2 = CH_2CO_2H, R^3 = 2,4,6-OMe) resulted in abolishment of activity. Substitution of methoxy with a hydroxyl as in **59g** (R^1 = NH_2, R^2 = H, R^3 = 2,4,6-OMe) resulted in abolishment of activity, indicating that an alkyloxy group is necessary at this position for activity. The increase in water solubility of the compounds may limit the intracellular concentration of the drug due to the lipophilic nature of the cell membrane which can limit the entry of highly polar molecules. Due to the importance of the methoxy group at this position for optimum antiproliferative activity, this group was retained and modifications were subsequently conducted at the R^3 position.

Similar to the (*E*)-3-((styrylsulfonyl)methyl)pyridine series of compounds, the methoxy group at the 4-position of the styryl ring is necessary for optimum antiproliferative activity. Replacement of the methoxy at this position with a hydroxyl (**61**), hydrogen (**63c**), or ethoxy (**63a**) resulted in a decrease in activity. Interestingly, **61** and **63c** were found to be significantly more active (GI_{50} = 0.041-0.084 μM) than their (*E*)-3-((styrylsulfonyl)methyl)pyridine counterparts **34** and **41c** (GI_{50} = 0.424-0.668 μM) (*vide supra*, section 2.3). This indicates that modifications to the 4-position are more tolerated in the (*E*)-2-((styrylsulfonyl)methyl)pyridine series compared to the (*E*)-3-((styrylsulfonyl)-methyl)pyridine series. Introduction of an ethoxy group at the 2-position of the styryl ring as in **63b** gave potent antiproliferative activity (GI_{50} = 0.005-0.008 μM), with its activity similar to that of **49**.

Table 3.1: **Summary of structure and biological activity**[a]



Code	Structure			Antiproliferative activity, GI_{50} (μmol/L) ± sd	
	R^1	R^2	R^3	A2780	HCT-116
48	NO_2	Me	2,4,6-OMe	> 10	> 10
49	NH_2	Me	2,4,6-OMe	0.007 ± 0.002	0.008 ± 0.001
50a	$NHSO_2Me$	Me	2,4,6-OMe	0.406 ± 0.051	0.610 ± 0.030
50b	NHCOMe	Me	2,4,6-OMe	0.500 ± 0.027	0.320 ± 0.385
50c	$NHCH_2CO_2Et$	Me	2,4,6-OMe	6.906 ± 0.518	5.450 ± 0.370
50d	$NHCH_2CO_2H$	Me	2,4,6-OMe	0.253 ± 0.021	0.329 ± 0.013
59a	NH_2	Et	2,4,6-OMe	0.012 ± 0.004	0.033 ± 0.006
59b	NH_2	*n*-Pr	2,4,6-OMe	0.455 ± 0.159	0.498 ± 0.063
59c	NH_2	C_2H_4OH	2,4,6-OMe	0.494 ± 0.025	0.506 ± 0.029
59e	NH_2		2,4,6-OMe	> 10	> 10
59f	NH_2		2,4,6-OMe	> 10	> 10
59g	NH_2	H	2,4,6-OMe	> 10	> 10
59h	NH_2	CH_2CO_2H	2,4,6-OMe	> 10	> 10
61	NH_2	Me	2,6-OMe, 4-OH	0.053 ± 0.015	0.084 ± 0.015
63a	NH_2	Me	2,6-OMe, 4-OEt	0.046 ± 0.001	0.052 ± 0.002
63b	NH_2	Me	2-OEt, 4,6-OMe	0.008 ± 0.004	0.005 ± 0.001
63c	NH_2	Me	2,6-OMe	0.041 ± 0.001	0.057 ± 0.003
ON01910	-	-	-	0.062 ± 0.004	0.070 ± 0.003

[a] Performed by Julian Adams

Table 3.2: Antiproliferative activity of 49, 50a and ON01910 against a panel of human cell lines[a]

Human cell lines		Antiproliferative activity, GI_{50} (μmol/L) ± sd		
Origin	**Designation**	**49**	**50a**	**ON01910**
Brain	DAOY	0.004 ± 0.001	-	0.047 ± 0.004
	D283	0.011 ± 0.007	-	0.035 ± 0.011
	D458	0.007 ± 0.003	-	0.007 ± 0.001
Breast	MCF-7	0.006 ± 0.001	0.468 ± 0.041	0.050 ± 0.010
	MDA-MB231	0.007 ± 0.001	0.641 ± 0.039	0.057 ± 0.001
Cervical	Hela	<0.001	0.556 ± 0.079	0.012 ± 0.001
Colon	HCT-116	0.008 ± 0.001	0.610 ± 0.030	0.070 ± 0.003
	Colo205	0.004 ± 0.001	-	0.050 ± 0.004
	HT-29	0.006 ± 0.001	-	0.075 ± 0.019
	KM12	0.006 ± 0.001	-	0.058 ± 0.004
Ovarian	A2780	0.007 ± 0.002	0.406 ± 0.051	0.062 ± 0.004
Pancreatic	PANC-1	<0.001	0.604 ± 0.093	0.039 ± 0.006
Prostate	LNCaP	0.003 ± 0.002	0.450 ± 0.021	0.025 ± 0.003
	DU-145	0.006 ± 0.008	0.484 ± 0.040	0.075 ± 0.006
	PC-3	0.006 ± 0.001	-	0.647 ± 0.011
Untransformed	WI-38	>10	>10	>10

[a] Performed by Julian Adams

Due to their potent antiproliferative activity and high oral bioavailabilities (*vide infra*, section 3.8), **49** and **50a** were tested against a panel of cell lines to further evaluate their antiproliferative activity. The results are summarized in **Table 3.2**. Similar to the antiproliferative profile of **17** and **18a**, **49** and **50a** were highly potent against a wide variety of cancer cell lines. While **49** was found to be tenfold more potent than ON01910, the activity of **50a** was significantly lower than ON01910. The compounds also exhibited no activity towards the untransformed WI-38 cell line, indicating the selectivity of these compounds toward cancer cells.

3.4 **Investigation of cellular mode of action**

To determine the effect of the compounds on the cell cycle, cell cycle analysis using flow cytometry was conducted on cancer cell lines. In this assay, the use of propidium iodide (PI), a fluorescent dye which stoichiometrically binds to DNA, allows the flow cytometer to determine the proportion of cells in the different phases of the cell cycle. This is made possible because the fluorescence emission is directly proportional to the amount of DNA in the cell.[250-251] This assay was conducted to determine whether the antiproliferative activity of the compound was due to the effect of the compound on the cell cycle. Flow cytometry studies on cancer cell lines have demonstrated the ability of PLK1 inhibitors in inducing cell cycle arrest in the G2/M phase, eventually leading to the apoptosis of the cells.[252-253] Cells treated with ON01910 have also been found to accumulate at the G_2/M phase of the cell cycle,[81] indicating the effectiveness of ON01910 in promoting cell cycle arrest.

Compounds **49**, **50a**, **59a**, **and 63b** were tested for their cell cycle effects, with ON01910 used as a comparator and the results are shown in **Figure 3.3** and **Figure 3.4**.

Treatment of A2780 ovarian cells with **49** at 0.06 μM caused cell accumulation at the G_2/M phase of the cell cycle. Both **50a** and ON01910 also exhibited similar G_2/M cell cycle effects, but only at the higher concentrations of 0.25 μM and 1 μM for ON01910 and **50a** respectively.

Meanwhile at a concentration of 0.025 μM, cells treated with **63b** exhibited severe perturbation of cell cycle progression while compounds treated with **59a** exhibited a small increase in cells arrested at the G_2/M phase. Significant G_2/M arrests were subsequently observed at a concentration of 0.25 μM for both compounds. Similar to the results shown in **Figure 3.3**, cells treated with ON01910 only exhibited a significant G_2/M arrest at a concentration of 1 μM.

Cell cycle effects were assessed on untransformed WI-38 cells upon treatment with **39** or **50a** for a period of 24h (**Figure 3.5**). In contrast to A2780 cells, both compounds showed minimal effects on the the WI-38 cells up to a concentration of 1 μM, consistent with the results obtained in the MTT cytotoxic assay (*vide supra*, **Table 3.2**)

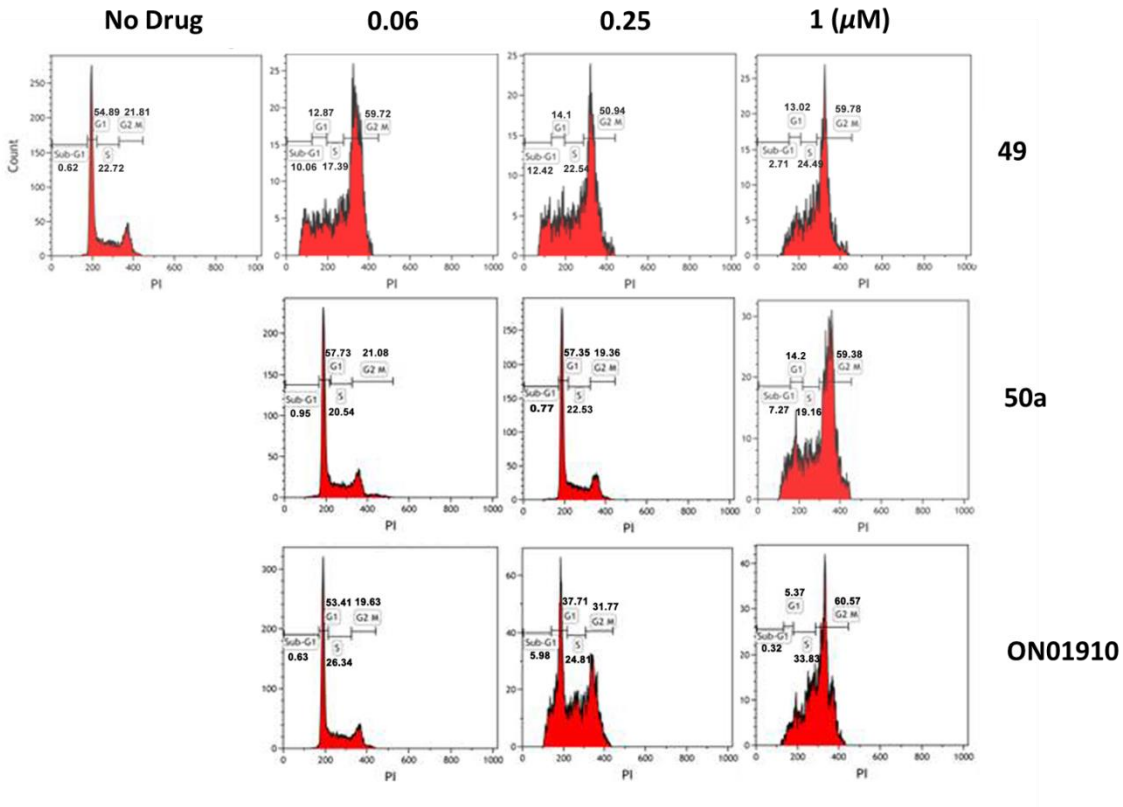


Figure 3.3: Cell cycle effects of **49** and **50a** on A2780 cells. Cells were treated with compound (or vehicle) for 24 h at the concentrations shown and the cell cycle effects were subjected to flow cytometric analysis of DNA content using propidium iodide (PI) staining demonstrating that the compounds can arrest A2780 cancer cells in G_2/M phase and that **49** is the most effective in this assay. (Performed by Julian Adams)

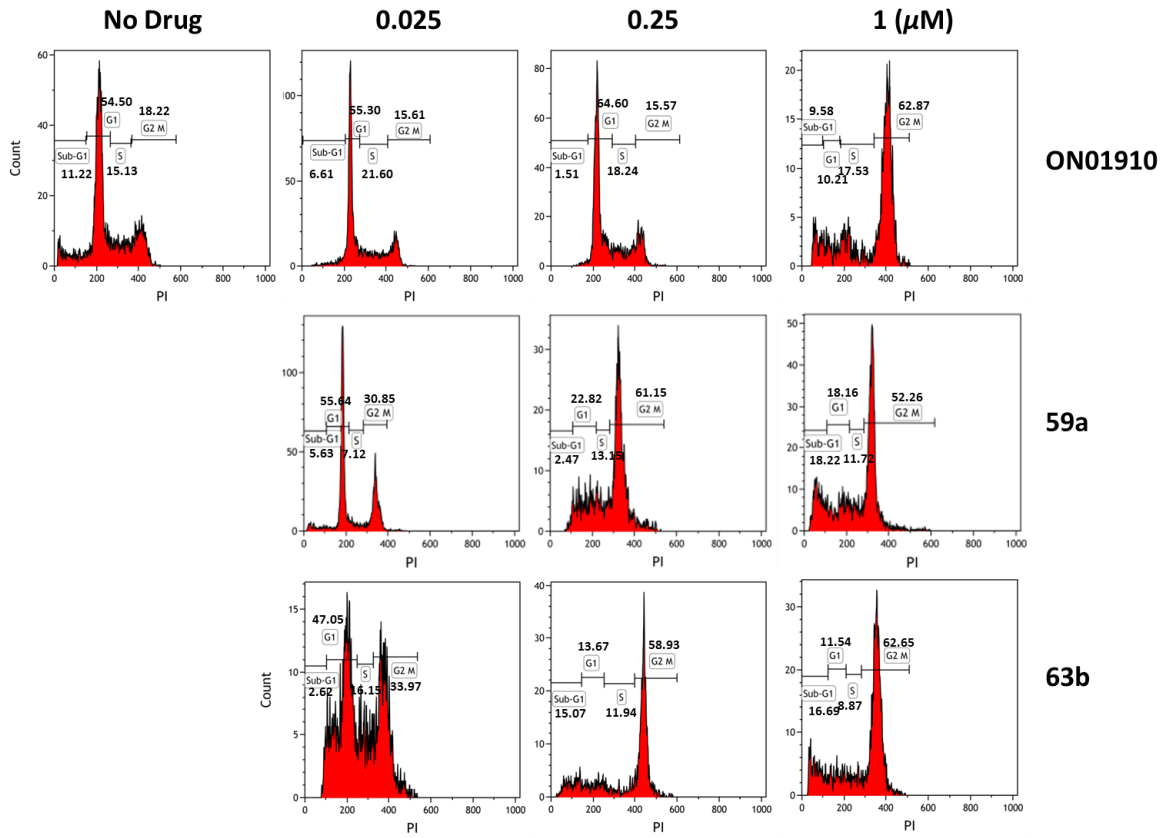


Figure 3.4: Cell cycle effects of **59a**, **63b** and ON01910 on A2780 cells. Cells were treated with DMSO diluent only (no drug) or compounds for 24 h at the concentrations shown. Flow cytometric analysis of DNA content using propidium iodide (PI) staining demonstrated that compounds **59a** and **63b** are significantly more potent than ON01910 in inducing G_2/M arrest. (Performed by Julian Adams)

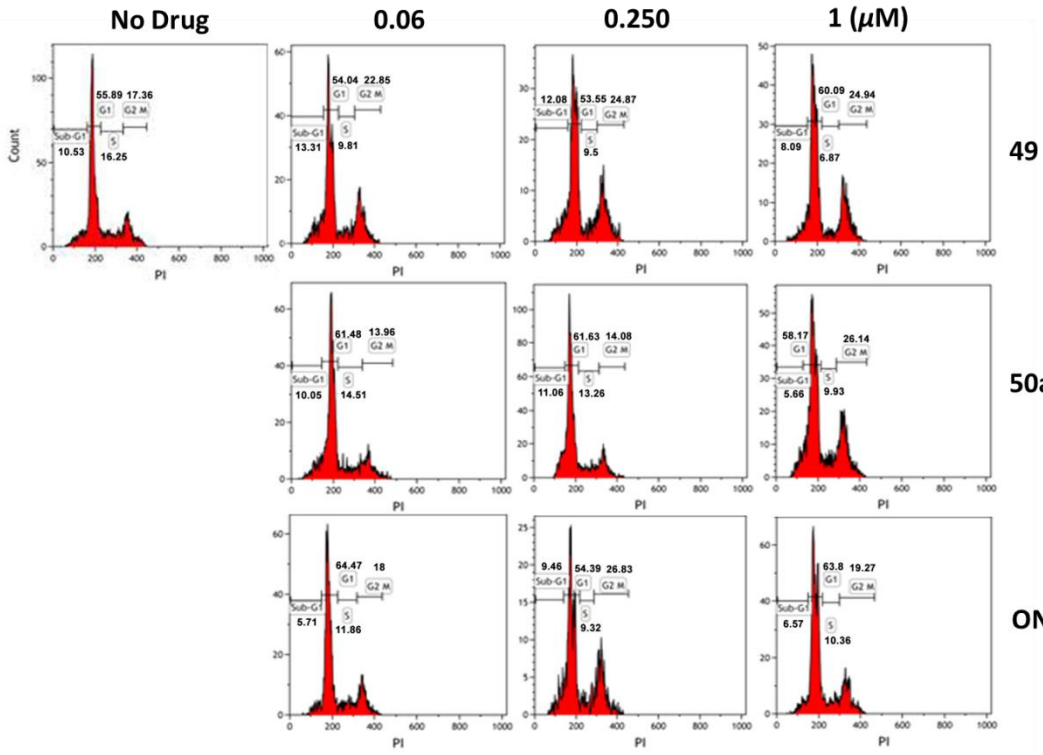


Figure 3.5: Cell cycle effects of **49**, **50a** and ON01910 on WI-38 cells. Cells were treated with DMSO diluent only (no drug) or compounds for 24 h at the concentrations shown. Flow cytometric analysis of DNA content using propidium iodide (PI) staining demonstrated that the compounds have minimal effect on the cells up to a concentration of 1 μM. (Performed by Julian Adams)

Induction of apoptosis was further evaluated using annexin V/PI double staining on A2780 cells after treated with the compounds. In the early phases of apoptosis, phosphatidylserine (PS), a protein which is normally located in the inner leaflet of the plasma membrane, is translocated to the outer leaflet of the membrane.[254] Fluorescein isothiocyanate (FTIC) labelled annexin V has a high binding affinity for PS binds, which allows identification of the apoptotic cells. The concomitant addition of PI allows the difference between early apoptotic cells and non-viable cells to be distinguished. This is possible because cells which are positively stained by PI are either in the final stage of apoptosis or are undergoing necrosis. The results obtained from the flow cytometry are displayed as contour diagrams, with the lower left quadrant representing viable cells, the upper right quadrant representing non-viable and necrotic cells, and the lower right quadrant representing early apoptotic cells.

A2780 cells were treated with varied concentrations of **49, 50a**, **59a**, **63b** or ON01910 for a period of 24 hours. Annexin V/PI assays (**Figure 3.6** and **Figure 3.7**) showed that like ON01910, **49**, **50a**, **59a** and **63b** were capable of inducing apotosis. Compound **49** was the most potent apoptotic inducer which caused a 31% increase in annexin V-positive cells at a concentration of 0.06 μM, whereas similar effects were observed with 0.25 and 1.0 μM of **50a** and ON01910, respectively.

While cells treated with 0.025 μM of **63b** resulted in a significant increase in the apoptotic cell population (**Figure 3.7**), higher concentrations resulted in a near complete loss of cell population. Concurrently, cells treated with **59a** exhibited a significant rise in apoptotic cell population at 0.25 μM while cells treated with ON01910 only displayed a significant increase at 1 μM. To determine whether **63b** had the same effect on other cell lines, the assay was subsequently repeated on HCT-116 cells treated with different concentrations of **63b** (**Figure 3.8**). HCT-116 was noticeably more tolerant to the effect of **63b** compared to A2780 cells. Similar to the results with A2780, a significant increase in apoptotic cell population was observed at a concentration of 0.025 and 1 μM for cells treated with **63b** and ON01910 respectively.

The same assay was conducted on WI-38 cells treated with **49** and **50a** to determine their effect on the apoptosis of normal cells. No effect on the apoptotic cell population was observed in this assay (**Figure 3.9**), reinforcing the high selectivity of the compounds towards cancer cells.

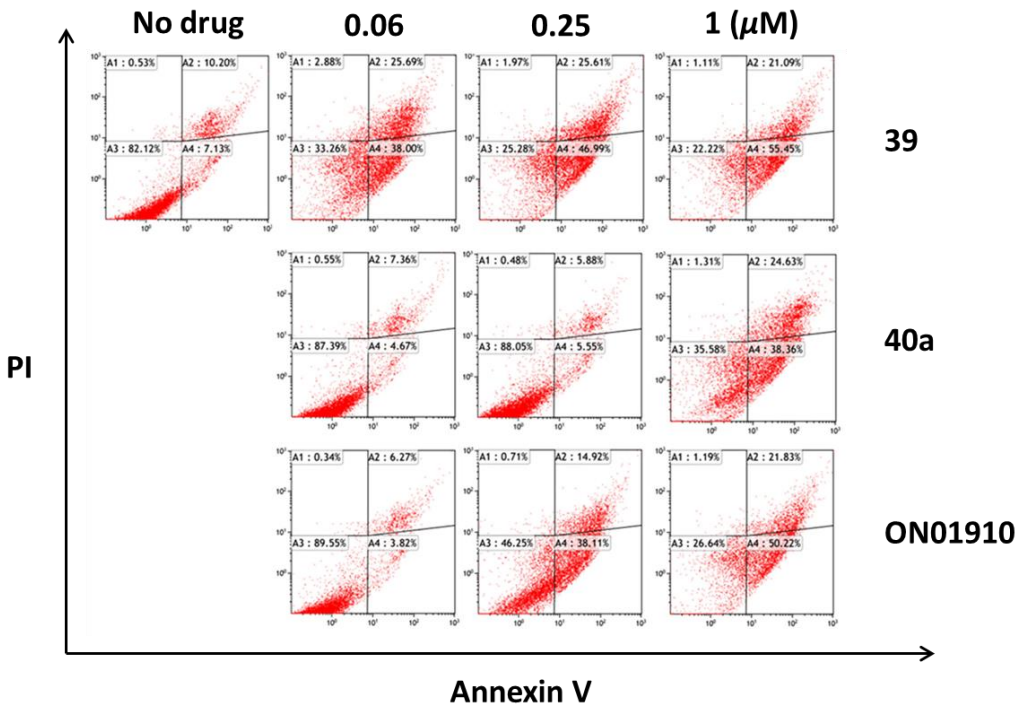


Figure 3.6: Annexin V/PI binding assay on A2780 cells treated with **49**, **50a**, and ON01910. Cells were exposed to DMSO diluent only (no drug), **49**, **50a**, and ON01910 for 48 h at the concentrations shown and analysed by annexin V/PI double staining. Treatment with **49** at 0.06 μM gave rise to an increase in annexin V positive apoptotic A2780 cells. Higher concentrations of ON01910 and **50a** were required for a significant increase in annexin V positive apoptotic cells. (Performed by Julian Adams)

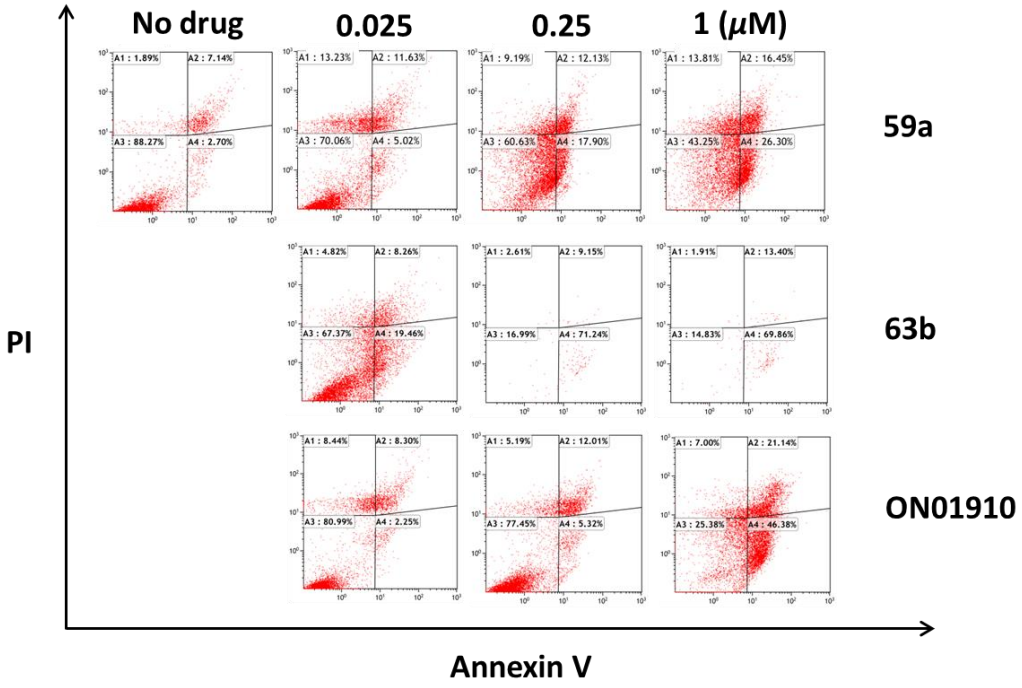


Figure 3.7: Annexin V/PI binding assay on A2780 cells treated with **59a**, **63b**, and ON01910. Cells were exposed to DMSO diluent only (no drug), **59a**, **63b**, and ON01910 for 48 h at the concentrations shown and analysed by annexin V/PI double staining. Treatment with **59a** at 0.025 μM gave rise to an increase in annexin V positive apoptotic A2780 cells. However at higher concentrations, loss of cell integrity was observed. (Performed by Julian Adams)

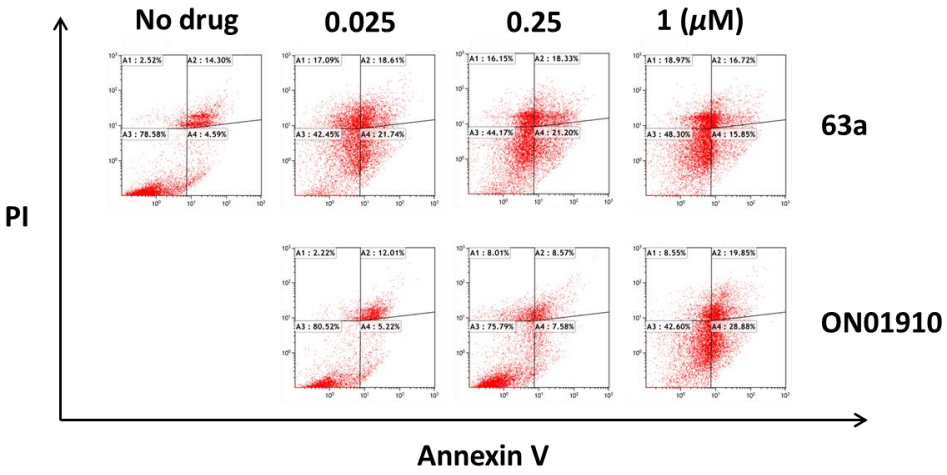


Figure 3.8: Annexin V/PI binding assay on HCT-116 cells treated with **63b** and ON01910. Cells were exposed to DMSO diluent only (no drug), **63b**, and ON01910 for 48 h at the concentrations shown and analysed by annexin V/PI double staining. (Performed by Julian Adams)

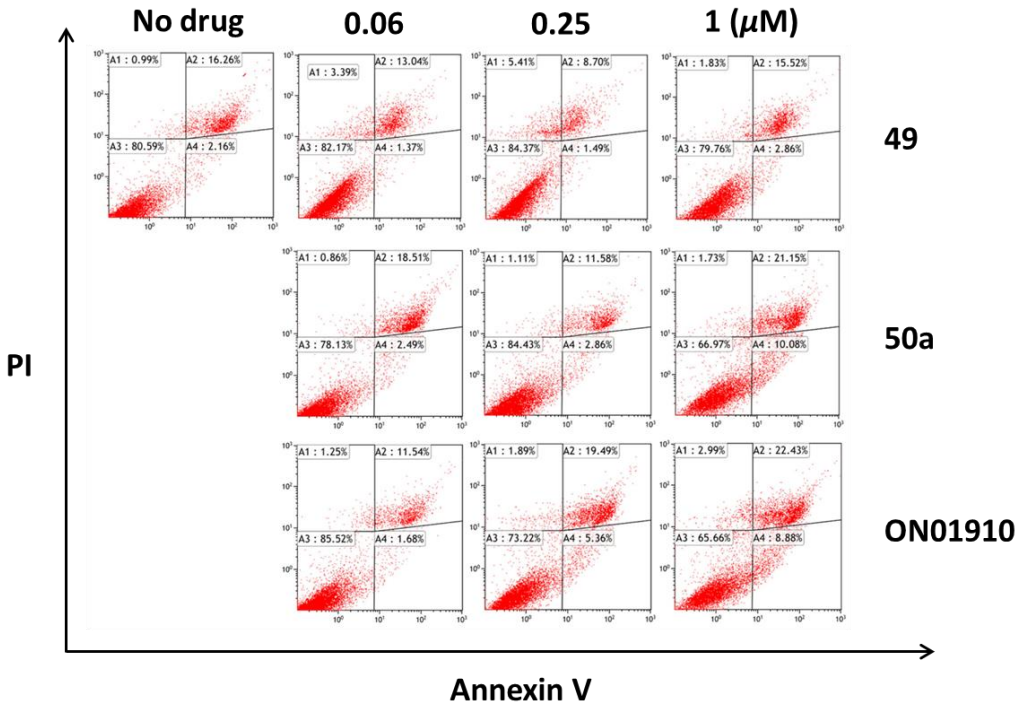


Figure 3.9: Annexin V/PI binding assay on WI-38 cells treated with **49**, **50a**, and ON01910. Cells were exposed to DMSO diluent only (no drug), **49**, **50a**, and ON01910 for 48 h at the concentrations shown and analysed by annexin V/PI double staining. No effect was observed on the apoptotic cell population, indicating their selectivity towards cancer cells. (Performed by Julian Adams)

3.5 **Caspase-3/7 activation**

Caspase-3/7 activation was further evaluated using an Apo-ONE® homogeneous caspase-3/7 assay.[255] Caspase-3 and -7 are important effector caspases that cleave key proteins that are essential for cell survival, leading to the morphological changes associated with apoptosis. In the Apo-ONE® homogeneous caspase-3/7 assay, the substrate Z-DEVD-R110 is cleaved by caspase-3/7 to form the fluorescent rhodamine 110. The measurement of fluorescence using a plate reader allows the evaluation of caspase-3/7 activity as the amount of fluorescent product generated is proportional to the caspase-3/7 activity in the cells.

The caspase-3/7 assay was also conducted on A2780 and WI-38 cells after treatment with **49**, **50a** and ON01910 for a period of 24h. As shown in **Figure 3.10**, **49** was capable of activating caspase 3/7 at a concentration of 0.06 μM ($p \leq 0.001$). ON01910 and **50a** showed the same effects but at higher concentrations i.e. 0.25 and 1.0 μM, respectively. The same treatment of WI-38 cells with **49**, **50a** and ON01910 resulted in minimal caspase-3/7 activity, confirming that these compounds induced the caspase-3/7 mediated apoptosis selectively in cancer cells over the untransformed cells.

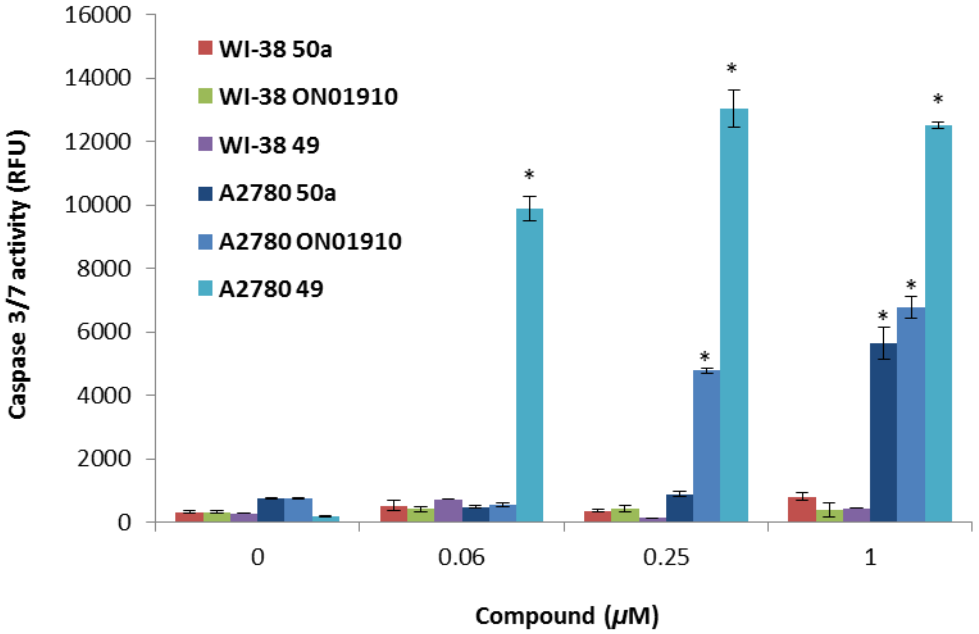


Figure 3.10: Caspase-3/7 activity in A2780 or WI-38 cells after treatment with **49**, **50a**, ON01910 for 24 h. All 3 compounds tested induced caspase-3/7 activity in A2780 cells. Compound **49** is the most potent, inducing significant caspase-3/7 activity at the lowest concentration of 0.06 μM. Vertical bars represent the mean relative fluorescence units (RFU) (±sd) of three independent experiments. Values significantly ($p \leq 0.001$) different from the assay diluent control only are marked with an asterisk (*). (Performed by Julian Adams)

3.6 Cellular mechanism of action

CDC25C, a protein that is regulated by PLK1, is important for the regulation of cell cycle (*vide supra*, section 1.4.1.1). Previous studies conducted by Gumireddy *et al* have demonstrated the ability of ON01910 in reducing the expression of CDC25C *via* PLK1 inhibition.[84] The expression of anti-apoptotic protein Mcl-1 in cancer cells are essential for the survival and growth of cancer cells while PARP cleavage is implicated in the execution of apoptosis.

To understand whether the induction of apoptosis of our compounds is the consequences of targeting PLK1-CDC25, western blot analysis was conducted. A2780 cells were treated with **49, 50a** or ON01910 for 24h. The antibodies against CDC25C

and Mcl-1 showed that **49,** ON01910 and **50a** downregulated the expression levels ofboth proteins at concentrations of 0.03, 0.25, and 1 μM respectively (**Figure 3.11**). The reduction in CDC25C level may be linked to the increase in CHK2 and p53 activity due to PLK1 inhibition.[121, 248] Studies have demonstrated the ability of PLK1 in inhibiting the activity of CHK2 and p53, two proteins that promote the downregulation of CDC25C.[110-111, 256-257] Studies have also demonstrated the ability of PLK1 polo-box domain (PBD) inhibitors including thymoquinone derivatives in reducing the expression of CDC25C,[96] suggesting that **49**, **50a** and ON01910 act predominantly by blocking the PBD.Similarly, induction of PARP cleavage in treated cells was observed at concentrations of 0.03, 0.25, and 1 μM for **49**, ON01910, and **50a** respectively. These concentrations were also found to be similar to the concentrations for the induction of caspase-3/7 activity obtained from the caspase-3/7 assay as the induction of PARP cleavage is promoted by the activation of caspase-3 activity.[258] Furthermore, the induction of apoptosis is also explained by the reduction of Mcl-1 level. Studies have shown that pharmacological inhibition of PLK1 in sarcoma cell lines is linked to the dose dependent down-regulation of Mcl-1.[259-260]

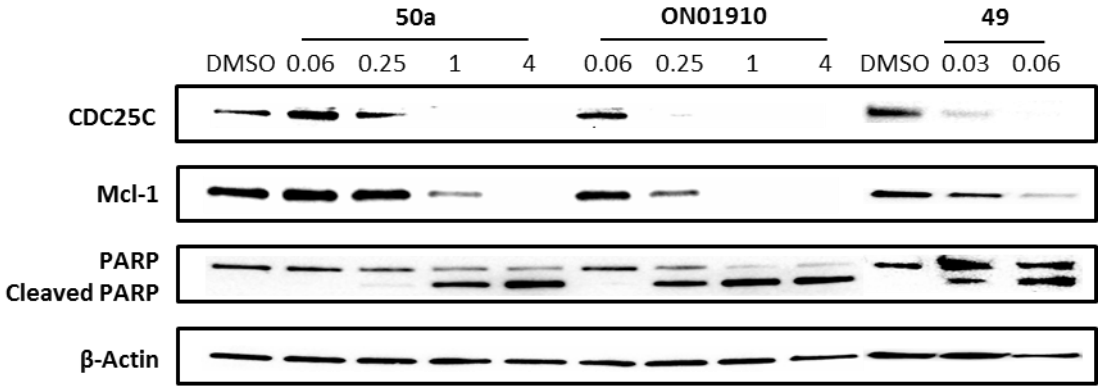


Figure 3.11: Western blot analysis of A2780 cells treated with **49**, **50a** or ON01910 for 24 h at the concentrations shown. Down regulation of CDC25C and Mcl-1, as well induction of PARP cleavage was observed with **49** being the most potent in inducing these changes. DMSO diluent was used as control in each experiment, and β-actin antibody was used as the internal control. (Performed by Julian Adams)

Compound **49** was also screened against a panel of 57 kinases using Eurofins Kinase Profiler® at a concentration of 1 μM, and the residual kinase activities are shown in **Figure 3.12**. This *in vitro* radiometric kinase assays involves the use of radiolabelled

[γ -^{33}P]ATP and is incubated with the kinase and inhibitor in the presence of Mg^{2+} and substrate.

The compound has no inhibitory activity against most of the kinases including PLK1, contradicting the kinase inhibitory profile of ON01910.[84] The failure of the panel screen to demonstrate PLK1 activity may be due to casein being used as a substrate instead of CDC25C which was utilized in the study of ON01910. As the PBD is essential for CDC25C binding to PLK1,[261-262] binding of ON01910 to the PBD is believed to be responsible for the inhibition of CDC25C phosphorylation.[263] Nevertheless, given that the Western blot results showed that the plausible mechanism of action align PLK1 inhibition, it is believed that **49** is a PLK1 inhibitor. To determine the ability of **49** in inhibiting PLK1, a filtration binding assay using different concentrations of CDC25C will need to be conducted in future studies to study the effect of increasing substrate concentration on the inhibitory activity of **49**.

Interestingly, **49** was found to inhibit CDK5 in the presence of its activator p35. However, **49** did not affect the activity of CDK5 in the presence of p25, the truncated form of p35. This suggests that **49** blocks the interaction between p35 and CDK5. Aurora-A, a mitotic regular implicated in the development of cancer, was also found to be inhibited by **49**, though its inhibitory activity on Aurora-A is lower compared to that on CDK5.

This inhibition warrants further investigation on its activity on CDK5/p35 and whether future drug development can be explored.

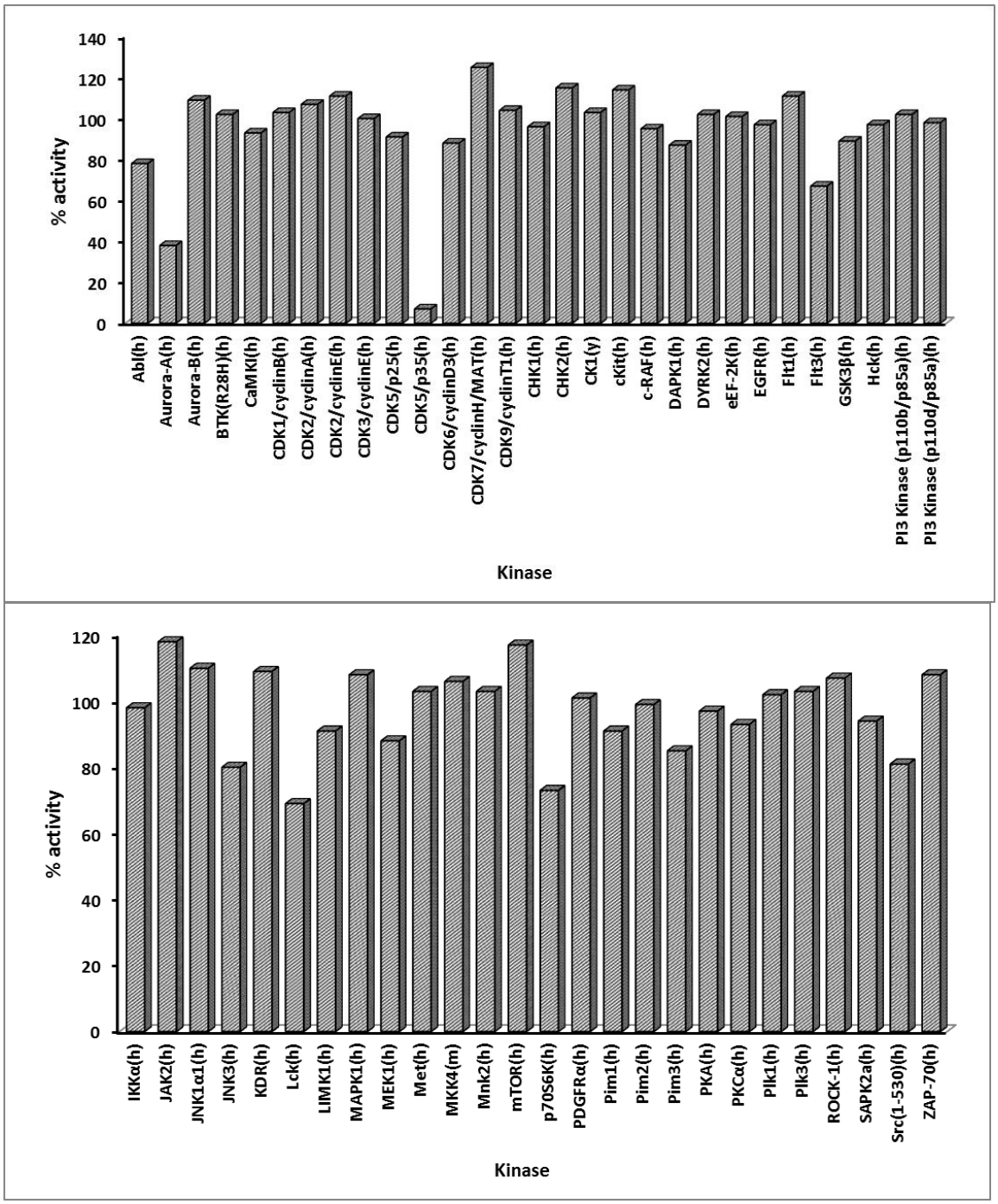


Figure 3.12: Screening of **49** against a panel of 57 kinases. Compounds were tested at the concentration of 1 μM by Eurofins Scientific.

3.7 **Microsomal stability assay**

Microsomal stability assays using rat liver microsomes were conducted on a selection of compounds, with the results summarized in **Table 3.3**.

Table 3.3: Metabolic stability of compounds in rat liver microsomes[a]

Compound code	Half-life, $t_{½}$ (min)[b]
49	15
50a	112
50d	>120
59a	10
61	17
63a	16
63b	>120
63c	5

[a] Performed by Ben Noll

[b] Values are means of at least two replicates

Compound **49** was found to have low metabolic stability ($t_{½}$ = 15 min), similar to that of **7**. The 2-methoxy group of the styryl ring was identified as the main site of metabolism for **49**, resulting in the formation of (*E*)-2-(2-(((6-amino-5-methoxypyridin-2-yl)methyl)sulfonyl)vinyl)-3,5-dimethoxyphenol (**Figure 3.13**). The difference in metabolism site between **17** and **49** may be attributed to the position of the N on the pyridine ring. In the structure of **17**, the pyridine N is ortho to the methoxy group. As oxidative O-dealkylation is dependent on the electronic effect of neighbouring groups,[232] the electron withdrawing effect of the N ortho to the methoxy group may have a significant impact on its demethylation. Meanwhile, the introduction of the highly polar methyl sulfonamide (**50a**) and acetic acid (**50d**) group at the the R^1 position resulted in a significant increase in metabolic stability (**50a** $t_{½}$ = 112 min; **50d** $t_{½}$ = >120 min).

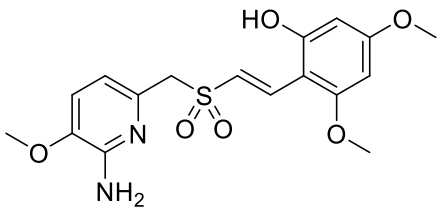


Figure 3.13: Proposed major metabolite of **49**.

In the modification of the R^2 position, introduction of an ethoxy group as in **59a** resulted in a decrease in metabolic stability ($t_{½}$ = 10 min) compared to **49** ($t_{½}$ = 15 min). The reduction in stability with the introduction of the ethoxy may be due to the

increased lipophilicity of the compound which makes it more susceptible to metabolism by CYP450.

It was initially envisioned that substitution of the methoxy group of the styryl ring with a hydroxyl group as in **61** would improve the metabolic stability of the compounds by increasing their polarity. However, no improvement was observed with this introduction ($t_{½}$ = 17 min). Replacement of the methoxy group of the 4-position with a hydrogen as in **63c** resulted in a significant decrease in metabolic stability ($t_{½}$ = 5 min), which may be due to the increased susceptibility of the styryl ring to be hydroxylated by CYP450 at the 4-position.[215, 234] Meanwhile, the introduction of an ethoxy group at this position as in **63a** had no effect on the microsomal stability ($t_{½}$ = 16 min).

Interestingly, the introduction of an ethoxy group on the 2-position of the styryl ring of **63b** significantly increased the metabolic stability of the compound despite the reduction in polarity of the molecule. Replacement of the methoxy group at this position in **49** with an ethoxy significantly prolonged the half-life as the latter is less susceptible to dealkylation compared to methoxy. In contrast, the opposite effect was observed in its counterpart **41b** whereby the introduction of an ethoxy at the 2-position of the styryl ring resulted in a significant decrease in stability. This indicates that this strategy of replacing a methoxy with an ethoxy to improve stability is only viable at positions where the methoxy is highly susceptible to demethylation.

3.8 Caco-2 permeability assay

Caco-2 permeability assay was conducted on **49** and **50a**, with the results summarized in **Table 3.4**. Similar to **17** (*vide supra*, section 2.7), **49** was demonstrated to have high permeability across the cell membrane (P_{app}A-B of 42.3 × 10^{-6} cm/s) and low susceptibility to active transport (efflux ratio < 1). In contrast, **50a** was found to have a relatively high efflux ratio efflux ratio = 16.9).

Table 3.4: Caco-2 permeability of 49 and 50a[a]

Compound	49	50a
P_{app} A-B (10^{-6} cm/s)	33.1	3.15
P_{app} B-A (10^{-6} cm/s)	26.2	53.4
Efflux ratio	0.79	16.9

[a] Performed by Cyprotex (Macclesfield, UK)

3.9 Pharmacokinetic studies

Pharmacokinetic studies of **49**, **50a**, and **63b** were conducted on rats to determine their drug clearance and oral bioavailability. The intravenous (IV) pharmacokinetic profiles were evaluated in rats following a single IV dose of 5 or 10 mg/kg, while the oral profiles were evaluated following an oral dose of 10 and/or 40 mg/kg.The plasma concentrations were measured using LC/MS and the results used to calculate the parameters are listed in **Table 3.5**.

In general, both compounds **49** and **50a** were found to have good half-lives and bioavailabilities,[264] with compound **50a** exhibiting a high bioavailability of 69%. Compound **49** was also found to have a significantly longer half life compared to **7**, indicating that **49** is less susceptible to drug elimination. The relatively low $AUC_{0\text{-}t}$ of **49** compared to **50a** is attributed to its relatively high volume of distribution (V_d) (V_d = 17) compared to that of **50a** (V_d = 3) as the AUC is inversely proportional to V_d. Increasing the oral dose of **49** from 10 to 40 mg/kg resulted in a ten-fold increase in half-life, as well as a slight increase in bioavailability. The same observation was also observed with **17** whereby the administration of the same oral dose resulted in a significant increase in half-life.

Compared to the impressive pharmacokinetic results of **49**, **63b** was found to have a significantly shorter half-life and bioavailability. The relatively low oral bioavailability ($F_{0\text{-}t}$ = 10%) of **63b** is attributable to the introduction of the ethoxy group which decreases the water solubility of the compound. In contrast, the hydrophilic **50a** has a much higher bioavailability ($F_{0\text{-}t}$ = 69%), indicating that water solubility of the compound has a significant impact on the bioavailability of these compounds.

Table 3.5: Rat pharmacokinetic comparison of IV and orally administered 49, 50a, and 63b[a]

Compound	Dose	Cmax (μM)	AUC_{0-t} (μM·h)	Half-life $t_{½}$ (h)	Bioavailability F_{0-t} (%)
49	IV 10 mg/kg	5.0	13.3	6.5	N/A
	Oral 10 mg/kg	0.9	4.6	7.5	34.9
	Oral 40 mg/kg	2.5	23.1	77.1	43.5
50a	IV 5 mg/kg	28.6	44.4	2.6	N/A
	Oral 10 mg/kg	10.8	64.4	2.7	69.4
63b	IV 5 mg/kg	26.9	19.4	2.1	N/A
	Oral 10 mg/kg	0.4	3.7	29	10

[a] Performed by Peng Li and Longjin Zhong

3.10 *In vivo* efficacy studies

The *in vivo* efficacy of **49** was subsequently studied using a human tumour xenograft model. This model is used for determining the efficacy and toxicities of anticancer agents before further clinical studies.[265] In the study of **49**, an oral dose of 50 mg/kg was administered to the A2780 tumour xenograft model in nude mice every 48 hours for two weeks. Cisplatin, a platinum based anticancer agent which induces G_2/M arrest in cancer cells,[266] was selected as a positive control to compare its efficacy and toxicity with **49**. Cisplatin was administered as a weekly dose of 4 mg/kg by intraperitoneal (IP) injection. The survival of the treated mice was also evaluated using a Kaplan-Meier analysis, an analytical method used to measure the survival of test animals during drug treatment.[267-268]

Adminstration of oral **49** was found to result in a significant 52% delay in tumour growth compared to the vehicle group (**Figure 3.14**), with the delay in tumour growth similar to the delay observed with cisplatin administration (49% delay). Both cisplatin and **49** also significantly increased the survival of the tested mice compared to the controls, with an increase in life span of 80% (median day of death = 9 days) observed compared to the control (median day of death = 5 days) (**Figure 3.15**). Adminstration of **49** on the mice was also found to be well tolerated, with no toxicity issues observed. These results indicated the anticancer efficacy of **49** when administered orally.

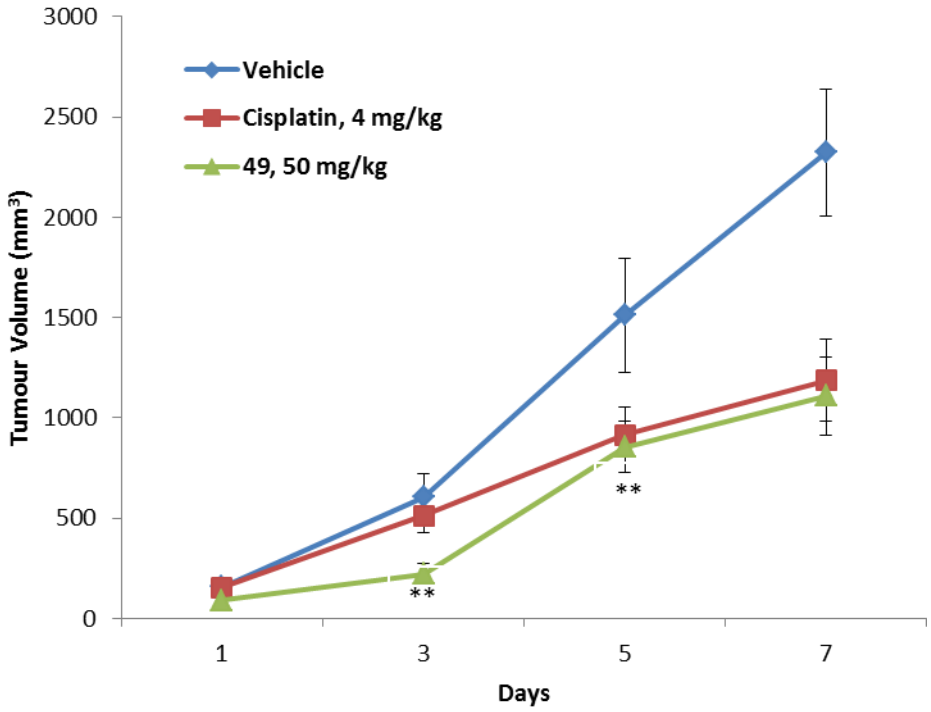


Figure 3.14: *In vivo* antitumour activity of **49** in an A2780 ovarian cancer xenograft model. Groups of eight animals bearing A2780 tumours were administered: vehicle 5% NMP/PEG400 (♦) or **49** at 50 mg/(kg·dose) (▲) by oral gavage (po) on every second day (days: 1, 3, 5 and 7). The positive control chemotherapy agent cisplatin was given by intraperitoneal injection (IP) at 4 mg/kg (■). A significant tumour growth delay was observed with the animals treated with **49** (**P < 0.01 on days 3 and 7) and with cisplatin at 4 mg/kg (**P = 0.01 on day 7 only) when compared to the vehicle control group. (Performed by Julian Adams)

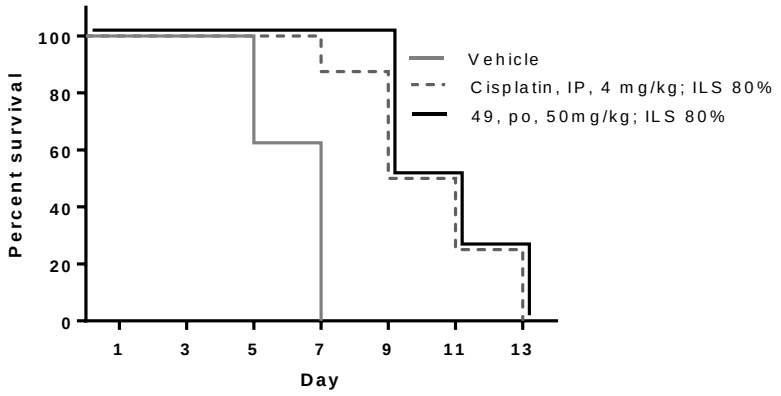


Figure 3.15: Kaplan−Meier analysis of animal survival in an A2780 ovarian cancer xenograft model treated with compound **49**. Groups of eight animals were administered either vehicle (gray solid line) or **49** at 50 mg/kg·dose (black line) on every second day (days: 1, 3, 5, 7, 9 and 11). Meanwhile, cisplatin (dashed gray line) was given at 4 mg/kg by weekly intraperitoneal injections (days 1 and 8). Treatment with **49** resulted in an increased life span (ILS) of 80% (median day of death = 9 days) when compared to the vehicle-treated group (median day of death = 5 days). Cisplatin treatment also showed a significantly increased animal life span (ILS = 80%). (Performed by Julian Adams)

3.11 **Conclusion**

In the continuous effort of developing styrylsulfonyl-methylpyridine derivatives with improved pharmacokinetic properties, the attention of this research shifted to the development of (*E*)-2-((styrylsulfonyl)methyl)pyridine derivatives.The synthesis of (*E*)-2-((styryl-sulfonyl)methyl)pyridine derivatives was described in this chapter. Modification at the R^1, R^2 and R^3 positions were conducted to study the SAR of substituents at these positions.

Evaluation of the antiproliferative activity using MTT assays led to identification of **49**, **59a** and **63b** which displayed potent antiproliferative activity. Evaluation of the cellular mechanism of action of these compounds using flow cytometry based assays indicates their ability to induce G_2/M arrest and apotosis. Preliminary western blot studies on **49** have shown its ability to inhibit PLK1, though further studies will need to be conducted to assess its activity on PLK1.

In vivo pharmacokinetic studies conducted on **49** demonstrated good oral bioavailability and drug clearance, with its elimination half-life significantly higher than its counterpart **7**. Similar to **17**, **49** was also found to have low susceptibility to the effects of efflux proteins. Meanwhile, **63b** was found to have low bioavailability and mediocre elimination half-life despite its high stability in microsomal preparations.

Compound **49** was subsequently evaluated for its *in vivo* anticancer activity in the A2780 tumour xenograft model in nude mice. Oral administration of **49** to treatment animals resulted in reduction in tumour growth and improvement in animal survival, with comparable efficacy to IV administered cisplatin. The results indicate the future potential for the development of **49** as an orally bioavailable anticancer agent.

4 Conclusions and future work

4.1 Conclusions

ON01910 is a type III multikinase inhibitor that is highly selective towards cancer cells, although it is plagued with poor pharmacokinetic properties including bioavailability and drug clearance. The main aim of this research was to develop novel styrylsulfonyl-methylpyridine derivatives that mimic the anticancer activity of ON01910 while having superior pharmacokinetic properties.

The introduction of a pyridine ring in the compounds was conducted to increase the water solubility of the compounds and to decrease the occurrence of CYP450 metabolism on the compound. The first series of derivatives that was developed is the (*E*)-3-((styrylsulfonyl)methyl)pyridine compounds. A series of synthetic schemes was developed and employed for the synthesis of these compounds. The derivatives were synthesised *via* the Verley-Doebner modification of Knoevenagel condensation of the pyridinylmethylsulfonyl acetic acid derivatives with substituted benzaldehydes, with subsequent synthetic steps to introduce functionality. The pyridinylmethylsulfonyl acetic acid derivatives were synthesised *via* the nucleophilic reaction between the bromomethyl derivatives with methylthioglycolate, with subsequent oxidation and ester hydrolysis to produce the acetic acid derivatives.

The first key position that was investigated was the R^1 position. Initial structure activity relationship (SAR) studies on the R^1 position led to the identification of **17** which was found to be significantly more potent than ON01910. Introduction of a primary amino group at this position was found to be essential for potent anticancer activity. The MTT assay of **17** on a variety of cell lines demonstrates its selectivity towards cancer cells.

Meanwhile, the investigation of the R^3 position indicates that the 2,4,6-trimethoxy moiety in **17** is necessary for optimum activity.

To assess the pharmacokinetic properties of **17**, a microsomal stability assay and an *in vivo* pharmacokinetic study using rats were conducted on these compounds. Although **17** was found to have low stability in rat liver microsomes, subsequent *in vivo* assays in rats exhibited superior pharmacokinetic properties compared to ON01910. Caco-2 assays on **17** also demonstrated the non-susceptibility of these compounds to the effects of efflux proteins.

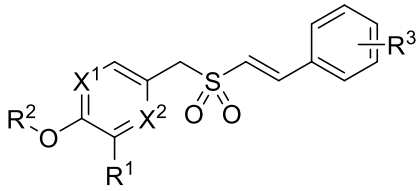


Figure 4.1: General structure of synthesised analogues.

The (*E*)-2-((styrylsulfonyl)methyl)pyridine analogues were subsequently developed to investigate the effect of changing the nitrogen position of the pyridine ring from the X^1 to the X^2 position. A selection of substituents was introduced at the key R^1, R^2, and R^3 positions to investigate the SAR at these positions. Similar to the (*E*)-3-((styrylsulfonyl)methyl)pyridine derivatives, the primary amino group is essential at the R^1 position for optimum antiproliferative activity. The primary amine analogue **49** was found to have comparable activity to **17**. At the R^2 position, methoxy (**49**) and ethoxy (**59a**) groups gave potent activity. Increasing the substituent size beyond that of an ethoxy group resulted in a significant drop in activity. Meanwhile, substitution of the R^3 position with 2,4,6-trimethoxy (**49**) or 2-ethoxy-4,6-methoxy (**63b**) moieties gave similar activity.

Further biological studies on **49**, **59a**, and **63b** indicated their ability in inducing G_2/M arrest and apoptosis. Pharmacokinetic studies conducted on **17** displayed good oral bioavailability while possessing low susceptibility to efflux proteins. Furthermore, **49** was found to be less susceptible to drug elimination compared to **17**. Although **63b** was found to be highly stable in the microsomal stability assay, *in vivo* pharmacokinetic studies demonstrated its poor oral bioavailability and mediocre half life. It can be deduced that the introduction of the more lipophilic ethoxy group resulted in a

significant drop in bioavailability, further indicating the importance of water solubility in the bioavailability of the compounds. *In vivo* efficacy studies conducted on the A2780 human tumour xenograft model also showed the ability of **49** in reducing tumour growth and improving treatment animal survival, with comparable activity to cisplatin. These results indicate the future potential of **49** as an orally bioavailable drug for the treatment of cancer.

4.2 Future work

Although preliminary western blot studies on **49** indicated its activity on PLK1, further studies will need to be conducted to elucidate its ability to inhibit the PBD of PLK1. To quantitatively measure the inhibition of the PBD, an enzyme-linked immuno-sorbent assay (ELISA) based PLK1 PBD competition assay which measures the competition between the inhibitor and PBIP1,[269-271] a protein that binds to the PBD of PLK1, can be employed.[272] To investigate the binding of the compounds to the PBD, computer based molecular docking which predicts the binding pose of the inhibitor can be utilized. Due to the flexibility of the binding site of the PBD,[273] an induced fit docking method, which accounts for structural changes of the protein during ligand binding, would be more suitable compared to conventional docking methods which assume that the protein is rigid.[274] Alternatively, advanced techniques such as molecular dynamic simulations, which take into consideration the full range of atomic motions in the protein, can be used.[275] These simulations can predict the binding energies of the ligands fairly accurately, allowing direct comparison between experimental competition assays and computations. Preliminary docking studies of **49** conducted by Kumarasiri *et al.* from our laboratory (unpublished results) have identified several amino acid residues of the PBD that may interact with **49** (**Figure 4.2**). The methoxy, sulfonyl oxygen, and amino groups of **49** were found to interact with amino acid residues including Leu491, Lys540, His538, and Trp414 *via* hydrogen bonding.

It has recently been revealed that ON01910 binds to the RAS-binding domain (RBD) and thus disrupts the interactions of RAS proteins and its effector proteins.[276] The finding has a significant impact on the development of ON01910 for RAS targeted cancer therapy. RAS proteins are members of a superfamily of GTP-binding proteins and are involved in the modulation of several pathways including the RAF/MEK/ERK

and the PI3K/AKT/mTOR pathways that regulate cell growth. Dysregulation of RAS signalling is found in 20% of human cancers.[277-279] Although RAS is an attractive target for the treatment of cancer, the development of direct inhibitors of RAS is challenging due to difficulties in blocking the nucleotide binding site of RAS.[280] Current strategies in disrupting the RAS signaling cascade in cancers are mainly concentrated on inhibiting downstream effector proteins (e.g. PI3K, AKT, and MEK). The development of farnesyltransferase inhibitors (FTI) is another strategy employed by pharmaceutical companies, as the farnesylation of RAS (catalysed by farsenyltransferase) is essential for its association with the plasma membrane.[281] However, results of clinical trials with FTIs have been disappointing due to a lack of anticancer activity *in vivo*.[282] Furthermore, it was subsequently discovered that KRAS, the RAS isoform most commonly mutated in cancer, can still associate with the plasma membrane via a compensatory mechanism involving the attachment of geranylgeranyl (catalysed by geranylgeranyltransferase 1) to its structure.[283]

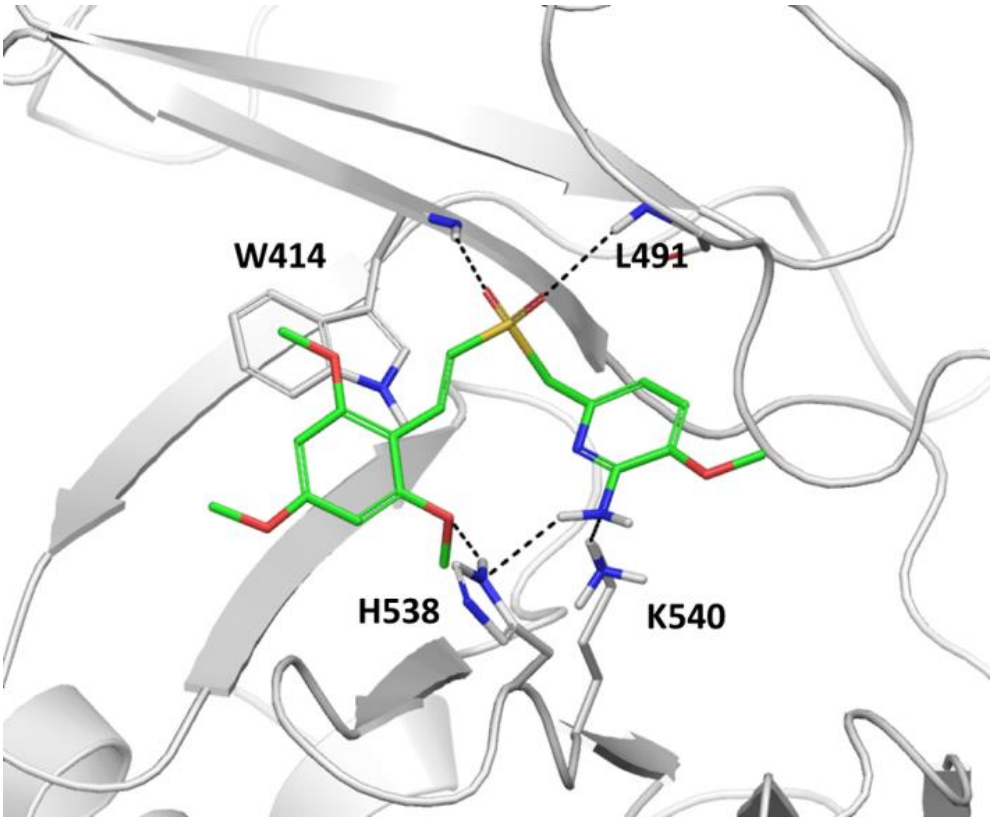


Figure 4.2: Binding model of **49** on the PBD of PLK1 (Schrödinger Suite). Amino acid residues including Leu491, Lys540, His538, and Trp414 were found to form hydrogen bonds with moieties of **49** including the methoxy, sulfonyl oxygen, and amino groups.

ON01910 was shown to bind to the RBD of effector proteins including the rapidly accelerated fibrosarcoma (RAF) (A-RAF, B-RAF, and C-RAF) and PI3K (PI3Kα, PI3Kβ, and PI3Kγ) isoforms.[284] NMR spectroscopic analysis structure elucidation of the complex between ON01910 and B-RAF has shown that ON01910 binds to the RBD of B-RAF in two different orientations which are complex I and II (**Figure 4.3A**). In complex I, the trimethoxystyryl moiety interacts with several amino acid residues of helix α1 (Lys183, Ala184, Met187, and Arg187) and strand β2 (Arg166, Thr167, and Val169), with Leu161 of the β1 interacting with a methoxy group (**Figure 4.3B**). Meanwhile, the methoxy benzyl sulfone moiety interacts with Lys154 and Ile156 of strand β1 and Val168 and Pro170 of strand β2. In complex II, inversion of ON01910 in the RBD relative to the orientation in complex I results in interaction between the trimethoxystyryl moiety with amino acid residues of strands β1 (Lys154 and Ile156) and β2 (Val168, Val169, and Pro170), with Lys183 of the helix α1 forming contact with a methoxy. The methoxy benzyl sulfone portion forms contacts with several amino acid residues of strand β1 (Leu161), strand β2 (Arg166, Thr167, and Val168), and helix α1 (Met187 and R188). The NH group of ON01910 also forms hydrogen bonds with Arg166 while the glycine moiety forms a salt bridge with Arg188. It is currently unknown whether the amino and hydroxyl groups of the more potent ON01500 and ON013100 have any specific intermolecular interactions with amino acid residues. While the amino and hydroxyl groups of these compounds may be involved in hydrogen bonding as seen in the NH group of ON01910, anticancer potency is also dependent on other factors including solubility and cell permeability. Therefore, binding studies on ON01500 and ON013100 are needed to truly understand the binding affinities of this series of compounds.

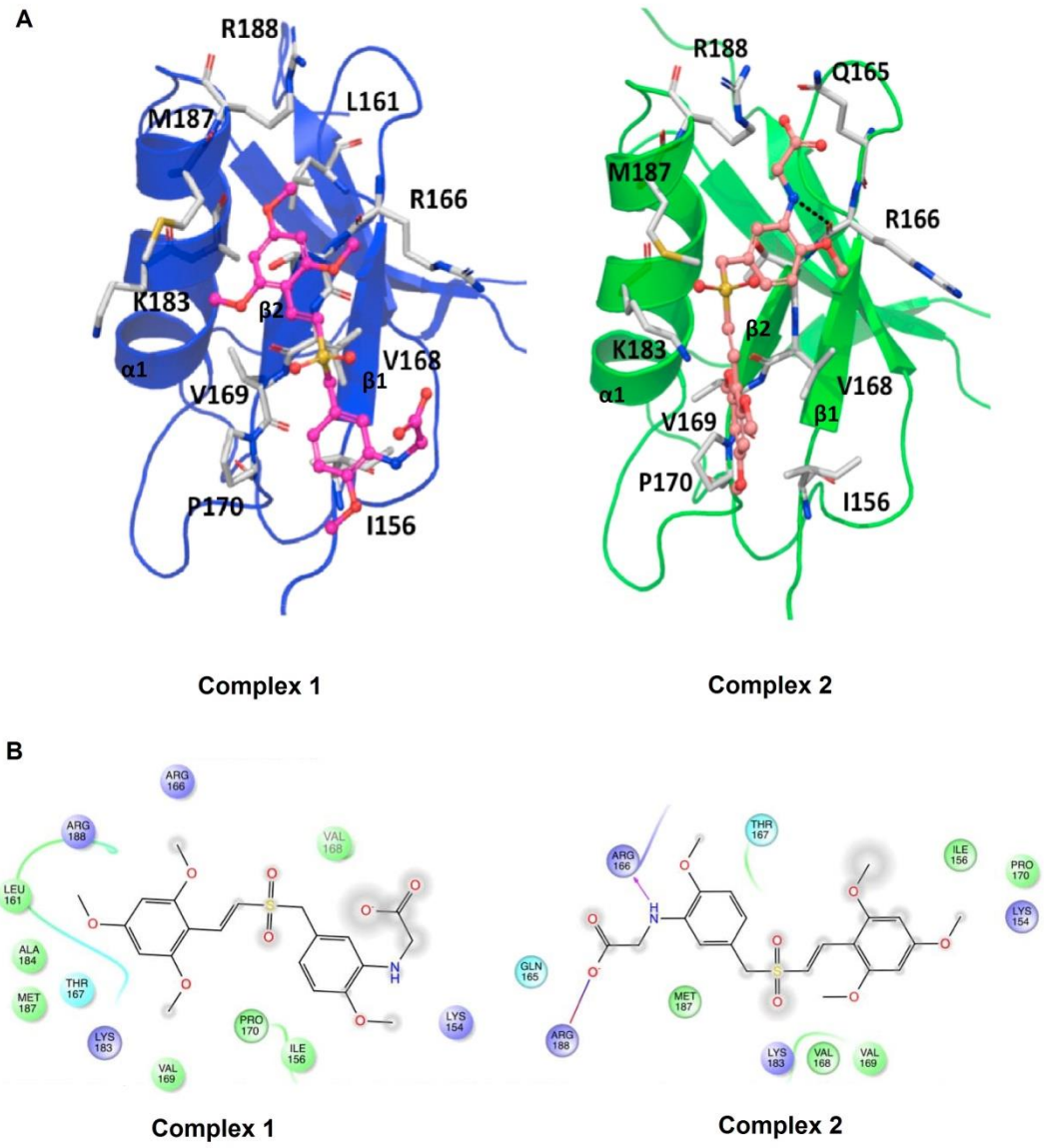


Figure 4.3: (A) The lowest energy structure of the RBD of B-RAF with ON01910 in complex I and II. (B) Interactions of ON01910 with the amino acid residues of the RBD in complex I and II. Charged residues are highlighted in indigo, polar in skyblue, and hydrophobic in green. Hydrogen binding is highlighted in purple while the salt bridge is highlighted in red/blue.[276] (Reprinted with permission from Cell, April 2016, Vol. 165, Pages 643–655.[276] Copyright (2016) Elsevier.)

As both ON01910 and our styrylsulfonyl-methylpyridine derivatives share a similar scaffold, it is likely that the styrylsulfonyl-methylpyridine derivatives possess similar abilities in blocking the RBD of effector proteins. Preliminary docking studies conducted by Kumarasiri *et al.* (unpublished results) have suggested that **49** displayed a similar mode of binding within the RBD of B-RAF compared to ON01910. As shown in

Figure 4.4, the 4-methoxy group of the styryl ring forms hydrogen bonding with Lys154 while the amino group of the pyridine ring interacts with Arg166 and Thr167. However, advanced modelling or experimental structure studies, including x-ray crystallography or NMR studies, are needed to generate a satisfactory binding hypothesis. The binding affinity of **49** to the RBD of effector proteins can be determined initially using microscale thermophoresis, a technique based on the directed motion of molecules in microscopic temperature gradients.[285-286] This technique allows the quantification of the interaction between protein and ligand as the thermophoresis of a ligand bound protein differs from the thermophoresis of an unbound protein.[287-288]

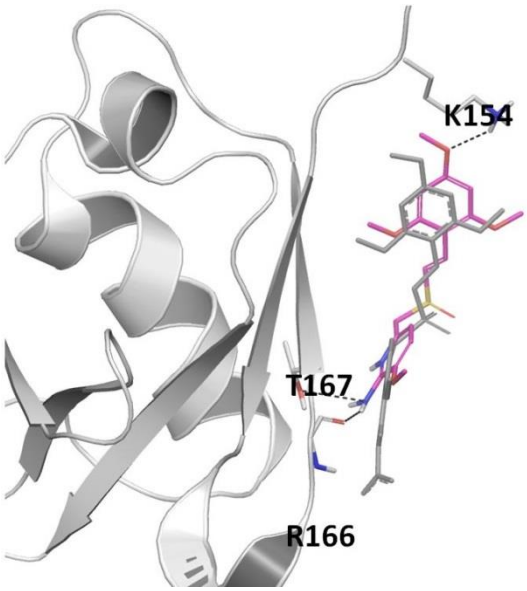


Figure 4.4: Preliminary binding model of **49** and ON01910 on the RBD of B-RAF (Schrödinger Suite). The structure of ON01910 is highlighted in grey while **49** is shown in magenta. Hydrogen bonding is representing by the dotted lines. On the styryl ring, the 4-methoxy of the styryl ring of **49** forms hydrogen bonding with Lys154. The amino moiety of **49** also forms hydrogen bonds with Arg166 and Thr167 of the RBD.

One question that still remains unanswered is the mechanism of how ON01910 and styrylsulfonyl-methylpyridine derivatives induce the cell cycle arrest at G_2/M phase. As RAF/MEK/ERK and PI3K/AKT/mTOR signalling disruption is commonly linked to G_1 arrest,[289-292] it is uncertain that the anticancer activity of **49** and ON01910 is predominantly due to RBD blockage of effector proteins. To investigate the ability of **49** in disrupting RAS signalling, western blot studies on proteins downstream of the

RAS signaling cascade including p-ERK and p-AKT will be required. A possible explanation for the potent antiproliferative activity of ON01910 and **49** is their ability to inhibit both the PI3K/AKT/mTOR and RAF/MEK/ERK pathways simultaneously. Crosstalk between the two pathways exists and negative regulation can occur (**Figure 4.5)**.[177, 293-294] The suppression of RAF activity by AKT is removed when AKT is inhibited, which leads to the activation of mTOR via the inhibition of TSC 2. Likewise, the inhibition of MEK, a protein that promotes the membrane localization of PTEN, reduces the dephosphorylation of PIP_3 which in turn leads to increased activation of AKT. Therefore, the inhibition of one pathway can lead to the activation of the other which compensates for this inhibition.

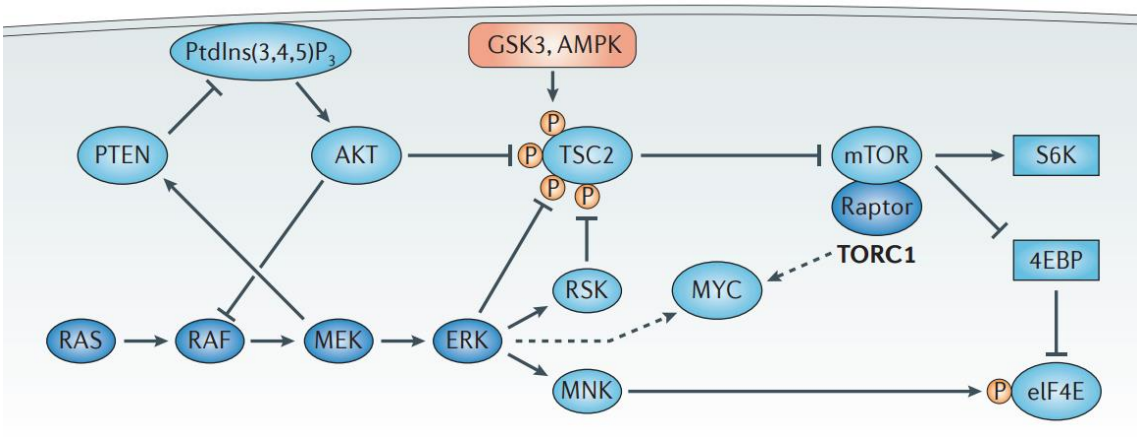


Figure 4.5: Crosstalk between the PI3K/AKT/mTOR and RAF/MEK/ERK signalling pathways. Inhibition of PI3K/AKT leads to the removal of the suppressive effect of AKT on RAF, leading to activation of the RAF/MEK/ERK signalling cascade. Likewise, inhibition of MEK activity results in PTEN activity reduction, causing enhanced AKT signalling. Activation of these pathways leads to the activation of mTOR. (Reprinted with permission from Nature Reviews Drug Discovery, February 2014, Vol. 13, Pages 140-156.[293] Copyright (2014) Nature Publishing Group.)

Other proteins that warrant investigation include p53 and the anti-apoptotic mouse double minute 2 homolog (mdm2), a protein that promotes the degradation of the apoptotic p53. The activity of mdm2 can be promoted by the activation of RAF/MEK/ERK[295-296] and the PI3K/AKT[297-299] pathways, which are both activated by RAS. As the inhibition of mdm2 activity is able to induce G_2 arrest,[300-301] it is worth investigating whether the expression of mdm2 and p53 are affected by **49**. Indeed,

preliminary Western blot studies on cells treated with **49** (*vide supra*, section 3.6) have exhibited reductions in CDC25C, a protein that is downregulated by p53.[257]

Kinase studies conducted on **49** have indicated its inhibitory activity against CDK5/p35, possibly by blocking the association of p35 with CDK5. The overexpression of CDK5/p35 has been found in a range of cancers including lung,[302] prostate,[303] and pancreatic cancers.[304] This overexpression is believed to aid in cancer cell motility and invasion, enhancing the metastatic potential of these cells.[305-306] Furthermore, inhibition of CDK5 activity in pancreatic cancer cells reduced cell migration in an *in vitro* migration assay and pancreatic cancer xenograft model.[307] Blocking CDK5 has been demonstrated to inhibit the RAS-RAL signaling pathway, a pathway involved in the metastatic potential of pancreatic cancer cells.[307] Moreover, treatment of CDK5 dependent pancreatic MIAPaCa-2 cancer cells with a combination of a CDK5 inhibitor with either a MEK or PI3K inhibitor resulted in a significant decrease in tumour growth compared to treatment with either inhibitor alone. However, it is currently unknown how CDK5 regulates the signaling of the RAS-RAL pathway. Nevertheless, the ability of **49** to inhibit the activity of CDK5/p35 is an interesting focus for future studies.

5 Experimental

5.1 Chemistry

All reagents and solvents were purchased from commercial sources, and were used as received unless otherwise specified. All reactions were carried out with continuous magnetic stirring in standard glassware. ^{1}H and ^{13}C NMR spectra were recorded at 295 K on a Bruker AVANCE III 500 spectrometer (^{1}H at 500 MHz and ^{13}C NMR at 125 MHz), and were processed using the Bruker Topspin 3.2 software. ^{1}H and ^{13}C NMR spectra are referenced to ^{1}H signals of residual nondeuterated solvents (or tetramethylsilane) and ^{13}C signals of the deuterated solvents respectively. ^{1}H NMR signals are reported with chemical shift values δ (ppm), multiplicity (s = singlet, d = doublet, t = triplet, q = quartet, m = multiplet and br = broad, dd = doublet of doublets, tt = triplet of triplets, app = apparent), relative integral, coupling constants *J* (Hz) and assignments. High resolution mass spectra (HRMS) were recorded on an AB SCIEX TripleTOF® 5600 mass spectrometer, and ionisation of all samples was carried out using ESI. Melting points (m.p.) were determined on a Stuart SMP10 melting point apparatus, and are uncorrected.

Analytic TLC was performed on Merck silica gel 60 F_{254} pre-coated aluminium plates (0.2 mm) and visualised under UV light (254 nm). Flash column chromatography, Biotage® FlashMaster Personal+ flash chromatography and Biotage® Isolera™ Four automated flash chromatography were performed using either Davisil silica gel 60 Å (0.040-0.063 mm) or Biotage® SNAP cartridges pre-packed with silica gel KP-SIL (ca. 0.050 mm). The purity of compounds used for biological assays were tested using analytical high performance liquid chromatography (HPLC) and were greater than 95%.

Analytic HPLC was performed on a Shimadzu Prominence ultrafast liquid chromatography (UFLC) system with a CBM-20A communications bus module, a DGU-20A5R degassing unit, an LC-20AD liquid 539 chromatograph pump, an SIL-20AHT autosampler, an SPD-M20A photo diode array detector, a CTO-20A column oven, and a Phenomenex Kinetex 5u C18 100A 250 mm × 4.60 mm column using method A (gradient 5−95% MeOH containing 0.1% FA over 7 min, followed by 95% MeOH containing 0.1% FA over 13min at a flow rate of 1mL/min) or method B (gradient 5−95% MeCN containing 0.1% FA over 7 min followed by 95% MeCN containing 0.1% FA over 13 min, at a flow rate of 1 mL/min).

General synthetic procedure A: Oxidation of thioether

To a solution of thioether (1.0 equiv.) in CH_3CO_2H was added 30% H_2O_2 (4.0 equiv.). The reaction mixture was heated at 50-60 °C for 4-12 h and concentrated under reduced pressure. The residue was either triturated with EtOH or purified with flash column chromatography to give the desired product.

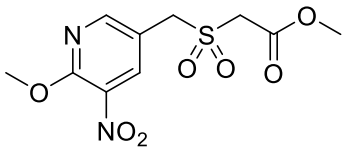
General synthetic procedure B: Verley-Doebner modification of the Knoevenagel condensation of carboxylic acids with benzaldehydes

To a solution of carboxylic acid (1.0 equiv.) in toluene was added benzaldehyde (1.1 equiv.), benzoic acid (0.15 equiv.), and piperidine (0.13 equiv.). The reaction mixture was heated at reflux for 2-4 h and concentrated under reduced pressure. The residue was purifiried either by washing with MeOH or flash column chromatography to give the desired product.

General synthetic procedure C: Reduction of nitro compounds to amines using iron powder

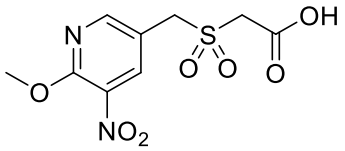
To a solution of nitro compound (1.0 equiv.) in MeOH/CH_3CO_2H was added iron powder (8.0 equiv.). The reaction mixture was heated at 50 °C for 2-3 h under a flow of N_2 and concentrated under reduced pressure. The residue was dissolved in CH_2Cl_2, and 1 M NaOH was added. The precipitate was removed by centrifugation. The aqueous layer was separated and extracted with CH_2Cl_2. The organic layer and extracts were combined, dried over $MgSO_4$, and concentrated under reduced pressure. The residue was purified either by washing with EtOAc, recrystallization, or flash column chromatography to give the desired product.

methyl 2-(((6-Methoxy-5-nitropyridin-3-yl)methyl)sulfonyl)acetate (13)



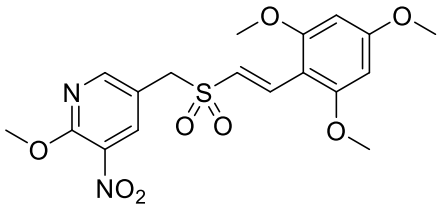
To a solution of 5-(bromomethyl)-2-methoxy-3-nitropyridine (5.00 g, 20.2 mmol) in MeOH (150 mL) was added Na_2CO_3 (2.57 g, 24.3 mmol) and methyl thioglycolate (2.00 mL, 21.6 mmol). The reaction mixture was stirred at room temperature for 2 h and concentrated under reduced pressure. The residue was diluted with EtOAc (500 mL), filtered, and the filtrate concentrated under reduced pressure. The residue was added 30% H_2O_2 (8.35 mL, 83.6 mmol) and CH_3CO_2H (85.0 mL). The mixture was heated at 60 °C for 14 h and concentrated under reduced pressure. The residue was triturated with EtOH (300 mL) and filtered to give **13** as a white solid (4.88 g, 79%). m.p. 137-138 °C. ^{1}H NMR (500 MHz, $CDCl_3$) δ 3.81 (s, 3H, $COOCH_3$), 3.82 (s, 2H, SO_2CH_2CO), 4.08 (s, 3H, pyridine-OCH_3), 4.50 (s, 2H, pyridine-CH_2SO_2), 8.35 (d, 1H, J = 2.0, pyridine-H), 8.43 (d, 1H, J = 2.5, pyridine-H). ^{13}C NMR (125 MHz, DMSO-d_6) δ 52.7, 54.0, 54.3, 54.5, 115.6, 132.8, 136.1, 152.4, 156.0, 162.6. HRMS (ESI) *m/z* 305.0437 $[M+H]^+$; calcd. for $C_{10}H_{13}N_2O_7S$ $[M+H]^+$ 305.0438.

2-(((6-methoxy-5-nitropyridin-3-yl)methyl)sulfonyl)acetic acid (14)



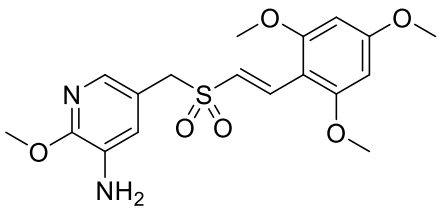
To a solution of compound **13** (11.0 g, 36.2 mmol) in MeOH/H_2O (1:1, 600 mL) was added Na_2CO_3 (4.18 g, 39.4 mmol). The reaction mixture was stirred at room temperature for 12 h and concentrated under reduced pressure. The residue was diluted with 1 M HCl (50 mL) and extracted with EtOAc (3 × 300 mL). The extracts were combined, dried over MgSO4 and concentrated under reduced pressure to give **14** as a light brown solid (10.2 g, 98%). m.p. 174-176 °C. ^{1}H NMR (500 MHz, $CDCl_3$) δ 4.06 (s, 3H, OCH_3), 4.30 (s, 2H), 4.78 (s, 2H) (total 4H, $CH_2SO_2CH_2$), 8.48 (d, 1H, J = 2.0, pyridine-H), 8.50 (d, 1H, J = 2.0, pyridine-H), 13.58 (s, 1H, COOH). ^{13}C NMR (125 MHz, DMSO-d_6) δ 55.1, 55.4, 57.2, 118.5, 133.7, 138.0, 154.3, 156.2, 164.9. HRMS (ESI) *m/z* 291.0280 $[M+H]^+$; calcd. for $C_9H_{11}N_2O_7S$ $[M+H]^+$ 291.0281.

(*E*)-2-methoxy-3-nitro-5-(((2,4,6-trimethoxystyryl)sulfonyl)methyl)pyridine (16)



Compound **14** (14.5 g, 50.0 mmol) and 2,4,6-trimethoxybenzaldehyde (10.8 g, 55.0 mmol), benzoic acid (0.915 g, 7.50 mmol) and piperidine (642 µL, 6.50 mmol). were reacted using general synthetic procedure B. The residue was washed with MeOH (300 mL) and CH_3CO_2H (200 mL) to give **16** as a pale brown solid (8.70 g, 41%). m.p. 185-188 °C. ^{1}H NMR (500 MHz, $CDCl_3$) δ 3.85 (s, 6H), 3.86 (s, 3H), 4.03 (s, 3H) (total 12H, 4 × OCH_3), 4.63 (s, 2H, CH_2), 6.29 (s, 2H, benzene-H), 7.09 (d, 1H, J = 15.5, SO_2CH=CH), 7.46 (d, 1H, J = 15.5, SO_2CH=C*H*), 8.44 (d, 1H, J = 2.0, pyridine-H), 8.45 (d, 1H, J = 2.0, pyridine-H). ^{13}C NMR (125 MHz, DMSO-d_6) δ 55.4, 56.1, 56.6, 91.4, 102.8, 120.0, 122.7, 133.4, 135.3, 137.8, 154.2, 156.0, 161.5, 164.5 (four carbon signals overlapping or obscured). HRMS (ESI) *m/z* 425.0991 $[M+H]^+$; calcd. for $C_{18}H_{21}N_2O_8S$ $[M+H]^+$ 425.1013. Anal. RP-HPLC: t_R = 13.24, purity >97% (method A); t_R = 11.18, purity >97% (method B).

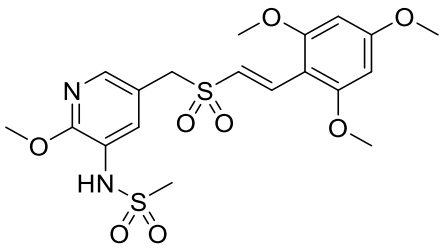
(*E*)-2-methoxy-5-(((2,4,6-trimethoxystyryl)sulfonyl)methyl)pyridin-3-amine (17)



Nitro compound **16** (5.00 g, 11.8 mmol) was reduced using general synthetic procedure C. The residue was washed with EtOAc (200 mL) to give **17** as a white solid (3.15 g, 68%). m.p. 170−172 °C. ^{1}H NMR (500 MHz, DMSO-d_6) δ 3.84 (s, 3H), 3.85 (s, 3H), 3.86 (s, 6H) (total 12H, 4 × OCH_3), 4.27 (s, 2H, CH_2), 5.04 (s, 2H, NH_2) 6.30 (s, 2H, benzene-H), 6.88 (s, 1H, pyridine-H), 7.09 (d, 1H, J = 15.5, SO_2CH=CH), 7.28 (s, 1H, pyridine-H), 7.57 (d, 1H, J = 15.5, SO_2CH=C*H*). ^{13}C NMR (125 MHz, DMSO-d_6) δ 53.4, 56.1, 56.6, 57.8, 91.4, 103.0, 119.0, 121.2, 123.9, 132.5, 133.5, 134.8, 152.3, 161.4, 164.1 (three carbon signals overlapping or obscured). HRMS (ESI) *m/z* 395.1250

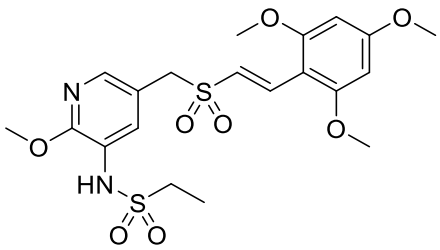
$[M + H]^+$; calcd. for $C_{18}H_{23}N_2O_6S$ $[M+H]^+$ 395.1271. Anal. RP-HPLC: t_R = 12.69 min, purity >98% (method A); t_R = 10.35 min, purity >98% (method B).

(*E*)-N-(2-methoxy-5-(((2,4,6-trimethoxystyryl)sulfonyl)methyl)pyridin-3-yl)methanesulfonamide (18a)



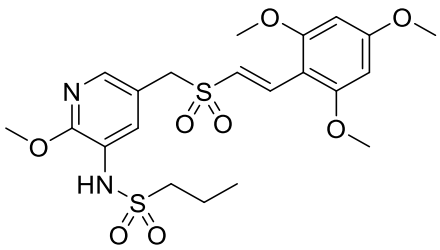
To a solution of compound **17** (1.00 g, 2.54 mmol) in anhydrous pyridine (25 mL) at 0 °C was added dropwise methanesulfonyl chloride (400 µL, 5.17 mmol). The reaction mixture was stirred at room temperature for 13 h and concentrated under reduced pressure. The residue was dissolved in CH_2Cl_2 (150 mL) and washed with H_2O(3 × 30 mL). The organic phase was concentrated under reduced pressure, and the residue was purified by an Isolera Four automated flash chromatography system using a 50 g KP-SIL SNAP flash cartridge (silica gel, EtOAc/hexane = 0:100 ramping to 100:0) to give **18a** as a white solid (0.914 g, 76%). m.p. 211−212 °C. ^{1}H NMR (500 MHz, DMSO-d_6) δ 2.96 (s, 3H, SO_2CH_3), 3.85 (s, 3H), 3.86 (s, 6H), 3.90 (s, 3H) (total 12H, 4 × OCH_3), 4.47 (s, 2H, CH_2), 6.29 (s, 2H, benzene-H), 7.12 (d, 1H, *J* = 15.5, SO_2C*H*=CH), 7.54 (d, 1H, *J* = 15.5, SO_2CH=C*H*), 7.65 (d, 1H, *J* = 2.5, pyridine-H), 7.91 (d, 1H, *J* = 2.0, pyridine-H), 9.25 (s, 1H, $NHSO_2$). ^{13}C NMR (125 MHz, DMSO) δ 53.7, 55.7, 56.1, 56.4, 91.0, 102.5, 118.8, 121.0, 122.9, 133.5, 133.8, 144.4, 156.2, 161.1, 163.9 (four carbon signals overlapping or obscured). HRMS (ESI) *m/z* 473.1061 $[M + H]^+$; calcd. for $C_{19}H_{25}N_2O_8S_2$ $[M+H]^+$ 473.1047. Anal. RP-HPLC: t_R = 12.74 min, purity >98% (method A); t_R = 10.16 min, purity >97% (method B).

(*E*)-N-(2-methoxy-5-(((2,4,6-trimethoxystyryl)sulfonyl)methyl)pyridin-3-yl)ethanesulfonamide (18b)



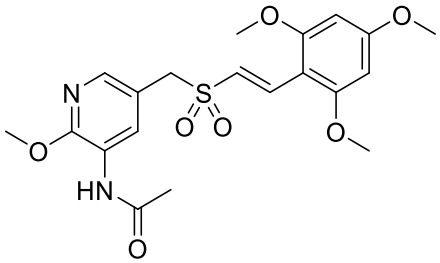
To a solution of compound **17** (59 mg, 0.15 mmol) in anhydrous pyridine (3 mL) at 0 °C was added dropwise ethanesulfonyl chloride (28 μL, 0.30 mmol). The reaction mixture was stirred at room temperature for 12 h and concentrated under reduced pressure. The residue was dissolved in CH_2Cl_2 (30 mL) and washed with H_2O (3 × 10 mL). The organic phase was concentrated under reduced pressure, and the residue was purified by FlashMaster Personal$^+$ flash chromatography (silica gel, CH_2Cl_2/acetone = 99:1 ramping to 94:6) to give **18b** as a white solid (61 mg, 84%). m.p. 130−131 °C. ^{1}H NMR (500 MHz, $CDCl_3$) δ 1.25 (t, 3H, *J* = 7.5, CH_2CH_3), 3.01 (q, 2H, *J* = 7.5, CH_2CH_3), 3.83 (s, 3H), 3.84 (s, 6H), 3.99 (s, 3H) (total 12H, 4 × OCH_3), 4.16 (s, 2H, pyridine-CH_2SO_2), 6.07 (s, 2H, benzene-H), 6.77 (s, 1H, $NHSO_2$), 7.09 (d, 1H, *J* = 15.5, SO_2CH=CH), 7.77 (d, 1H, *J* = 2.0, pyridine-H), 7.80 (d, 1H, *J* = 15.5, SO_2CH=C*H*), 7.89 (d, 1H, *J* = 2.0, pyridine-H). ^{13}C NMR (125 MHz, $CDCl_3$) δ 8.2, 46.1, 54.4, 55.6, 55.9, 58.5, 90.4, 103.7, 118.7, 121.6, 122.0, 128.0, 136.4, 143.1, 153.8, 161.7, 164.2 (three carbon signals overlapping or obscured). HRMS (ESI) *m/z* 509.1007 $[M + Na]^+$; calcd. for $C_{20}H_{26}N_2NaO_8S_2$ $[M+Na]^+$ 509.1023. Anal. RP-HPLC: t_R = 10.75 min, purity >96% (method A); t_R = 10.14 min, purity >95% (method B).

(*E*)-N-(2-methoxy-5-(((2,4,6-trimethoxystyryl)sulfonyl)methyl)pyridin-3-yl)propane-1-sulfonamide (18c)



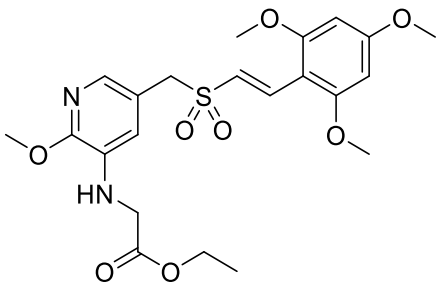
To a solution of compound **17** (59 mg, 0.15 mmol) in anhydrous pyridine (3 mL) at 0 °C was added dropwise propane-1-sulfonyl chloride (34 μL, 0.30 mmol). The reaction mixture was stirred at room temperature for 12 h and concentrated under reduced pressure. The residue was dissolved in CH_2Cl_2 (30 mL) and washed with H_2O (3 × 10 mL). The organic phase was concentrated under reduced pressure, and the residue was purified by FlashMaster Personal$^+$ flash chromatography (silica gel, CH_2Cl_2/EtOAc = 9:1 ramping to 2:1) to give **18c** as a white solid (53 mg, 71%). m.p. 139−140 °C. ^{1}H NMR (500 MHz, $CDCl_3$) δ 0.93 (t, 3H, *J* = 7.5, $CH_2CH_2CH_3$), 1.74 (m, 2H, $CH_2CH_2CH_3$), 2.95 (m, 2H, $CH_2CH_2CH_3$), 3.83 (s, 3H), 3.84 (s, 6H), 3.99 (s, 3H) (total 12H, 4 × OCH_3), 4.17 (s, 2H, pyridine-CH_2SO_2), 6.07 (s, 2H, benzene-H), 6.75 (s, 1H, $NHSO_2$), 7.10 (d, 1H, *J* = 16.0, SO_2CH=CH), 7.78 (d, 1H, *J* = 2.0, pyridine-H), 7.80 (d, 1H, *J* = 15.5, SO_2CH=C*H*), 7.89 (d, 1H, *J* = 2.0, pyridine-H). 13C NMR (125 MHz, $CDCl_3$) δ 12.8, 17.3, 53.4, 54.3, 55.6, 55.9, 58.5, 90.4, 103.7, 118.7, 121.6, 122.0, 128.1, 136.3, 143.1, 153.8, 161.7, 164.2 (three carbon signals overlapping). HRMS (ESI) 523.1141 $[M + Na]^+$; calcd. for $C_{21}H_{28}N_2NaO_8S_2$ $[M + Na]^+$ 523.1179. Anal. RP-HPLC: t_R = 11.03 min, purity >95% (method A); t_R = 10.43 min, purity >95% (method B).

(*E*)-N-(2-methoxy-5-(((2,4,6-trimethoxystyryl)sulfonyl)methyl)pyridin-3-yl)acetamide (18d)



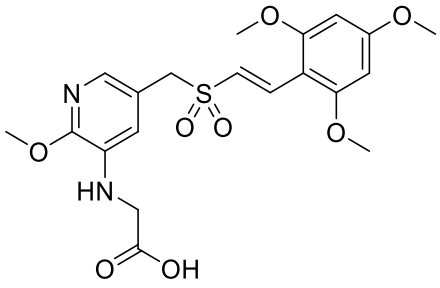
To a solution of compound **17** (200 mg, 0.507 mmol) in anhydrous pyridine (5 mL) at 0 °C was added dropwise acetyl chloride (100 µL, 1.41 mmol). The reaction mixture was stirred at room temperature for 2 h, quenched with H_2O (1 mL), and concentrated under reduced pressure. The residue was diluted with 1 M HCl (50 mL) and extracted with CH_2Cl_2 (3 × 50 mL). The extracts were combined, dried over $MgSO_4$, and concentrated under reduced pressure. The residue was purified by flash column chromatography (silica gel, petroleum ether ramping to EtOAc) to give **18d** as a white solid (189 mg, 86%). m.p. 199-201 °C. ^{1}H NMR (500 MHz, DMSO-d_6) δ 2.10 (s, 3H, $NCOCH_3$), 3.84 (s, 6H), 3.85 (s, 3H), 3.92 (s, 3H) (total 12H, 4 × OCH_3), 4.42 (s, 2H, CH_2), 6.29 (s, 2H, benzene-H), 7.11 (d, 1H, J = 16.0, SO_2CH=CH), 7.55 (d, 1H, J = 15.5, SO_2CH=C*H*), 7.79 (app s, 1H, pyridine-H), 8.37 (app s, 1H, pyridine-H), 9.37 (s, 1H, NH). ^{13}C NMR (125 MHz, DMSO-d_6) δ 24.3, 54.1, 56.1, 56.5, 57.3, 91.4, 103.0, 118.7, 122.6, 123.6, 131.1, 134.0, 142.7, 154.3, 161.5, 164.2, 169.7 (three carbon signals overlapping or obscured). HRMS (ESI) *m/z* 437.1386 $[M + H]^+$; calcd. for $C_{20}H_{25}N_2O_7S$ $[M + H]^+$ 437.1377. Anal. RP-HPLC: t_R = 13.74 min, purity >99% (method A); t_R = 10.09 min, purity >98% (method B).

ethyl (*E*)-(2-methoxy-5-(((2,4,6-trimethoxystyryl)sulfonyl)methyl)pyridin-3-yl)glycinate (18e)



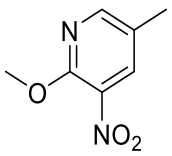
To a solution of compound **17** (300 mg, 0.761 mmol) in DMF (10 mL) was added ethyl bromoacetate (0.1 mL, 0.902 mmol) and K_2CO_3 (315 mg, 2.28 mmol). The reaction mixture was heated at 60 °C for 16 h and concentrated under reduced pressure. The residue was diluted with saturated $NaHCO_3$ (200 mL) and extracted with EtOAc (3 × 100 mL). The extracts were combined, dried over $MgSO_4$, and concentrated under reduced pressure. The residue was purified by an Isolera Four automated flash chromatography system using a 25 g KP-SIL SNAP flash cartridge (silica gel, EtOAc/hexane = 0:100 ramping to 100:0) to give **18e** as a white solid (187 mg, 51%). m.p. 155-157 °C. ^{1}H NMR (500 MHz, DMSO-d_6) δ 1.17 (t, 3H, J = 7.0, CH_2CH_3), 3.81 (d, 2H, J = 6.5, $NHCH_2$), 3.84 (s, 3H), 3.85 (s, 6H), 3.88 (s, 3H) (total 12H, 4 × OCH_3), 4.07 (q, 2H, J = 7.0, CH_2CH_3), 4.30 (s, 2H, pyridine-CH_2SO_2), 5.55 (t, 1H, J = 6.5, $NHCH_2$), 6.29 (s, 2H, benzene-H), 6.63 (d, 1H, J = 2.0, pyridine-H), 7.09 (d, 1H, J = 16.0, SO_2CH=CH), 7.34 (d, 1H, J = 2.0, pyridine-H), 7.53 (d, 1H, J = 15.5, SO_2CH=C*H*). ^{13}C NMR (125 MHz, DMSO-d_6) δ 14.1, 44.0, 53.1, 55.7, 56.1, 57.4, 60.5, 91.0, 102.5, 116.8, 118.8, 123.3, 131.7, 133.3, 134.3, 151.7, 161.0, 163.7, 170.5 (three carbon signals overlapping or obscured). HRMS (ESI) *m/z* 481.1633 $[M + H]^+$; calcd. for $C_{22}H_{28}NO_9S$ $[M+H]^+$ 481.1639. Anal. RP-HPLC: t_R = 11.80 min, purity >96% (method A); t_R = 10.80 min, purity >95% (method B).

(*E*)-(2-methoxy-5-(((2,4,6-trimethoxystyryl)sulfonyl)methyl)pyridin-3-yl)glycine (18f)



To a solution of compound **18e** (50 mg, 0.10 mmol) in H_2O/MeOH (1:2, 3 mL) was added 1 M NaOH (0.20 mL, 0.21 mmol). The reaction mixture was stirred at room temperature for 12 h and concentrated under reduced pressure. The residue was acidified with 1 M HCl (3 mL), diluted with H_2O (3 mL), and the precipitate was filtered and washed with acetone (6 mL) to give **18f** as a white solid (28 mg, 60%). m.p. >300 °C. ^{1}H NMR (500 MHz, DMSO-d_6) δ 3.73 (s, 2H, NHCH_2), 3.84 (s, 3H), 3.85 (s, 6H), 3.88 (s, 3H) (total 12H, 4 × OCH_3), 4.31 (s, 2H, pyridine-CH_2SO_2), 6.29 (s, 2H, benzene-H), 6.65 (d, 1H, *J* = 2.0, pyridine-H), 7.11 (d, 1H, *J* = 16.0, SO_2C*H*=CH), 7.34 (d, 1H, *J* = 2.0, pyridine-H), 7.54 (d, 1H, *J* = 16.0, SO_2CH=C*H*) (one carboxylic acid proton signal and one secondary amine proton signal not observed). ^{13}C NMR (125 MHz, DMSO-d_6) δ 43.9, 53.2, 55.7, 56.1, 57.4, 91.0, 102.5, 116.8, 118.8, 123.3, 131.8, 133.4, 134.1, 151.7, 161.0, 163.8, 171.8 (three carbon signals overlapping or obscured). HRMS (ESI) *m/z* 453.1331 $[M+H]^+$; calcd. for $C_{20}H_{25}N_2O_8S$ $[M+H]^+$ 453.1326. Anal. RP-HPLC: t_R = 11.09 min, purity >97% (method A); t_R 9.78 min, purity >96% (method B).

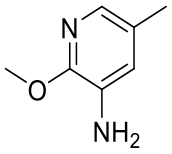
2-methoxy-5-methyl-3-nitropyridine (21)



To a solution of NaOMe (4.70 g, 87.0 mmol) in anhydrous MeOH (240 mL) was added 2-chloro-5-methyl-3-nitropyridine (10.0 g, 57.9 mmol). The reaction mixture was heated at reflux for 1 h and added with H_2O (250 mL). The precipitate was filtered and washed with H_2O (50 mL) to give **21** as a pale yellow solid (9.36 g, 96%). m.p. 75-76 °C. ^{1}H NMR (500 MHz, DMSO-d_6) δ 2.31 (s, 3H, pyridine-CH_3), 3.98 (s, 3H, OCH_3),

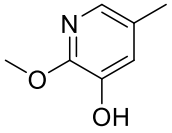
8.29 (m, 1H, pyridine-H), 8.35 (m, 1H, pyridine-H). ^{13}C NMR (125 MHz, DMSO-d_6) δ 16.8, 54.9, 127.4, 133.7, 135.9, 152.0, 154.3. HRMS (ESI) *m/z* 169.0679 $[M+H]^+$; calcd. for $C_7H_9N_2O_3$ $[M+H]^+$ 169.0608.

2-methoxy-5-methylpyridin-3-amine (22)



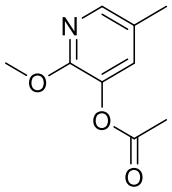
To a solution of compound **21** (2.00 g, 11.9 mmol) in MeOH (40 mL) was added 10 % Pd in C (127 mg, 0.19 mmol). The reaction mixture was stirred at room temperature for 5 h under H_2, filtered, and the filtrate concentrated under reduced pressure to give **22** as a light purple solid (1.55 g, 94%). m.p. 58-60 °C. ^{1}H NMR (500 MHz, DMSO-d_6) δ 2.08 (s, 3H, pyridine-CH_3), 3.80 (s, 3H, OCH_3), 4.81 (s, 2H, NH_2), 6.69 (m, 1H, pyridine-H), 7.15 (m, 1H, pyridine-H). ^{13}C NMR (125 MHz, DMSO-d_6) δ 17.7, 53.1, 120.4, 126.4, 132.1, 132.3, 150.8. HRMS (ESI) *m/z* 139.0846 $[M+H]^+$; calcd. for $C_7H_{11}N_2O$ $[M+H]^+$ 139.0866.

2-methoxy-5-methylpyridin-3-ol (23)



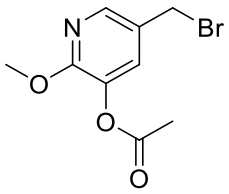
To a solution of compound **22** (1.55 g, 11.2 mmol) in 10% H_2SO_4 (60 mL) at 0 °C was added a solution of $NaNO_2$ (850 mg, 12.3 mmol) in H_2O (5 mL). The reaction mixture was stirred on a salt ice bath for 30 min, heated at 70 °C for 1 h, basified to pH 6 with Na_2CO_3 powder, and extracted with EtOAc (3 × 200 mL). The organic extracts were combined, dried over $MgSO_4$ and concentrated under reduced pressure. The residue was purified by flash column chromatography (silica gel, petroleum ether ramping to EtOAc:petroleum ether = 1:4) to give **23** as a white solid (1.26 g, 81%). m.p. 86-87 °C. ^{1}H NMR (500 MHz, DMSO-d_6) δ 2.13 (s, 3H, pyridine-CH_3), 3.81 (s, 3H, OCH_3), 6.89 (m, 1H, pyridine-H), 7.39 (m, 1H, pyridine-H), 9.34 (br s, 1H, OH). ^{13}C NMR (125 MHz, DMSO-d_6) δ 17.4, 53.2, 123.2, 126.7, 135.2, 141.3, 152.2. HRMS (ESI) *m/z* 140.0670 $[M+H]^+$; calcd. for $C_7H_{10}NO_2$ $[M+H]^+$ 140.0706.

2-methoxy-5-methylpyridin-3-yl acetate (24)



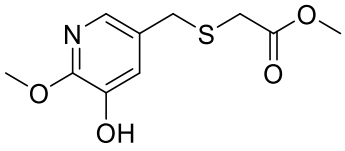
To a solution of compound **23** (1.00 g, 7.19 mmol) in anhydrous pyridine (20 mL) at 0 °C was added acetic anhydride (7.00 mL, 74.2 mmol). The reaction mixture was stirred at room temperature for 15 h and concentrated under reduced pressure. The residue was added 1 M HCl (50 mL) and the mixture was extracted with CH_2Cl_2 (3 × 100 mL). The organic extracts were combined, dried over $MgSO_4$ and concentrated under reduced pressure to give **24** as a light yellow liquid (1.30 g, 100%). ^{1}H NMR (500 MHz, CD_3OD) δ 2.26 (app s, 6H, $COCH_3$ & pyridine-CH_3), 3.89 (s, 3H, pyridine-OCH_3), 7.28 (m, 1H, pyridine-H), 7.82 (m, 1H, pyridine-H).^{13}C NMR (125 MHz, CD_3OD) δ 17.1, 20.4, 54.0, 128.2, 133.1, 135.9, 143.9, 156.0, 170.3. HRMS (ESI) *m/z* 182.0746 $[M+H]^+$; calcd. for $C_9H_{12}NO_3$ $[M+H]^+$ 182.0812.

5-(bromomethyl)-2-methoxypyridin-3-yl acetate (25)



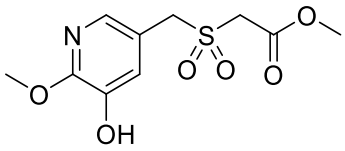
To a solution of compound **24** (5.80 g, 32.0 mmol) in anhydrous CH_2Cl_2 (50 mL) was added *N*-bromosuccinimide (5.69 g, 32.0 mmol) and AIBN (530 mg, 3.23 mmol). The reaction mixture was heated at reflux for 24 h, added with N-bromosuccinimide (1.14 g, 6.41 mmol), further heated at reflux for 18 h, and concentrated under reduced pressure. The residue was purified by flash column chromatography (silica gel, hexane ramping to CH_2Cl_2:hexane = 1:1) to give **25** as a colourless liquid (3.88 g, 47%). ^{1}H NMR (500 MHz, $CDCl_3$) δ 2.33 (s, 3H, $COCH_3$), 3.97 (s, 3H, pyridine-OCH_3), 4.45 (s, 2H, CH_2), 7.40 (d, 1H, *J* = 2.0, pyridine-H), 8.03 (d, 1H, *J* = 2.5, pyridine-H). ^{13}C NMR (125 MHz, $CDCl_3$) δ 20.8, 29.6, 54.2, 127.3, 131.6, 134.9, 143.5, 156.5, 168.5. HRMS (ESI) *m/z* 259.9817 [M (^{79}Br)+H]$^+$, 261.9795 [M(^{81}Br)+H]$^+$; calcd. for $C_9H_{11}BrNO_3$ [M (^{79}Br)+H]$^+$ 259.9917, [M(^{81}Br)+H]$^+$ 261.9896.

methyl 2-(((5-hydroxy-6-methoxypyridin-3-yl)methyl)thio)acetate (26)



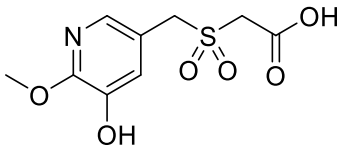
To a solution of compound **25** (2.68 g, 10.3 mmol) in anhydrous MeOH (40 mL) was added methyl thioglycolate (1.15 mL, 12.9 mmol) and Na_2CO_3 (1.35 g, 12.7 mmol). The reaction mixture was stirred at room temperature for 2 h, added with methyl thioglycolate (300 μL, 3.36 mmol), further stirred for 2 h, and concentrated under reduced pressure. The residue was added EtOAc (200 mL), the solid filtered, and the filtrate concentrated under reduced pressure. The residue was purified by flash column chromatography (silica gel, petroleum ether ramping to EtOAc:petroleum ether = 2:3) to give **26** as a yellow liquid (2.12 g, 84%). ^{1}H NMR (500 MHz, $CDCl_3$) δ 3.07 (s, 2H, SCH_2CO), 3.73 (app s, 5H, $COOCH_3$ & pyridine-CH_2S), 4.01 (s, 3H, pyridine-OCH_3), 5.60 (br s, 1H, OH), 7.16 (d, 1H, *J* = 2.0, pyridine-H), 7.60 (d, 1H, *J* = 2.5, pyridine-H). ^{13}C NMR (125 MHz, $CDCl_3$) δ 32.0, 33.1, 52.5, 54.0, 121.7, 127.2, 136.9, 140.7, 152.5, 170.9. HRMS (ESI) *m/z* 244.0690 $[M+H]^+$; calcd. for $C_{10}H_{14}NO_4S$ $[M+H]^+$ 244.0638.

methyl 2-(((5-hydroxy-6-methoxypyridin-3-yl)methyl)sulfonyl)acetate (27)



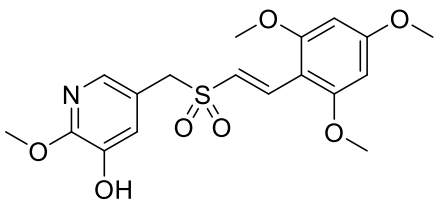
Thioether **26** (2.12 g, 8.71 mmol) was oxidised according to general synthetic procedure A. The residue was purified by flash column chromatography (silica gel, petroleum ether ramping to EtOAc:petroleum ether = 1:1) to give **27** as a white solid (1.98 g, 83%). m.p. 132-134 °C. ^{1}H NMR (500 MHz, $CDCl_3$) δ 3.83 (s, 2H, SO_2CH_2CO), 3.86 (s, 3H, $COOCH_3$), 4.05 (s, 3H, pyridine-OCH_3), 4.43 (s, 2H, pyridine-CH_2SO_2), 5.46 (s, 1H, OH), 7.29 (d, 1H, *J* = 2.0, pyridine-H), 7.78 (d, 1H, *J* = 2.5, pyridine-H). 13C NMR (125 MHz, $CDCl_3$) δ 53.5, 54.0, 54.5, 56.2, 117.8, 122.6, 139.1, 140.7, 153.6, 163.7. HRMS (ESI) *m/z* 276.0611 $[M+H]^+$; calcd. for $C_{10}H_{14}NO_6S$ $[M+H]^+$ 276.0536.

2-(((5-hydroxy-6-methoxypyridin-3-yl)methyl)sulfonyl)acetic acid (28)



To a solution of compound **27** (1.98 g, 7.19 mmol) in MeOH/H_2O (1:1, 160 mL) was added Na_2CO_3 (1.83 g, 17.3 mmol). The reaction mixture was stirred at room temperature for 12 h and concentrated under reduced pressure. The residue was added 1M HCl (40 mL) and extracted with EtOAc (3 × 100 mL). The organic extracts were combined, dried over $MgSO_4$, and concentrated under reduced pressure to give **28** as a light yellow solid (1.77 g, 94%). m.p. 182-183 °C. ^{1}H NMR (500 MHz, CD_3OD) δ 3.98 (s, 3H, OCH_3), 4.04 (s, 2H, SO_2CH_2CO), 4.53 (s, 2H, pyridine-CH_2SO_2), 7.20 (d, 1H, *J* = 2.0, pyridine-H), 7.67 (d, 1H, *J* = 2.0, pyridine-H) (one carboxylic acid proton not observed). ^{13}C NMR (125 MHz, CD_3OD) δ 54.1, 56.7, 56.9, 119.1, 124.9, 139.3, 142.9, 155.8, 166.2. HRMS (ESI) *m/z* 262.0171 $[M+H]^+$, 284.0250 $[M+Na]^+$; calcd. for $C_9H_{12}NO_6S$ $[M+H]^+$ 262.0380, $[M+Na]^+$ 284.0199.

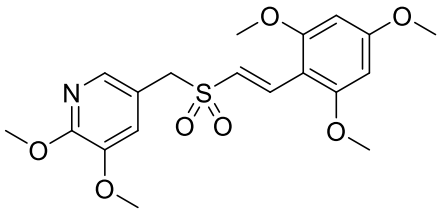
(*E*)-2-methoxy-5-(((2,4,6-trimethoxystyryl)sulfonyl)methyl)pyridin-3-ol (29)



Compound **28** (500 mg, 1.91 mmol) and 2,4,6-trimethoxybenzaldehyde (413 mg, 2.10 mmol) were reacted using general synthetic procedure B. The residue was added 1M NaOH (50 mL) and washed with CH_2Cl_2 (3 × 100 mL). The aqueous layer was acidified to pH 2 with 2M HCl and extracted with EtOAc (3 × 100 mL). The organic extracts were combined, dried over $MgSO_4$ and concentrated under reduced pressure. The residue was purified by flash column chromatography (silica gel, CH_2Cl_2 ramping to MeOH:CH_2Cl_2 = 5:95) and triturated with MeOH (20 mL) to give **29** as a white solid (309 mg, 41%). m.p. 121-122 °C. ^{1}H NMR (500 MHz, acetone-d_6) δ 3.88 (s, 3H), 3.91 (m, 9H) (total 12H, 4 ×OCH_3), 4.26 (s, 2H, CH_2), 6.30 (s, 2H, benzene-H), 7.11 (d, 1H, *J* = 15.5, SO_2CH=CH), 7.22 (d, 1H, *J* = 2.0, pyridine-H), 7.65 (d, 1H, *J* = 2.0, pyridine-H), 7.71 (d, 1H, *J* = 16.0, SO_2CH=C*H*), 8.09 (s, 1H, OH).^{13}C NMR (125 MHz, acetone-

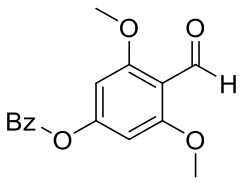
d_6) δ 53.6, 56.0, 56.4, 58.5, 91.6, 104.2, 120.5, 124.4, 124.6, 135.3, 139.4, 141.7, 154.5, 162.4, 165.1 (three carbon signals overlapping or obscured). HRMS (ESI) *m/z* 396.0956 $[M+H]^+$; calcd. for $C_{18}H_{22}NO_7S$ $[M+H]^+$ 396.1111. Anal. RP-HPLC: t_R = 11.04, purity >97% (method A); t_R = 9.90, purity >99% (method B).

(*E*)-2,3-dimethoxy-5-(((2,4,6-trimethoxystyryl)sulfonyl)methyl)pyridine (30)



To a solution of compound **29** (50 mg, 0.13 mmol) in DMF (5 mL) was added K_2CO_3 (20 mg, 0.14 mmol) and MeI (100 μL, 1.6 mmol). The reaction mixture was stirred at room temperature for 12 h and concentrated under reduced pressure. The residue was diluted with 1 M NaOH (50 mL) and extracted with CH_2Cl_2 (3 × 50 mL). The extracts were combined, dried over $MgSO_4$, and concentrated under reduced pressure. The residue was crystallized with CH_2Cl_2/hexane (1:1, 20 mL) to give **30** as white solid (34 mg, 65%). m.p. 165-167 °C. ^{1}H NMR (500 MHz, $CDCl_3$) δ 3.84 (s, 6H), 3.85 (s, 3H), 3.88 (s, 3H), 4.05 (s, 3H) (total 15H, 5 × OCH_3), 4.18 (s, 2H, CH_2), 6.09 (s, 2H, benzene-H), 7.02 (d, 1H, *J* = 15.5, SO_2CH=CH), 7.22 (d, 1H, *J* = 1.5, pyridine-H), 7.66 (d, 1H, *J* = 1.5, pyridine-H), 7.79 (d, 1H, *J* = 15.5, SO_2CH=C*H*). ^{13}C NMR (125 MHz, $CDCl_3$) δ 54.0, 55.6, 55.9, 59.0, 90.5, 103.8, 118.,4, 119.2, 122.0, 136.5, 138.9, 144.0, 154.7, 161.7, 164.1 (four carbon signals overlapping or obscured). HRMS (ESI) *m/z* 410.1272 $[M+H]^+$; calcd. for $C_{19}H_{24}NO_7S$ $[M+H]^+$ 410.1268. Anal. RP-HPLC: t_R = 11.36, purity >95% (method A); t_R = 9.18, purity >95% (method B).

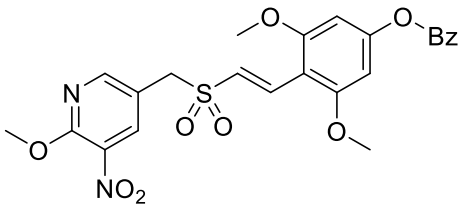
4-formyl-3,5-dimethoxyphenyl benzoate (32b)



To a solution of 4-hydroxy-2,6-dimethoxybenzaldehyde (1.00 g, 5.49 mmol) in EtOAc (20 mL) was added with Et_3N (900 μL, 6.45 mmol) and benzoyl chloride (640 μL, 5.51 mmol). The reaction mixture was stirred at room temperature for 12 h and concentrated

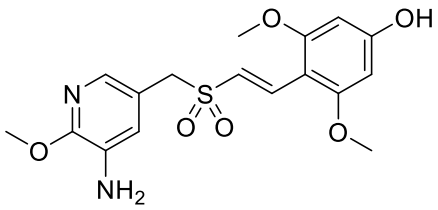
under reduced pressure. The residue was purified by flash column chromatography (silica gel, petroleum ether ramping to EtOAc:petroleum ether = 1:1) to give **32b** as a white solid (611 mg, 39%). m.p. 88-89 °C. ^{1}H NMR (500 MHz, $CDCl_3$) δ 3.91 (s, 6H, OCH_3), 6.50 (s, 2H, benzene-H), 7.54 (app t, 2H, *J* = 8.0, benzene-H), 7.67 (tt, 1H, *J* = 7.0 & 1.5, benzene-H), 8.19 (dd, 2H, *J* = 8.0 & 1.0, benzene-H). ^{13}C NMR (125 MHz, $CDCl_3$) δ 56.4, 98.4, 112.3, 128.9, 129.0, 130.4, 134.2, 157.2, 163.3, 164.5, 188.5. HRMS (ESI) *m/z* 287.0905 $[M+H]^+$; calcd. for $C_{16}H_{15}O_5$ $[M+H]^+$ 287.0914.

(*E*)-3,5-dimethoxy-4-(2-(((6-methoxy-5-nitropyridin-3-yl)methyl)sulfonyl)vinyl)-phenyl benzoate (33b)



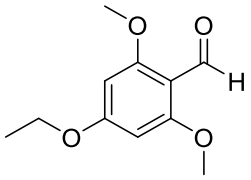
Compound **4** (120 mg, 0.413 mmol) and **32b** (113 mg, 0.395 mmol) were reacted using general synthetic procedure B. The residue was purified by flash column chromatography (silica gel, petroleum ether ramping to EtOAc:petroleum ether = 1:1) to give **33b** as a white solid (124 mg, 58%). m.p. 202-203 °C. ^{1}H NMR (500 MHz, $CDCl_3$) δ 3.88 (s, 6H, benzene-OCH_3), 4.13 (s, 3H, pyridine-OCH_3), 4.27 (s, 2H, pyridine-CH_2SO_2), 6.49 (s, 2H, benzene-H), 7.20 (d, 1H, *J* = 15.5, SO_2C*H*=CH), 7.54 (t, 2H, *J* = 7.5, benzene-H), 7.67 (tt, 1H, *J* = 1, 7.5, benzene-H), 7.84 (d, 1H, *J* = 15.5, SO_2CH=C*H*), 8.19 (dd, 2H, *J* = 8.5 & 1.0, benzene-H), 8.35 (d, 1H, *J* = 2.0, pyridine-H), 8.39 (d, 1H, *J* = 2.5, pyridine-H). ^{13}C NMR (125 MHz, $CDCl_3$) δ 55.3, 56.3, 57.7, 60.5, 98.3, 107.7, 118.3, 124.3, 128.9, 129.0, 130.4, 133.7, 134.2, 137.1, 153.5, 155.3, 156.8, 161.0, 164.8 (five carbon signals overlapping or obscured). HRMS (ESI) *m/z* 515.1055 $[M+H]^+$; calcd. for $C_{24}H_{23}N_2O_9S$ $[M+H]^+$ 515.1119.

(*E*)-4-(2-(((5-amino-6-methoxypyridin-3-yl)methyl)sulfonyl)vinyl)-3,5-dimethoxyphenol (34)



To a solution of compound **33b** (100 mg, 0.194 mmol) in MeOH/CH_3CO_2H (1:1, 10 mL) was added Fe powder (87 mg, 1.56 mmol). The mixture reaction mixture was heated at 50 °C for 2 h under N_2 gas and concentrated under reduced pressure. The residue was filtered through a silica plug eluted with EtOAc (250 mL) to yield the amino ester as a colourless liquid. The compound was dissolved in H_2O/MeOH (1:1, 10 mL) and added 1 M NaOH (1 mL). The reaction mixture was stirred at room temperature for 24 h and concentrated under reduced pressure. The residue was neutralized to pH = 7 with 1 M HCl, and the mixture extracted with EtOAc (3 × 50 mL). The extracts were combined, dried over $MgSO_4$ and concentrated under reduced pressure. The residue was purified by flash column chromatography (silica gel, CH_2Cl_2 ramping to MeOH:CH_2Cl_2 = 1:9) to give **34** as a white solid (15 mg, 20%). m.p. 220-221 °C. ^{1}H NMR (500 MHz, DMSO-d_6) δ 3.79 (s, 6H, benzene-OCH_3), 3.84 (s, 3H, pyridine-OCH_3), 4.25 (s, 2H, CH_2), 5.05 (s, 2H, NH_2), 6.12 (s, 2H, benzene-H), 6.87 (app s, 1H, pyridine-H), 7.01 (d, 1H, J = 15.5, $SO_2C\mathit{H}$=CH), 7.27 (app s, 1H, pyridine-H), 7.56 (d, 1H, J = 15.5, SO_2CH=CH). ^{13}C NMR (125 MHz, DMSO-d_6) δ 53.1, 55.9, 57.5, 92.2, 101.4, 118.8, 120.9, 122.2, 132.1, 133.5, 134.5, 152.0, 161.3, 162.6 (three carbon signals overlapping or obscured). HRMS (ESI) *m/z* 381.1094 $[M+H]^+$; calcd. for $C_{17}H_{21}N_2O_6S$ $[M+H]^+$ 381.1115. Anal. RP-HPLC: t_R = 8.96, purity >97% (method A); t_R = 7.85, purity >98% (method B).

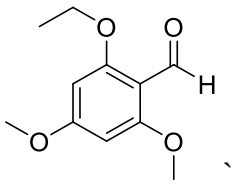
4-ethoxy-2,6-dimethoxybenzaldehyde (39a)



To a solution of 4-hydroxy-2,6-dimethoxybenzaldehyde (400 mg, 2.20 mmol) in DMF (10 mL) was added with K_2CO_3 (364 mg, 2.63 mmol) and EtI (360 µL, 4.48 mmol).

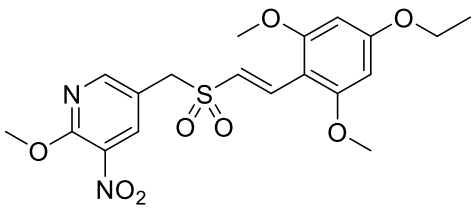
The reaction mixture was stirred at room temperature for 15 h and concentrated under reduced pressure. The residue was added H_2O (50 mL) and extracted with EtOAc (3 × 50 mL). The extracts were combined, dried under $MgSO_4$, and concentrated under reduced pressure to give **39a** as a yellow solid (231 mg, 87%). m.p. 86-88 °C. ^{1}H NMR (500 MHz, DMSO-d_6) δ 1.35 (t, 3H, J = 7.0, CH_2CH_3), 3.81 (s, 6H, OCH_3), 4.16 (q, 2H, J = 7.0, CH_2CH_3), 6.24 (s, 2H, benzene-H), 10.19 (s, 1H, aldehyde-H). ^{13}C NMR (125 MHz, DMSO-d_6) δ 14.5, 56.1, 63.9, 91.1, 107.8, 163.5, 165.3, 185.7. HRMS (ESI) *m/z* 211.0964 $[M+H]^+$; calcd. for $C_{11}H_{15}O_4$ $[M+H]^+$ 211.0965.

2-ethoxy-4,6-dimethoxybenzaldehyde (39b)



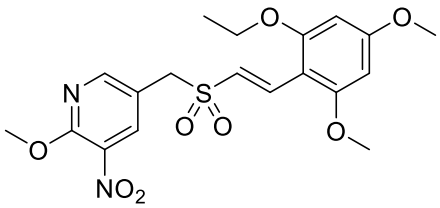
To a solution of 2-hydroxy-4,6-dimethoxybenzaldehyde (500 mg, 2.75 mmol) in DMF (20 mL) was added K_2CO_3 (455 mg, 3.29 mmol) and EtI (400 µL, 4.98 mmol). The reaction mixture was stirred at room temperature for 12 h and concentrated under reduced pressure. The residue was added H_2O (50 mL) and extracted with CH_2Cl_2 (3 × 50 mL). The extracts were combined, dried under $MgSO_4$, and concentrated under reduced pressure to give **39b** product as a white solid (515 mg, 89%). m.p. 78-79 °C. ^{1}H NMR (500 MHz, $CDCl_3$) δ 1.46 (t, 3H, J = 7.0, CH_2CH_3), 3.86 (s, 3H), 3.88 (s, 3H) (total 6H, 2 ×OCH_3), 4.09 (q, 2H, J = 7.0, CH_2CH_3), 6.06 (app s, 2H, benzene-H), 10.38 (s, 1H, aldehyde-H). ^{13}C NMR (125 MHz, $CDCl_3$) δ 14.7, 55.6, 56.1, 64.7, 90.4, 91.0, 109.0, 163.6, 164.2, 166.2, 188.1. HRMS (ESI) *m/z* 211.0957 $[M+H]^+$; calcd. for $C_{11}H_{15}O_4$ $[M+H]^+$ 211.0965.

(*E*)-5-(((4-ethoxy-2,6-dimethoxystyryl)sulfonyl)methyl)-2-methoxy-3-nitropyridine (40a)



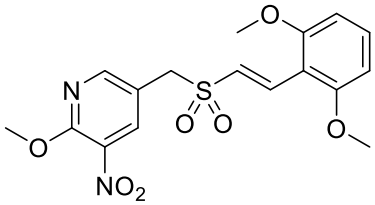
Compound **32** (200 mg, 0.689 mmol) and **39a** (159 mg, 0.756 mmol) were reacted using general synthetic procedure B. The residue was purified by flash column chromatography (silica gel, petroleum ether ramping to EtOAc:petroleum ether = 2:3) and triturated with MeOH (50 mL) to give **40a** as a white solid (167 mg, 55%). m.p. 176-178 °C. ^{1}H NMR (500 MHz, DMSO-d_6) δ 1.34 (t, 3H, J = 7.0, CH_2CH_3), 3.83 (s, 6H, benzene-OCH_3), 4.03 (s, 3H, pyridine-OCH_3), 4.13 (q, 2H J = 7.0, CH_2CH_3, 4.62 (s, 2H, pyridine-CH_2SO_2), 6.27 (s, 2H, benzene-H), 7.08 (d, 1H, J = 15.5, SO_2CH=CH), 7.44 (d, 1H, J = 15.5, SO_2CH=C*H*), 8.43 (d, 1H, J = 2.0, pyridine-H), 8.45 (d, 1H, J = 2.5, pyridine-H). 13C NMR (125 MHz, DMSO-d_6) δ 14.5, 54.9, 55.6, 56.1, 63.8, 91.3, 102.2, 119.6, 122.1, 132.9, 134.9, 137.3, 153.7, 155.5, 161.1, 163.3 (three carbon signals overlapping or obscured). HRMS (ESI) *m/z* 439.1170 $[M+H]^+$; calcd. for $C_{19}H_{23}N_2O_8S$ $[M+H]^+$ 439.1170.

(*E*)-5-(((2-ethoxy-4,6-dimethoxystyryl)sulfonyl)methyl)-2-methoxy-3-nitropyridine (40b)



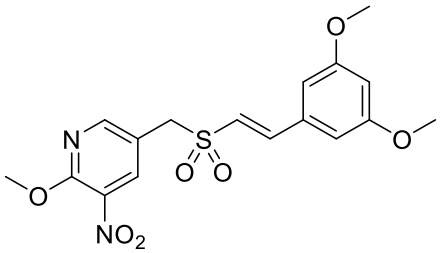
Compound **14** (200 mg, 0.689 mmol) and **39b** (159 mg, 0.756 mmol) were reacted using general synthetic procedure B. The residue was purified by flash column chromatography (silica gel, petroleum ether ramping to EtOAc:petroleum ether = 1:1) to give **40b** as a pale yellow solid (201 mg, 67%). m.p. 173-174 °C. ^{1}H NMR (500 MHz, $CDCl_3$) δ 1.42 (t, 3H, J = 7.0, CH_2CH_3), 3.84 (m, 6H, benzene-OCH_3), 4.07 (q, 2H, J = 7.0, CH_2CH_3), 4.12 (s, 1H, pyridine-OCH_3), 4.24 (s, 2H, pyridine-CH_2SO_2), 7.05 (d, 1H, J = 15.5, SO_2CH=CH), 7.81 (d, 1H, J = 15.5, SO_2CH=C*H*), 8.33 (d, 1H, J = 2.0, pyridine-H), 8.39 (d, 1H, J = 2.0, pyridine-H). ^{13}C NMR (125 MHz, $CDCl_3$) δ 14.7, 55.3, 55.6, 55.9, 57.8, 64.7, 90.4, 91.2, 103.6, 118.8, 120.9, 133.6, 137.2, 137.9, 153.5, 156.7, 161.2, 161.8, 164.5. HRMS (ESI) *m/z* 439.1158 $[M+H]^+$; calcd. for $C_{19}H_{23}N_2O_8S$ $[M+H]^+$ 439.1170.

(*E*)-5-(((2,6-dimethoxystyryl)sulfonyl)methyl)-2-methoxy-3-nitropyridine (40c)



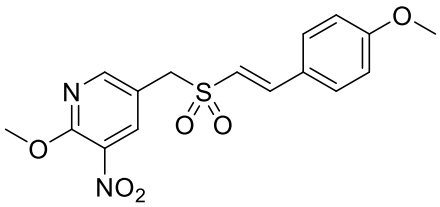
Compound **14** (200 mg, 0.689 mmol) and 2,6-dimethoxybenzaldehyde (0.130 mg, 0.782 mmol) (159 mg, 0.756 mmol) were reacted using general synthetic procedure B. The residue was purified by flash column chromatography (silica gel, petroleum ether ramping to EtOAc:petroleum ether = 1:1) to give **40c** as a white solid (206 mg, 76%). m.p. 181-183 °C. ^{1}H NMR (500 MHz, $CDCl_3$) δ 3.87 (s, 6H, benzene-OCH_3), 4.12 (s, 3H, pyridine-OCH_3), 4.26 (s, 2H, CH_2), 6.56 (d, 2H, *J* = 8.5, benzene-H), 7.22 (d, 1H, *J* = 15.5, SO_2CH=CH), 7.35 (app t, 1H, *J* = 8.5, benzene-H), 7.87 (d, 1H, *J* = 15.5, SO_2CH=CH), 8.33 (d, 1H, *J* = 2.5, pyridine-H), 8.39 (d, 1H, *J* = 2.5, pyridine-H). ^{13}C NMR (125 MHz, $CDCl_3$) δ 55.3, 56.0, 57.7, 77.7, 103.8, 109.9, 118.4, 124.7, 133.4, 137.1, 137. 9, 153.5, 156.8, 160.5 (three carbon signals overlapping or obscured). HRMS (ESI) *m/z* 395.0903 $[M+H]^+$; calcd. for $C_{17}H_{19}N_2O_7S$ $[M+H]^+$ 395.0907.

(*E*)-5-(((3,5-dimethoxystyryl)sulfonyl)methyl)-2-methoxy-3-nitropyridine (40d)



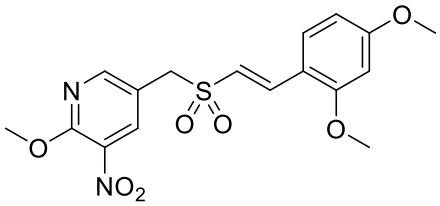
Compound **14** (200 mg, 0.689 mmol) and 3,5-dimethoxybenzaldehyde (126 mg, 0.758 mmol) were reacted using general synthetic procedure B. The residue was washed with MeOH (30 mL) to give **40d** as a grey solid (117 mg, 47%). m.p. 180-182 °C. ^{1}H NMR (500 MHz, $CDCl_3$) δ 3.82 (s, 6H, benzene-OCH_3), 4.13 (s, 3H, pyridine-OCH_3), 4.30 (s, 2H, CH_2), 6.56 (m, 1H, benzene-H), 6.59 (d, 2H, *J* = 2.0, benzene-H), 6.75 (d, 1H, *J* = 15.0, SO_2CH=CH), 7.45 (d, 1H, *J* = 15.5, SO_2CH=C*H*), 8.34 (d, 1H, *J* = 2.0, pyridine-H), 8.38 (d, 1H, *J* = 2.0, pyridine-H) .^{13}C NMR (125 MHz, $CDCl_3$) δ 55.4, 55.7, 57.5, 104.1, 106.8, 117.4, 123.8, 133.6, 133.8, 137.1, 147.5, 153.3, 157.0, 161.4 (three carbon signals overlapping or obscured). HRMS (ESI) *m/z* 395.0912 $[M+H]^+$; calcd. for $C_{17}H_{19}N_2O_7S$ $[M+H]^+$ 395.0907.

(*E*)-2-methoxy-5-(((4-methoxystyryl)sulfonyl)methyl)-3-nitropyridine (40e)



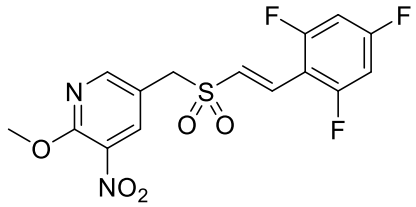
Compound **14** (200 mg, 0.689 mmol) and 4-methoxybenzaldehyde (103 mg, 0.757 mmol) were reacted using general synthetic procedure B. The residue was washed with MeOH (30 mL) to give **40e** as a grey solid (88 mg, 35%). m.p. 193-195 °C. ^{1}H NMR (500 MHz, $CDCl_3$) δ 3.86 (s, 3H), 4.12 (s, 3H) (total 6H, 2 × OCH_3), 4.28 (s, 2H, CH_2), 6.62 (s, 1H, *J* = 15.5, SO_2CH=CH), 6.93 (m, 2H, benzene-H), 7.45 (m, 3H, benzene-H & SO_2CH=C*H*), 8.34 (d, 1H, *J* = 2.0, pyridine-H), 8.38 (d, 1H, *J* = 2.5, pyridine-H). ^{13}C NMR (125 MHz, $CDCl_3$) δ 55.4, 55.7, 57.7, 114.9, 117.8, 120.2, 124.5, 130.8, 133.8, 137.1, 147.0, 153.3, 156.9, 162.8 (two carbon signals overlapping or obscured). HRMS (ESI) *m/z* 365.0777 $[M+H]^+$; calcd. for $C_{16}H_{17}N_2O_6S$ $[M+H]^+$ 365.0802.

(*E*)-5-(((2,4-dimethoxystyryl)sulfonyl)methyl)-2-methoxy-3-nitropyridine (40f)



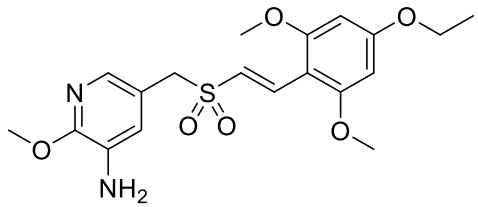
Compound **14** (200 mg, 0.689 mmol) and 2,4-dimethoxybenzaldehyde (126 mg, 0.758 mmol) were reacted using general synthetic procedure B. The residue was washed with MeOH (35 mL) to give **40f** as a grey solid (149 mg, 55%). m.p. 176-178 °C. ^{1}H NMR (500 MHz, $CDCl_3$) δ 3.86 (s, 3H), 3.87 (s, 3H), 4.12 (s, 3H) (total 9H, 3 × OCH_3), 4.26 (s, 2H, CH_2), 6.46 (d, 1H, *J* = 2.5, benzene-H), 6.52 (dd, 1H, *J* = 8.5 & 2.5, benzene-H), 6.88 (d, 1H, *J* = 15.5, SO_2CH=CH), 7.30 (d, 1H, *J* = 8.5, benzene-H), 7.51 (d, 1H, *J* = 15.5, SO_2CH=C*H*), 8.33 (d, 1H, *J* = 2.5, pyridine-H), 8.38 (d, 1H, *J* = 2.0, pyridine-H).^{13}C NMR (125 MHz, $CDCl_3$) δ 55.3, 55.7, 55.8, 57.7, 98.7, 105.7, 114.0, 118.2, 120.9, 133.5, 133.7, 137.1, 143.3, 153.4, 156.8, 160.9, 164.1. HRMS (ESI) *m/z* 395.0904 $[M+H]^+$; calcd. for $C_{17}H_{19}N_2O_7S$ $[M+H]^+$ 395.0907.

(*E*)-2-methoxy-3-nitro-5-(((2,4,6-trifluorostyryl)sulfonyl)methyl)pyridine (40g)



Compound **14** (200 mg, 0.689 mmol) and 2,4,6-trifluorobenzaldehyde (121 mg, 0.756 mmol) were reacted using general synthetic procedure B. The residue was purified by flash column chromatography (silica gel, petroleum ether ramping to EtOAc:petroleum ether = 1:1) to give **40g** as a yellow solid (162 mg, 60%). m.p. 193-194 °C. ^{1}H NMR (500 MHz) δ 4.14 (s, 3H, OCH_3), 4.31 (s, 2H, CH2), 6.79 (t, 2H, *J* = 9.0, benzene-H), 7.07 (d, 1H, *J* = 16.0, SO_2CH=CH), 7.56 (d, 1H, *J* = 16.0, SO_2CH=C*H*), 8.33 (d, 1H, *J* = 2.5, pyridine-H), 8.40 (d, 1H, *J* = 2.0, pyridine-H). ^{13}C NMR (125 MHz) δ 55.3, 57.1, 101.5 (td, *J* = 26.3 & 3.5), 106.9 (td, *J* = 14.9 & 4.7), 117.0, 128.6 (td, *J* = 8.7 & 2.5), 132.2, 133.6, 137.0, 153.2, 156.9, 162.2 (m), 164.5 (td, *J* = 256.1 & 13.0) (two carbon signals overlapping or obscured). HRMS (ESI) *m/z* 389.0392 $[M+H]^+$; calcd. for $C_{15}H_{11}F_3N_2O_5S$ $[M+H]^+$ 389.0414.

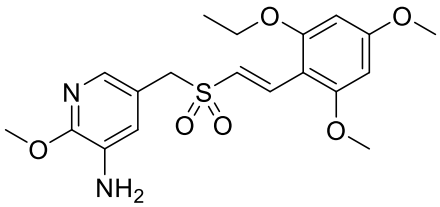
(*E*)-5-(((4-ethoxy-2,6-dimethoxystyryl)sulfonyl)methyl)-2-methoxypyridin-3-amine (41a)



Nitro compound **40a** (100 mg, 0.228 mmol) was reduced using general synthetic procedure C. The residue was purified by flash column chromatography (silica gel, CH_2Cl_2 ramping to acetone:CH_2Cl_2 = 1:9) to give **41a** as a white solid (58 mg, 62%). m.p. 142-144 °C. ^{1}H NMR (500 MHz, DMSO-d_6) δ 1.34 (t, 3H, *J* = 7.0, CH_2CH_3), 3.83 (s, 3H, pyridine-OCH_3), 3.84 (s, 6H, benzene-OCH_3), 4.13 (q, 2H, *J* = 7.0, CH_2CH_3), 4.26 (s, 2H, pyridine-CH_2SO_2), 5.03 (s, 2H, NH_2), 6.27 (s, 2H, benzene-H), 6.87 (d, 1H, *J* = 2.0, pyridine-H), 7.08 (d, 1H, *J* = 15.5, SO_2CH=CH), 7.27 (d, 1H, *J* = 2.0, pyridine-H), 7.56 (d, 1H, *J* = 15.5, SO_2CH=C*H*). ^{13}C NMR (125 MHz, DMSO-d_6) δ 14.5, 52.9, 56.1, 57.3, 63.7, 91.3, 102.4, 118.6, 120.7, 123.3, 132.1, 133.1, 134.3, 151.9, 161.0,

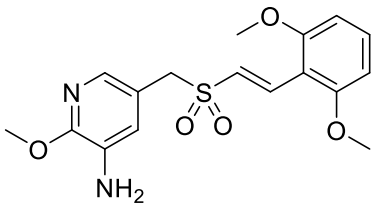
163.0 (three carbon signals overlapping or obscured). HRMS (ESI) *m/z* 409.1465 $[M+H]^+$; calcd. for $C_{19}H_{25}N_2O_6S$ $[M+H]^+$ 409.1428. Anal. RP-HPLC: t_R = 11.51, purity >97% (method A); t_R = 10.67, purity >98% (method B).

(*E*)-5-(((2-ethoxy-4,6-dimethoxystyryl)sulfonyl)methyl)-2-methoxypyridin-3-amine (41b)



Nitro compound **40b** (100 mg, 0.228 mmol) was reduced using general synthetic procedure C. The residue was purified by flash column chromatography (silica gel, CH_2Cl_2 ramping to acetone:CH_2Cl_2 = 2:98) and crystallized (diethyl ether/hexane = 1:1) to give **41b** as a white solid (29 mg, 31%). m.p. 141-143 °C. ^{1}H NMR (500 MHz, DMSO-d_6) δ 1.31 (t, 3H, *J* = 7.0, CH_2CH_3), 3.83 (s, 3H), 3.84 (s, 3H), 3.85 (s, 3H) (total 9H, 3 × OCH_3), 4.10 (q, 2H, *J* = 7.0, CH_2CH_3), 4.28 (s, 2H, pyridine-CH_2SO_2), 5.05 (s, 2H, NH_2), 6.27 (d, 1H, *J* = 2.0, benzene-H), 6.28 (d, 1H, *J* = 2.5, benzene-H), 6.89 (d, 1H, *J* = 2.5, pyridine-H), 7.04 (d, 1H, *J* = 15.5, SO_2CH=CH), 7.28 (d, 1H, *J* = 2.0, pyridine-H), 7.61 (d, 1H, *J* = 16.0, SO_2CH=C*H*). ^{13}C NMR (125 MHz, DMSO-d_6) δ 14.3, 52.9, 55.6, 56.1, 57.4, 64.4, 90.9, 91.6, 102.5, 118.7, 120.6, 123.0, 132.1, 133.3, 134.3, 151.9, 160.4, 160.9, 163.7. HRMS (ESI) *m/z* 409.1422 $[M+H]^+$; calcd. for $C_{19}H_{25}N_2O_6S$ $[M+H]^+$ 409.1428. Anal. RP-HPLC: t_R = 11.69, purity >99% (method A); t_R = 10.51, purity >98% (method B).

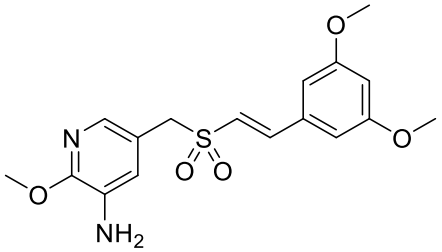
(*E*)-5-(((2,6-dimethoxystyryl)sulfonyl)methyl)-2-methoxypyridin-3-amine (41c)



Nitro compound **40c** (100 mg, 0.254 mmol) was reduced using general synthetic procedure C. The residue was purified by flash column chromatography (silica gel, CH_2Cl_2 ramping to acetone:CH_2Cl_2 = 1:9) and crystallized (CH_2Cl_2/hexane = 1:1) to

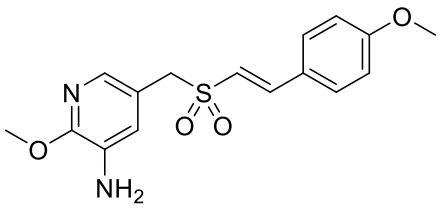
give **41c** as a pale yellow solid (52 mg, 56%). m.p. 194-196 °C. ^{1}H NMR (500 MHz, DMSO-d_6) δ 3.83 (s, 3H, pyridine-OCH_3), 3.86 (s, 6H, benzene-OCH_3), 4.32 (s, 2H, CH_2), 5.04 (s, 2H, NH_2), 6.73 (d, 2H, J = 8.5, benzene-H), 6.89 (d, 1H, J = 2.0, pyridine-H), 7.29 (m, 2H, pyridine-H & SO_2C*H*=CH), 7.41 (t, 1H, J = 8.5 Hz, benzene-H), 7.64 (d, 1H, J = 16.0, SO_2CH=C*H*). ^{13}C NMR (125 MHz, DMSO-d_6) δ 53.0, 56.1, 57.1, 104.2, 109.1, 118.4, 120.7, 127.0, 132.2, 132.9, 133.1, 134.4, 152.0, 159.7 (four carbon overlapping or obscured). HRMS (ESI) *m/z* 365.1179 $[M+H]^+$; calcd. for $C_{18}H_{23}N_2O_5S$ $[M+H]^+$ 365.1166. Anal. RP-HPLC: t_R = 9.50, purity >98% (method A); t_R = 8.70, purity >98% (method B).

(*E*)-5-(((3,5-dimethoxystyryl)sulfonyl)methyl)-2-methoxypyridin-3-amine (41d)



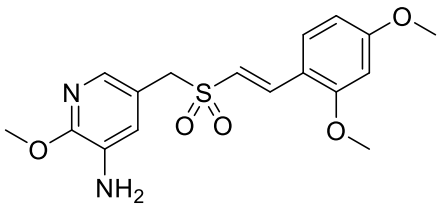
Nitro compound **40d** (100 mg, 0.254 mmol) was reduced using general synthetic procedure C. The residue was purified by flash column chromatography (silica gel, CH_2Cl_2 ramping to MeOH:CH_2Cl_2 = 2:98) to give **41d** as a white solid (79 mg, 86%). m.p. 149-151 °C. ^{1}H NMR (500 MHz, DMSO-d_6) δ 3.76 (s, 6H), 3.82 (s, 3H) (total 9H, 3 × OCH_3), 4.34 (s, 2H, CH_2), 5.05 (s, 2H, NH_2), 6.58 (t, 1H, J = 2.0, benzene-H), 6.87 (m, 3H, benzene-H & pyridine-H), 7.27 (d, 1H, J = 15.5, SO_2C*H*=CH), 7.29 (d, 1H, J = 2.0, pyridine-H), 7.43 (d, 1H, J = 15.5, SO_2CH=C*H*). ^{13}C NMR (125 MHz, DMSO-d_6) δ 53.1, 55.6, 57.2, 103.3, 106.7, 118.2, 120.8, 127.1, 131.3, 132.3, 134.5, 143.3, 152.2, 160.9 (three carbon signals overlapping or obscured). HRMS (ESI) *m/z* 365.1164 $[M+H]^+$; calcd. for $C_{17}H_{21}N_2O_5S$ $[M+H]^+$ 365.1166. Anal. RP-HPLC: t_R =11.31, purity >98% (method A); t_R = 10.31, purity >98% (method B).

(*E*)-2-methoxy-5-(((4-methoxystyryl)sulfonyl)methyl)pyridin-3-amine (41e)



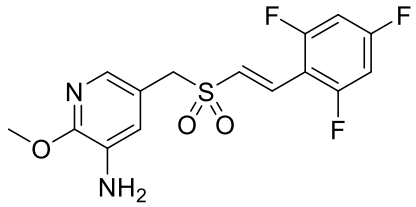
Nitro compound **40e** (70 mg, 0.192 mmol) was reduced using general synthetic procedure C. The residue was purified by flash column chromatography (silica gel, CH_2Cl_2 ramping to MeOH:CH_2Cl_2 = 2:98) to give **41e** as a white solid (37 mg, 58%). m.p. 127-129 °C. ^{1}H NMR (500 MHz, DMSO-d_6) δ 3.80 (s, 3H), 3.83 (s, 3H) (total 6H, 2 × OCH_3), 4.34 (s, 2H, CH_2), 6.92 (d, 1H, *J* = 2.0, pyridine-H), 7.00 (d, 1H, *J* = 8.5, benzene-H), 7.20 (d, 1H, *J* = 15.5, SO_2C*H*=CH), 7.30 (d, 1H, *J* = 15.0, SO_2CH=C*H*), 7.32 (d, 1H, *J* = 2.5, pyridine-H), 7.65 (d, 1H, *J* = 8.5, benzene-H). ^{13}C NMR (125 MHz, DMSO-d_6) δ 53.0, 55.4, 57.2, 114.5, 118.3, 121.1, 123.3, 125.0, 130.6, 131.6, 134.7, 142.9, 152.1, 161.6 (two carbon signals overlapping or obscured). HRMS (ESI) *m/z* 335.1070 $[M+H]^+$; calcd. for $C_{16}H_{19}N_2O_4S$ $[M+H]^+$ 335.1060. Anal. RP-HPLC: t_R = 11.00, purity >97% (method A); t_R = 10.04, purity >96% (method B).

(*E*)-5-(((2,4-dimethoxystyryl)sulfonyl)methyl)-2-methoxypyridin-3-amine (41f)



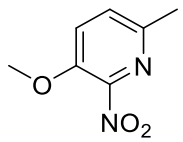
Nitro compound **40f** (100 mg, 0.254 mmol) was reduced using general synthetic procedure C. The residue was purified by flash column chromatography (silica gel, CH_2Cl_2 ramping to MeOH:CH_2Cl_2 = 1:9) to give **41f** as a white solid (80 mg, 87%). m.p. 182-184 °C. ^{1}H NMR (500 MHz, DMSO-d_6) δ 3.82 (s, 6H), 3.86 (s, 3H) (total 9H, 3 × OCH_3), 4.30 (s, 2H, CH_2), 5.06 (s, 2H, NH_2), 6.61 (m, 2H, benzene-H), 6.87 (app s, 1H, pyridine-H), 7.12 (d, 1H, *J* = 16.0, SO_2C*H*=CH), 7.28 (app s, 1H, pyridine-H), 7.42 (d, 1H, *J* = 15.5, SO_2CH=C*H*), 7.59 (d, 1H, *J* = 8.5, benzene-H). ^{13}C NMR (125 MHz, DMSO-d_6) δ 52.9, 55.6, 55.9, 57.3, 98.4, 106.4, 113.5, 118.4, 120.6, 123.0, 131.3, 132.2, 134.3, 138.0, 151.9, 159.8, 163.3. HRMS (ESI) *m/z* 365.1160 $[M+H]^+$; calcd. for $C_{17}H_{21}N_2O_5S$ $[M+H]^+$. Anal. RP-HPLC: t_R = 12.73, purity >99% (method A); t_R = 10.75, purity >98% (method B).

(*E*)-2-methoxy-5-(((2,4,6-trifluorostyryl)sulfonyl)methyl)pyridin-3-amine (41g)



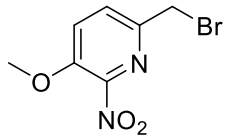
Nitro compound **40g** (100 mg, 0.258 mmol) was reduced using general synthetic procedure C. The residue was purified by flash column chromatography (silica gel, CH_2Cl_2 ramping to acetone:CH_2Cl_2 = 1:9) and crystallized (CH_2Cl_2/hexane = 1:1) to give **41g** as a white solid (19 mg, 21%). m.p. 150-151 °C. ^{1}H NMR (500 MHz, DMSO-d_6) δ 3.83 (s, 3H, CH_3), 4.46 (s, 2H, CH_2), 5.06 (s, 2H, NH_2), 6.88 (d, 1H, J = 2.0, pyridine-H), 7.20 (d, 1H, J = 16.0, $SO_2C\mathit{H}$=CH), 7.30 (d, 1H, J = 2.0, pyridine-H), 7.34 (d, 1H, J = 16.0, SO_2CH=CH), 7.39 (t, 2H, J = 9.5, benzene-H). ^{13}C NMR (125 MHz, DMSO-d_6) δ 53.0, 56.6, 101.9 (td, J = 21.5 & 2.1), 107.1 (td, J = 12.3 & 3.8), 117.9, 120.6, 127.9, 131.4, 132.3, 134.4, 152.1, 161.3 (m), 164.5 (two carbon signals overlapping or obscured). (HRMS (ESI) *m/z* 359.0685 $[M+H]^+$; calcd. for $C_{15}H_{13}F_3N_2O_3S$ $[M+H]^+$ 359.0672. Anal. RP-HPLC: t_R = 12.21, purity >96% (method A); t_R = 10.42, purity >95% (method B).

3-methoxy-6-methyl-2-nitropyridine (43)



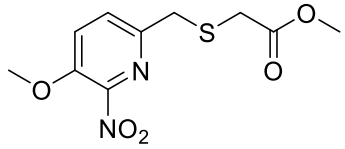
To a solution of 6-methyl-2-nitropyridin-3-ol (10.0 g, 64.9 mmol) in acetone/H_2O (5:2, 350 mL) were added K_2CO_3 (14.0 g, 101 mmol) and MeI (11.1 mL, 178 mmol). The reaction mixture was heated at reflux for 24 h and concentrated under reduced pressure. The residue was extracted with EtOAc (3 × 100 mL). The organic extracts were combined, dried over $MgSO_4$ and concentrated under reduced pressure. The residue was crystallized (acetone:H_2O = 1:1) to give **43** as a white solid (10.5 g, 96%). m.p. 87-89 °C. ^{1}H NMR (500 MHz, DMSO-d_6) δ 2.44 (s, 3H, pyridine-CH_3), 3.93 (s, 3H, OCH_3), 7.62 (d, 1H, J = 8.5, pyridine-H), 7.86 (d, 1H, J = 8.5, pyridine-H). ^{13}C NMR (125 MHz, DMSO-d_6) δ 22.6, 57.3, 125.3, 129.4, 145.2, 147.7, 148.6. HRMS (ESI) *m/z* 169.0572 $[M+H]^+$; calcd. for $C_7H_9N_2O_3$ ($[M+H]^+$) 169.0608.

6-(bromomethyl)-3-methoxy-2-nitropyridine (44)



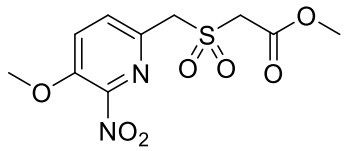
To a solution of compound **43** (16.0 g, 95.2 mmol) in MeCN (160 mL) were added *N*-bromosuccinimide (20.3 g, 114 mmol) and benzoyl peroxide (2.30 g, 9.50 mmol). The reaction mixture was heated at 120 °C under microwave irradiation for 45 min, cooled down to room temperature and concentrated under reduced pressure. The residue was diluted with 1 M NaOH (200 mL), and extracted with EtOAc (3 × 300 mL). The extracts were combined, dried over $MgSO_4$ and concentrated under reduced pressure. The residue was purified by flash column chromatography (silica gel, hexane ramping to acetone:hexane = 1:4) to give **44** as a white solid (9.90 g, 42%). m.p. 65-67 °C. ^{1}H NMR (500 MHz, DMSO-d_6) δ 3.98 (s, 3H, OCH_3), 4.72 (s, 2H, CH_2), 7.93 (d, 1H, J = 8.5, pyridine-H), 7.99 (d, 1H, J = 8.5, pyridine-H). ^{13}C NMR (125 MHz, DMSO-d_6) δ 30.5, 55.8, 122.6, 127.8, 145.8, 146.0, 146.5. HRMS (ESI) *m/z* 246.9656 ([M(^{79}Br)+H]$^+$), 248.9632 ([M(^{81}Br)+H]$^+$); calcd. for $C_7H_8BrN_2O_3$ ([M(^{79}Br)+H]$^+$) 246.9713, ([M(^{81}Br)+H]$^+$) 248.9693.

methyl 2-(((5-methoxy-6-nitropyridin-2-yl)methyl)thio)acetate (45)



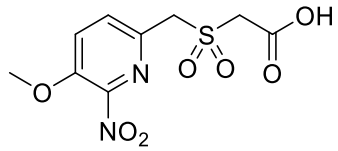
To a solution of compound **44** (5.00 g, 20.2 mmol) and K_2CO_3 (3.72 g, 26.9 mmol) in MeOH (200 mL) at 0 °C was added methyl thioglycolate (2.20 mL, 24.6 mmol). The reaction mixture was stirred at room temperature for 12 h, acidified to pH 2 with 1 M HCl and concentrated under reduced pressure. The precipitate was filtered and washed with Et_2O (20 mL) to give **45** as a white solid (5.00 g, 91%). m.p. 70-71 °C. ^{1}H NMR (500 MHz, DMSO-d_6) δ 3.39 (s, 2H, SCH_2CO), 3.59 (s, 3H, $COOCH_3$), 3.91 (s, 2H, pyridine-CH_2S), 3.96 (s, 3H, pyridine-OCH_3), 7.76 (d, 1H, J = 9.0, pyridine-H), 7.95 (d, 1H, J = 8.5, pyridine-H). ^{13}C NMR (125 MHz, DMSO-d_6) δ 33.1, 36.1, 55.5, 57.5, 125.8, 129.4, 146.1, 147.7, 148.5, 170.7. HRMS (ESI) *m/z* 311.0116 [M+K]$^+$; calcd. for $C_{10}H_{12}KN_2O_5S$ [M+K]$^+$ 311.0099.

methyl 2-(((5-methoxy-6-nitropyridin-2-yl)methyl)sulfonyl)acetate (46)



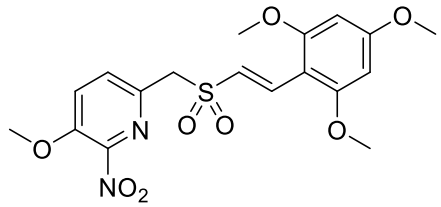
Thioether **45** (10.0 g, 36.7 mmol) was oxidised according to general synthetic procedure A. The residue was triturated with EtOH (100 mL) and filtered to give **46** as a white solid (10.9 g, 98%). m.p. 151-153 °C. ^{1}H NMR (500 MHz, DMSO-d_6) δ 3.72 (s, 3H, $COOCH_3$), 3.99 (s, 3H, pyridine-OCH_3), 4.50 (s, 2H), 4.85 (s, 2H), (total 4H, $CH_2SO_2CH_2$), 7.86 (d, 1H, J = 9.0, pyridine-H), 8.05 (d, 1H, J = 8.5, pyridine-H). ^{13}C NMR (125 MHz, DMSO-d_6) δ 53.3, 57.2, 57.7, 59.5, 126.0, 132.5, 138.8, 147.4, 147.8, 163.9. HRMS (ESI) *m/z* 327.0065 $[M+Na]^+$; calcd. for $C_{10}H_{12}N_2NaO_7S$ $[M+Na]^+$ 327.0252.

2-(((5-methoxy-6-nitropyridin-2-yl)methyl)sulfonyl)acetic acid (47)



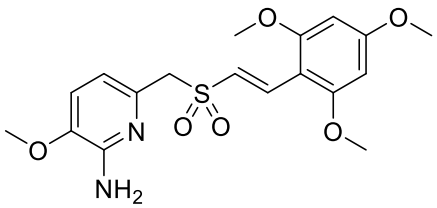
To a solution of compound **46** (10.0 g, 32.9 mmol) in MeOH/H_2O (3:2, 500 mL) was added K_2CO_3 (5.40 g, 39.1 mmol). The reaction mixture was stirred at room temperature for 12 h and concentrated under reduced pressure. The residue was acidified to pH 2 with 1 M HCl. The precipitate was filtered and washed with Et_2O (20 mL) to give **47** as a white solid (9.50 g, 100%). m.p. 97-100 °C. ^{1}H NMR (500 MHz, DMSO-d_6) δ 4.00 (s, 3H, OCH_3), 4.35 (s, 2H), 4.83 (s, 2H) (total 4H, $CH_2SO_2CH_2$), 7.85 (d, 1H, J = 8.5, pyridine-H), 8.04 (d, 1H, J = 9.0, pyridine-H) (one carboxylic acid proton signal not observed). ^{13}C NMR (125 MHz, DMSO-d_6) δ 57.5, 57.6, 59.3, 125.9, 132.4, 138.9, 147.5, 147.8, 164.9. HRMS (ESI) *m/z* 291.0316 ($[M+H]^+$); calcd. for $C_9H_{11}N_2O_7S$ $[M+H]^+$ 291.0281.

(*E*)-3-methoxy-2-nitro-6-(((2,4,6-trimethoxystyryl)sulfonyl)methyl)pyridine (48)



Compound **47** (5.00 g, 17.2 mmol) and 2,4,6-trimethoxybenzaldehyde (3.70 g, 18.9 mmol) were reacted using general synthetic procedure B. The residue was washed with MeOH (10 mL) to give **48** as a white solid (2.30 g, 31%). m.p. 218-219 °C. ^{1}H NMR (500 MHz, DMSO-d_6) δ 3.85 (s, 9H), 3.98 (s, 3H) (total 12H, 4 × OCH_3), 4.66 (s, 2H, CH_2), 6.30 (s, 2H, benzene-H), 7.14 (d, 1H, J = 15.5, $SO_2C\mathit{H}$=CH), 7.55 (d, 1H, J = 16.0, SO_2CH=CH), 7.82 (d, 1H, J = 8.5, pyridine-H), 8.02 (d, 1H, J = 9.0, pyridine-H). ^{13}C NMR (125 MHz, DMSO-d_6) δ 56.1, 56.5, 57.6, 61.0, 91.4, 102.9, 123.5, 125.5, 132.0, 134.2, 140.2, 147.0, 147.8, 148.0, 161.5, 164.4 (two carbon signals overlapping or obscured). HRMS (ESI) *m/z* 425.0925 ([M+H]$^+$); calcd. for $C_{18}H_{21}N_2O_8S$ [M+H]$^+$ 425.1013. Anal. RP-HPLC Method A: t_R 12.99 min, purity > 99%; Method B: t_R 11.10 min, purity >98%.

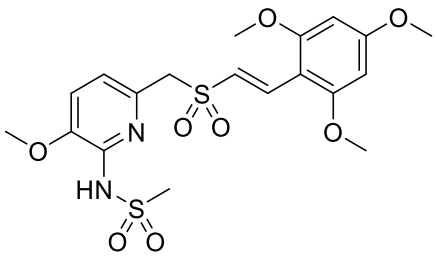
(*E*)-3-methoxy-6-(((2,4,6-trimethoxystyryl)sulfonyl)methyl)pyridin-2-amine (49)



Nitro compound **48** (500 mg, 1.18 mmol) was reduced using general synthetic procedure C. The residue was crystallized (acetone:petroleum ether = 2:1) to give **49** as a white solid (438 mg, 94%). m.p. 211-212 °C. ^{1}H NMR (500 MHz, DMSO-d_6) δ 3.77 (s, 3H), 3.85 (s, 3H), 3.86 (s, 6H) (total 12H, 4 × OCH_3), 4.24 (s, 2H, CH_2), 5.73 (s, 2H, NH_2), 6.30 (s, 2H, benzene-H), 6.59 (d, 1H, J = 8.0, pyridine-H), 7.01 (d, 1H, J = 8.0, pyridine-H), 7.12 (d, 1H, J = 16.0, $SO_2C\mathit{H}$=CH), 7.59 (d, 1H, J = 15.5, SO_2CH=CH). ^{13}C NMR (125 MHz, DMSO-d_6) δ 55.8, 56.1, 56.6, 62.7, 91.4, 103.1, 114.5, 115.8, 124.6, 132.7, 138.2, 141.9, 150.8, 161.4, 164.1 (three carbon signals overlapping or obscured). HRMS (ESI) *m/z* 395.1184 [M+H]$^+$; calcd. for $C_{18}H_{23}N_2O_6S$ [M+H]$^+$

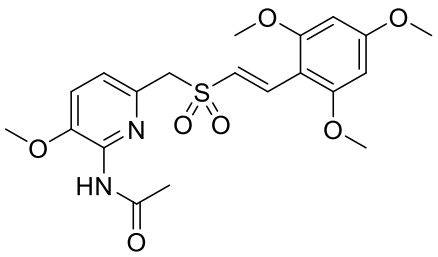
395.1271. Anal. RP-HPLC Method A: t_R 12.23 min, purity >98%; Method B: t_R 9.22 min, purity >98%.

(*E*)-*N*-(3-methoxy-6-(((2,4,6-trimethoxystyryl)sulfonyl)methyl)pyridine-2-yl)methanesulfonamide (50a)



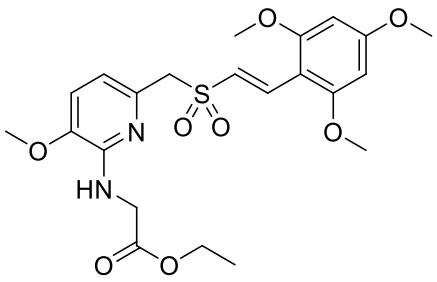
To a solution of compound **49** (1.1 g, 2.8 mmol) in anhydrous pyridine (25 mL) at 0 °C was added dropwise methanesulfonyl chloride (0.60 mL, 7.8 mmol). The reaction mixture was stirred at room temperature for 14 h and concentrated under reduced pressure. The residue was diluted with H_2O (5 mL) and 1 M NaOH (14 mL), and extracted with EtOAc (3 × 50 mL). The organic extracts were combined, washed with brine (20 mL), dried over $MgSO_4$ and concentrated under reduced pressure. The residue was purified by FlashMaster Personal$^+$ flash chromatography (silica gel, EtOAc:petroleum ether = 0:100 ramping to 100:0) and crystallized (EtOAc:hexane = 99:1) to give **50a** as a white solid (0.66 g, 50%). m.p. 171-173 °C. ^{1}H NMR (500 MHz, DMSO-d_6) δ 3.25 (s, 3H, SO_2CH_3), 3.82 (s, 3H), 3.84 (s, 6H), 3.85 (s, 3H) (total 12H, 4 × OCH_3), 4.46 (s, 2H, CH_2), 6.29 (s, 2H, benzene-H), 7.13 (d, 1H, J = 15.5, SO_2CH=CH), 7.14 (s, 1H, J = 8.0, pyridine-H), 7.41 (d, 1H, J = 8.0, pyridine-H), 7.55 (d, 1H, J = 15.5, SO_2CH=C*H*), 9.73 (s, 1H, $NHSO_2$). ^{13}C NMR (125 MHz, DMSO-d_6) δ 42.4, 29.1, 56.1, 56.3, 56.5, 62.1, 91.4, 102.9, 119.2, 121.7, 124.2, 133.5, 138.5, 144.8, 161.4, 164.2 (three carbon signals overlapping or obscured). HRMS (ESI) *m/z* 473.1045 $[M+H]^+$; calcd. for $C_{19}H_{25}N_2O_8S_2$ $[M+H]^+$ 473.1047. Anal. RP-HPLC Method A: t_R 10.09 min, purity >99%; Method B: t_R 10.09 min, purity >95%.

(*E*)-N-(3-methoxy-6-(((2,4,6-trimethoxystyryl)sulfonyl)methyl)pyridin-2-yl)acetamide (50b)



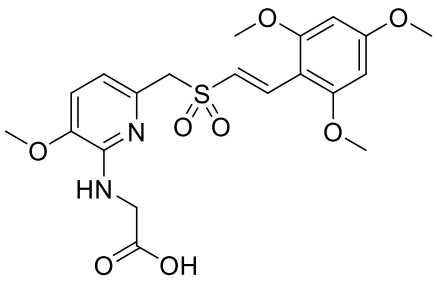
To a solution of compound **49** (100 mg, 0.254 mmol) in anhydrous pyridine (5 mL) was added dropwise acetyl chloride (500 μL, 7.03 mmol). The reaction mixture was stirred at room temperature for 2 h under N_2 and concentrated under reduced pressure. The residue was diluted with 1 M NaOH (100 mL) and extracted with CH_2Cl_2 (3 × 50 mL). The organic extracts were combined, dried over $MgSO_4$ and concentrated under reduced pressure. The residue was purified by an Isolera Four automated flash chromatography system using a 50 g KP-SIL SNAP flash cartridge (silica gel, hexane ramping to acetone:hexane = 4:1) to give **50b** as a yellow solid (47 mg, 42%). m.p. 107-109 °C. ^{1}H NMR (500 MHz, DMSO-d_6) δ 2.02 (s, 3H, $COCH_3$), 3.81 (s, 3H), 3.85 (s, 9H) (total 12H, 4 × OCH_3), 4.48 (s, 2H, CH_2), 6.30 (s, 2H, benzene-H), 7.15 (d, 1H, J = 15.5, SO_2CH=CH), 7.28 (d, 1H, J = 8.0, pyridine-H), 7.48 (d, 1H, J = 8.5, pyridine-H), 7.60 (d, 1H, J = 15.5, SO_2CH=C*H*), 9.54 (br s, 1H, NHCO). ^{13}C NMR (125 MHz, DMSO-d_6) δ 23.6, 56.1, 56.3, 56.5, 62.1, 91.4, 103.0, 120.3, 124.2, 124.3, 133.2, 139.2, 141.4, 148.4, 161.5, 164.2, 169.4 (three carbon signals overlapping or obscured). HRMS (ESI) *m/z* 437.1374 $[M+H]^+$; calcd. for $C_{20}H_{25}N_2O_7S$ $[M+H]^+$ 437.1377. Anal. RP-HPLC Method A: t_R 10.69 min, purity >95%; Method B: t_R 9.46 min, purity >95%.

(*E*)-ethyl 2-((3-methoxy-6-(((2,4,6-trimethoxystyryl)sulfonyl)methyl)pyridin-2-yl)amino)acetate (50c)



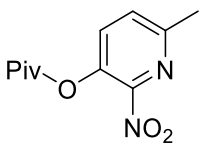
To a solution of compound **49** (100 mg, 0.254 mmol) in DMF (5 mL) was added NaH (20.0 mg, 0.833 mmol). The reaction mixture was stirred for 1 h, and ethyl bromoacetate (200 μL, 1.81 mmol) was added. The reaction mixture was stirred at room temperature for 18 h, cooled down to 0 °C, diluted with H_2O (50 mL) and extracted with EtOAc (3 × 50 mL). The organic extracts were combined, dried over $MgSO_4$ and concentrated under reduced pressure. The residue was purified by an Isolera Four automated flash chromatography system using a 25 g KP-SIL SNAP flash cartridge (silica gel, EtOAc:hexane = 1:9 ramping to EtOAc) to give **50c** as a white solid (31 mg, 25%). m.p. 129-132 °C. ^{1}H NMR (500 MHz, DMSO-d_6) δ 1.12 (t, 3H, J = 7.0, CH_2CH_3), 3.81 (s, 3H), 3.84 (s, 3H), 3.85 (s, 6H) (total 12H, 4 × OCH_3), 3.94 (d, 2H, J = 5.0, $NHCH_2$), 4.00 (q, 2H, J = 7.0, CH_2CH_3), 4.25 (s, 2H, pyridine-CH_2SO_2), 6.30 (s, 2H, benzene-H), 6.35 (t, 1H, J = 5.5, $NHCH_2$), 6.62 (d, 1H, J = 7.5, pyridine-H), 7.03 (d, 1H, J = 8.0, pyridine-H), 7.11 (d, 1H, J = 15.5, SO_2CH=CH), 7.56 (d, 1H, J = 15.5, SO_2CH=C*H*). ^{13}C NMR (125 MHz, DMSO-d_6) δ 14.5, 55.9, 56.1, 56.5, 60.5, 61.1, 62.9, 91.4, 103.1, 114.5, 115.2, 124.8, 132.6, 138.0, 142.3, 148.8, 161.4, 164.0, 171.4 (three carbon signals overlapping or obscured). HRMS (ESI) *m/z* 481.1687 $[M+H]^+$; calcd. for $C_{22}H_{29}N_2O_8S$ $[M+H]^+$ 481.1639. Anal. RP-HPLC Method A: t_R 13.14 min, purity >95%; Method B: t_R 10.00 min, purity >96%.

(*E*)-2-((3-methoxy-6-(((2,4,6-trimethoxystyryl)sulfonyl)methyl)pyridin-2-yl)amino)acetic acid (50d)



To a solution of compound **50c** (20 mg, 0.042 mmol) in MeOH (5 mL) was added a solution of NaOH (40 mg, 1.0 mmol) in H_2O (10 mL). The reaction mixture was stirred at room temperature for 18 h, and MeOH was removed under reduced pressure. The remaining aqueous mixture was acidified to pH 2 with 1 M HCl, and the precipitate was filtered and washed with H_2O (10 mL) to give **50d** as a white solid (14 mg, 74%). m.p. > 300 °C. ^{1}H NMR (500 MHz, DMSO-d_6) δ 3.83 (s, 3H), 3.85 (s, 9H) (total 12H, 4 × OCH_3), 3.95 (s, 2H, NHCH_2), 4.33 (s, 2H, pyridine-CH_2SO_2), 6.29 (s, 2H, benzene-H), 6.65 (d, 1H, J = 7.5, pyridine-H), 7.09 (d, 1H, J = 7.0, pyridine-H), 7.13 (d, 1H, J = 15.5, SO_2C*H*=CH), 7.56 (d, 1H, J = 15.5, SO_2CH=C*H*) (one carboxylic acid proton signal and one secondary amine proton signal not observed). ^{13}C NMR (125 MHz, DMSO-d_6) δ 42.0, 55.6, 56.1, 91.0, 102.5, 114.1, 115.0, 124.0, 132.5, 142.1, 148.2, 42.0, 55.6, 56.1, 91.0, 102.5, 114.1, 115.0, 124.0, 132.5, 142.1, 148.2, 161.0, 163.7, 172.0 (six carbon signals overlapping or obscured). HRMS (ESI) *m/z* 453.1260 $[M+H]^+$; calcd. for $C_{20}H_{25}N_2O_8S$ $[M+H]^+$ 453.1326. Anal. RP-HPLC: t_R = 11.03 min, purity >96% (method A); t_R 9.56 min, purity >96% (method B).

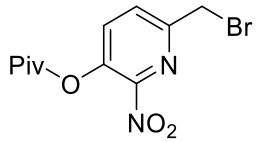
6-methyl-2-nitropyridin-3-yl pivalate (52)



To a solution of 6-methyl-2-nitropyridin-3-ol (20.0 g, 130 mmol) in CH_2Cl_2 (300 mL) was added Et_3N (27.1 mL, 194 mmol) and pivaloyl chloride (19.2 mL, 156 mmol). The reaction mixture was stirred at room temperature for 15 h and concentrated under reduced pressure. The residue was added 0.1M HCl (100 mL) and extracted with CH_2Cl_2 (3 × 200 mL). The extracts were combined, dried under $MgSO_4$, and

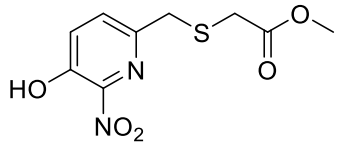
concentrated under reduced pressure to give **52** as a yellow liquid (31.8 g, 100%). ^{1}H NMR (500 MHz, $CDCl_3$) δ 1.36 (s, 9H, pivalate-CH_3), 2.63 (s, 3H, pyridine-CH_3), 7.48 (d, 1H, *J* = 8.5, pyridine-H), 7.57 (d, 1H, *J* = 8.0, pyridine-H). ^{13}C NMR (125 MHz, $CDCl_3$) δ 23.7, 26.6, 27.0, 39.4, 129.1, 135.1, 137.9, 155.6, 175.7. HRMS (ESI) *m/z* 239.1048 $[M+H]^+$; calcd. for $C_{11}H_{15}N_2O_4$ $[M+H]^+$ 239.1026.

6-(bromomethyl)-2-nitropyridin-3-yl pivalate (53)



To a solution of compound **52** (16.5 g, 69.3 mmol) in MeCN (200 mL) was added N-bromosuccinimide (7.39 g, 41.5 mmol) and AIBN (0.568 g, 3.46 mmol). The reaction mixture was heated at reflux for 6 h, added with N-bromosuccinimide (7.39 g, 41.5 mmol) and AIBN (0.568 g, 3.46 mmol), further heated at reflux for 12 h, and concentrated under reduced pressure. The residue was briefly purified by flash column chromatography (silica gel, petroleum ether ramping to CH_2Cl_2:petroleum ether = 1:1) to give the crude **53** as a yellow liquid which was used without further characterization.

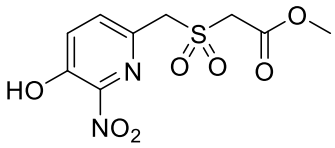
methyl 2-(((5-hydroxy-6-nitropyridin-2-yl)methyl)thio)acetate (54)



To a solution of compound **53** (354 mg, 1.12 mmol) in MeOH (10 mL) was added Na_2CO_3 (142 mg, 1.34 mmol) and methyl thioglycolate (100 μL, 1.12 mmol). The reaction mixture was stirred at room temperature for 2 h and concentrated under reduced pressure. The residue was added 0.1 M HCl (50 mL) and extracted with EtOAc (3 × 50 mL). The extracts were combined, dried over $MgSO_4$, and concentrated under reduced pressure. The residue was purified by flash column chromatography (silica gel, petroleum ether ramping to CH_2Cl_2, then ramping from CH_2Cl_2 to EtOAc:CH_2Cl_2 = 1:4) to give **54** as a yellow solid (200 mg, 69.4%). m.p. 56-58 °C. ^{1}H NMR (500 MHz, $CDCl_3$) δ 3.27 (s, 2H, SCH_2CO), 3.71 (s, 3H, OCH_3), 3.95 (s, 2H, pyridine-CH_2S), 7.62 (d, 1H, *J* = 8.5, pyridine-H), 7.73 (d, 1H, *J* = 8.5, pyridine-H), 10.21 (s, 1H, OH). ^{13}C NMR (125 MHz, $CDCl_3$) δ 33.0, 37.0, 52.7, 131.0, 132.3, 141.3, 149.5, 150.0, 170.5.

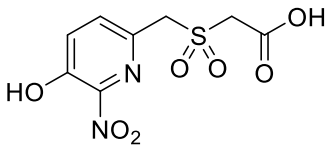
HRMS (ESI) *m/z* 259.0384 $[M+H]^+$, 281.0202 $[M+Na]^+$; calcd. for $C_9H_{11}N_2O_5S$ $[M+H]^+$ 259.0383, $C_9H_{10}N_2NaO_5S$ $[M+Na]^+$ 281.0203.

methyl 2-(((5-hydroxy-6-nitropyridin-2-yl)methyl)sulfonyl)acetate (55)



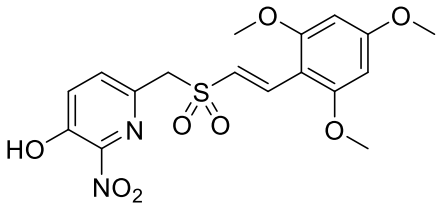
Thioether **54** (786 mg, 3.04 mmol) was oxidised according to general synthetic procedure A. The residue was triturated with EtOH (30 mL) and filtered to give **55** as a white solid (776 mg, 88%). m.p. 174-176 °C. ^{1}H NMR (500 MHz, DMSO-d_6) δ 3.71 (s, 3H, OCH_3), 4.48 (s, 2H, SO_2CH_2CO), 4.78 (s, 2H, pyridine-CH_2SO_2), 7.69 (app m, 2H, pyridine-H). ^{13}C NMR (125 MHz, DMSO-d_6) δ 52.9, 56.7, 59.2, 129.6, 132.3, 137.3, 146.3, 146.8, 163.6. HRMS (ESI) *m/z* 291.0347 $[M+H]^+$; calcd. for $C_9H_{11}N_2O_7S$ $[M+H]^+$ 291.0281.

2-(((5-hydroxy-6-nitropyridin-2-yl)methyl)sulfonyl)acetic acid (56)



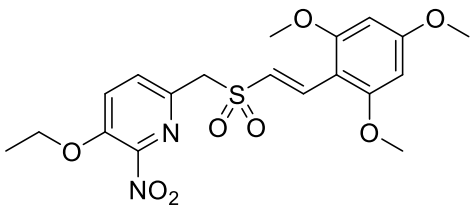
To a solution of compound **55** (500 mg, 1.72 mmol) in H_2O/MeOH (1:1, 20 mL) was added sodium carbonate (438 mg, 4.13 mmol). The reaction mixture was stirred at room temperature for 14 h and concentrated under reduced pressure. The residue was acidified to pH = 2 with 1 M HCl, added with H_2O (20 mL), and extracted with EtOAc (3 × 50 mL). The extracts were combined, dried over $MgSO_4$ and concentrated under reduced pressure to give **56** as a white solid (441 mg, 93%). m.p. 185-187 °C. ^{1}H NMR (500 MHz, DMSO-d_6) δ 4.33 (s, 2H, SO_2CH_2CO), 4.78 (s, 2H, pyridine-CH_2SO_2), 7.70 (app s, 2H, pyridine-H) (one carboxylic acid proton not observed). ^{13}C NMR (125 MHz, DMSO-d_6) δ 57.0, 58.9, 129.4, 132.2, 137.5, 146.3, 146.6, 164.5. HRMS (ESI) *m/z* 277.0123 $[M+H]^+$; calcd. for $C_8H_9N_2O_7S$ $[M+H]^+$ 277.0125.

(*E*)-2-nitro-6-(((2,4,6-trimethoxystyryl)sulfonyl)methyl)pyridin-3-ol (57)



Compound **56** (4.50 g, 16.3 mmol) and 2,4,6-trimethoxybenzaldehyde (3.20 g, 16.3 mmol) were reacted using general synthetic procedure B. The residue was washed with MeOH (150 mL) to give **57** as a yellow solid (2.48 g, 43%). m.p. 216-218 °C. ^{1}H NMR (500 MHz, $CDCl_3$) δ 3.84 (s, 6H), 3.85 (s, 3H) (total 9H, 3× OCH_3), 4.50 (s, 2H, CH_2), 6.08 (s, 2H, benzene-H), 7.15 (d, 1H, *J* = 15.5, SO_2CH=CH), 7.66 (d, 1H, *J* = 8.5, pyridine-H), 7.72 (d, 1H, *J* = 15.5, SO_2CH=C*H*), 7.88 (d, 1H, *J* = 8.5, pyridine-H), 10.24 (s, 1H, OH). ^{13}C NMR (125 MHz, $CDCl_3$) δ 55.6, 55.9, 62.4, 90.5, 103.7, 122.0, 130.9, 134.3, 136.9, 141.4, 141.6, 150.8, 161.8, 164.4 (three carbon signals overlapping or obscured). HRMS (ESI) *m/z* 411.0874 $[M+H]^+$; calcd. for $C_{17}H_{19}N_2O_8S$ $[M+H]^+$ 411.0857.

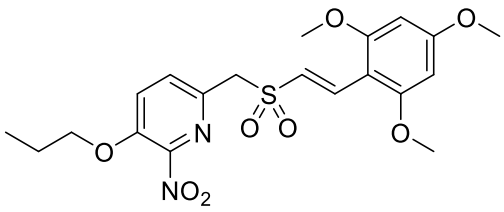
(*E*)-3-ethoxy-2-nitro-6-(((2,4,6-trimethoxystyryl)sulfonyl)methyl)pyridine (58a)



To a solution of compound **57** (100 mg, 0.244 mmol) in DMF (10 mL) was added K_2CO_3 (40 mg, 0.289 mmol) and EtI (100 µL, 1.24 mmol). The reaction mixture was stirred at room temperature for 14 h and concentrated under reduced pressure. The residue was diluted with H_2O (50 mL) and extracted with CH_2Cl_2 (3 × 50 mL). The extracts were combined, dried over $MgSO_4$, and concentrated under reduced pressure. The residue was triturated with MeOH (20 mL) and filtered to give **58a** as a white powder (66 mg, 62%). m.p. 165-167 °C. ^{1}H NMR (500 MHz, $CDCl_3$) δ 1.47 (t, 3H, *J* = 7.0, CH_2CH_3), 3.84 (s, 6H), 3.85 (s, 3H) (total 9H, 3 × OCH_3), 4.21 (q, 2H, *J* = 7.0, CH_2CH_3), 4.43 (s, 2H, pyridine-CH_2SO_2), 6.08 (s, 2H, benzene-H), 7.10 (d, 1H, *J* = 15.5, SO_2CH=CH), 7.51 (d, 1H, *J* = 8.5, pyridine-H), 7.76 (d, 1H, *J* = 8.5, pyridine-H), 7.81 (d, 1H, *J* = 15.5, SO_2CH=C*H*). ^{13}C NMR (125 MHz, $CDCl_3$) δ 14.5, 55.6, 55.9,

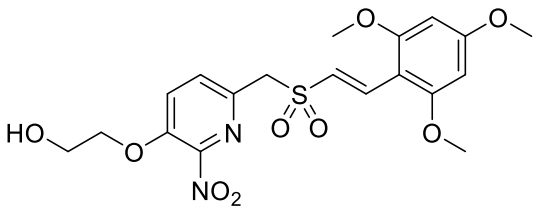
62.3, 66.0, 90.4, 103.8, 121.8, 124.1, 130.7, 136.3, 139.8, 146.8, 148.4, 161.8, 164.2 (three carbon signals overlapping or obscured). HRMS (ESI) *m/z* 439.1218 $[M+H]^+$; calcd. for $C_{19}H_{23}N_2O_8S$ $[M+H]^+$ 439.1170.

(*E*)-2-nitro-3-propoxy-6-(((2,4,6-trimethoxystyryl)sulfonyl)methyl)pyridine (58b)



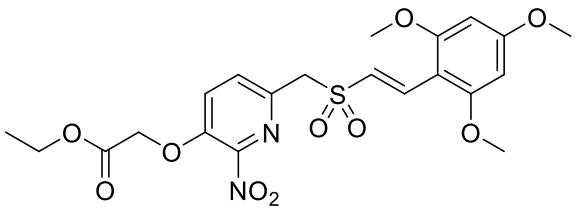
To a solution of compound **57** (100 mg, 0.244 mmol) in DMF (10 mL) was added K_2CO_3 (40 mg, 0.289 mmol) and 1-iodopropane (35 μL, 0.359 mmol). The reaction mixture was stirred at room temperature for 48 h and concentrated under reduced pressure. The residue was added H_2O (50 mL) and extracted with CH_2Cl_2 (3 × 50 mL). The extracts were combined, dried over $MgSO_4$, and concentrated under reduced pressure. The residue was purified by flash column chromatography (silica gel, petroleum ether ramping to EtOAc:petroleum ether = 3:2) to give **58b** as a yellow solid (86 mg, 78%). m.p. 152-153 °C. ^{1}H NMR (500 MHz, $CDCl_3$) δ 1.04 (t, 3H, *J* = 7.5, $CH_2CH_2CH_3$), 1.85 (m, 2H, $CH_2CH_2CH_3$), 3.84 (s, 6H), 3.85 (s, 3H) (total 9H, 3 × OCH_3), 4.09 (t, 2H, *J* = 6.5, $CH_2CH_2CH_3$), 4.43 (s, 2H, pyridine-CH_2SO_2), 6.08 (s, 2H, benzene-H), 7.11 (app dd, 1H, *J* = 15.5 & 0.5, SO_2CH=CH), 7.51 (d, 1H, *J* = 8.5, pyridine-H), 7.76 (d, 1H, *J* = 8.5, pyridine-H), 7.82 (d, 1H, *J* = 15.5, SO_2CH=C*H*). ^{13}C NMR (125 MHz, $CDCl_3$) δ 10.4, 22.3, 55.6, 55.9, 62.3, 71.6, 90.4, 103.8, 121.9, 124.1, 130.8, 136.3, 139.7, 147.0, 148.4, 161.8, 164.2 (three carbon signals overlapping or obscured). HRMS (ESI) *m/z* 453.1318 $[M+H]^+$; calcd. for $C_{20}H_{25}N_2O_8S$ $[M+H]^+$ 453.1326.

(*E*)-2-((2-nitro-6-(((2,4,6-trimethoxystyryl)sulfonyl)methyl)pyridin-3-yl)oxy)ethan-1-ol (58c)



To a solution of compound **57** (200 mg, 0.488 mmol) in DMF (10 mL) was added K_2CO_3 (81.0 mg, 0.586 mmol) and 2-bromoethanol (69.0 µL, 0.974 mmol). The reaction mixture was stirred at room temperature for 6 h, heated at 50 °C for 18 h, and concentrated under reduced pressure. The residue was added H_2O (25 mL), acidified to pH = 2 with 2 M HCl, and extracted with CH_2Cl_2 (3 × 50 mL). The extracts were combined, dried over $MgSO_4$, and concentrated under reduced pressure. The residue was purified by flash column chromatography (silica gel, petroleum ether ramping to EtOAc) to give **58c** as a yellow powder (168 mg, 76%). m.p. 179-182 °C. ^{1}H NMR (500 MHz, DMSO-d_6) δ 3.70 (q, 2H, J = 5.0, CH_2CH_2OH), 3.84 (s, 9H, OCH_3), 4.25 (t, 2H, J = 5.0, CH_2CH_2OH), 4.99 (t, 1H, J = 5.0, OH), 7.13 (d, 1H, J = 15.5, SO_2CH=CH), 7.53 (d, 1H, J = 16.0, SO_2CH=C*H*), 7.77 (d, 1H, J = 8.5, pyridine-H), 8.01 (d, 1H, J = 8.5, pyridine-H). ^{13}C NMR (125 MHz, DMSO-d_6) δ 55.8, 56.2, 59.3, 60.7, 71.8, 91.0, 102.5, 123.1, 126.0, 131.5, 133.9, 139.8, 146.2, 147.8, 161.2, 164.1 (three carbon signals overlapping or obscured). HRMS (ESI) *m/z* 455.1125 $[M+H]^+$; calcd. for $C_{19}H_{23}N_2O_9S$ $[M+H]^+$ 455.1119.

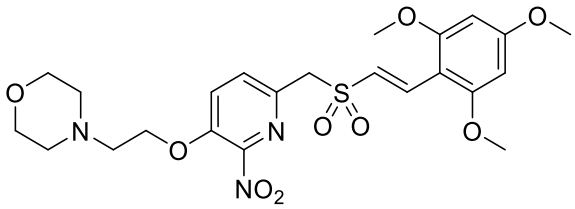
Ethyl (*E*)-2-((2-nitro-6-(((2,4,6-trimethoxystyryl)sulfonyl)methyl)pyridin-3-yl)oxy)-acetate (58d)



To a solution of compound **57** (200 mg, 0.488 mmol) in DMF (10 mL) was added K_2CO_3 (81 mg, 0.586 mmol) and ethyl bromoacetate (70 µL, 0.633 mmol). The reaction mixture was stirred at room temperature for 12 h and concentrated under reduced pressure. The residue was triturated with MeOH (50 mL) and filtered to give **58d** as a

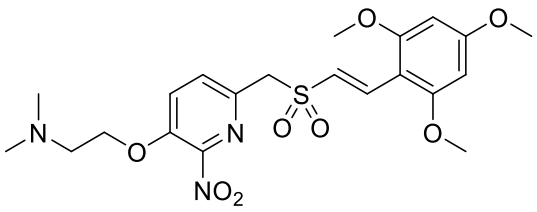
white solid (201 mg, 83%). m.p. 147-148 °C. ^{1}H NMR (500 MHz, DMSO-d_6) δ 1.20 (t, 3H, J = 7.0, CH_2CH_3), 3.86 (s, 9H, OCH_3), 4.17 (q, 2H, J = 7.0, CH_2CH_3), 4.68 (s, 2H, pyridine-CH_2SO_2), 5.11 (s, 2H, OCH_2CO), 6.31 (s, 2H, benzene-H), 7.15 (d, 1H, J = 15.5, SO_2CH=CH), 7.58 (d, 1H, J = 15.5, SO_2CH=CH), 7.79 (d, 1H, J = 9.0, pyridine-H), 7.99 (d, 1H, J = 9.0, pyridine-H). ^{13}C NMR (125 MHz, DMSO-d_6) δ 14.0, 55.7, 56.1, 60.5, 61.1, 65.6, 90.9, 102.4, 123.0, 126.1, 131.3, 133.8, 140.7, 145.0, 147.6, 161.1, 163.9, 167.5 (three carbon signals overlapping or obscured). HRMS (ESI) *m/z* 497.1228 $[M+H]^+$; calcd. for $C_{21}H_{25}N_2O_{10}S$ $[M+H]^+$ 497.1224.

(*E*)-4-(2-((2-nitro-6-(((2,4,6-trimethoxystyryl)sulfonyl)methyl)pyridin-3-yl)oxy)ethyl)morpholine (58e)



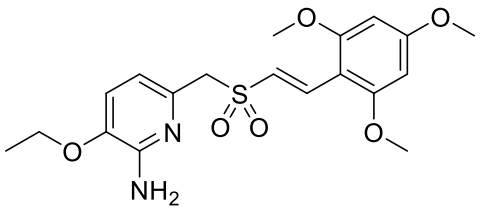
To a solution of compound **57** (200 mg, 0.488 mmol) in DMF (10 mL) was added K_2CO_3 (162 mg, 1.17 mmol) and 4-(2-chloroethyl)morpholine hydrochloride (109 mg, 0.586 mmol). The reaction mixture was heated at 50 °C for 48 h and concentrated under reduced pressure. The residue was diluted with CH_2Cl_2 (50 mL), filtered, and the filtrate concentrated under reduced pressure. The residue was purified by flash column chromatography (silica gel, CH_2Cl_2 ramping to MeOH:CH_2Cl_2 = 6:94) to give **60e** as a brown liquid (255 mg, 98%). ^{1}H NMR (500 MHz, $CDCl_3$) δ 2.59 (app s, 4H, morpholine-CH_2), 2.85 (t, 2H, J = 5.0, OCH_2CH_2N), 3.71 (t, 4H, J = 4.5, morpholine-CH_2), 3.84 (s, 6H), 3.85 (s, 3H) (total 9H, 3 × OCH_3), 4.28 (t, 2H, J = 5.0,OCH_2CH_2N), 4.44 (s, 2H, pyridine-CH_2SO_2), 6.08 (s, 2H, benzene-H), 7.12 (d, 1H, J = 15.5, SO_2CH=CH), 7.55 (d, 1H, J = 8.5, pyridine-H), 7.77 (d, 1H, J = 8.5, pyridine-H), 7.83 (d, 1H, J = 15.5, SO_2CH=CH). ^{13}C NMR (125 MHz, $CDCl_3$) δ 54.2, 55.6, 55.9, 57.0, 62.3, 66.9, 68.7, 90.4, 103.8, 121.9, 124.6, 130.8, 136.3, 140.3, 146.7, 148.4, 161.8, 164.3 (five carbon signals overlapping or obscured). HRMS (ESI) *m/z* 524.1688 $[M+H]^+$; calcd. for $C_{23}H_{30}N_3O_9S$ $[M+H]^+$ 524.1697.

(*E*)-N,N-dimethyl-2-((2-nitro-6-(((2,4,6-trimethoxystyryl)sulfonyl)methyl)pyridin-3-yl)oxy)ethan-1-amine (58f)



To a solution of compound **57** (200 mg, 0.488 mmol) in DMF (10 mL) was added K_2CO_3 (324 mg, 2.34 mmol) and 2-chloro-N,N-dimethylethylamine hydrochloride (140 mg, 0.972 mmol). The reaction mixture was heated at 50 °C for 48 h and concentrated under reduced pressure. The residue was dissolved in CH_2Cl_2 (50 mL), filtered, and the filtrate concentrated under reduced pressure. The residue was purified by flash column chromatography (silica gel, CH_2Cl_2 ramping to MeOH:CH_2Cl_2 = 8:92) to give **58f** as a yellow liquid (128 mg, 55%). ^{1}H NMR (500 MHz, $CDCl_3$) δ 2.37 (s, 6H, NCH_3), 2.83 (t, 2H, *J* = 5.5, OCH_2CH_2N), 3.83 (s, 6H), 3.84 (s, 3H) (total 9H, 3 × OCH_3), 4.26 (t, 2H, *J* = 5.5, OCH_2CH_2N), 4.43 (s, 2H, pyridine-CH_2SO_2), 6.07 (s, 2H, benzene-H), 7.11 (d, 1H, *J* = 15.5, SO_2CH=CH), 7.56 (d, 1H, *J* = 8.5, pyridine-H), 7.76 (d, 1H, *J* = 8.5, pyridine-H), 7.82 (d, 1H, *J* = 15.5, SO_2CH=C*H*). ^{13}C NMR (125 MHz, $CDCl_3$) δ 46.0, 55.6, 55.9, 57.5, 62.3, 68.8, 90.4, 103.8, 121.9, 124.6, 130.9, 136.3, 140.3, 146.8, 148.3, 161.8, 164.2 (four carbon signals overlapping or obscured). HRMS (ESI) *m/z* 482.1596 $[M+H]^+$; calcd. for $C_{21}H_{28}N_3O_8S$ $[M+H]^+$ 482.1592.

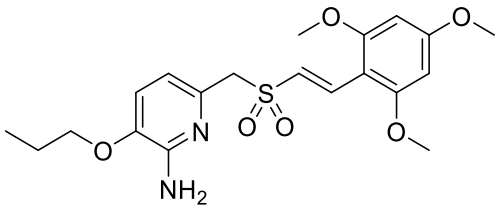
(*E*)-3-ethoxy-6-(((2,4,6-trimethoxystyryl)sulfonyl)methyl)pyridin-2-amine (59a)



Nitro compound **58a** (100 mg, 0.228 mmol) was reduced using general synthetic procedure C. The residue was purified by flash column chromatography (silica gel, CH_2Cl_2 ramping to acetone:CH_2Cl_2 = 1:4) and washed with MeOH (20 mL) to give **59a** as a white solid (63 mg, 68%). m.p. 185-187 °C. ^{1}H NMR (500 MHz, DMSO-d_6) δ 1.33 (t, 3H, *J* = 7.0, CH_2CH_3), 3.84 (s, 3H), 3.85 (s, 6H) (total 9H, 3 × OCH_3), 4.00 (q, 2H, *J* = 7.0, CH_2CH_3), 4.23 (s, 2H, pyridine-CH_2SO_2), 5.65 (s, 2H, NH_2), 6.29 (s, 2H,

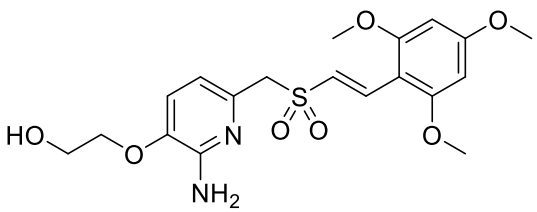
benzene-H), 6.57 (d, 1H, *J* = 8.0, pyridine-H), 6.99 (d, 1H, *J* = 8.0, pyridine-H), 7.11 (d, 1H, *J* = 15.5, SO_2C*H*=CH), 7.58 (d, 1H, *J* = 16.0, SO_2CH=C*H*). ^{13}C NMR (500 MHz, DMSO-d_6) δ 14.6, 55.7, 56.2, 62.3, 63.6, 91.1, 102.7, 114.3, 116.3, 124.1, 132.4, 137.7, 140.7, 150.6, 161.1, 163.7 (three carbon signals overlapping or obscured). HRMS (ESI) *m/z* 409.1398 $[M+H]^+$; calcd. for $C_{19}H_{25}N_2O_6S$ $[M+H]^+$ 409.1428. Anal. RP-HPLC: t_R =10.46, purity >98% (method A); t_R = 8.99, purity >98% (method B).

(*E*)-3-propoxy-6-(((2,4,6-trimethoxystyryl)sulfonyl)methyl)pyridin-2-amine (59b)



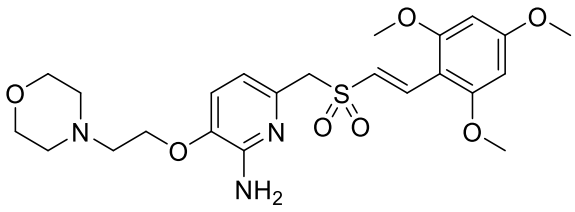
Nitro compound **58b** (80 mg, 0.18 mmol) was reduced using general synthetic procedure C. The residue was purified by flash column chromatography (silica gel, CH_2Cl_2 ramping to acetone:CH_2Cl_2 = 1:9) to give **59b** as a white solid (56 mg, 75%). m.p. 165-167 °C. ^{1}H NMR (500 MHz, DMSO-d_6) δ 0.99 (t, 3H, *J* = 7.0, $CH_2CH_2CH_3$), 1.73 (m, 2H, $CH_2CH_2CH_3$), 3.85 (s, 3H), 3.86 (s, 6H) (total 9H, 3 × OCH_3), 3.91 (t, 2H, *J* = 6.5, $CH_2CH_2CH_3$), 4.24 (s, 2H, pyridine-CH_2SO_2), 5.69 (s, 2H, NH_2), 6.30 (s, 2H, benzene-H), 6.57 (d, 1H, *J* = 8.0, pyridine-H), 6.99 (d, 1H, *J* = 8.0, pyridine-H), 7.12 (d, 1H, *J* = 16.0, SO_2C*H*=CH), 7.59 (d, 1H, *J* = 16.0, SO_2CH=C*H*). ^{13}C NMR (500 MHz, DMSO-d_6) δ 10.5, 21.9, 55.7, 56.1, 62.2, 69.2, 91.0, 102.6, 114.1, 116.1, 124.1, 132.2, 137.6, 140.7, 150.5, 161.0, 163.6 (three carbon signals overlapping or obscured). HRMS (ESI) *m/z* 423.1578 $[M+H]^+$; calcd. for $C_{20}H_{27}N_2O_6S$ $[M+H]^+$ 423.1584. Anal. RP-HPLC: t_R = 10.74, purity >98% (method A); t_R = 9.12, purity >98% (method B).

(*E*)-2-((2-amino-6-(((2,4,6-trimethoxystyryl)sulfonyl)methyl)pyridin-3-yl)oxy)ethan-1-ol (59c)



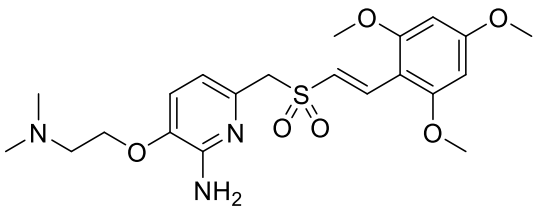
Nitro compound **58c** (100 mg, 0.220 mmol) was reduced using general synthetic procedure C. The residue was purified by flash column chromatography (silica gel, CH_2Cl_2 ramping to MeOH:CH_2Cl_2 = 4:96) to give **59c** as a white solid (70 mg, 75%). m.p. 88-90 °C. ^{1}H NMR (500 MHz, DMSO-d_6) δ 3.71 (m, 2H, CH_2CH_2OH), 3.83 (s, 3H), 3.85 (s, 6H) (total 9H, 3 × OCH_3), 3.92 (t, 2H, J = 4.5, CH_2CH_2OH), 4.23 (s, 2H, pyridine-CH_2SO_2), 5.04 (t, 1H, J = 6.0, OH), 5.85 (s, 2H, NH_2), 6.28 (s, 2H, benzene-H), 6.55 (d, 1H, J = 8.0, pyridine-H), 6.97 (d, 1H, J = 7.5, pyridine-H), 7.11 (d, 1H, J = 15.5, SO_2CH=CH), 7.58 (d, 1H, J = 15.5, SO_2CH=CH). ^{13}C NMR (500 MHz, DMSO-d_6) δ 55.8, 56.3, 59.7, 62.4, 70.0, 91.1, 102.7, 114.2, 116.3, 124.1, 132.5, 137.9, 140.9, 150.8, 161.1, 163.8 (three carbon signals overlapping or obscured). HRMS (ESI) *m/z* 425.1385 $[M+H]^+$; calcd. for $C_{19}H_{25}N_2O_7S$ $[M+H]^+$ 425.1377. Anal. RP-HPLC: t_R = 10.03, purity >98% (method A); t_R = 8.34, purity >98% (method B).

(*E*)-3-(2-morpholinoethoxy)-6-(((2,4,6-trimethoxystyryl)sulfonyl)methyl)pyridin-2-amine (59e)



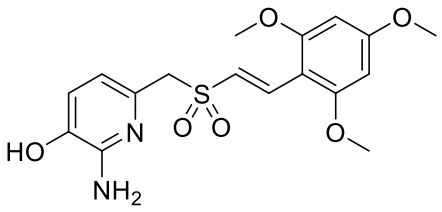
Nitro compound **58e** (250 mg, 0.478 mmol) was reduced using general synthetic procedure C. The residue was purified by flash column chromatography (silica gel, CH_2Cl_2 ramping to MeOH:CH_2Cl_2 = 1:9) to give **59e** as a white solid (87 mg, 37%). m.p. 148-150 °C. ^{1}H NMR (500 MHz, DMSO-d_6) δ 2.46 (app s, 4H, morpholine-H), 2.69 (t, 2H, J = 5.5, OCH_2CH_2N), 3.56 (t, 4H, J = 4.5, morpholine-H), 3.85 (s, 3H), 3.86 (s, 6H) (total 9H, 3 × OCH_3), 4.06 (t, 2H, J = 5.5, OCH_2CH_2N), 4.24 (s, 2H, pyridine-CH_2SO_2), 5.75 (s, 2H, NH_2), 6.30 (s, 2H, benzene-H), 6.57 (d, 1H, J = 8.0, pyridine-H), 7.05 (d, 1H, J = 8.0, pyridine-H), 7.12 (d, 1H, J = 15.5, SO_2CH=CH), 7.59 (d, 1H, J = 15.5, SO_2CH=CH). ^{13}C NMR (500 MHz, DMSO-d_6) δ 53.6, 55.7, 56.1, 56.9, 62.2, 66.1, 66.2, 91.0, 102.6, 114.1, 117.2, 124.0, 132.3, 138.2, 140.5, 150.8, 161.0, 163.6 (five carbon signals overlapping or obscured). HRMS (ESI) *m/z* 494.1966 $[M+H]^+$; calcd. for $C_{23}H_{32}N_3O_7S$ $[M+H]^+$ 494.1955. Anal. RP-HPLC: t_R = 10.98, purity >95% (method A); t_R = 8.68, purity >97% (method B).

(*E*)-3-(2-(dimethylamino)ethoxy)-6-(((2,4,6-trimethoxystyryl)sulfonyl)methyl)-pyridin-2-amine (59f)



Nitro compound **58f** (100 mg, 0.208 mmol) was reduced using general synthetic procedure C. The residue was purified by flash column chromatography (silica gel, CH_2Cl_2 ramping to MeOH:CH_2Cl_2 = 8:92) to give **59f** as a white solid (45 mg, 48%). m.p. 76-79 °C. ^{1}H NMR (500 MHz, acetone-d_6) δ 2.28 (s, 6H, NCH_3), 2.70 (app s, 2H, OCH_2CH_2N), 3.88 (s, 3H), 3.91 (s, 6H) (total 9H, 3 × OCH_3), 4.10 (t, 2H, *J* = 6.0, OCH_2CH_2N), 4.17 (s, 2H, pyridine-CH_2SO_2), 6.30 (s, 2H, benzene-H), 6.70 (d, 1H, *J* = 7.5, pyridine-H), 7.04 (d, 1H, *J* = 8.0, pyridine-H), 7.18 (d, 1H, *J* = 15.5, SO_2CH=CH), 7.76 (d, 1H, *J* = 16.0, SO_2CH=C*H*). ^{13}C NMR (500 MHz, acetone-d_6) δ 46.0, 55.9, 56.4, 58.8, 63.8, 67.7, 91.5, 104.3, 115.4, 117.9, 125.6, 133.6, 139.9, 141.9, 151.8, 162.3, 164.8 (four carbon signals overlapping or obscured). HRMS (ESI) *m/z* 452.1856 $[M+H]^+$; calcd. for $C_{21}H_{30}N_3O_6S$ $[M+H]^+$ 452.1850. Anal. RP-HPLC: t_R =10.93, purity >97% (method A); t_R =8.63, purity >97% (method B).

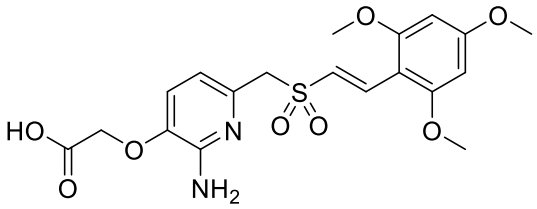
(*E*)-2-amino-6-(((2,4,6-trimethoxystyryl)sulfonyl)methyl)pyridin-3-ol (59g)



To a solution of compound **57** (100 mg, 0.244 mmol) in MeOH (10 mL) was added 10 % Pd in C (3 mg, 2.82 nmol). The reaction mixture was stirred at room temperature for 6 h under H_2, filtered, and the filtrate concentrated under reduced pressure. The residue was purified by flash column chromatography (silica gel, CH_2Cl_2 ramping to MeOH:CH_2Cl_2 = 3:97) and washed with Et_2O (10 mL) to give **59g** as a light yellow solid (49 mg, 53%). m.p. 175-177 °C. ^{1}H NMR (500 MHz, DMSO-d_6) δ 3.85 (s, 3H), 3.86 (s, 6H) (total 9H, 3 × OCH_3), 4.20 (s, 2H, pyridine-CH_2SO_2), 5.51 (s, 2H, NH_2), 6.30 (s, 2H, benzene-H), 6.48 (d, 1H, *J* = 8.0, pyridine-H), 6.81 (d, 1H, *J* = 7.5,

pyridine-H), 7.11 (d, 1H, *J* = 16.0, $SO_2C\mathit{H}$=CH), 7.59 (d, 1H, *J* = 15.5, SO_2CH=C*H*), 9.62 (s, 1H, OH). ^{13}C NMR (125 MHz, DMSO-d_6) δ 55.6, 56.1, 65.0, 91.0, 102.6, 114.5, 118.7, 124.1, 132.1, 136.6, 139.1, 150.2, 160.9, 163.6 (three carbon signals overlapping or obscured). HRMS (ESI) *m/z* 381.1142 $[M+H]^+$; calcd. for $C_{17}H_{21}N_2O_6S$ $[M+H]^+$ 381.1115. Anal. RP-HPLC: t_R = 9.82, purity >99% (method A); t_R = 8.35, purity >99% (method B).

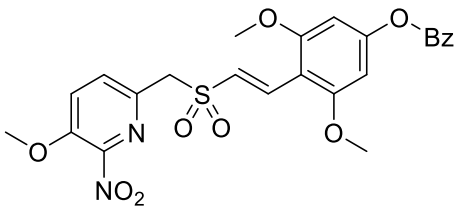
(*E*)-2-((2-amino-6-(((2,4,6-trimethoxystyryl)sulfonyl)methyl)pyridin-3-yl)oxy)acetic acid (59h)



To a solution of **58d** (50 mg, 0.10 mmol) in MeOH/CH_2CO_2H (1:1, 10 mL) was added Fe powder (45 mg, 0.81 mmol). The reaction mixture was heated at 50 °C for 2 h under N_2 gas and concentrated under reduced pressure. The residue was diluted with saturated aqueous $NaHCO_3$ (25 mL) and H_2O (75 mL). The mixture was extracted with CH_2Cl_2 (3 × 50 mL). The organic layer and extract were combined, dried over $MgSO_4$, and concentrated under reduced pressure. The residue was purified by flash column chromatography (silica gel, CH_2Cl_2 ramping to MeOH:CH_2Cl_2 = 2:98) to give a mixture of ester and carboxylic acid as a white solid which was dissolved in H_2O/MeOH (1:1, 10 mL) and added 1 M NaOH (1 mL). The reaction mixture was stirred at room temperature for 12 h, added 1 M NaOH (5 mL), heated at 80 °C for 2 h and concentrated under reduced pressure. The residue was acidified to pH = 2 with 1 M HCl. The precipitate was filtered and washed with MeOH (5 mL) to give **59h** as a white solid (21 mg, 48%). m.p. 270-272 °C. ^{1}H NMR (500 MHz, DMSO-d_6) δ 3.85 (s, 3H), 3.86 (s, 6H) (total 9H, 3 × OCH_3), 4.25 (s, 2H, pyridine-CH_2SO_2), 4.67 (s, 2H, OCH_2CO), 5.77 (s, 2H, NH_2), 6.30 (s, 2H, benzene-H), 6.56 (d, 1H, *J* = 7.5, pyridine-H), 6.94 (d, 1H, *J* = 8.0, pyridine-H), 7.13 (d, 1H, *J* = 16.0, $SO_2C\mathit{H}$=CH), 7.61 (d, 1H, *J* = 15.5, SO_2CH=C*H*). ^{13}C NMR (500 MHz, DMSO-d_6) δ 55.7, 56.1, 62.1, 64.9, 89.2, 91.0, 102.6, 114.0, 117.1, 124.0, 132.3, 140.0, 150.4, 161.0, 163.7, 170.0 (three carbon signals overlapping or obscured). HRMS (ESI) *m/z* 439.1176 $[M+H]^+$; calcd. for

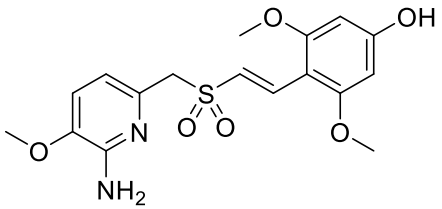
$C_{19}H_{23}N_2O_8S$ $[M+H]^+$ 439.1170. Anal. RP-HPLC: t_R = 12.08, purity >95% (method A); t_R = 9.24, purity >95% (method B).

(*E*)-3,5-dimethoxy-4-(2-(((5-methoxy-6-nitropyridin-2-yl)methyl)sulfonyl)vinyl)-phenyl benzoate (60)



Compound **47** (300 mg, 1.03 mmol) and **32b** (295 mg, 1.03 mmol) were reacted using general synthetic procedure B. The residue was washed with MeOH (50 mL) to give **60** as a yellow solid (156 mg, 29%). m.p. 198-200 °C. ^{1}H NMR (500 MHz, DMSO-d_6) δ 3.86 (s, 6H, benzene-OCH_3), 3.98 (s, 3H, pyridine-OCH_3), 4.73 (s, 2H, CH_2), 6.80 (s, 2H, benzene-H), 7.37 (d, 1H, *J* = 16.0, SO_2C*H*=CH), 7.60 (d, 1H, *J* = 16.0, SO_2CH=C*H*), 7.63 (t, 2H, *J* = 7.5, benzene-H), 7.78 (tt, 1H, *J* = 7.5 & 1.5, benzene-H), 7.84 (d, 1H, *J* = 9.0, pyridine-H), 8.03 (d, 1H, *J* = 9.0, pyridine-H), 8.15 (dd, 2H, *J* = 8.5 & 1.0, benzene-H). ^{13}C NMR (125 MHz, DMSO-d_6) δ 56.5, 57.1, 60.3, 99.1, 106.8, 125.2, 126.5, 128.7, 129.1, 129.9, 131.7, 133.0, 134.3, 139.5, 146.6, 147.4, 154.8, 160.3, 164.1 (five carbon overlapping or obscured). HRMS (ESI) *m/z* 515.1128 $[M+H]^+$; calcd. for $C_{24}H_{23}N_2O_9S$ $[M+H]^+$ 515.1119.

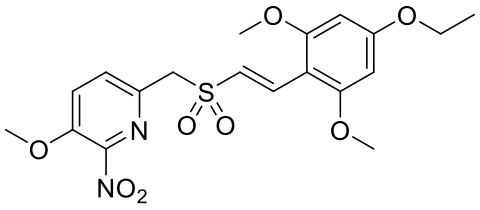
(*E*)-4-(2-(((6-amino-5-methoxypyridin-2-yl)methyl)sulfonyl)vinyl)-3,5-dimethoxyphenol (61)



To a solution of compound **60** (100 mg, 0.194 mmol) in MeOH/CH_3CO_2H (1:1, 10 mL) was added Fe powder (87 mg, 1.56 mmol). The mixture reaction mixture was heated at 50 °C for 2 h under N_2 gas and concentrated under reduced pressure. The residue was filtered through a silica plug eluted with EtOAc (250 mL) to yield the amino ester as a yellow powder. The compound was dissolved in H_2O/MeOH (1:1, 10 mL) and added 1

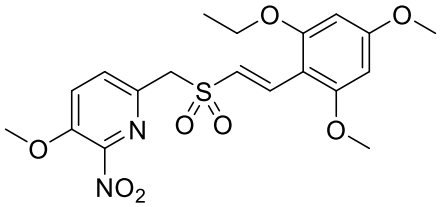
M NaOH (1 mL). The reaction mixture was stirred at room temperature for 24 h and concentrated under reduced pressure. The residue was neutralized to pH = 7 with 1 M HCl, and the mixture extracted with EtOAc (3 × 50 mL). The extracts were combined, dried over $MgSO_4$ and concentrated under reduced pressure. The residue was purified by flash column chromatography (silica gel, CH_2Cl_2 ramping to MeOH:CH_2Cl_2 = 6:94) to give **61** as a white solid (28 mg, 38%). m.p. 211-213 °C. ^{1}H NMR (500 MHz, DMSO-d_6) δ 3.76 (s, 3H, pyridine-OCH_3), 3.79 (s, 6H, benzene-OCH_3), 4.22 (s, 2H, CH_2), 5.70 (s, 2H, NH_2), 6.12 (s, 2H, benzene-H), 6.58 (d, 1H, *J* = 7.5, pyridine-H), 7.01 (d, 1H, *J* = 8.0, pyridine-H), 7.04 (d, 1H, *J* = 15.5, SO_2C*H*=CH), 7.57 (d, 1H, *J* = 15.5, SO_2CH=C*H*) (one phenolic proton signal not observed). ^{13}C NMR (125 MHz, DMSO-d_6) δ 55.4, 55.9, 62.4, 92.2, 101.4, 114.2, 115.5, 122.9, 132.7, 137.8, 141.6, 150.4, 161.3, 162.5 (three carbon signals overlapping or obscured). HRMS (ESI) *m/z* 381.1108 $[M+H]^+$; calcd. for $C_{17}H_{21}N_2O_6S$ $[M+H]^+$ 381.1115. Anal. RP-HPLC: t_R = 9.38, purity >96% (method A) ; t_R = 8.03, purity >96% (method B).

(*E*)-6-(((4-ethoxy-2,6-dimethoxystyryl)sulfonyl)methyl)-3-methoxy-2-nitropyridine (62a)



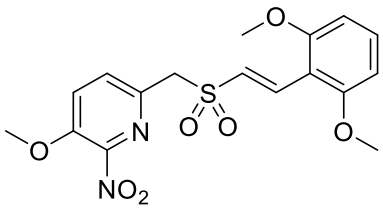
Compound **47** (400 mg, 1.38 mmol) and **39a** (318 mg, 1.51 mmol) were reacted using general synthetic procedure B. The residue was purified by flash column chromatography (silica gel, petroleum ether ramping to EtOAc:petroleum ether = 1:1) to give **62a** as a white solid (250 mg, 41%). m.p. 178-180 °C. ^{1}H NMR (500 MHz, $CDCl_3$) δ 1.43 (t, 3H, *J* = 7.0, CH_2C*H*$_3$), 3.83 (s, 6H, benzene-OCH_3), 3.98 (s, 3H, pyridine-OCH_3), 4.07 (q, 2H, *J* = 7.0, C*H*$_2$CH$_3$), 4.44 (s, 2H, pyridine-CH_2SO_2), 7.10 (d, 1H, *J* = 15.5, SO_2C*H*=CH), 7.54 (d, 1H, *J* = 8.5, pyridine-H), 7.79 (d, 1H, *J* = 8.5, pyridine-H), 7.81 (d, 1H, *J* = 15.5, SO_2CH=C*H*). ^{13}C NMR (125 MHz, $CDCl_3$) δ 14.8, 55.9, 56.9, 62.3, 63.9, 77.7, 90.9, 103.7, 121.7, 123.4, 130.9, 136.4, 140.1, 147.5, 161.8, 163.7 (three carbon signals overlapping or obscured). HRMS (ESI) *m/z* 439.1172 $[M+H]^+$; calcd. for $C_{19}H_{23}N_2O_8S$ $[M+H]^+$ 439.1170.

(*E*)-6-(((2-ethoxy-4,6-dimethoxystyryl)sulfonyl)methyl)-3-methoxy-2-nitropyridine (62b)



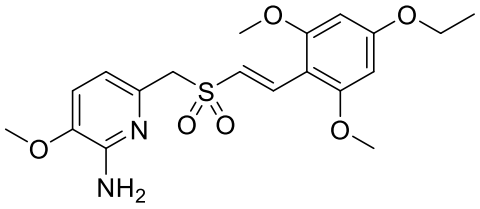
Compound **47** (300 mg, 1.03 mmol) and **39b** (159 mg, 0.756 mmol) were reacted using general synthetic procedure B. The residue was washed with MeOH (100 mL) to give **62b** as a white solid (112 mg, 37%). m.p. 163-165 °C. ^{1}H NMR (500 MHz, $CDCl_3$) δ 1.42 (t, 3H, *J* = 7.0, CH_2CH_3), 3.83 (m, 6H, benzene-OCH_3), 3.98 (s, 3H, pyridine-OCH_3), 4.06 (q, 2H, *J* = 7.0, CH_2CH_3), 4.44 (s, 2H, pyridine-CH_2SO_2), 6.06 (s, 2H, benzene-H), 7.10 (d, 1H, *J* = 15.5, SO_2CH=CH), 7.54 (d, 1H, *J* = 9.0, pyridine-H), 7.81 (d, 1H, *J* = 8.5, pyridine-H), 7.83 (d, 1H, *J* = 15.5, SO_2CH=C*H*).^{13}C NMR (125 MHz, $CDCl_3$) δ 14.7, 55.6, 55.9, 56.9, 62.2, 64.6, 90.3, 91.1, 103.8, 121.7, 123.3, 130.9, 136.6, 140.1, 147.5, 148.1, 161.2, 161.8, 164.2. HRMS (ESI) *m/z* 439.1154 $[M+H]^+$; calcd. for $C_{19}H_{23}N_2O_8S$ $[M+H]^+$ 439.1170.

(*E*)-6-(((2,6-dimethoxystyryl)sulfonyl)methyl)-3-methoxy-2-nitropyridine (62c)



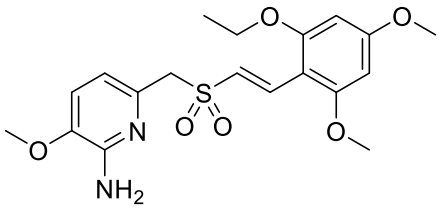
Compound **47** (200 mg, 0.689 mmol) and 2,6-dimethoxybenzaldehyde (0.126 mg, 0.758 mmol) were reacted using general synthetic procedure B. The residue was washed with MeOH (50 mL) to give **62c** as a brown solid (117 mg, 43%). m.p. 199-200 °C.^{1}H NMR (500 MHz, $CDCl_3$) δ 3.85 (s, 6H, benzene-OCH_3), 3.99 (s, 3H, pyridine-OCH_3), 4.46 (s, 2H, CH_2), 6.54 (d, 2H, *J* = 8.5, benzene-H), 7.29 (d, 1H, *J* = 15.5, SO_2CH=CH), 7.32 (t, 1H, *J* = 8.5, benzene-H), 7.55 (d, 1H, *J* = 8.5, pyridine-H), 7.79 (d, 1H, *J* = 8.5, pyridine-H), 7.90 (d, 1H, *J* = 15.5, SO_2CH=C*H*). ^{13}C NMR (125 MHz, $CDCl_3$) δ 56.0, 56.9, 62.1, 103.7, 110.1, 123.4, 125.3, 130.9, 133.1, 136.3, 139.9, 147.6, 148.1, 160.5 (three carbon signals overlapping or obscured). HRMS (ESI) *m/z* 395.0906 $[M+H]^+$; calcd. for $C_{17}H_{19}N_2O_7S$ $[M+H]^+$ 3950907.

(*E*)-6-(((4-ethoxy-2,6-dimethoxystyryl)sulfonyl)methyl)-3-methoxypyridin-2-amine (63a)



Nitro compound **62a** (100 mg, 0.228 mmol) was reduced using general synthetic procedure C. The residue was purified by flash column chromatography (silica gel, CH_2Cl_2 ramping to acetone:CH_2Cl_2 = 1:9) to give **63a** as a white solid (67 mg, 72%). m.p. 172-174 °C. ^{1}H NMR (500 MHz, DMSO-d_6) δ 1.34 (t, 3H, J = 7.0, CH_2CH_3), 3.76 (s, 3H, pyridine-OCH_3), 3.84 (s, 6H, benzene-OCH_3), 4.13 (q, 2H, J = 7.0, CH_2CH_3), 4.23 (s, 2H, pyridine-CH_2SO_2), 5.71 (s, 2H, NH_2), 6.27 (s, 2H, benzene-H), 6.59 (d, 1H, J = 8.0, pyridine-H), 7.01 (d, 1H, J = 8.0, pyridine-H), 7.11 (d, 1H, J = 15.5, SO_2CH=CH), 7.58 (d, 1H, J = 16.0, SO_2CH=C*H*). ^{13}C NMR (125 MHz, DMSO-d_6) δ 14.6, 55.4, 56.1, 62.3, 63.7, 91.4, 102.6, 114.2, 115.4, 124.0, 132.4, 137.7, 141.6, 150.4, 161.0, 163.0. HRMS (ESI) *m/z* 409.1407 $[M+H]^+$; calcd. for $C_{19}H_{25}N_2O_6S$ $[M+H]^+$ 409.1428. Anal. RP-HPLC: t_R =11.47, purity >96% (method A); t_R = 9.17, purity >96% (method B).

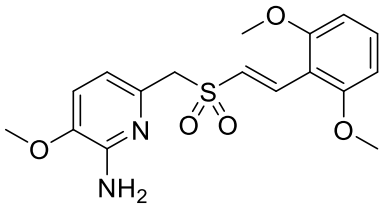
(*E*)-6-(((2-ethoxy-4,6-dimethoxystyryl)sulfonyl)methyl)-3-methoxypyridin-2-amine (63b)



Nitro compound **62b** (100 mg, 0.228 mmol) was reduced using general synthetic procedure C. The residue was purified by flash column chromatography (silica gel, CH_2Cl_2 ramping to acetone:CH_2Cl_2 = 2:98) to give **63b** as a white solid (39 mg, 42%). m.p. 211-213 °C. ^{1}H NMR (500 MHz, DMSO-d_6) δ 1.32 (t, 3H, J = 7.0, CH_2CH_3), 3.76 (s, 3H), 3.83 (s, 3H), 3.85 (s, 3H) (total 9H, 3 × OCH_3), 4.10 (q, 2H, J = 7.0, CH_2CH_3), 4.24 (s, 2H, pyridine-CH_2SO_2), 5.75 (s, 2H, NH_2), 6.27 (d, 1H, J = 2.0, benzene-H), 6.28 (d, 1H, J = 2.0, benzene-H), 6.59 (d, 1H, J = 8.0, pyridine-H), 7.01 (d, 1H, J = 8.0,

pyridine-H), 7.09 (d, 1H, *J* = 15.5, $SO_2C\mathit{H}$=CH), 7.63 (d, 1H, *J* = 16.0, SO_2CH=C*H*). ^{13}C NMR (125 MHz, DMSO-d_6) δ 14.3, 55.3, 55.6, 56.1, 62.3, 64.4, 90.9, 91.6, 102.6, 114.0, 115.3, 123.8, 132.5, 137.7, 141.5, 150.4, 160.3, 160.9, 163.6. HRMS (ESI) *m/z* 409.1463 $[M+H]^+$; calcd. for $C_{19}H_{25}N_2O_6S$ $[M+H]^+$ 409.1428. Anal. RP-HPLC: t_R = 10.59, purity >98% (method A); t_R = 8.91, purity >98% (method B).

(*E*)-6-(((2,6-dimethoxystyryl)sulfonyl)methyl)-3-methoxypyridin-2-amine (63c)



Nitro compound **62c** (100 mg, 0.254 mmol) was reduced using general synthetic procedure C. The residue was purified by flash column chromatography (silica gel, CH_2Cl_2 ramping to acetone:CH_2Cl_2 = 1:9) and crystallized (CH_2Cl_2/hexane = 1:1) to give **63c** as a white solid (61 mg, 66%). m.p. 158-160 °C. ^{1}H NMR (500 MHz, DMSO-d_6) δ 3.76 (s, 3H, pyridine-OCH_3), 3.86 (s, 6H, benzene-OCH_3), 4.28 (s, 2H, CH_2), 5.73 (s, 2H, NH_2), 6.60 (d, 1H, *J* = 8.0, pyridine-H), 6.73 (d, 2H, *J* = 8.5, benzene-H), 7.01 (d, 1H, *J* = 8.0, pyridine-H), 7.33 (d, 1H, *J* = 16.0, $SO_2C\mathit{H}$=CH), 7.41 (t, 1H, *J* = 8.5, benzene-H), 7.67 (d, 1H, *J* = 15.5, SO_2CH=C*H*). ^{13}C NMR (125 MHz, DMSO-d_6) δ 55.4, 56.1, 62.1, 104.2, 109.1, 114.2, 115.4, 127.6, 132.1, 133.0, 137.5, 141.6, 150.4, 159.7 (three carbon signals overlapping or obscured). HRMS (ESI) *m/z* 365.1143 $[M+H]^+$; calcd. for $C_{17}H_{21}N_2O_5S$ $[M+H]^+$ 365.1166. Anal. RP-HPLC: t_R = 8.21, purity >99% (method A); t_R = 7.12, purity >99% (method B).

5.2 **Antiproliferative assay**

MTT (3-(4,5-dimethylthiazol-2-yl)-2,5-diphenyltetrazolium bromide) assays were conducted using the method reported by Wang *et al.*[308] Cells were seeded onto 96 well cell culture plates and incubated overnight at 37 °C, 5% CO_2. Test compounds were diluted in DMSO to form a 10 mM stock solution which was used to prepare a fivefold dilution series in 100 μL cell medium. The cells were added with the dilution series and incubated for 72 h at 37 °C, 5% CO_2. MTT was made up as a stock solution of 5 mg/mL in cell medium, and filter sterilized before use. Medium was removed from the wells

which were subsequently washed with 200 μL/well phosphate buffered saline (PBS). MTT stock solution was added at 200 μL/well and the plates were further incubated for 4 h at 37 °C. MTT dye was solubilized with 200 μL/well of DMSO with agitation. Absorbance was read at 585 nm using an EnVision multi label plate reader (PerkinElmer, Beaconsfield, Buckinghamshire, UK). Compound concentrations required to inhibit 50% of cell growth (GI_{50}) were calculated using nonlinear regression analysis. Data presented are the mean values of at least two replicates.

5.3 Cell-Cycle Analysis and Detection of Apoptosis

Cells were seeded at 8×10^4 and incubated overnight at 37 °C, 5% CO_2. After treatment with the compounds, cells were trypsinized and centrifuged at 300g for 5 min. Cell pellets were collected and fixed with 70% ethanol on ice for 15 min and collected again after being centrifuged at 300g for 5 min. The collected pellets were incubated with staining solution (50 μg/mL propidium iodide, 0.1 mg/mL RNase A, 0.05% Triton X-100) at rt for 1 h and analyzed with FACS Gallios (Beckman Coulter). Apoptosis was detected with cells collected and processed as described by the annexin-V FITC/PI commercial kit (Becton Dickenson). Samples were analyzed with fluorescence-activated cell sorting (FACS) within 1 h of staining. The data were analyzed using Kaluza v1.2 (Beckman Coulter).

5.4 Caspase-3/7 assay

Activity of caspase-3/7 was measured using the Apo-ONE® Homogeneous caspase-3/7 kit (Promega) according to the manufacturer's instructions. A2780 or WI-38 Cells were seeded onto black 96 well cell culture plates and incubated for 24 hours at 37 °C, 5% CO_2. Diluted test compounds were added to the cells and the plates were further incubated for 48 hours at 37 °C, 5% CO_2. Each well were added with 100 μl of Apo-ONE® Caspase-3/7 Reagent and the contents mixed using a shaker at 200-400 rpm for one minute. The plates were placed on ice and incubated in the dark for two hours. After incubation, the fluorescence was read using an EnVision multi label plate reader (PerkinElmer, Beaconsfield, Buckinghamshire, UK). The excitation wavelength for detection was set at 468 nm and the emission wavelength was set 508 nm. Data obtained was transferred to Microsoft Excel for analysis.

5.5 Western blots

Western blots were conducted based on the method described previously. Cell lysates (20 µg) were run on SDS-PAGE gels (Mini-PROTEAN® TGX™ precast gels). Seperated proteins were transferred onto membranes and probed with antibodies. Antibodies used are detailed as follows: CDC25C (5H9) rabbit monoclonal, Mcl-1 (D35A5) rabbit monoclonal antibody, PARP (46D11) rabbit monoclonal, Cleaved PARP (Asp214) (D64E10) XP® rabbit monoclonal, β-actin (13E5) rabbit monoclonal. All primary antibodies used were purchased from Cell Signaling Technologies. Antirabbit immunoglobulin G (IgG) horseradish peroxidase conjugated antibodies (secondary antibody) were obtained from Dako. Enhanced chemiluminescence (ECL) reagents were obtained from Amersham (GE Life Sciences).

5.6 Kinase assay

Kinase panel screen was conducted by Eurofins Scientific (Dundee, UK) using KinaseProfiler™ service, with ATP within 15 μM of the K_M.

5.7 Microsomal stability assay

The microsomal stability assay was performed using rat liver microsomes (Life Technologies, Victoria, Australia) with protein concentrations of 0.5 mg/mL. Incubation of the test compounds (2 μM) was performed at 37 °C with 100 mM potassium phosphate buffer, pH 7.4, containing 10 mM $MgCl_2$ in the presence or absence of the NADPH-regenerating system (total volume 400 μL). The glucose-6-phosphate based NADPH-regenerating system consisted of 0.5 mM NADP, 10 mM glucose 6-phosphate, and 1.0 unit/mL glucose 6-phosphate dehydrogenase. During the incubation, 50 μL were collected at 0, 15, 30, 45 min, 1, 1.5, and 2 h from the incubation media. The reaction of the microsomes in the collected samples was terminated by the addition of 50 μL ice-cold MeCN. The remaining concentrations of the compounds in the samples were quantified using a validated LC/MS/MS method with a triple TOF-MS 5600 (AB Sciex) to determine the half-life of the compounds in microsomal medium. The samples were injected into a Shimadzu Nexera HPLC system, and resolved on a Kinetex C18 2.6u 50 mm × 3 mm column (Phenomenex) at a mobile phase flow rate of 0.4 mL/min.

Mobile phase A (MPA) was 5% acetonitrile and 0.1% formic acid in water and mobile phase B (MPB) was 95% acetonitrile and 0.1% formic acid. The mobile phase timetable was set as a gradient from 20% MPB initially to 95% MPB in 1 min, held at 95% MPB for 2 min, then 20% MPB for 30 s in preparation for the next sample. Peak areas were obtained from the compounds, and internal standards and known concentrations of calibrators were used to construct a calibration curve from compounds/internal standard area ratios.

5.8 Pharmacokinetic determinations

Pharmacokinetic studies were conducted in male adult CD1 mice or Wistar rats. After an overnight fast, the compounds were administrated to the animal through oral gavage or IV *via* the tail vein. Blood samples were collected at predose and a series of time points up to 24 h post drug administration. Plasma was separated and stored at −20 °C until analysis. The samples were extracted with EtOAc, the organic extract collected, and dried under N_2. The extracts were reconstituted in acetonitrile/water (50:50), and the concentration quantified using the method as described above.

5.9 Caco-2 permeability assay

Caco-2 permeability assay was conducted by Cyprotex (Macclesfield, UK), with a concentration of 10 μM of test compound used during the assay.

5.10 *In vivo* efficacy studies

Female nude (nu/nu) BALB/c mice at 6−8 weeks were subcutaneously inoculated on their hind flanks with with 2.5×10^6 human ovarian A2780 cancer cells suspended in RPMI medium. Tumours were grown to an average size of 100 mm^3 before being allocated into groups of eight mice (control or treated). Compound **15** and vehicle control 5% N-methyl-2-pyrrolidone (NMP)/95% PEG400 were administered by oral gavage (po) every second day. The positive control cisplatin was dissolved in 0.9% normal saline was administered by ip injection once per week. The effects of the compounds were assessed by monitoring tumour volume (in cubic millimeters = length × width × height) and body weight of the mice on treatment days. Animals were euthanized if the tumour volume exceeded 2000 mm^3 or if weight loss exceeded 15% of

their pretreatment mass. Animal experiments where performed under the approval of the South Australian Pathology ethics committee.

1. Hanahan, D.; Weinberg, R. A., *Cell* **2011,** *144*, 646-74.
2. Hanahan, D.; Weinberg, R. A., *Cell* **2000,** *100*, 57-70.
3. Kiechle, F. L.; Zhang, X., *Clin Chim Acta* **2002,** *326*, 27-45.
4. Czabotar, P. E.; Lessene, G.; Strasser, A.; Adams, J. M., *Nat Rev Mol Cell Biol* **2014,** *15*, 49-63.
5. Huang, D. C. S.; Strasser, A., *Cell* **2000,** *103*, 839-42.
6. Korsmeyer, S. J.; Wei, M. C.; Saito, M.; Weller, S.; Oh, K. J.; Schlesinger, P. H., *Cell Death Differ* **2000,** *7*, 1166-73.
7. Ow, Y. P.; Green, D. R.; Hao, Z.; Mak, T. W., *Nat Rev Mol Cell Biol* **2008,** *9*, 532-42.
8. Sartorius, U. A.; Krammer, P. H., *Int J Cancer* **2002,** *97*, 584-92.
9. Altieri, D. C., *Oncogene* **2003,** *22*, 8581-8589.
10. Cheng, Q.; Lee, H. H.; Li, Y.; Parks, T. P.; Cheng, G., *Oncogene* **2000,** *19*, 4936-40.
11. Bruchim, I.; Attias, Z.; Werner, H., *Expert Opin Ther Targets* **2009,** *13*, 1179-92.
12. Bargou, R. C.; Wagener, C.; Bommert, K.; Mapara, M. Y.; Daniel, P. T.; Arnold, W.; Dietel, M.; Guski, H.; Feller, A.; Royer, H. D.; Dorken, B., *J Clin Invest* **1996,** *97*, 2651-9.
13. Liu, Q. Y.; Stein, C. A., *Clin Cancer Res* **1997,** *3*, 2039-46.
14. Bartek, J.; Bartkova, J.; Lukas, J., *Exp Cell Res* **1997,** *237*, 1-6.
15. Wilentz, R. E.; Geradts, J.; Maynard, R.; Offerhaus, G. J.; Kang, M.; Goggins, M.; Yeo, C. J.; Kern, S. E.; Hruban, R. H., *Cancer Res* **1998,** *58*, 4740-4.
16. Hu, B.; Gilkes, D. M.; Farooqi, B.; Sebti, S. M.; Chen, J., *J Biol Chem* **2006,** *281*, 33030-5.
17. Fine, B.; Hodakoski, C.; Koujak, S.; Su, T.; Saal, L. H.; Maurer, M.; Hopkins, B.; Keniry, M.; Sulis, M. L.; Mense, S.; Hibshoosh, H.; Parsons, R., *Science* **2009,** *325*, 1261-5.
18. Mulligan, L. M.; Matlashewski, G. J.; Scrable, H. J.; Cavenee, W. K., *Proc Natl Acad Sci U S A* **1990,** *87*, 5863-7.
19. Kourea, H. P.; Orlow, I.; Scheithauer, B. W.; Cordon-Cardo, C.; Woodruff, J. M., *Am J Pathol* **1999,** *155*, 1855-60.
20. Williams, R. T.; Roussel, M. F.; Sherr, C. J., *Proc Natl Acad Sci U S A* **2006,** *103*, 6688-93.
21. Graff, J. R.; Herman, J. G.; Lapidus, R. G.; Chopra, H.; Xu, R.; Jarrard, D. F.; Isaacs, W. B.; Pitha, P. M.; Davidson, N. E.; Baylin, S. B., *Cancer Res* **1995,** *55*, 5195-9.
22. Hollstein, M.; Sidransky, D.; Vogelstein, B.; Harris, C. C., *Science* **1991,** *253*, 49-53.
23. Arbeit, J. M.; Olson, D. C.; Hanahan, D., *Oncogene* **1996,** *13*, 1847-57.
24. Holash, J.; Wiegand, S. J.; Yancopoulos, G. D., *Oncogene* **1999,** *18*, 5356-62.
25. Blasco, M. A., *Curr Opin Genet Dev* **2003,** *13*, 70-6.
26. Hiyama, E.; Hiyama, K., *Oncogene* **2002,** *21*, 643-9.
27. Muta, H.; Noguchi, M.; Kanai, Y.; Ochiai, A.; Nawata, H.; Hirohashi, S., *Jpn J Cancer Res* **1996,** *87*, 843-8.
28. Herrera-Gayol, A.; Jothy, S., *Exp Mol Pathol* **1999,** *66*, 149-56.
29. Hazan, R. B.; Phillips, G. R.; Qiao, R. F.; Norton, L.; Aaronson, S. A., *J Cell Biol* **2000,** *148*, 779-90.
30. Hanks, S. K.; Hunter, T., *FASEB J* **1995,** *9*, 576-96.
31. Zhang, J.; Yang, P. L.; Gray, N. S., *Nat Rev Cancer* **2009,** *9*, 28-39.

32. Endicott, J. A.; Noble, M. E.; Johnson, L. N., *Annu Rev Biochem* **2012,** *81*, 587-613.
33. Peng, Y. H.; Shiao, H. Y.; Tu, C. H.; Liu, P. M.; Hsu, J. T.; Amancha, P. K.; Wu, J. S.; Coumar, M. S.; Chen, C. H.; Wang, S. Y.; Lin, W. H.; Sun, H. Y.; Chao, Y. S.; Lyu, P. C.; Hsieh, H. P.; Wu, S. Y., *J Med Chem* **2013,** *56*, 3889-903.
34. Bennett, B. L.; Sasaki, D. T.; Murray, B. W.; O'Leary, E. C.; Sakata, S. T.; Xu, W.; Leisten, J. C.; Motiwala, A.; Pierce, S.; Satoh, Y.; Bhagwat, S. S.; Manning, A. M.; Anderson, D. W., *Proc Natl Acad Sci U S A* **2001,** *98*, 13681-6.
35. Cookson, M. R.; Dauer, W.; Dawson, T.; Fon, E. A.; Guo, M.; Shen, J., *J Neurosci* **2007,** *27*, 11865-8.
36. Hardie, D. G., *FEBS Lett* **2008,** *582*, 81-9.
37. Fogarty, S.; Hardie, D. G., *Biochim Biophys Acta* **2010,** *1804*, 581-91.
38. Fedorov, O.; Muller, S.; Knapp, S., *Nat Chem Biol* **2010,** *6*, 166-9.
39. Sharma, S. V.; Settleman, J., *Genes Dev* **2007,** *21*, 3214-31.
40. Ren, R., *Nat Rev Cancer* **2005,** *5*, 172-83.
41. Stegmeier, F.; Warmuth, M.; Sellers, W. R.; Dorsch, M., *Clin Pharmacol Ther* **2010,** *87*, 543-52.
42. Kaelin, W. G., Jr., *Nat Rev Cancer* **2005,** *5*, 689-98.
43. Reinhardt, H. C.; Jiang, H.; Hemann, M. T.; Yaffe, M. B., *Cell Cycle* **2009,** *8*, 3112-9.
44. Watanabe, R.; Wei, L.; Huang, J., *J Nucl Med* **2011,** *52*, 497-500.
45. Cheng, C. K.; Gustafson, W. C.; Charron, E.; Houseman, B. T.; Zunder, E.; Goga, A.; Gray, N. S.; Pollok, B.; Oakes, S. A.; James, C. D.; Shokat, K. M.; Weiss, W. A.; Fan, Q. W., *Proc Natl Acad Sci U S A* **2012,** *109*, 12722-7.
46. Luo, J.; Emanuele, M. J.; Li, D.; Creighton, C. J.; Schlabach, M. R.; Westbrook, T. F.; Wong, K. K.; Elledge, S. J., *Cell* **2009,** *137*, 835-48.
47. Shibuya, M., *Genes Cancer* **2011,** *2*, 1097-105.
48. Presta, M.; Dell'Era, P.; Mitola, S.; Moroni, E.; Ronca, R.; Rusnati, M., *Cytokine Growth Factor Rev* **2005,** *16*, 159-78.
49. Christofk, H. R.; Vander Heiden, M. G.; Harris, M. H.; Ramanathan, A.; Gerszten, R. E.; Wei, R.; Fleming, M. D.; Schreiber, S. L.; Cantley, L. C., *Nature* **2008,** *452*, 230-3.
50. Young, P. R.; McLaughlin, M. M.; Kumar, S.; Kassis, S.; Doyle, M. L.; McNulty, D.; Gallagher, T. F.; Fisher, S.; McDonnell, P. C.; Carr, S. A.; Huddleston, M. J.; Seibel, G.; Porter, T. G.; Livi, G. P.; Adams, J. L.; Lee, J. C., *J Biol Chem* **1997,** *272*, 12116-21.
51. Skora, L.; Mestan, J.; Fabbro, D.; Jahnke, W.; Grzesiek, S., *Proc Natl Acad Sci U S A* **2013,** *110*, 4437-45.
52. Park, J. H.; Liu, Y.; Lemmon, M. A.; Radhakrishnan, R., *Biochem J* **2012,** *448*, 417-23.
53. Kufareva, I.; Abagyan, R., *J Med Chem* **2008,** *51*, 7921-32.
54. Weisberg, E.; Manley, P.; Mestan, J.; Cowan-Jacob, S.; Ray, A.; Griffin, J. D., *Br J Cancer* **2006,** *94*, 1765-9.
55. Norman, R. A.; Toader, D.; Ferguson, A. D., *Trends Pharmacol Sci* **2012,** *33*, 273-8.
56. Liu, Y.; Gray, N. S., *Nat Chem Biol* **2006,** *2*, 358-64.
57. Bikker, J. A.; Brooijmans, N.; Wissner, A.; Mansour, T. S., *J Med Chem* **2009,** *52*, 1493-509.
58. Xu, Y.; Liu, H.; Chen, J.; Zhou, Q., *Cancer Biol Ther* **2010,** *9*, 572-82.
59. Bradham, C.; McClay, D. R., *Cell Cycle* **2006,** *5*, 824-8.

60. McInnes, C.; Mezna, M.; Fischer, P. M., *Curr Top Med Chem* **2005,** *5*, 181-97.
61. Coley, H. M.; Hatzimichael, E.; Blagden, S.; McNeish, I.; Thompson, A.; Crook, T.; Syed, N., *Oncotarget* **2012,** *3*, 78-83.
62. Fasano, M.; Della Corte, C. M.; Califano, R.; Capuano, A.; Troiani, T.; Martinelli, E.; Ciardiello, F.; Morgillo, F., *Expert Opin Investig Drugs* **2014,** *23*, 809-21.
63. Karve, S.; Werner, M. E.; Sukumar, R.; Cummings, N. D.; Copp, J. A.; Wang, E. C.; Li, C.; Sethi, M.; Chen, R. C.; Pacold, M. E.; Wang, A. Z., *Proc Natl Acad Sci U S A* **2012,** *109*, 8230-5.
64. Senderowicz, A. M., *Invest New Drugs* **1999,** *17*, 313-20.
65. Knight, Z. A.; Shokat, K. M., *Chem Biol* **2005,** *12*, 621-37.
66. Lewis, J. A.; Lebois, E. P.; Lindsley, C. W., *Curr Opin Chem Biol* **2008,** *12*, 269-80.
67. Branford, S.; Rudzki, Z.; Walsh, S.; Parkinson, I.; Grigg, A.; Szer, J.; Taylor, K.; Herrmann, R.; Seymour, J. F.; Arthur, C., *Blood* **2003,** *102*, 276-83.
68. Khateb, M.; Ruimi, N.; Khamisie, H.; Najajreh, Y.; Mian, A.; Metodieva, A.; Ruthardt, M.; Mahajna, J., *BMC Cancer* **2012,** *12*, 563.
69. Zhang, J.; Adrian, F. J.; Jahnke, W.; Cowan-Jacob, S. W.; Li, A. G.; Iacob, R. E.; Sim, T.; Powers, J.; Dierks, C.; Sun, F.; Guo, G. R.; Ding, Q.; Okram, B.; Choi, Y.; Wojciechowski, A.; Deng, X.; Liu, G.; Fendrich, G.; Strauss, A.; Vajpai, N.; Grzesiek, S.; Tuntland, T.; Liu, Y.; Bursulaya, B.; Azam, M.; Manley, P. W.; Engen, J. R.; Daley, G. Q.; Warmuth, M.; Gray, N. S., *Nature* **2010,** *463*, 501-6.
70. Jahnke, W.; Blommers, M. J.; Fernandez, C.; Zwingelstein, C.; Amstutz, R., *Chembiochem* **2005,** *6*, 1607-10.
71. Singh, J.; Petter, R. C.; Baillie, T. A.; Whitty, A., *Nat Rev Drug Discov* **2011,** *10*, 307-17.
72. Yun, C. H.; Mengwasser, K. E.; Toms, A. V.; Woo, M. S.; Greulich, H.; Wong, K. K.; Meyerson, M.; Eck, M. J., *Proc Natl Acad Sci U S A* **2008,** *105*, 2070-5.
73. Bowles, D. W.; Diamond, J. R.; Lam, E. T.; Weekes, C. D.; Astling, D. P.; Anderson, R. T.; Leong, S.; Gore, L.; Varella-Garcia, M.; Vogler, B. W.; Keysar, S. B.; Freas, E.; Aisner, D. L.; Ren, C.; Tan, A. C.; Wilhelm, F.; Maniar, M.; Eckhardt, S. G.; Messersmith, W. A.; Jimeno, A., *Clin Cancer Res* **2014,** *20*, 1656-65.
74. Olnes, M. J.; Shenoy, A.; Weinstein, B.; Pfannes, L.; Loeliger, K.; Tucker, Z.; Tian, X.; Kwak, M.; Wilhelm, F.; Yong, A. S.; Maric, I.; Maniar, M.; Scheinberg, P.; Groopman, J.; Young, N. S.; Sloand, E. M., *Leuk Res* **2012,** *36*, 982-9.
75. ClinicalTrials.gov. Oral Rigosertib in Combination With Azacitidine. https://clinicaltrials.gov/ct2/show/NCT01926587 (accessed 15 December 2015).
76. Odchimar-Reissig, R.; Reddy, E. P.; Demakos, E. P.; Holland, J. F.; Wilhelm, F.; Silverman, L. R., *Blood* **2013,** *122*, 1527-1527.
77. Fang, S. H.; Padmavathi, V.; Rao, Y. K.; Venkata Subbaiah, D. R.; Thriveni, P.; Geethangili, M.; Padmaja, A.; Tzeng, Y. M., *Int Immunopharmacol* **2006,** *6*, 1699-705.
78. Vedula, M. S.; Pulipaka, A. B.; Venna, C.; Chintakunta, V. K.; Jinnapally, S.; Kattuboina, V. A.; Vallakati, R. K.; Basetti, V.; Akella, V.; Rajgopal, S.; Reka, A. K.; Teepireddy, S. K.; Mamnoor, P. K.; Rajagopalan, R.; Bulusu, G.; Khandelwal, A.; Upreti, V. V.; Mamidi, S. R., *Eur J Med Chem* **2003,** *38*, 811-24.
79. Sharma, V. M.; Adi Seshu, K. V.; Chandra Sekhar, V.; Madan, S.; Vishnu, B.; Babu, P. A.; Vamsee Krishna, C.; Sreenu, J.; Ravi Krishna, V.; Venkateswarlu, A.; Rajagopal, S.; Ajaykumar, R.; Kumar, T. S., *Bioorg Med Chem Lett* **2004,** *14*, 67-71.
80. Reddy, M. V.; Mallireddigari, M. R.; Pallela, V. R.; Venkatapuram, P.; Boominathan, R.; Bell, S. C.; Reddy, E. P., *Bioorg Med Chem* **2005,** *13*, 1715-23.

81. Reddy, M. V.; Mallireddigari, M. R.; Cosenza, S. C.; Pallela, V. R.; Iqbal, N. M.; Robell, K. A.; Kang, A. D.; Reddy, E. P., *J Med Chem* **2008,** *51*, 86-100.
82. Reddy, M. V.; Venkatapuram, P.; Mallireddigari, M. R.; Pallela, V. R.; Cosenza, S. C.; Robell, K. A.; Akula, B.; Hoffman, B. S.; Reddy, E. P., *J Med Chem* **2011,** *54*, 6254-76.
83. Preda, A.; Ohnuma, T.; Jiang, J. D.; Holland, J. F.; Reddy, E. P., *Cancer Res* **2006,** *2006*, 1106.
84. Gumireddy, K.; Reddy, M. V.; Cosenza, S. C.; Boominathan, R.; Baker, S. J.; Papathi, N.; Jiang, J.; Holland, J.; Reddy, E. P., *Cancer Cell* **2005,** *7*, 275-86.
85. Emery, C. M.; Vijayendran, K. G.; Zipser, M. C.; Sawyer, A. M.; Niu, L.; Kim, J. J.; Hatton, C.; Chopra, R.; Oberholzer, P. A.; Karpova, M. B.; MacConaill, L. E.; Zhang, J.; Gray, N. S.; Sellers, W. R.; Dummer, R.; Garraway, L. A., *Proc Natl Acad Sci U S A* **2009,** *106*, 20411-6.
86. Adrian, F. J.; Ding, Q.; Sim, T.; Velentza, A.; Sloan, C.; Liu, Y.; Zhang, G.; Hur, W.; Ding, S.; Manley, P.; Mestan, J.; Fabbro, D.; Gray, N. S., *Nat Chem Biol* **2006,** *2*, 95-102.
87. Pezuk, J. A.; Brassesco, M. S.; Morales, A. G.; de Oliveira, J. C.; de Oliveira, H. F.; Scrideli, C. A.; Tone, L. G., *Cancer Biother Radiopharm* **2013,** *28*, 516-22.
88. Oussenko, I. A.; Holland, J. F.; Reddy, E. P.; Ohnuma, T., *Cancer Res* **2011,** *71*, 4968-76.
89. Swaminathan, S.; Kiendl, F.; Korner, R.; Lupetti, R.; Hengst, L.; Melchior, F., *J Cell Biol* **2004,** *164*, 965-71.
90. Prasad, A.; Park, I. W.; Allen, H.; Zhang, X.; Reddy, M. V.; Boominathan, R.; Reddy, E. P.; Groopman, J. E., *Oncogene* **2009,** *28*, 1518-28.
91. Chapman, C. M.; Sun, X.; Roschewski, M.; Aue, G.; Farooqui, M.; Stennett, L.; Gibellini, F.; Arthur, D.; Perez-Galan, P.; Wiestner, A., *Clin Cancer Res* **2012,** *18*, 1979-91.
92. Pelicano, H.; Carney, D.; Huang, P., *Drug Resist Updat* **2004,** *7*, 97-110.
93. Huang, X.; Li, X.; Guo, B., *J Biol Chem* **2008,** *283*, 29795-801.
94. Davis, R. J., *Cell* **2000,** *103*, 239-52.
95. Tonino, S. H.; van Laar, J.; van Oers, M. H.; Wang, J. Y.; Eldering, E.; Kater, A. P., *Oncogene* **2011,** *30*, 701-13.
96. Reindl, W.; Yuan, J.; Kramer, A.; Strebhardt, K.; Berg, T., *Chem Biol* **2008,** *15*, 459-66.
97. McInnes, C.; Estes, K.; Baxter, M.; Yang, Z.; Farag, D. B.; Johnston, P.; Lazo, J. S.; Wang, J.; Wyatt, M. D., *Mol Cancer Ther* **2012,** *11*, 1683-92.
98. Liu, J.; Lewellyn, A. L.; Chen, L. G.; Maller, J. L., *J Biol Chem* **2004,** *279*, 21367-73.
99. Lowery, D. M.; Lim, D.; Yaffe, M. B., *Oncogene* **2005,** *24*, 248-259.
100. Zitouni, S.; Nabais, C.; Jana, S. C.; Guerrero, A.; Bettencourt-Dias, M., *Nat Rev Mol Cell Biol* **2014,** *15*, 433-52.
101. Strebhardt, K., *Nat Rev Drug Discov* **2010,** *9*, 643-60.
102. Song, B.; Liu, X. S.; Liu, X., *Cell Div* **2012,** *7*, 3.
103. Lu, L. Y.; Wood, J. L.; Minter-Dykhouse, K.; Ye, L.; Saunders, T. L.; Yu, X. C.; Chen, J. J., *Mol Cell Biol* **2008,** *28*, 6870-6.
104. Graves, P. R.; Lovly, C. M.; Uy, G. L.; Piwnica-Worms, H., *Oncogene* **2001,** *20*, 1839-51.
105. Fattaey, A.; Booher, R. N., *Prog Cell Cycle Res* **1997,** *3*, 233-40.
106. Schmit, T. L.; Ahmad, N., *Mol Cancer Ther* **2007,** *6*, 1920-31.

107. Toyoshima-Morimoto, F.; Taniguchi, E.; Shinya, N.; Iwamatsu, A.; Nishida, E., *Nature* **2001,** *410*, 215-20.
108. Toyoshima-Morimoto, F.; Taniguchi, E.; Nishida, E., *EMBO Rep* **2002,** *3*, 341-8.
109. Chaturvedi, P.; Eng, W. K.; Zhu, Y.; Mattern, M. R.; Mishra, R.; Hurle, M. R.; Zhang, X.; Annan, R. S.; Lu, Q.; Faucette, L. F., *Oncogene* **1999,** *18*, 4047-54.
110. Chehab, N. H.; Malikzay, A.; Appel, M.; Halazonetis, T. D., *Genes Dev* **2000,** *14*, 278-88.
111. Ahn, J.; Prives, C., *J Biol Chem* **2002,** *277*, 48418-26.
112. Porter, L. A.; Donoghue, D. J., *Prog Cell Cycle Res* **2003,** *5*, 335-47.
113. Casenghi, M.; Barr, F. A.; Nigg, E. A., *J Cell Sci* **2005,** *118*, 5101-8.
114. Petronczki, M.; Lenart, P.; Peters, J. M., *Dev Cell* **2008,** *14*, 646-59.
115. McInnes, C.; Mazumdar, A.; Mezna, M.; Meades, C.; Midgley, C.; Scaerou, F.; Carpenter, L.; Mackenzie, M.; Taylor, P.; Walkinshaw, M.; Fischer, P. M.; Glover, D., *Nat Chem Biol* **2006,** *2*, 608-17.
116. Lenart, P.; Petronczki, M.; Steegmaier, M.; Di Fiore, B.; Lipp, J. J.; Hoffmann, M.; Rettig, W. J.; Kraut, N.; Peters, J. M., *Curr Biol* **2007,** *17*, 304-15.
117. Zhao, C.; Gong, L.; Li, W.; Chen, L., *J Cancer Res Clin Oncol* **2010,** *136*, 9-16.
118. Wang, Z. X.; Xue, D.; Liu, Z. L.; Lu, B. B.; Bian, H. B.; Pan, X.; Yin, Y. M., *Int J Biochem Cell Biol* **2012,** *44*, 200-10.
119. Schmit, T. L.; Zhong, W.; Nihal, M.; Ahmad, N., *Cell Cycle* **2009,** *8*, 2697-702.
120. Reagan-Shaw, S.; Ahmad, N., *IUBMB Life* **2005,** *57*, 677-82.
121. He, Z. L.; Zheng, H.; Lin, H.; Miao, X. Y.; Zhong, D. W., *World J Gastroenterol* **2009,** *15*, 4177-82.
122. de Oliveira, J. C.; Brassesco, M. S.; Pezuk, J. A.; Morales, A. G.; Valera, E. T.; Montaldi, A. P.; Sakamoto-Hojo, E. T.; Scrideli, C. A.; Tone, L. G., *J Drugs Dermatol* **2012,** *11*, 587-92.
123. Green, D. R.; Kroemer, G., *Nature* **2009,** *458*, 1127-30.
124. Chipuk, J. E.; Green, D. R., *Cell Cycle* **2004,** *3*, 429-31.
125. Shibue, T.; Takeda, K.; Oda, E.; Tanaka, H.; Murasawa, H.; Takaoka, A.; Morishita, Y.; Akira, S.; Taniguchi, T.; Tanaka, N., *Genes Dev* **2003,** *17*, 2233-8.
126. Ando, K.; Ozaki, T.; Yamamoto, H.; Furuya, K.; Hosoda, M.; Hayashi, S.; Fukuzawa, M.; Nakagawara, A., *J Biol Chem* **2004,** *279*, 25549-61.
127. Nakano, K.; Vousden, K. H., *Mol Cell* **2001,** *7*, 683-94.
128. Yang, X.; Li, H.; Zhou, Z.; Wang, W. H.; Deng, A.; Andrisani, O.; Liu, X., *J Biol Chem* **2009,** *284*, 18588-92.
129. Rudolph, D.; Steegmaier, M.; Hoffmann, M.; Grauert, M.; Baum, A.; Quant, J.; Haslinger, C.; Garin-Chesa, P.; Adolf, G. R., *Clin Cancer Res* **2009,** *15*, 3094-102.
130. Olmos, D.; Barker, D.; Sharma, R.; Brunetto, A. T.; Yap, T. A.; Taegtmeyer, A. B.; Barriuso, J.; Medani, H.; Degenhardt, Y. Y.; Allred, A. J.; Smith, D. A.; Murray, S. C.; Lampkin, T. A.; Dar, M. M.; Wilson, R.; de Bono, J. S.; Blagden, S. P., *Clin Cancer Res* **2011,** *17*, 3420-30.
131. Lin, C. C.; Su, W. C.; Yen, C. J.; Hsu, C. H.; Su, W. P.; Yeh, K. H.; Lu, Y. S.; Cheng, A. L.; Huang, D. C.; Fritsch, H.; Voss, F.; Taube, T.; Yang, J. C., *Br J Cancer* **2014,** *110*, 2434-40.
132. Jimeno, A.; Chan, A.; Cusatis, G.; Zhang, X.; Wheelhouse, J.; Solomon, A.; Chan, F.; Zhao, M.; Cosenza, S. C.; Ramana Reddy, M. V.; Rudek, M. A.; Kulesza, P.; Donehower, R. C.; Reddy, E. P.; Hidalgo, M., *Oncogene* **2009,** *28*, 610-8.

133. Steegmaier, M.; Hoffmann, M.; Baum, A.; Lenart, P.; Petronczki, M.; Krssak, M.; Gurtler, U.; Garin-Chesa, P.; Lieb, S.; Quant, J.; Grauert, M.; Adolf, G. R.; Kraut, N.; Peters, J. M.; Rettig, W. J., *Curr Biol* **2007,** *17*, 316-22.
134. Lan, R. F.; Lin, G. M.; Yin, F.; Xu, J.; Zhang, X. M.; Wang, J.; Wang, Y. C.; Gong, J. X.; Ding, Y. H.; Yang, Z.; Lu, F.; Zhang, H., *Lab Invest* **2012,** *92*, 1503-14.
135. Janku, F.; Wheler, J. J.; Westin, S. N.; Moulder, S. L.; Naing, A.; Tsimberidou, A. M.; Fu, S.; Falchook, G. S.; Hong, D. S.; Garrido-Laguna, I.; Luthra, R.; Lee, J. J.; Lu, K. H.; Kurzrock, R., *J Clin Oncol* **2012,** *30*, 777-82.
136. Philp, A. J.; Campbell, I. G.; Leet, C.; Vincan, E.; Rockman, S. P.; Whitehead, R. H.; Thomas, R. J. S.; Phillips, W. A., *Cancer Res* **2001,** *61*, 7426-9.
137. Downward, J., *Nat Med* **2008,** *14*, 1315-6.
138. Gao, N.; Flynn, D. C.; Zhang, Z.; Zhong, X. S.; Walker, V.; Liu, K. J.; Shi, X.; Jiang, B. H., *Am J Physiol Cell Physiol* **2004,** *287*, 281-91.
139. Tee, A. R.; Manning, B. D.; Roux, P. P.; Cantley, L. C.; Blenis, J., *Curr Biol* **2003,** *13*, 1259-68.
140. Summers, S. A.; Kao, A. W.; Kohn, A. D.; Backus, G. S.; Roth, R. A.; Pessin, J. E.; Birnbaum, M. J., *J Biol Chem* **1999,** *274*, 17934-40.
141. Shukla, S.; Maclennan, G. T.; Hartman, D. J.; Fu, P.; Resnick, M. I.; Gupta, S., *Int J Cancer* **2007,** *121*, 1424-32.
142. Shen, W. H.; Balajee, A. S.; Wang, J.; Wu, H.; Eng, C.; Pandolfi, P. P.; Yin, Y., *Cell* **2007,** *128*, 157-70.
143. Nardella, C.; Clohessy, J. G.; Alimonti, A.; Pandolfi, P. P., *Nat Rev Cancer* **2011,** *11*, 503-11.
144. Li, J.; Yen, C.; Liaw, D.; Podsypanina, K.; Bose, S.; Wang, S. I.; Puc, J.; Miliaresis, C.; Rodgers, L.; McCombie, R.; Bigner, S. H.; Giovanella, B. C.; Ittmann, M.; Tycko, B.; Hibshoosh, H.; Wigler, M. H.; Parsons, R., *Science* **1997,** *275*, 1943-7.
145. Wu, Z.; Cho, H.; Hampton, G. M.; Theodorescu, D., *Neoplasia* **2009,** *11*, 66-76.
146. Sun, H.; Lesche, R.; Li, D. M.; Liliental, J.; Zhang, H.; Gao, J.; Gavrilova, N.; Mueller, B.; Liu, X.; Wu, H., *Proc Natl Acad Sci U S A* **1999,** *96*, 6199-204.
147. Slipicevic, A.; Holm, R.; Nguyen, M. T.; Bohler, P. J.; Davidson, B.; Florenes, V. A., *Am J Clin Pathol* **2005,** *124*, 528-36.
148. Chalhoub, N.; Baker, S. J., *Annu Rev Pathol* **2009,** *4*, 127-50.
149. Risinger, J. I.; Hayes, K.; Maxwell, G. L.; Carney, M. E.; Dodge, R. K.; Barrett, J. C.; Berchuck, A., *Clin Cancer Res* **1998,** *4*, 3005-10.
150. Ming, M.; He, Y. Y., *J Invest Dermatol* **2009,** *129*, 2109-12.
151. Cully, M.; You, H.; Levine, A. J.; Mak, T. W., *Nat Rev Cancer* **2006,** *6*, 184-92.
152. Huang, C. H.; Mandelker, D.; Gabelli, S. B.; Amzel, L. M., *Cell Cycle* **2008,** *7*, 1151-6.
153. Samuels, Y.; Wang, Z.; Bardelli, A.; Silliman, N.; Ptak, J.; Szabo, S.; Yan, H.; Gazdar, A.; Powell, S. M.; Riggins, G. J.; Willson, J. K.; Markowitz, S.; Kinzler, K. W.; Vogelstein, B.; Velculescu, V. E., *Science* **2004,** *304*, 554.
154. Bader, A. G.; Kang, S.; Zhao, L.; Vogt, P. K., *Nat Rev Cancer* **2005,** *5*, 921-9.
155. Ravi, R.; Bedi, A., *Drug Resist Updat* **2004,** *7*, 53-67.
156. Wang, W.; Hu, Y., *Med Res Rev* **2012,** *32*, 1159-96.
157. Elkholi, R.; Floros, K. V.; Chipuk, J. E., *Genes Cancer* **2011,** *2*, 523-37.
158. Engelman, J. A., *Nat Rev Cancer* **2009,** *9*, 550-62.
159. Hou, J.; Lam, F.; Proud, C.; Wang, S., *Oncotarget* **2012,** *3*, 118-131.
160. Le Tourneau, C.; Faivre, S.; Serova, M.; Raymond, E., *Br J Cancer* **2008,** *99*, 1197-203.
161. Liu, E.; Marincola, P.; Oberg, K., *Therap Adv Gastroenterol* **2013,** *6*, 412-9.

162. Svejda, B.; Kidd, M.; Kazberouk, A.; Lawrence, B.; Pfragner, R.; Modlin, I. M., *Cancer* **2011,** *117*, 4141-54.
163. Witzig, T. E.; Reeder, C. B.; LaPlant, B. R.; Gupta, M.; Johnston, P. B.; Micallef, I. N.; Porrata, L. F.; Ansell, S. M.; Colgan, J. P.; Jacobsen, E. D.; Ghobrial, I. M.; Habermann, T. M., *Leukemia* **2011,** *25*, 341-7.
164. Johnston, P. B.; Inwards, D. J.; Colgan, J. P.; Laplant, B. R.; Kabat, B. F.; Habermann, T. M.; Micallef, I. N.; Porrata, L. F.; Ansell, S. M.; Reeder, C. B.; Roy, V.; Witzig, T. E., *Am J Hematol* **2010,** *85*, 320-4.
165. Zoncu, R.; Efeyan, A.; Sabatini, D. M., *Nat Rev Mol Cell Biol* **2011,** *12*, 21-35.
166. O'Reilly, K. E.; Rojo, F.; She, Q. B.; Solit, D.; Mills, G. B.; Smith, D.; Lane, H.; Hofmann, F.; Hicklin, D. J.; Ludwig, D. L.; Baselga, J.; Rosen, N., *Cancer Res* **2006,** *66*, 1500-8.
167. Sun, S. Y.; Rosenberg, L. M.; Wang, X.; Zhou, Z.; Yue, P.; Fu, H.; Khuri, F. R., *Cancer Res* **2005,** *65*, 7052-8.
168. Manara, M. C.; Nicoletti, G.; Zambelli, D.; Ventura, S.; Guerzoni, C.; Landuzzi, L.; Lollini, P. L.; Maira, S. M.; Garcia-Echeverria, C.; Mercuri, M.; Picci, P.; Scotlandi, K., *Clin Cancer Res* **2010,** *16*, 530-40.
169. Baumann, P.; Schneider, L.; Mandl-Weber, S.; Oduncu, F.; Schmidmaier, R., *Anticancer Drugs* **2012,** *23*, 131-8.
170. Leung, E.; Kim, J. E.; Rewcastle, G. W.; Finlay, G. J.; Baguley, B. C., *Cancer Biol Ther* **2011,** *11*, 938-46.
171. Rodon, J.; Dienstmann, R.; Serra, V.; Tabernero, J., *Nat Rev Clin Oncol* **2013,** *10*, 143-53.
172. Zaytseva, Y. Y.; Valentino, J. D.; Gulhati, P.; Evers, B. M., *Cancer Lett* **2012,** *319*, 1-7.
173. Hyoda, T.; Tsujioka, T.; Nakahara, T.; Suemori, S.; Okamoto, S.; Kataoka, M.; Tohyama, K., *Cancer Sci* **2015,** *106*, 287-93.
174. Liang, J.; Pan, Y.; Zhang, D.; Guo, C.; Shi, Y.; Wang, J.; Chen, Y.; Wang, X.; Liu, J.; Guo, X.; Chen, Z.; Qiao, T.; Fan, D., *FASEB J* **2007,** *21*, 2247-56.
175. Alao, J. P., *Mol Cancer* **2007,** *6*, 24.
176. Seetharam, M.; Fan, A. C.; Tran, M.; Xu, L.; Renschler, J. P.; Felsher, D. W.; Sridhar, K.; Wilhelm, F.; Greenberg, P. L., *Leuk Res* **2012,** *36*, 98-103.
177. Mendoza, M. C.; Er, E. E.; Blenis, J., *Trends Biochem Sci* **2011,** *36*, 320-8.
178. Serra, V.; Scaltriti, M.; Prudkin, L.; Eichhorn, P. J. A.; Ibrahim, Y. H.; Chandarlapaty, S.; Markman, B.; Rodriguez, O.; Guzman, M.; Rodriguez, S.; Gili, M.; Russillo, M.; Parra, J. L.; Singh, S.; Arribas, J.; Rosen, N.; Baselga, J., *Oncogene* **2011,** *30*, 2547-57.
179. Ilic, N.; Utermark, T.; Widlund, H. R.; Roberts, T. M., *Proc Natl Acad Sci U S A* **2011,** *108*, 699-708.
180. Herman, S. E.; Gordon, A. L.; Wagner, A. J.; Heerema, N. A.; Zhao, W.; Flynn, J. M.; Jones, J.; Andritsos, L.; Puri, K. D.; Lannutti, B. J.; Giese, N. A.; Zhang, X.; Wei, L.; Byrd, J. C.; Johnson, A. J., *Blood* **2010,** *116*, 2078-88.
181. Vijapurkar, U.; Robillard, L.; Zhou, S.; Degtyarev, M.; Lin, K.; Truong, T.; Tremayne, J.; Ross, L. B.; Pei, Z.; Friedman, L. S.; Blackwood, E. M.; Belvin, M., *Cancer Lett* **2012,** *326*, 168-75.
182. ClinicalTrials.gov. Efficacy and safety of IV rigosertib in MDS patients with excess blasts progressing after azacitidine or decitabine. https://clinicaltrials.gov/ct2/show/NCT01928537 (accessed 5th November).

183. ClinicalTrials.gov. Efficacy and Safety of Oral Rigosertib in Transfusion-dependent, Low or Int-1 or Trisomy 8 Int-2 Myelodysplastic Syndrome (ONTARGET). https://clinicaltrials.gov/ct2/show/NCT01584531 (accessed 5th November).
184. ClinicalTrials.gov. Randomized Study of ON 01910.Na in Refractory Myelodysplastic Syndrome Patients With Excess Blasts (ONTIME). https://www.clinicaltrials.gov/ct2/show/NCT01241500 (accessed 5th November).
185. Corey, S. J.; Minden, M. D.; Barber, D. L.; Kantarjian, H.; Wang, J. C. Y.; Schimmer, A. D., *Nat Rev Cancer* **2007,** *7*, 118-129.
186. Nyakern, M.; Tazzari, P. L.; Finelli, C.; Bosi, C.; Follo, M. Y.; Grafone, T.; Piccaluga, P. P.; Martinelli, G.; Cocco, L.; Martelli, A. M., *Leukemia* **2006,** *20*, 230-8.
187. Yee, K. W.; Zeng, Z.; Konopleva, M.; Verstovsek, S.; Ravandi, F.; Ferrajoli, A.; Thomas, D.; Wierda, W.; Apostolidou, E.; Albitar, M.; O'Brien, S.; Andreeff, M.; Giles, F. J., *Clin Cancer Res* **2006,** *12*, 5165-73.
188. Roschewski, M.; Farooqui, M.; Aue, G.; Wilhelm, F.; Wiestner, A., *Leukemia* **2013,** *27*, 1920-3.
189. Jimeno, A.; Li, J.; Messersmith, W. A.; Laheru, D.; Rudek, M. A.; Maniar, M.; Hidalgo, M.; Baker, S. D.; Donehower, R. C., *J Clin Oncol* **2008,** *26*, 5504-10.
190. Ohnuma, T.; Lehrer, D.; Ren, C.; Cho, S. Y.; Maniar, M.; Silverman, L.; Sung, M.; Gretz, H. F., 3rd; Benisovich, V.; Navada, S.; Akahoho, E.; Wilck, E.; Taft, D. R.; Roboz, J.; Wilhelm, F.; Holland, J. F., *Am J Cancer Res* **2013,** *3*, 323-38.
191. Silverman, L. R.; Greenberg, P.; Raza, A.; Olnes, M. J.; Holland, J. F.; Reddy, P.; Maniar, M.; Wilhelm, F., *Hematol Oncol* **2015,** *33*, 57-66.
192. Raza, A.; Mukherjee, S.; Eisenberger, A.; Mears, J. G.; Wilhelm, F., *J Clin Oncol* **2013,** *31*.
193. Frost, A.; Mross, K.; Steinbild, S.; Hedbom, S.; Unger, C.; Kaiser, R.; Trommeshauser, D.; Munzert, G., *Curr Oncol* **2012,** *19*, 28-35.
194. Ellis, P. M.; Chu, Q. S.; Leighl, N.; Laurie, S. A.; Fritsch, H.; Gaschler-Markefski, B.; Gyorffy, S.; Munzert, G., *Clin Lung Cancer* **2013,** *14*, 19-27.
195. Schoffski, P.; Blay, J. Y.; De Greve, J.; Brain, E.; Machiels, J. P.; Soria, J. C.; Sleijfer, S.; Wolter, P.; Ray-Coquard, I.; Fontaine, C.; Munzert, G.; Fritsch, H.; Hanft, G.; Aerts, C.; Rapion, J.; Allgeier, A.; Bogaerts, J.; Lacombe, D., *Eur J Cancer* **2010,** *46*, 2206-15.
196. Raza, A.; Tycko, B.; Lee, S.; Galili, N.; Ali, A.; Eisenberger, A.; Mears, J. G.; Al-Kali, A.; Tibes, R.; Spitzer, G., *Blood* **2013,** *122*, 2745.
197. Lu, T.; Goh, A. W.; Yu, M.; Adams, J.; Lam, F.; Teo, T.; Li, P.; Noll, B.; Zhong, L.; Diab, S.; Chahrour, O.; Hu, A.; Abbas, A. Y.; Liu, X.; Huang, S.; Sumby, C. J.; Milne, R.; Midgley, C.; Wang, S., *J Med Chem* **2014,** *57*, 2275-91.
198. White, M. P.; Babayeva, M.; Taft, D. R.; Maniar, M., *J Pharm Pharmacol* **2013,** *65*, 960-9.
199. Komrokji, R. S.; Raza, A.; Lancet, J. E.; Ren, C.; Taft, D.; Maniar, M.; Wilhelm, F.; List, A. F., *Br J Haematol* **2013,** *162*, 517-24.
200. Molsa, M.; Heikkinen, T.; Hakkola, J.; Hakala, K.; Wallerman, O.; Wadelius, M.; Wadelius, C.; Laine, K., *Clin Pharmacol Ther* **2005,** *78*, 123-31.
201. Su, L.; Mruk, D. D.; Lui, W. Y.; Lee, W. M.; Cheng, C. Y., *Proc Natl Acad Sci U S A* **2011,** *108*, 19623-8.
202. Gottesman, M. M., *Annu Rev Med* **2002,** *53*, 615-27.
203. Ros, J. E.; Libbrecht, L.; Geuken, M.; Jansen, P. L.; Roskams, T. A., *J Pathol* **2003,** *200*, 553-60.
204. Schinkel, A. H., *Adv Drug Deliv Rev* **1999,** *36*, 179-94.

205. Szakacs, G.; Paterson, J. K.; Ludwig, J. A.; Booth-Genthe, C.; Gottesman, M. M., *Nat Rev Drug Discov* **2006,** *5*, 219-34.
206. Smith, D. A.; Di, L.; Kerns, E. H., *Nat Rev Drug Discov* **2010,** *9*, 929-939.
207. Chun, A. W.; Cosenza, S. C.; Taft, D. R.; Maniar, M., *Cancer Chemother Pharmacol* **2009,** *65*, 177-86.
208. Almond, L. M.; Hoggard, P. G.; Edirisinghe, D.; Khoo, S. H.; Back, D. J., *J Antimicrob Chemother* **2005,** *56*, 738-44.
209. Trainor, G. L., *Expert Opin Drug Discov* **2007,** *2*, 51-64.
210. Jones, K.; Hoggard, P. G.; Khoo, S.; Maher, B.; Back, D. J., *Br J Clin Pharmacol* **2001,** *51*, 99-102.
211. Fricker, G.; Gutmann, H.; Droulle, A.; Drewe, J.; Miller, D. S., *Pharm Res* **1999,** *16*, 1570-5.
212. Gutmann, H.; Miller, D. S.; Droulle, A.; Drewe, J.; Fahr, A.; Fricker, G., *Br J Pharmacol* **2000,** *129*, 251-6.
213. Okamura, N.; Hirai, M.; Tanigawara, Y.; Tanaka, K.; Yasuhara, M.; Ueda, K.; Komano, T.; Hori, R., *J Pharmacol Exp Ther* **1993,** *266*, 1614-9.
214. Tanigawara, Y.; Okamura, N.; Hirai, M.; Yasuhara, M.; Ueda, K.; Kioka, N.; Komano, T.; Hori, R., *J Pharmacol Exp Ther* **1992,** *263*, 840-5.
215. Meanwell, N. A., *J Med Chem* **2011,** *54*, 2529-91.
216. Yu, K. L.; Sin, N.; Civiello, R. L.; Wang, X. A.; Combrink, K. D.; Gulgeze, H. B.; Venables, B. L.; Wright, J. J.; Dalterio, R. A.; Zadjura, L.; Marino, A.; Dando, S.; D'Arienzo, C.; Kadow, K. F.; Cianci, C. W.; Li, Z.; Clarke, J.; Genovesi, E. V.; Medina, I.; Lamb, L.; Colonno, R. J.; Yang, Z.; Krystal, M.; Meanwell, N. A., *Bioorg Med Chem Lett* **2007,** *17*, 895-901.
217. Samuel, K.; Yin, W.; Stearns, R. A.; Tang, Y. S.; Chaudhary, A. G.; Jewell, J. P.; Lanza, T., Jr.; Lin, L. S.; Hagmann, W. K.; Evans, D. C.; Kumar, S., *J Mass Spectrom* **2003,** *38*, 211-21.
218. Bell, S. C.; Wong, A.; Maniar, M., Formulations for parenteral administration of (e)-2, 6-dialkoxystyryl 4-substituted benzylsulfones. Google Patents: 2011.
219. Kolb, K. E.; Field, K. W.; Schatz, P. F., *J Chem Educ* **1990,** *67*, 304.
220. Mayo, D. W.; Pike, R. M.; Forbes, D. C., *Microscale organic laboratory: with multistep and multiscale syntheses*. John Wiley & Sons: 2010.
221. Tsou, H. R.; Overbeek-Klumpers, E. G.; Hallett, W. A.; Reich, M. F.; Floyd, M. B.; Johnson, B. D.; Michalak, R. S.; Nilakantan, R.; Discafani, C.; Golas, J.; Rabindran, S. K.; Shen, R.; Shi, X.; Wang, Y. F.; Upeslacis, J.; Wissner, A., *J Med Chem* **2005,** *48*, 1107-31.
222. Nelson, D. W.; Gregg, R. J.; Kort, M. E.; Perez-Medrano, A.; Voight, E. A.; Wang, Y.; Grayson, G.; Namovic, M. T.; Donnelly-Roberts, D. L.; Niforatos, W.; Honore, P.; Jarvis, M. F.; Faltynek, C. R.; Carroll, W. A., *J Med Chem* **2006,** *49*, 3659-66.
223. Testa, B., Chapter 32 - Biotransformation Reactions and Their Enzymes. In *The Practice of Medicinal Chemistry (Third Edition)*, Wermuth, C. G., Ed. Academic Press: New York, 2008; pp 655-73.
224. Baur, B.; Storch, K.; Martz, K. E.; Goettert, M. I.; Richters, A.; Rauh, D.; Laufer, S. A., *J Med Chem* **2013,** *56*, 8561-78.
225. Protection for the Hydroxyl Group, Including 1,2- and 1,3-Diols. In *Greene's Protective Groups in Organic Synthesis*, John Wiley & Sons, Inc.: 2014; pp 17-471.
226. Wang, Z., Wohl-Ziegler Bromination. In *Comprehensive Organic Name Reactions and Reagents*, John Wiley & Sons, Inc.: 2010.

227. Parke, D. V., Chapter 3 - Metabolic transformations catalysed by hepatic microsomal enzymes. In *The Biochemistry of Foreign Compounds*, Parke, D. V., Ed. Pergamon: 1968; pp 34-55.
228. Silverman, R. B.; Holladay, M. W., Chapter 8 - Drug Metabolism. In *The Organic Chemistry of Drug Design and Drug Action (Third Edition)*, Holladay, R. B. S. W., Ed. Academic Press: Boston, 2014; pp 357-422.
229. Lemke, T. L.; Williams, D. A., *Foye's principles of medicinal chemistry*. Wolters Kluwer Health: 2012.
230. Zhang, C.; Sun, X.; Ren, Y.; Lou, Y.; Zhou, J.; Liu, M.; Li, D., *Cancer Biol Ther* **2012,** *13*, 1214-20.
231. Liu, X.; Lei, M.; Erikson, R. L., *Mol Cell Biol* **2006,** *26*, 2093-108.
232. Williams, D., *Foye's principles of medicinal chemistry* **2008,** *6*.
233. Wermuth, C. G., Chapter 38 - Preparation of Water-Soluble Compounds by Covalent Attachment of Solubilizing Moieties. In *The Practice of Medicinal Chemistry (Third Edition)*, Wermuth, C. G., Ed. Academic Press: New York, 2008; pp 767-85.
234. Ioannides, C.; Lewis, D. F., *Curr Top Med Chem* **2004,** *4*, 1767-88.
235. St Jean, D. J., Jr.; Fotsch, C., *J Med Chem* **2012,** *55*, 6002-20.
236. van Breemen, R. B.; Li, Y., *Expert Opin Drug Metab Toxicol* **2005,** *1*, 175-85.
237. Stephens, R. H.; O'Neill, C. A.; Warhurst, A.; Carlson, G. L.; Rowland, M.; Warhurst, G., *J Pharmacol Exp Ther* **2001,** *296*, 584-91.
238. Zornoza, T.; Cano-Cebrian, M. J.; Hipolito, L.; Granero, L.; Polache, A., *Biopharm Drug Dispos* **2006,** *27*, 305-11.
239. Barwell, N. P.; Davis, A. P., *J Org Chem* **2011,** *76*, 6548-57.
240. Diez-Barra, E.; Garcia-Martinez, J. C.; Merino, S.; del Rey, R.; Rodriguez-Lopez, J.; Sanchez-Verdu, P.; Tejeda, J., *J Org Chem* **2001,** *66*, 5664-70.
241. Kang, S. U.; Worthy, K. M.; Bindu, L. K.; Zhang, M.; Yang, D.; Fisher, R. J.; Burke, T. R., Jr., *J Med Chem* **2005,** *48*, 5369-72.
242. Shimasaki, T.; Kato, S.; Ideta, K.; Goto, K.; Shinmyozu, T., *J Org Chem* **2007,** *72*, 1073-87.
243. Upadhyay, S. K.; Jursic, B. S., *Synth Commun* **2011,** *41*, 3177-3185.
244. Amijs, C. H. M.; van Klink, G. P. M.; van Koten, G., *Green Chem* **2003,** *5*, 470-4.
245. Katritzky, A. R.; Ramsden, C. A.; Joule, J. A.; Zhdankin, V. V., 3.2 - Reactivity of Six-membered Rings. In *Handbook of Heterocyclic Chemistry (Third Edition)*, Elsevier: Amsterdam, 2010; pp 242-382.
246. Stewart, R.; Harris, M. G., *J Org Chem* **1978,** *43*, 3123-6.
247. Theodorou, V.; Gogou, M.; Giannoussi, A.; Skobridis, K., *ARKIVOC* **2014,** *4*, 11-23.
248. Harris, M. H.; Stewart, R., *Can. J. Chem.* **1977,** *55*, 3800-3806.
249. Ohmatsu, K.; Ito, M.; Kunieda, T.; Ooi, T., *Nat Chem* **2012,** *4*, 473-7.
250. Riccardi, C.; Nicoletti, I., *Nat Protoc* **2006,** *1*, 1458-61.
251. Ormerod, M. G., *J Immunol Methods* **2002,** *265*, 73-80.
252. Gleixner, K. V.; Ferenc, V.; Peter, B.; Gruze, A.; Meyer, R. A.; Hadzijusufovic, E.; Cerny-Reiterer, S.; Mayerhofer, M.; Pickl, W. F.; Sillaber, C.; Valent, P., *Cancer Res* **2010,** *70*, 1513-23.
253. Santamaria, A.; Neef, R.; Eberspacher, U.; Eis, K.; Husemann, M.; Mumberg, D.; Prechtl, S.; Schulze, V.; Siemeister, G.; Wortmann, L.; Barr, F. A.; Nigg, E. A., *Mol Biol Cell* **2007,** *18*, 4024-36.
254. Logue, S. E.; Elgendy, M.; Martin, S. J., *Nat Protoc* **2009,** *4*, 1383-95.
255. Riss, T.; O'Brien, M.; Moravec, R., *Cell Notes* **2003,** *6*, 6.

256. Chaturvedi, P.; Eng, W. K.; Zhu, Y.; Mattern, M. R.; Mishra, R.; Hurle, M. R.; Zhang, X.; Annan, R. S.; Lu, Q.; Faucette, L. F.; Scott, G. F.; Li, X.; Carr, S. A.; Johnson, R. K.; Winkler, J. D.; Zhou, B. B., *Oncogene* **1999,** *18*, 4047-54.
257. Krause, K.; Haugwitz, U.; Wasner, M.; Wiedmann, M.; Mossner, J.; Engeland, K., *Biochem Biophys Res Commun* **2001,** *284*, 743-50.
258. Boulares, A. H.; Yakovlev, A. G.; Ivanova, V.; Stoica, B. A.; Wang, G.; Iyer, S.; Smulson, M., *J Biol Chem* **1999,** *274*, 22932-40.
259. Liu, X.; Choy, E.; Harmon, D.; Yang, S.; Yang, C.; Mankin, H.; Hornicek, F. J.; Duan, Z., *Anticancer Drugs* **2011,** *22*, 444-53.
260. Nair, J. S.; Schwartz, G. K., *Cell Cycle* **2015,** *14*, 3101-11.
261. Elia, A. E.; Rellos, P.; Haire, L. F.; Chao, J. W.; Ivins, F. J.; Hoepker, K.; Mohammad, D.; Cantley, L. C.; Smerdon, S. J.; Yaffe, M. B., *Cell* **2003,** *115*, 83-95.
262. van de Weerdt, B. C.; Littler, D. R.; Klompmaker, R.; Huseinovic, A.; Fish, A.; Perrakis, A.; Medema, R. H., *Biochim Biophys Acta* **2008,** *1783*, 1015-22.
263. Chahrour, O.; Xiangrui, L.; Lam, F.; Abdullah, A.; Midgley, C.; Shudong, W. In *Synthesis, Design, and biological evaluation of thymoquinone derivatives and ON01910 derivatives as anticancer agents*, Abstract in National Cancer Research Institute Conference, BT Convention Center, 2010.
264. Veber, D. F.; Johnson, S. R.; Cheng, H. Y.; Smith, B. R.; Ward, K. W.; Kopple, K. D., *J Med Chem* **2002,** *45*, 2615-23.
265. Morton, C. L.; Houghton, P. J., *Nat Protoc* **2007,** *2*, 247-50.
266. Ormerod, M. G.; Orr, R. M.; Peacock, J. H., *Br J Cancer* **1994,** *69*, 93-100.
267. Goel, M. K.; Khanna, P.; Kishore, J., *Int J Ayurveda Res* **2010,** *1*, 274-8.
268. Rich, J. T.; Neely, J. G.; Paniello, R. C.; Voelker, C. C.; Nussenbaum, B.; Wang, E. W., *Otolaryngol Head Neck Surg* **2010,** *143*, 331-6.
269. Murugan, R. N.; Park, J. E.; Lim, D.; Ahn, M.; Cheong, C.; Kwon, T.; Nam, K. Y.; Choi, S. H.; Kim, B. Y.; Yoon, D. Y.; Yaffe, M. B.; Yu, D. Y.; Lee, K. S.; Bang, J. K., *Bioorg Med Chem* **2013,** *21*, 2623-34.
270. Dai, W.; Wang, X., *Mol Cell* **2006,** *24*, 489-90.
271. Ahn, M.; Han, Y. H.; Park, J. E.; Kim, S.; Lee, W. C.; Lee, S. J.; Gunasekaran, P.; Cheong, C.; Shin, S. Y., Sr.; Kim, H. Y.; Ryu, E. K.; Murugan, R. N.; Kim, N. H.; Bang, J. K., *J Med Chem* **2015,** *58*, 294-304.
272. Kang, Y. H.; Park, J. E.; Yu, L. R.; Soung, N. K.; Yun, S. M.; Bang, J. K.; Seong, Y. S.; Yu, H.; Garfield, S.; Veenstra, T. D.; Lee, K. S., *Mol Cell* **2006,** *24*, 409-22.
273. Liao, C.; Park, J. E.; Bang, J. K.; Nicklaus, M. C.; Lee, K. S., *ACS Med Chem Lett* **2010,** *1*, 110-4.
274. Sherman, W.; Beard, H. S.; Farid, R., *Chem Biol Drug Des* **2006,** *67*, 83-4.
275. Huggins, D. J.; McKenzie, G. J.; Robinson, D. D.; Narvaez, A. J.; Hardwick, B.; Roberts-Thomson, M.; Venkitaraman, A. R.; Grant, G. H.; Payne, M. C., *PLoS Comput Biol* **2010,** *6*.
276. Athuluri-Divakar, S. K.; Vasquez-Del Carpio, R.; Dutta, K.; Baker, S. J.; Cosenza, S. C.; Basu, I.; Gupta, Y. K.; Reddy, M. R.; Ueno, L.; Hart, J. R., *Cell* **2016,** *165*, 643-655.
277. Lievre, A.; Bachet, J.-B.; Le Corre, D.; Boige, V.; Landi, B.; Emile, J.-F.; Côté, J.-F.; Tomasic, G.; Penna, C.; Ducreux, M., *Cancer Res* **2006,** *66*, 3992-3995.
278. Mitsudomi, T.; Viallet, J.; Mulshine, J.; Linnoila, R.; Minna, J.; Gazdar, A., *Oncogene* **1991,** *6*, 1353-1362.
279. Mok, S. C.-H.; Bell, D. A.; Knapp, R. C.; Fishbaugh, P. M.; Welch, W. R.; Muto, M. G.; Berkowitz, R. S.; Tsao, S.-W., *Cancer Res* **1993,** *53*, 1489-1492.

280. Gysin, S.; Salt, M.; Young, A.; McCormick, F., *Genes Cancer* **2011,** *2*, 359-372.
281. Baines, A. T.; Xu, D.; Der, C. J., *Future Med Chem* **2011,** *3*, 1787-808.
282. Downward, J., *Nat Rev Cancer* **2003,** *3*, 11-22.
283. Cox, A. D.; Hisaka, M. M.; Buss, J. E.; Der, C. J., *Mol Cell Biol* **1992,** *12*, 2606-15.
284. Athuluri-Divakar, Sai K.; Vasquez-Del Carpio, R.; Dutta, K.; Baker, Stacey J.; Cosenza, Stephen C.; Basu, I.; Gupta, Yogesh K.; Reddy, M. V. R.; Ueno, L.; Hart, Jonathan R.; Vogt, Peter K.; Mulholland, D.; Guha, C.; Aggarwal, Aneel K.; Reddy, E. P., *Cell 165*, 643-655.
285. Jerabek-Willemsen, M.; André, T.; Wanner, R.; Roth, H. M.; Duhr, S.; Baaske, P.; Breitsprecher, D., *J Mol Struct* **2014,** *1077*, 101-13.
286. Wienken, C. J.; Baaske, P.; Rothbauer, U.; Braun, D.; Duhr, S., *Nat Commun* **2010,** *1*, 100.
287. Seidel, S. A.; Wienken, C. J.; Geissler, S.; Jerabek-Willemsen, M.; Duhr, S.; Reiter, A.; Trauner, D.; Braun, D.; Baaske, P., *Angew Chem Int Ed Engl* **2012,** *51*, 10656-9.
288. Jerabek-Willemsen, M.; Wienken, C. J.; Braun, D.; Baaske, P.; Duhr, S., *Assay Drug Dev Technol* **2011,** *9*, 342-353.
289. Matsui, T. A.; Murata, H.; Sowa, Y.; Sakabe, T.; Koto, K.; Horie, N.; Tsuji, Y.; Sakai, T.; Kubo, T., *Oncol Rep* **2010,** *24*, 329-33.
290. Weng, L. P.; Smith, W. M.; Dahia, P. L.; Ziebold, U.; Gil, E.; Lees, J. A.; Eng, C., *Cancer Res* **1999,** *59*, 5808-14.
291. Weng, L.-P.; Brown, J. L.; Eng, C., *Hum Mol Genet* **2001,** *10*, 599-604.
292. Joseph, E. W.; Pratilas, C. A.; Poulikakos, P. I.; Tadi, M.; Wang, W.; Taylor, B. S.; Halilovic, E.; Persaud, Y.; Xing, F.; Viale, A.; Tsai, J.; Chapman, P. B.; Bollag, G.; Solit, D. B.; Rosen, N., *Proc Natl Acad Sci U S A* **2010,** *107*, 14903-8.
293. Fruman, D. A.; Rommel, C., *Nat Rev Drug Discov* **2014,** *13*, 140-56.
294. Bradley, E. W.; Ruan, M. M.; Vrable, A.; Oursler, M. J., *J Cell Biochem* **2008,** *104*, 1439-51.
295. Halaschek-Wiener, J.; Wacheck, V.; Kloog, Y.; Jansen, B., *Cell Signal* **2004,** *16*, 1319-27.
296. Ries, S.; Biederer, C.; Woods, D.; Shifman, O.; Shirasawa, S.; Sasazuki, T.; McMahon, M.; Oren, M.; McCormick, F., *Cell* **2000,** *103*, 321-330.
297. Ogawara, Y.; Kishishita, S.; Obata, T.; Isazawa, Y.; Suzuki, T.; Tanaka, K.; Masuyama, N.; Gotoh, Y., *J Biol Chem* **2002,** *277*, 21843-50.
298. Mayo, L. D.; Donner, D. B., *Proc Natl Acad Sci U S A* **2001,** *98*, 11598-603.
299. Gottlieb, T. M.; Leal, J. F.; Seger, R.; Taya, Y.; Oren, M., *Oncogene* **2002,** *21*, 1299-303.
300. Wang, W.; Qin, J. J.; Voruganti, S.; Wang, M. H.; Sharma, H.; Patil, S.; Zhou, J.; Wang, H.; Mukhopadhyay, D.; Buolamwini, J. K.; Zhang, R., *Gastroenterology* **2014,** *147*, 893-902
301. Shangary, S.; Wang, S., *Annu Rev Pharmacol Toxicol* **2009,** *49*, 223-41.
302. Liu, J.-L.; Wang, X.-Y.; Huang, B.-X.; Zhu, F.; Zhang, R.-G.; Wu, G., *Med Oncol* **2011,** *28*, 673-8.
303. Strock, C. J.; Park, J.-I.; Nakakura, E. K.; Bova, G. S.; Isaacs, J. T.; Ball, D. W.; Nelkin, B. D., *Cancer Res* **2006,** *66*, 7509-7515.
304. Eggers, J. P.; Grandgenett, P. M.; Collisson, E. C.; Lewallen, M. E.; Tremayne, J.; Singh, P. K.; Swanson, B. J.; Andersen, J. M.; Caffrey, T. C.; High, R. R., *Clin Cancer Res* **2011,** *17*, 6140-50.

305. Bisht, S.; Nolting, J.; Schutte, U.; Haarmann, J.; Jain, P.; Shah, D.; Brossart, P.; Flaherty, P.; Feldmann, G., *Transl Oncol* **2015,** *8*, 295-307.
306. Strock, C. J.; Park, J. I.; Nakakura, E. K.; Bova, G. S.; Isaacs, J. T.; Ball, D. W.; Nelkin, B. D., *Cancer Res* **2006,** *66*, 7509-15.
307. Feldmann, G.; Mishra, A.; Hong, S. M.; Bisht, S.; Strock, C. J.; Ball, D. W.; Goggins, M.; Maitra, A.; Nelkin, B. D., *Cancer Res* **2010,** *70*, 4460-9.
308. Wang, S.; Meades, C.; Wood, G.; Osnowski, A.; Anderson, S.; Yuill, R.; Thomas, M.; Mezna, M.; Jackson, W.; Midgley, C.; Griffiths, G.; Fleming, I.; Green, S.; McNae, I.; Wu, S. Y.; McInnes, C.; Zheleva, D.; Walkinshaw, M. D.; Fischer, P. M., *J Med Chem* **2004,** *47*, 1662-75.